Cell fate and signalling in chick limb bud development

A thesis submitted for the degree of

Doctor of Philosophy

at the University of London

By
Neil Andrew Vargesson

Department of Anatomy and Developmental Biology
University College London

February 1998

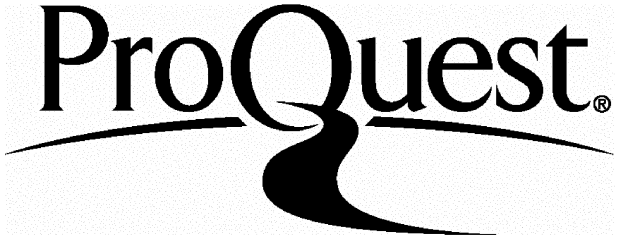

ABSTRACT

The chick limb develops from a bud of apparently homogeneous mesenchyme cells encased in ectoderm. Mesenchymal-epithelial interactions and mesenchymal signalling pathways are important in controlling the patterning and positioning of the skeletal elements and other tissues of the limb. I have produced detailed and comprehensive fatemaps for mesenchyme and apical ridge of a stage 20 chick wing bud. The mesenchyme fate maps show that the majority of the limb including the digits arises from posterior subapical mesenchyme. Fatemaps of the apical ridge show that apical ridge and mesenchyme do not remain in concert as development proceeds; the apical ridge expands more anteriorly than mesenchyme. The detailed behaviour of cells in the fate maps is not consistent with the model of vertebrate limb evolution which suggests an anterior bending of the posterior metapterygial axis led to the evolution of the hand plate. I have used these fate maps to investigate the relationship between cell lineage and gene expression. I show that the *Hoxa-13* and *Hoxd-13* expression domains expand by different mechanisms. I investigated activation of 5' *HoxA* genes in response to FGF-4, and show that *Hoxa-13* gene expression may require FGF-4 for elaboration but not initiation. I have also used the fate maps to investigate cell fate in regulating and 'regenerating' limbs. I show that regulation and regeneration can only operate in the progress zone. Furthermore I show polarising signals act over a very short distance in reprogramming cells in the anterior tip to produce posterior digits. Finally I investigated expression of genes in the *Notch* signalling pathway in chick limb outgrowth and patterning. I show that genes in the *Notch* signalling pathway are expressed at different stages of chick limb development, and are implicated in bud outgrowth, formation of the musculature and vasculature and in digit spacing and positioning.

CONTENTS

CHAPTER TWO - Materials and Methods

CHAPTER THREE - Cell fate in the chick limb bud and relationship to gene expression

List of Figures

List of Tables

Abbreviations used in text

ATP	adenosine triphosphate
BMP	Bone morphogenetic protein
CTP	cytosine triphosphate
DiI	1,1-dioctadecyl-3,3,3',3'-tetramethylindo-carbocyanine perchloride
DiA	4-Di-16-Asp
EDTA	ethylenediamine tetra acetic acid
En-1	*Engrailed-1* - homeobox containing transcription factor
FGF	Fibroblast growth factor
GTP	guanine triphosphate
Lmx-1	LIM-homeodomain containing transcription factor
Msx	muscle segmentation homeobox containing gene
PBS	phosphate buffered saline
PBST	phosphate buffered saline with 0.1% Tween
psi	per square inch
R-fri	*Radical fringe*
rpm	revolutions per minute
Shh	*Sonic hedgehog*
Slug	zinc finger transcription factor
SSC	standard saline citrate
UTP	uracil triphosphate
Wnt-7a	secreted signalling molecule

Acknowledgements

I feel very privileged to have carried out my Ph.D in such a fantastic, friendly and vibrant lab, with such outstanding colleagues. I would like to thank Professor Lewis Wolpert for allowing me to carry out this Ph.D and for his support and inspiration throughout the course of my studies.

I owe a great deal to Professor Cheryll Tickle who has been a constant source of guidance, advice, help, inspiration, infectious enthusiasm and support.

I thank Dr Jon Clarke for introducing me to the DiI labelling technique as well help, advice and useful discussions throughout my Ph.D. I thank Dr Paris Ataliotis for his advice and help, Dr Ketan Patel for advice and guidance on whole mount in situ hybridisation as well as for stimulating discussions and Professor Paul Brickell for discussions and guidance on molecular biology. I would also like to thank Dr Julian Lewis and members of staff in his lab for many helpful discussions on the *Notch* signalling pathway. I also thank Anne Sheasby for various experimental support throughout the course of my Ph.D and Maureen Maloney for advice on admin issues. I am indebted to Professor Lewis Wolpert, Dr Jon Clarke and especially Professor Cheryll Tickle for reading and guiding the production of this thesis.

I would like to thank the many past and present members of the lab who have made my stay at UCL so fruitful, enjoyable and memorable, not just in advice and help on experimental issues but also for allowing me to relax and socialise with them. I would like to particularly thank Lynda Erskine, Adrian Hardy, Mel McGonnell, Richard Leigh, Bryony Green and Mark George for being great friends and colleagues and always being available for beer!.

Finally, I thank Lynda for her support and patience and for allowing me to share her life.

Dedication

To my parents, brother and sister.

CHAPTER ONE

General Introduction

The mechanisms of developmental patterning and morphogenesis in vertebrate embryos have been studied extensively using the chick wing bud as a model system. The wing develops from a small mass of mesenchyme enclosed in ectoderm and interactions between signalling pathways in the mesenchyme and ectoderm control the patterning and outgrowth of the limb. Thus an initially homogeneous population of cells gives rise to many different cell and tissue types. Although great advances in understanding the mechanisms and molecular basis of the processes underlying limb development have occurred in recent years, many questions still remain. I will review current knowledge of limb developmental biology and then outline the focus of this thesis.

1.1 Review of limb development

1.1.1 Early development of the chick limb bud

The wing and leg buds of the chick embryo grow out at specific levels along the main body axis from lateral plate mesenchyme on either side of the somites and consist of a mass of mesenchyme encased in an ectodermal jacket. The wing bud forms opposite somites 15-20 at stage 15 and the leg bud opposite somites 26-32 at stage 16 (Hamburger and Hamilton, 1951). These buds are clearly seen as outgrowths from the flank by stage 17. The budding of the limb from flank mesenchyme is due to a decrease in the rate of proliferation in mesenchyme bordering each limb region, while the proliferation rate of mesenchyme cells within the presumptive limb forming regions remains the same (Searls and Janners, 1971). By approximately stage 17, an apical ectodermal ridge is observed around the antero-posterior rim of the limb bud at the interface between dorsal and ventral ectoderm. The apical ridge is a specialised thickening of the ectoderm and is initiated by a mesenchymal signal (Saunders and Reuss, 1974; see also Ohuchi et al., 1997; Altabef et al., 1997). By stage 20, the apical ridge is considerably thicker and wider in medial and posterior regions of the bud (Carrington and Fallon, 1984; Todt and Fallon, 1984).

The limb grows and develops along three axes, the antero-posterior axis (e.g. thumb to little finger), the dorsal-ventral axis (e.g. back of hand to palm) and proximo-distal axis (e.g. shoulder girdle to tips of digits; Fig. 1.1).

1.1.2 Antero-posterior axis

1.1.2.1 *The zone of polarising activity*

The hand plate of the chick wing bud consists of three digits, digit **2** the most anterior digit, digit **3** the middle digit and digit **4** near the posterior margin (Fig. 1.2A). The digits are thought to be patterned by the polarising region. Saunders and Gasseling (1968) showed that grafting the posterior distal mesenchyme of one wing to the anterior margin of a second host wing resulted in a duplication of the pattern across the antero-posterior axis. Full duplication of digits was seen in mirror image symmetry to the normal digit pattern of **2**, **3** and **4** (thus, the pattern **432234** was achieved; Saunders and Gasseling, 1968; Fig. 1.2B). Hence the posterior distal mesenchyme of early chick wings can polarise the antero-posterior axis and is termed the zone of polarising activity (ZPA) or polarising region (Fig. 1.1).

The polarising region is found in limbs from the time the limb bud is first seen, around stage 16/17. Polarising potential, the ability of tissue to form a polarising region, is found in both the presumptive limb areas and intervening flank up to stage 17 (Hornbruch and Wolpert, 1991). The polarising region, once formed, remains and is restricted to the posterior distal margin of the limb as outgrowth occurs and strongest activity is found adjacent to the apical ridge (MacCabe and Parker, 1975; Honig and Summerbell, 1985). As development proceeds, the activity of the polarising region gets weaker, until stage 29, when the polarising region can not be detected (Honig and Summerbell, 1985).

A universal signalling mechanism

The posterior distal mesenchyme of the limb is only one area of the developing chick embryo that has polarising activity. Grafts of Hensen's node (Hornbruch and Wolpert, 1986) and the floor plate of the neural tube (Wagner et al., 1990), induce mirror image duplications of the digits when grafted to the anterior margin of the wing. This suggests a common signalling mechanism may be used in different regions of the embryo to organise and pattern tissue. Furthermore, grafts of posterior distal mesenchyme from different species, for example mouse, can induce mirror image digit duplications in the chick limb (Tickle et al., 1976; Izpisua-Belmonte et al., 1992a).

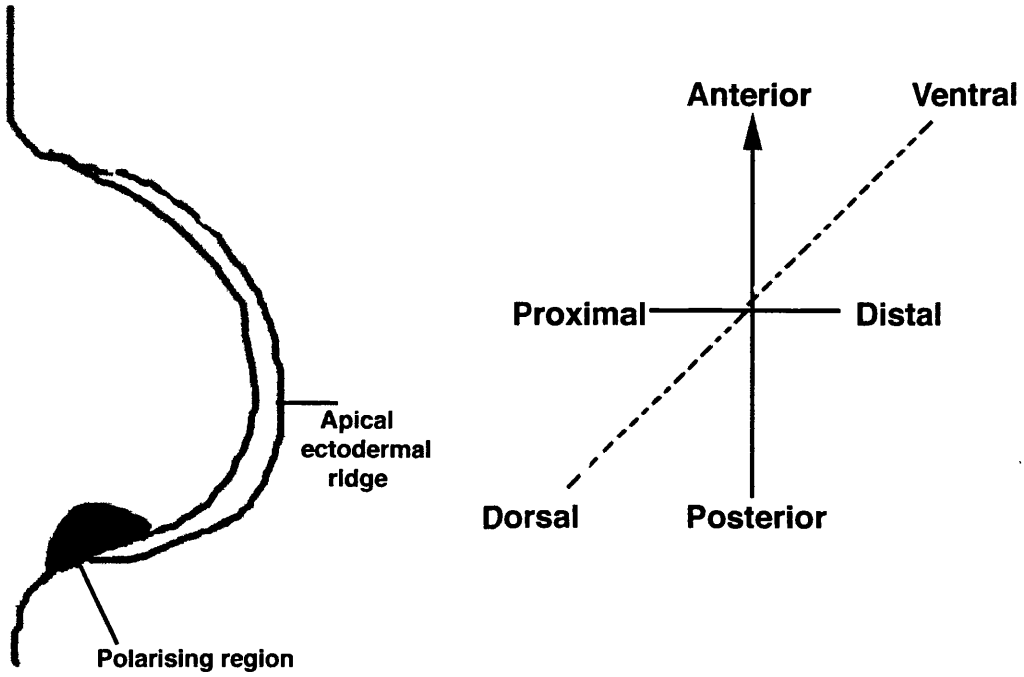

Figure 1.1

Stage 21 wing bud showing the position of polarising region in posterior distal mesenchyme and the apical ectodermal ridge around the rim of the bud.The three axes are indicated on the right.

Figure 1.2

A) A normal stage 21 wing bud left to develop for 7 days produces a wing with a humerus (H), ulna (U), radius (R) and three digits (digit **2** anteriorly, digit **3** mid limb and digit **4** posteriorly). On far right, proposed morphogen model where a morphogen diffuses across the anterior-posterior axis and the digits are determined at specific thresholds. Cells exposed to a low concentration form digit **2** in anterior of limb, while cells exposed to a high concentration in the posterior limb form a digit **4**. **B)** Example of the effect of ectopic polarising region, retinoic acid soaked bead or graft of *Shh* expressing cells placed beneath anterior apical ridge in stage 21 wing upon limb pattern 7 days later. Both normal and ectopic signalling regions produce morphogen giving a 'U' shaped morphogen profile. Digit **4** now forms at both margins of the limb, and digit **2**'s farthest away. Note when the ectopic source of polarising morphogen is grafted closer to the limb polarising region, then as a higher concentration of morphogen would be encountered in the middle of the limb, the digit **2**'s would not form.

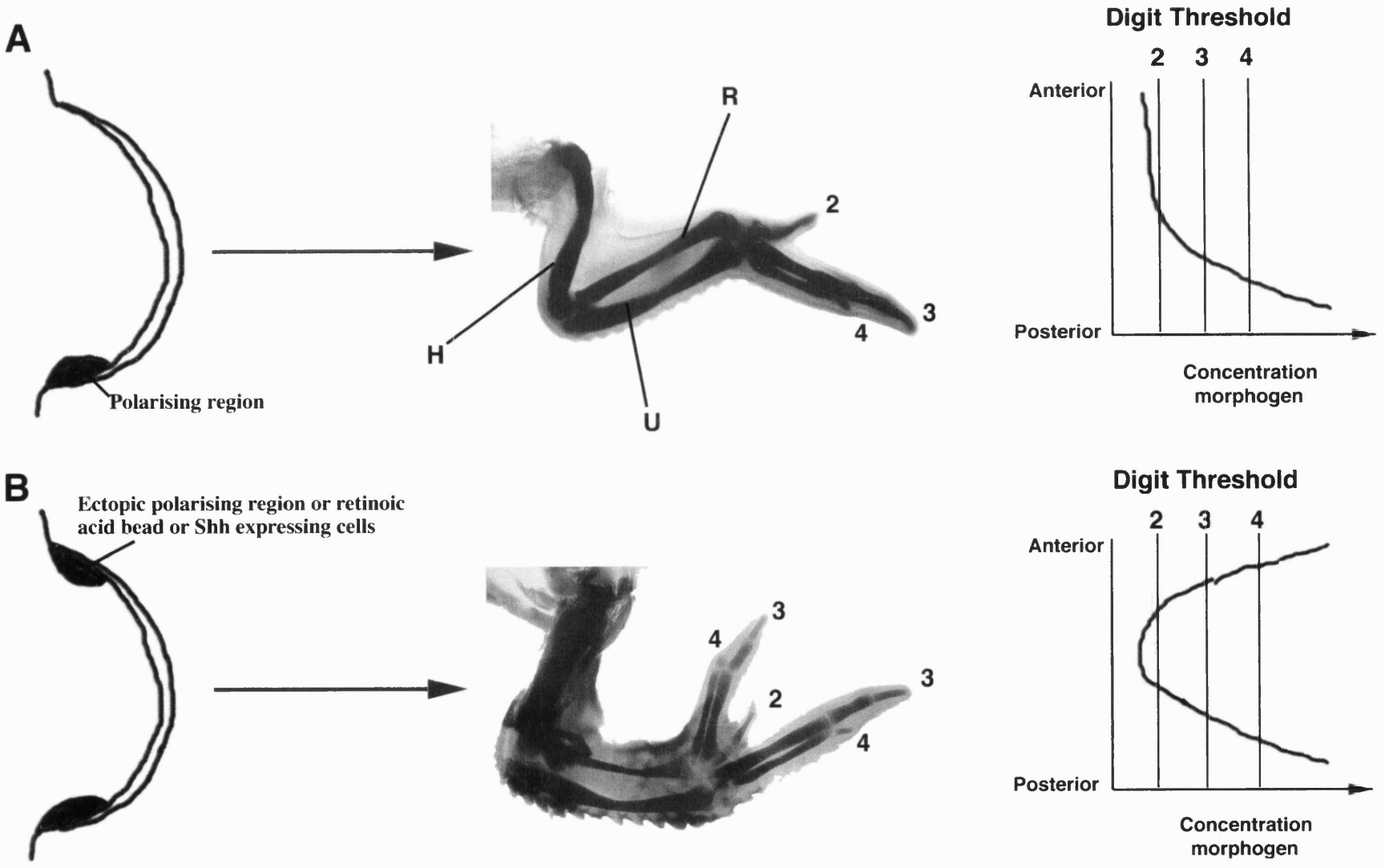
A
Polarising region
R
2
3
4
H
U
Digit Threshold
2 3 4
Anterior
Posterior
Concentration morphogen
B
Ectopic polarising region or retinoic acid bead or Shh expressing cells
3
4
2
3
4
Digit Threshold
2 3 4
Anterior
Posterior
Concentration morphogen

1.1.2.2 *The morphogen model*

The polarising region is thought to assign different positional identities across the antero-posterior axis of the limb. A digit **4** is specified nearest the polarising region and digit **2** is specified the farthest from the polarising region. To explain how this could be accomplished a model was proposed based on a diffusible morphogen being released from the polarising region and diffusing from posterior to anterior in the limb (Fig. 1.2A; Wolpert, 1969; Tickle et al., 1975). The cells along the antero-posterior axis then interpret the concentration of the morphogen and differentiate accordingly. Data consistent with this model was obtained by placing polarising region grafts at different positions along the antero-posterior axis, which gave rise to different combinations of duplicated digits (Tickle et al., 1975). Grafts placed at the anterior of the limb bud gave rise to a full duplication, resulting in a **432234** digit pattern where the duplicated digit **4** is nearest the polarising region graft, hence highest morphogen concentration, and the duplicated digit **2** at the furthest point from the graft, the lowest morphogen concentration (Fig. 1.2B). When the grafted polarising region was placed closer to the limb polarising region, the resulting digit pattern was **4334** (Tickle et al., 1975; see also Wolpert and Hornbruch, 1981). Thus, when the grafted polarising region is closer to the host region this results in a higher concentration of morphogen between the two sources resulting in the loss of digit **2**.

Further evidence for a morphogen based mechanism of antero-posterior digit patterning is shown when the polarising region was exposed to gamma radiation (Smith et al., 1978) or ultra-violet light (Honig, 1982) posterior digits were not specified, suggesting that some cells that produce the morphogen were killed and less morphogen was produced. Moreover, Tickle (1981), showed a graded effect by grafting specific numbers of polarising region cells beneath the anterior apical ridge with 34 cells specifying a digit **2**, 79 cells a digit **3** and 100 a digit **4**.

The molecule responsible for the morphogenetic properties of the polarising region has been the subject of intense investigation. Recently, two different molecules that mimic the effect of the polarising region have been discovered, retinoic acid (Tickle et al., 1982) and the amino terminal product of the *Sonic hedgehog* gene (*Shh*; Riddle et al., 1993; Lopez-Martinez et al., 1995).

1.1.2.3 *Polarising region signals*

Retinoic acid

Retinoic acid, a metabolite of Retinol (vitamin A), when soaked onto filter paper and placed into the anterior of the chick limb bud can mimic the effects of a polarising region and produce full limb duplications (Tickle et al., 1982). Extensive work, in the chick limb, added weight to the idea that retinoic acid could be the signal released from the polarising region which patterns the antero-posterior axis. For example retinoic acid can induce digits in a concentration dependent manner (Tickle et al., 1985) and is present within the limb bud, in an antero-posterior gradient (Thaller and Eichele, 1987, Stratford et al., 1996; for review see Tabin, 1991; Tickle and Eichele, 1994). Moreover, cellular retinoic acid binding proteins (CRABP1 and CRAPB2) which are believed to present retinoic acid to nuclear retinoid receptors (receptors that bind retinoic acid and other metabolites of retinol) have been isolated in limb tissue (for review see Tabin, 1991; Mendelsohn et al., 1992; Tickle and Eichele, 1994). Two families of retinoid receptors have been isolated; the retinoic acid receptors (RARα, RARβ and RARγ) of which all three subtypes are expressed in limb tissue in overlapping expression domains; and the retinoid-X-receptors (RXRα, RXRβ and RXRγ) of which the RXRα and RXRγ subtypes are expressed in limb tissue (for review see Tickle and Eichele, 1994). The retinoid receptors, once activated, are thought to form RAR-RXR heterodimers which activate gene expression by binding to retinoic acid response elements contained in target gene promoter regions (for review see Tabin, 1991; Mendelsohn et al., 1992). Moreover, in mutant mice containing two loss of function retinoic acid receptors, limb defects are observed including syndactyly, a supernumerary anterior digit, shortened limb elements and loss of digits (Lohnes et al., 1994).

However recent work suggests retinoic acid is not the signal mediating the effects of the polarising region (Noji et al., 1991; Wanek et al., 1991; for review see Tabin, 1991). Beads soaked in retinoic acid placed beneath the anterior apical ridge have been shown to induce a polarising region adjacent to the bead, as when tissue adjacent to the bead is removed and grafted to the anterior margin of a new limb, duplicated structures are induced (Wanek et al., 1991; Noji et al., 1991). Furthermore, Noji et al (1991), showed that in response to a retinoic acid bead placed anteriorly, expression of the retinoic acid receptor β is induced in tissue around the bead. This does not happen following polarising region grafts and suggests that retinoic acid may not directly specify digits. It has recently been proposed that retinoic acid has roles in initiation of limb outgrowth and formation of the polarising region (Stratford et al., 1996, 1997).

Sonic hedgehog

Another candidate was identified recently as the mediator of polarising signalling, the amino-terminal product of *Shh* (Sonic hedgehog; Riddle et al., 1993; Lopez-Martinez et al., 1995; for review see Hammerschmidt et al., 1997). *Shh* is a vertebrate homologue of *Drosophila Hedgehog*, a segment-polarity gene involved in *Drosophila* wing patterning (for review see Hammerschmidt et al., 1997). In the *Drosophila* wing imaginal disc, *Hh* is expressed on the posterior side of the antero-posterior compartment boundary. *Hh* signals and activates *Dpp* on the anterior side of the compartment boundary which then patterns the antero-posterior compartment of the wing (for review see Hammerschmidt et al., 1997). Current views suggest that in *Drosophila, Hh* is acting as a short range signal activating *Dpp* to mediate the long range effects of *Hh* (for review see Hammerschmidt et al., 1997). *Shh* transcripts are found in the chick limb from stage 17 until stage 29 and are expressed in the same region as the polarising region (Riddle et al., 1993). In the chick limb, *Shh* is thought to mediate polarising activity as *Shh* expressing cells, beads soaked in *Shh* protein and viral misexpression of *Shh* can induce mirror image digit duplications (Riddle et al., 1993; Lopez-Martinez et al., 1995). Furthermore retinoic acid can activate *Shh* (Riddle et al., 1993; Niswander et al., 1994; Laufer et al., 1994). That *Shh* may mediate the polarising signal and digit patterning is further emphasised by the *Shh* knock out mouse where a rudimentary limb forms but no distal structures develop (Chiang et al., 1996). Furthermore, removal of the entire *Shh* expressing area i.e. the polarising region, in early limb buds results in limbs with pattern defects (Pagan et al., 1996). However it is not clear over what distance *Shh* acts in the vertebrate limb and whether it is a true morphogen or acts via producing cascades of short range signals (for review see Johnson and Tabin, 1997; Hammerschmidt et al., 1997). *Shh* is a protein which requires to be cleaved in order to release the active amino terminal fragment and the inactive carboxy terminal fragment (Lopez-Martinez et al., 1995; Roelink et al., 1995). The *Shh* amino terminal fragment appears to be restricted to the polarising region domain, as shown by immunohistochemistry, suggesting that *Shh* acts short range via inducing cascades of signals (for review see Hammerschmidt et al., 1997; Johnson and Tabin, 1997). *Shh* is also expressed in several other regions of the developing embryo, most notably in the notochord and floor plate that are involved in specifying cell type and pattern in the spinal cord (Echelard et al., 1993; Roelink et al., 1995; for review see Roelink et al., 1996; Hammerschmidt et al., 1997).

Shh is thought to act through a receptor, *Patched* which once bound to *Shh* allows the activation of *Smoothened* (for review see Hammerschmidt et al., 1997; Johnson and Tabin, 1997) initiating a signal transduction pathway. This pathway includes Protein kinase A and *Gli* genes and results in activation of downstream target

genes such as *Bmp-2* in the vertebrate limb, which is a homologue of *Dpp* (Decapentaplegic) in the *Drosophila* wing (for review see Hammerschmidt et al., 1997).

Bmp-2

Bmp-2 is a member of the Bone Morphogenetic Protein family (BMPs) which is part of the TGF-β superfamily of growth factors (for review see Hogan et al., 1996), one of six major families of signalling molecules in development (for review see Wolpert et al., 1998). BMPs are involved in cartilage formation but also have other roles in somite patterning, skeletal development, neural patterning and mesoderm induction (for review see Hogan, 1996) as well as in cartilage formation (Duprez et al., 1996a) and programmed cell death in chick limbs (Yokouchi et al., 1996). *Bmp-2* expression is seen from around stage 17 in the posterior mesenchyme and is observed in the apical ridge (Francis et al., 1994). *Bmp-2* expression co-localises with the polarising region and is activated by *Shh* in the limb bud, showing that *Bmp-2* is involved in the *Shh* signalling pathway (Francis et al., 1994; Laufer et al., 1994). Moreover *Shh* and *Bmp-2* are co-expressed in many diverse sites in mouse embryogenesis, suggesting a functional relationship (Bitgood and McMahon, 1995). However *Bmp-2* does not appear to act alone as the primary polarising signal as *Bmp-2* protein soaked beads or grafts of cells expressing *Bmp-2* cannot induce full duplications of limb pattern (Francis et al., 1994; Duprez et al., 1996b).

1.1.2.4 *Positioning of the polarising region*

What mechanisms confine the polarising region to distinct posterior limb mesenchyme? The region of cells that possesses polarising potential and hence the ability to form a polarising region initially exceeds the region that will actually produce a polarising region (Hornbruch and Wolpert, 1991). Recent work has suggested that retinoic acid and *Hoxb-8* are important in defining the polarising region.

The expression of *Hoxb-8* is observed throughout the presumptive wing and in the interlimb flank region to just above the presumptive leg region at stage 12 (Stratford et al., 1997; Lu et al., 1997). As development proceeds, expression of *Hoxb-8* is reduced so that, by stage 16/17, *Hoxb-8* expression is located in interlimb flank mesenchyme up to somite 18 (Stratford et al., 1997; Lu et al., 1997). The expression of *Hoxb-8* marks exactly the extent of polarising potential throughout early development as mapped by Hornbruch and Wolpert (1991). By stage 18, *Hoxb-8* expression has gone completely from the wing, which is the same time as the polarising region is induced and *Shh* expression is strongly observed (Stratford et al.,

1997; Lu et al., 1997). Stratford et al (1997) and Lu et al (1997), suggest that *Hoxb-8* marks the extent of polarising potential. They further suggest that retinoic acid is required for the establishment of the polarising region and *Hoxb-8* expression. and beads of retinoic acid placed anteriorly in chick limb buds induce *Hoxb-8* expression in a dose responsive manner (Stratford et al., 1997; Lu et al., 1997). Moreover retinoid antagonists and disulphiram treatment prevent polarising region formation and prevent *Hoxb-8* expression (Stratford et al., 1997; Lu et al., 1997). These results suggest that retinoic acid induces expression of *Hoxb-8* which marks polarising potential within the embryo and plays a role in localising the polarising region and hence establishing initial antero-posterior asymmetry within the limb. The position of the polarising region is restricted to the posterior margin as polarising activity can only be induced in cells that have expressed *Hoxb-8* (Stratford et al., 1997; Lu et al., 1997). It is likely that inhibitory signals from the apical ridge and from the newly formed polarising region inhibit *Hoxb-8* expression in polarising region cells which further restricts of expansion of the polarising region (Stratford et al., 1997). Moreover, it is likely that negative signals in the anterior mesenchyme may prevent or suppress *Shh*/polarising region expression, thus further limiting the extent of the polarising region. Ectopic expression of *Shh* (and *Fgf-4*) occurs in polydactylous mouse mutants such as *Hemimelic extra toes* (*Hx*), *Extra toes* (*Xt*) and *Recombination induced mutant 4* (*Rim4*; Masuya et al., 1995, 1997). This suggests the normal products of these genes may act as transcriptional repressors of *Shh* activity, particularly as the molecular basis of *Xt* is due to the loss of *Gli-3* expression (Hui and Joyner, 1993) which is implicated in repression of *Shh* signalling (Marigo et al., 1996; see also Masuya et al., 1995).

1.1.3 Proximo-distal axis

1.1.3.1 *Apical ridge and the control of outgrowth and pattern*

Patterning of the proximo-distal axis of the limb (shoulder to digit tips; Fig. 1.1, 1.2A) is under the control of the apical ectodermal ridge, which is essential for distal outgrowth. The importance of the apical ridge is shown by removing the apical ridge which results in a truncated limb in which distal structures are missing (Saunders, 1948; Summerbell, 1974). When the apical ridge is removed at progressively later stages of limb development, the state of truncation gets less severe. For example, at stage 20 only a humerus forms but at stage 26 the whole limb, except the distal parts of the digits, develops (Saunders, 1948; Summerbell, 1974; Rowe and Fallon, 1981, 1982). By stage 28, ridge removal does not affect limb

pattern, suggesting that by this stage the entire limb pattern has been irreversibly laid down (Summerbell, 1974). Ridge removal seems to halt proximo-distal development and whatever was patterned or specified at the time of ridge removal will develop but nothing more distally.

1.1.3.2 *Progress zone model*

The progress zone (Summerbell et al., 1973) is a region of mesenchyme directly beneath the apical ridge that is proliferative and undifferentiated. The model for proximo-distal patterning proposes that progress zone cells are rapidly dividing and that the length of time that a cell remains within the progress zone determines its eventual fate (Summerbell et al., 1973). Cells leaving the progress zone early would be specified to contribute to proximal structures and cells leaving the progress zone late would contribute to distal structures. The mechanism by which cells know how long they have been in the progress zone and hence what structures to form could be by recording the number of cell divisions they have undergone (Summerbell et al., 1973; Lewis, 1975). The progress zone is proposed to be maintained by the apical ridge. Hence apical ridge removal would cause the loss of the progress zone and cells would differentiate according to the structure being specified at the time. The apical ridge and the progress zone therefore control patterning along the proximo-distal axis.

1.1.3.3 *Apical ridge signalling*

The apical ectodermal ridge forms at the border between dorsal and ventral ectoderm just after the bud is first seen. The apical ridge is thought to be induced by a mesenchymal factor as prospective wing mesenchyme grafted to a host flank between stages 12 and 17 results in a normal limb with an apical ridge (Saunders and Reuss, 1974). An alternative theory was postulated recently where a mesenchymal factor makes ectoderm competent to produce a ridge which actually occurs under the control of the dorsal-ventral ectoderm (Altabef et al., 1997). Once the apical ridge has been induced it is maintained throughout development by a mesenchymal factor, as shown by the apical tip reorientation and barrier experiments of Saunders and Gasseling (1963).

Several signals emanating from the apical ridge have been proposed to have a role in the maintenance of the progress zone and in proximo-distal signalling (for review see Tickle and Eichele, 1994). A number of Fibroblast Growth Factors (FGF) are expressed in the apical ridge and have been shown to be involved in limb initiation, controlling limb outgrowth and proximo-distal patterning as well as maintaining the

progress zone (Niswander et al., 1993; Fallon et al., 1994; Cohn et al., 1995; Crossley et al., 1996, Vogel et al., 1996; Ohuchi et al., 1997). Furthermore, *Bmp-2* and *Bmp-4* are expressed in the apical ridge, in addition to the subapical mesenchyme, and may have roles in maintaining apical ridge signalling and activity (Francis et al., 1994).

The FGF family consists of at least ten members (FGF 1-10; Ohuchi et al., 1997) all of which are highly conserved and have diverse functions throughout development including growth, differentiation and migration. FGFs bind to FGF receptors, which are transmembrane receptor tyrosine kinases (for review see Wilkie et al., 1995). Four FGF receptors are known (FGFR1-4; for review see Wilkie et al., 1995; Webster and Donoghue, 1997). FGFs bind to the receptors, in concert with heparan sulphate proteoglycans, causing the receptors to dimerise, which leads to phosphorylation of the kinase domain of the receptor and activation of downstream targets (for review see Wilkie et al., 1995; Webster and Donoghue, 1997). Mutations in FGF receptors have shown that they have essential functions in bone and limb development. For example, mutations in FGFR3 are responsible for human achondroplasia and mutations in FGFR2 cause hand and foot defects in humans (for review see Wilkie et al., 1995; Yamaguchi and Rossant, 1995; Webster and Donoghue, 1997). Of the FGFRs, only FGFR1 and FGFR2 are expressed in the limb from early limb bud stages. FGFR1 is expressed throughout limb mesenchyme, including the progress zone and FGFR2 is expressed in the apical ridge and ectoderm, although one isoform (FGFR2c) is expressed in subapical mesenchyme (Peters et al., 1992; see also Xu et al., 1998). Furthermore in FGFR1 loss of function mice, the limb is patterned normally but growth is retarded suggesting the progress zone may be affected (Deng et al., 1997). In contrast, in FGFR2 loss of function mice, limb initiation is blocked and a limbless embryo is obtained (Xu et al., 1998) suggesting FGFR1 and FGFR2 have distinct functions in limb bud outgrowth and development.

At least four FGF family members play important roles in the chick limb; FGF-2, -4 and -8 which are expressed in the apical ridge and play important roles in the outgrowth of the proximo-distal axis of the limb and FGF-10 which is expressed in the mesenchyme and may maintain the apical ridge. FGF-2, FGF-4 and FGF-8 can bind to FGFR1 or FGFR2 and FGF-10 binds to FGFR2 (see Crossley and Martin, 1995; Mahmood et al., 1995; Vogel et al., 1996; Xu et al., 1998). I shall discuss each of these FGFs in turn.

FGF-2

Fgf-2 (mRNA and protein) is initially expressed at stage 16 in dorsal and apical ectoderm and later in dorsal ectoderm, apical ridge and dorsal and apical mesenchyme of the developing limb bud until stage 25 (Savage et al., 1993; Fallon et

al., 1994). Following apical ridge removal, FGF-2 soaked beads can rescue limb pattern (Fallon et al., 1994) and FGF-2 is able to maintain polarising activity in cultured posterior limb cells, which, without FGF-2 would lose polarising ability (Anderson et al., 1993). Furthermore, in experiments where anterior limb bud mesenchyme was dissociated and cultured alone, polarising activity was observed 24 hours later. When the experiment was repeated with FGF-2 also added up to 24 hours following the dissociation and culturing, polarising activity was not induced earlier than 24 hours. However FGF-2 added 24 hours after dissociation and culturing maintained polarising activity (Anderson et al., 1994). This suggests that FGF-2 could be an endogenous apical ridge signal that normally inhibits anterior cells from forming a polarising region and perhaps inhibits cell differentiation (Anderson et al., 1994). FGF-2 has also been postulated to have a potential role in the initiation of the limb, but the fact that its expression is so widespread and that FGF-2 expression is not seen until stage 16 argues against this (Savage et al., 1993; Fallon et al., 1994). FGF-2 expression in the apical ridge and apical mesenchyme may maintain the progress zone in early limb outgrowth, however the progress zone remains in the limb for several stages after the loss of FGF-2 expression at stage 25.

FGF-4

Fgf-4 transcripts are found in the posterior apical ridge from stage 18. As development proceeds, *Fgf-4* transcripts come to fill the majority of the ridge and remain until stage 26 (Niswander and Martin, 1992; Duprez et al., 1996b). FGF-4 can maintain and rescue limb outgrowth following apical ridge removal (Vogel and Tickle, 1993; Niswander and Martin, 1993), and maintain cell proliferation in culture (Vogel and Tickle, 1993). FGF-4 may be signalling to posterior mesenchyme to increase the proliferation rate above that of the anterior (see also Mahmood et al., 1995). FGF-4 like FGF-2 can maintain polarising activity in culture and following ridge removal (Vogel and Tickle, 1993) but FGF-4 is unlikely to be the signal that maintains the progress zone early in development as FGF-4 transcripts are only seen in posterior ridge but might maintain the progress zone later in development.

FGF-8

Fgf-8 transcripts are detected from stage 13 in intermediate mesoderm, which, by stage 15, is found opposite the prospective wing region. By stage 16 *Fgf-8* is also expressed in the ectoderm overlying the prospective limb mesenchyme (Heikinheimo et al., 1994; Mahmood et al., 1995; Crossley et al., 1996; Vogel et al., 1996). *Fgf-8* is eventually expressed throughout the apical ridge and is still expressed in the ridge when the ridge starts to regress at stage 29 (Crossley et al., 1996). The spatial and temporal features of *Fgf-8* expression suggest very strongly a role in maintenance of the progress zone. Furthermore, FGF-8 can rescue limb outgrowth following apical

ridge removal and rescue *Shh* expression (Crossley et al., 1996; Vogel et al., 1996). FGF-8 has been strongly implicated in initiation of limb bud outgrowth and as the endogenous apical ridge factor because FGF-8 expression marks the entire presumptive apical ridge before limb outgrowth is observed (see later; Crossley et al., 1996; Vogel et al., 1996; for review see Johnson and Tabin, 1997).

1.1.3.4 *Mesenchyme signalling and apical ridge maintenance*

FGF-10 expression is observed from stage 15 throughout the limb mesenchyme including the progress zone abutting the apical ridge up to stage 28 (Ohuchi et al., 1997). FGF-10 can rescue limb outgrowth following apical ridge removal and rescue *Shh* expression (Ohuchi et al., 1997). FGF-10 has been postulated to have 3 main roles in limb development. First a role in limb initiation in which FGF-10 initiates outgrowth of the limb from the flank. Since the expression of FGF-10 is throughout the prospective limb mesenchyme at stage 15 but not in flank outside the limb forming regions, it is possible that FGF-10 could be the signal allowing outgrowth of the limb by maintaining the proliferation rate in presumptive limb tissue (Searls and Janners, 1971; Ohuchi et al., 1997; for review see Johnson and Tabin, 1997). Second, FGF-10 may have a role in inducing an apical ridge, since addition of FGF-10 to a ridgeless limb rescues the limb and also induces FGF-8, which is normally expressed in the apical ridge (Ohuchi et al., 1997). Third, FGF-10 expression is apical ridge dependent and may set up a positive feedback loop with the apical ridge to maintain the ridge once it is established which hence also maintains the progress zone (Ohuchi et al., 1997; see also Xu et al., 1998).

1.1.3.5 *Genes involved in maintenance of the Progress zone*

Along with members of the FGF family (see above) other genes have been postulated to have roles in maintenance of the progress zone (see Tickle and Eichele, 1994). *Msx-1* is a homeobox containing gene, related to the *Drosophila* gene *msh* (*muscle segment homeobox*; Robert et al., 1989; Davidson et al., 1991; Yokouchi et al., 1991a; for review see Davidson, 1995). *Msx* genes are found expressed not only in the limb but also in neural crest, cranial placodes and teeth (for review see Davidson, 1995). Initially transcripts for *Msx-1* are found throughout the limb bud mesenchyme but by stage 22 expression is restricted to the distal mesenchyme underlying the apical ridge. Later in development, expression of *Msx-1* is restricted to interdigital regions (Robert et al., 1989; Yokouchi et al., 1991a). The expression pattern of *Msx-1* is suggestive of a role in the maintenance of the progress zone particularly as *Msx-1*

expression is lost following apical ridge removal (Davidson et al., 1991). Moreover, muscle cells that normally differentiate in culture, were prevented from doing so, remaining in a proliferative state after being transfected with *Msx-1* suggesting that *Msx-1* promotes proliferation and inhibits cell differentiation, like cells in the progress zone (Song et al., 1992). Furthermore *Msx-1* has been shown to play a role in regeneration following digit tip amputation in the mouse embryo (for review see Muneoka and Sassoon, 1992; Reginelli et al., 1995).

Slug a zinc finger transcription factor, has also been proposed to have a role in maintenance of the progress zone (Buxton et al., 1997; Ros et al., 1997). Expression of *Slug* is first observed in mesenchyme at stage 19 in posterior progress zone. As development proceeds expression expands distally and anteriorly to occupy the entire progress zone from stage 22. *Slug* expression is found interdigitally from stage 28 (Buxton et al., 1997; Ros et al., 1997). *Slug* expression is apical ridge dependent, expression is lost following ridge removal however expression can be rescued by application of FGF-4 following ridge removal. This has led to the suggestion that *Slug* is involved in progress zone maintenance by transcriptionally repressing differentiation and maintaining cells in a proliferative state (Buxton et al., 1997; Ros et al., 1997).

1.1.4 Dorsal-ventral axis

Ectoderm signalling has been implicated in dorsal-ventral axis patterning. Reversal of the ectoderm by 180° about the dorsal-ventral axis in limbs from stage 16, causes the inversion of dorsal-ventral polarity of the distal limb muscle, tendon and cartilage elements; proximal limb develops in accordance with mesoderm polarity prior to ectoderm rotation (MacCabe et al., 1974; Geduspan and MacCabe, 1987, 1989; Akita, 1996). Very early ectoderm reversals, up to stage 15, results in normal dorsal-ventral pattern proximally and distally, suggesting that some mesenchymal factor induces dorsal-ventral information within the ectoderm between stage 14 and 15 which then controls mesenchymal pattern (Geduspan and MacCabe, 1987, 1989). Michaud et al (1997) suggest that a mesenchymal factor emitted from the somites dorsalises ectoderm. Furthermore they also propose that a signal from the lateral somatopleure may pattern and determine ventral ectoderm. That dorsal and ventral ectoderm release signals to pattern the dorsal-ventral axis was shown by grafting an apical ridge to the dorsal surface of a host limb bud, which induces an ectopic limb with a bi-dorsal character (Saunders et al., 1976). Moreover an apical ridge grafted to the ventral surface of a limb bud also induces an ectopic limb, but it has a bi-ventral character (Saunders et al., 1976; see also Michaud et al., 1997).

Signals involved in dorsal-ventral limb patterning and apical ridge patterning have recently been identified (for review see Zeller and Duboule, 1997; Irvine and Vogt, 1997; Johnson and Tabin, 1997; Fig. 1.3). *Wnt-7a*, a secreted signalling molecule, is expressed throughout the dorsal ectoderm (Dealy et al., 1993; Parr and McMahon, 1995; Yang and Niswander, 1995), which activates *Lmx-1*, a LIM homeodomain containing factor, in the dorsal mesenchyme (Riddle et al., 1995; Vogel et al., 1995b; Fig. 1.3A). More recently *Radical fringe* (*R-fri*), a vertebrate homologue of *Drosophila Fringe* a secreted signalling molecule related to glycosyltransferases, was also shown to be expressed in dorsal ectoderm and the apical ridge (Laufer et al., 1997; Rodriguez-Esteban et al., 1997; Yuan et al., 1997; Fig. 1.3A). *Engrailed-1* (*En-1*), a transcription factor, is expressed in ventral ectoderm and plays a role in dorsal-ventral pattern but also apical ridge positioning (Fig. 1.3B; Loomis et al., 1996; Logan et al., 1997). By gain and loss of function experiments the function of these molecules has been ascertained. *Wnt-7a* and *Lmx-1* can dorsalise ventral mesoderm, which also occurs in *En-1* loss of function mutants (Riddle et al., 1995; Vogel et al., 1995b; Loomis et al., 1996). In contrast, in *Wnt-7a* loss of function mutants, ventralisation of dorsal mesenchyme is seen (Parr and McMahon, 1995). It is likely that *Wnt-7a* is a dorsal signal activating *Lmx-1* in the mesenchyme and thus instructing dorsal mesenchyme patterning. *En-1* represses *Wnt-7a* expression keeping *Wnt-7a* restricted to dorsal ectoderm and also as a consequence restricting *Lmx-1* to dorsal mesenchyme thus, allowing the correct patterning of the dorsal-ventral axis (Loomis et al., 1996; Logan et al., 1997).

Positioning of the apical ridge

The apical ridge is initiated by a mesenchymal signal (Saunders and Reuss, 1974; see also Altabef et al., 1997), potentially FGF-10 (Ohuchi et al., 1997). Fate mapping studies in pre-limb bud embryos have shown that the apical ridge forms at the border of dorsal and ventral ectoderm (Altabef et al., 1997; Michaud et al., 1997) originating from progenitors widely spread amongst non-ridge cells in early presumptive dorsal and ventral ectoderm (Altabef et al., 1997).

Prior to apical ridge formation at around stage 17-18, expression of *En-1* is observed in ventral ectoderm and expression of *Wnt-7a* and *R-fri* in dorsal ectoderm. The interface between *R-fri* expressing and *R-fri* non-expressing cells is precisely where the apical ridge forms and *En-1* is thought to be vital in restricting *R-fri* to the dorsal ectoderm in pre-ridge limbs and to the dorsal ectoderm and ridge once the ridge has been established (Fig. 1.3B; Laufer et al., 1997; Rodriguez-Esteban et al., 1997). When the apical ridge is formed *R-fri* is expressed throughout and *En-1* is expressed only in the ventral part (Fig. 1.3A). Elimination of *R-fri* expression, by *En-1*

Figure 1.3

Adapted from Johnson and Tabin (1997). **A**) Diagram of a longitudinal view of the dorsal-ventral axis showing gene expression along the dorsal-ventral axis. *Wnt-7a* is expressed in dorsal ectoderm and *R-fri* (Radical fringe) is expressed in dorsal ectoderm and throughout the apical ridge. *Lmx-1* is expressed in dorsal mesenchyme and is activated by *Wnt-7a*. *En-1* (Engrailed-1) is expressed in ventral ectoderm and ventral apical ridge. **B**) Diagram showing the genetic interactions involved in apical ridge formation and dorsal-ventral polarity which both involve *En-1*. *En-1*, in ventral ectoderm restricts expression of *Wnt-7a* and *R-fri* to dorsal ectoderm. *Wnt-7a* activates *Lmx-1* in dorsal mesenchyme which specifies dorsal pattern. The apical ridge forms at the juxtaposition of *R-fri* expressing and *R-fri* non-expressing cells.

A

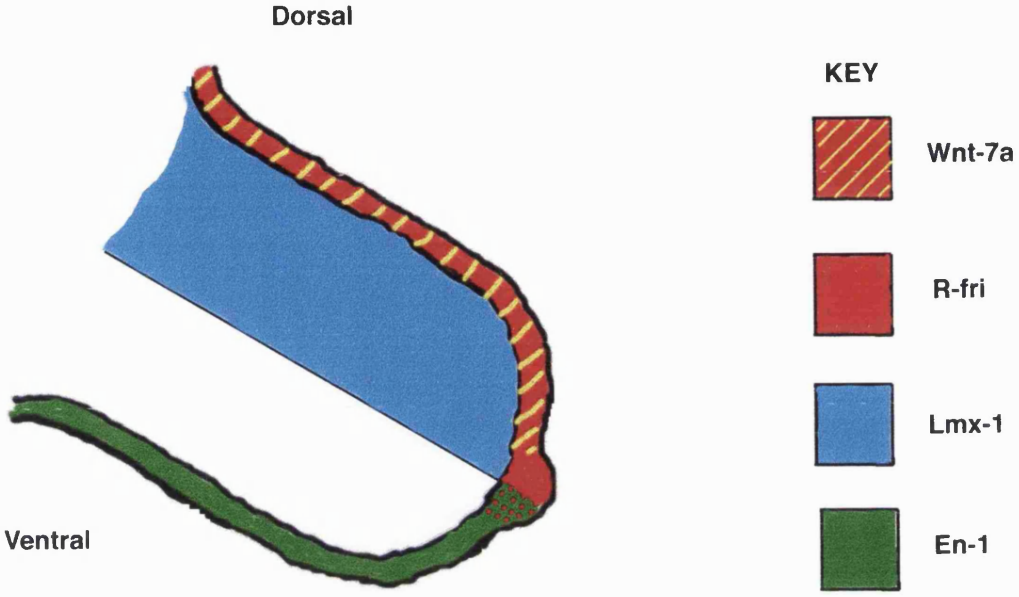
Dorsal
Ventral
KEY
Wnt-7a
R-fri
Lmx-1
En-1

B

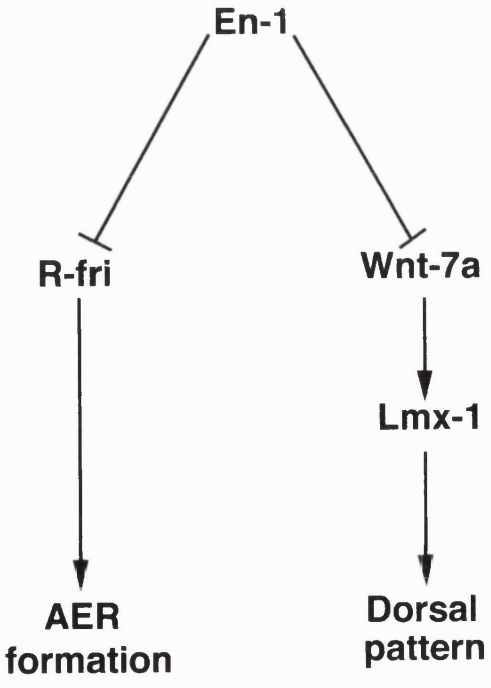
En-1
R-fri
Wnt-7a
Lmx-1
AER formation
Dorsal pattern

misexpression (Logan et al., 1997), or the ectopic expression of *R-fri* in ventral ectoderm results in the formation of ectopic apical ridges at the boundaries of *R-fri* expressing and non-expressing cells, which may mediate its effect via the *Notch* signalling pathway (Laufer et al., 1997; Rodriguez-Esteban et al., 1997). Moreover, in loss of function, *En-1* mutants dorsalisation of mesenchyme occurs and the apical ridge is flattened and extended ventrally suggesting *En-1* is essential in restricting the position of ventral apical ridge (Loomis et al., 1996; for review see Zeller and Duboule, 1997). These data suggest that the apical ridge is initiated by a mesenchymal factor, possibly FGF-10 inducing ridge precursors in dorsal and ventral ectoderm. The precursors are positioned to form the apical ridge at the juxtaposition of *R-fri* expressing and non-expressing cells which requires *En-1* to restrict *R-fri* expression to dorsal ectoderm (Fig. 1.3A, B; for review see Zeller and Duboule, 1997; Johnson and Tabin, 1997; see also Altabef et al., 1997).

1.1.5 Interdependence of limb signalling pathways

Specific signals are now known to operate in each of the three limb axes; antero-posterior axis by *Shh* from the polarising region; dorsal-ventral axis by *Wnt-7a* from the dorsal ectoderm and the proximo-distal axis by FGF from the apical ridge. However, recent evidence strongly suggests interdependence between the three axes (Fig. 1.4). For example, expression of *Fgf-4* in posterior ridge suggests it may have some role in maintaining the polarising region. Apical ridge removal results in the loss of *Shh* expression, but FGF-4 beads can rescue *Shh* expression (Niswander et al., 1994; Laufer et al., 1994). Furthermore, ectopic *Shh* expression in anterior limb induces FGF-4 expression in the overlying apical ridge. These results suggest that *Shh* and FGF-4 are part of a feedback loop co-ordinating growth and patterning (Fig. 1.4). Once *Shh* is induced in the polarising region, then this induces *Fgf-4* expression in the posterior apical ridge and FGF-4 is secreted to maintain *Shh* expression in the polarising region but also maintain the posterior progress zone (Niswander et al., 1994; Laufer et al., 1994). Furthermore, *Wnt-7a* is thought to not only play a role in regulating dorsal-ventral pattern but also in antero-posterior pattern. Dorsal ectoderm removal results in the loss of *Wnt-7a* and loss of *Shh* expression causing not only double ventral distal limb structures but also loss of posterior skeletal elements (Yang and Niswander, 1995). Furthermore, *Wnt-7a* knockout mice show reduced *Shh* and FGF-4 expression and loss of posterior structures (Parr and McMahon, 1995). *Shh* expression can be maintained following application of a *Wnt-7a* source (Yang and Niswander, 1995) but *Shh* can not be activated by *Wnt-7a*. These data suggest that *Wnt-7a* is required to maintain *Shh* expression in the polarising region. In summary,

Figure 1.4

Interdependence of signalling pathways maintains limb outgrowth

Summary diagram showing a stage 21 limb bud, outlining the interdependence of the antero-posterior (*Shh*), proximo-distal (FGF) and dorsal-ventral (*Wnt-7a*) signalling pathways. *Shh*, FGF and *Wnt-7a* are associated with patterning along a single axis respectively, however affecting expression of any single factor will lead to defects in other axes i.e. loss of *Wnt-7a* expression causes dorsal patterning defects but also loss of posterior structures due to reduced *Shh* and FGF (see Yang and Niswander, 1995).

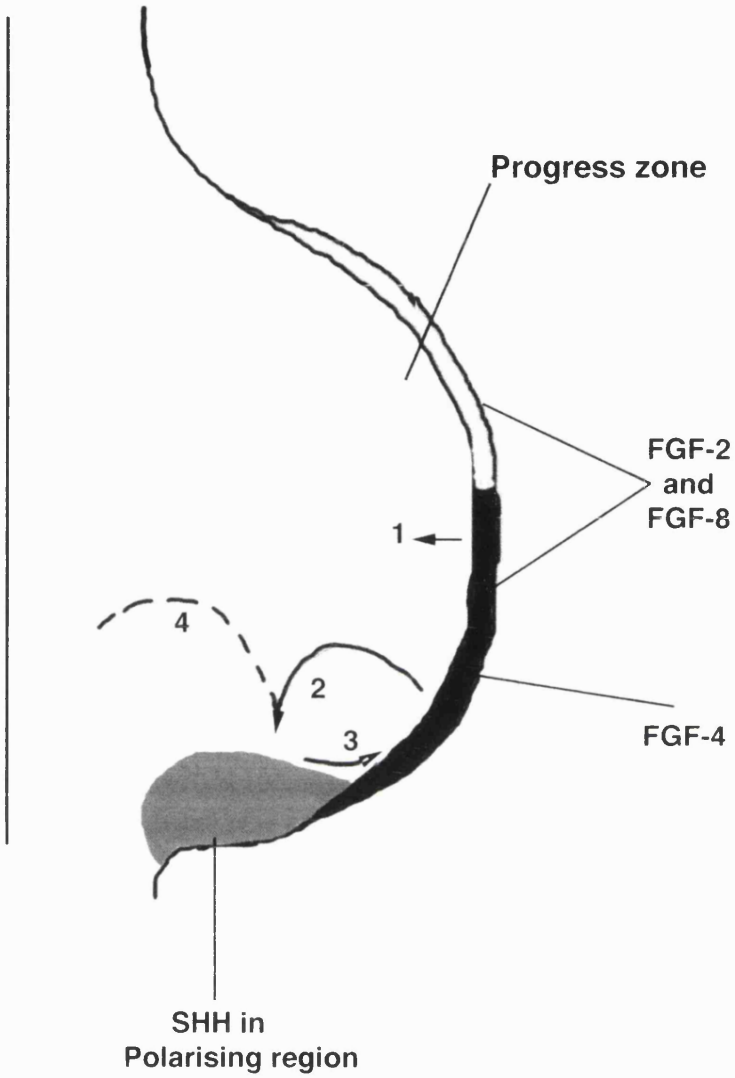

1. FGFs from the apical ridge help maintain the progress zone

2. FGF-4 from the posterior ridge maintains the polarising region and SHH expression

3. SHH maintains FGF-4 expression and the apical ridge

4. Wnt-7a from the dorsal ectoderm maintains SHH and polarising region which enables downstream target genes to be activated, such as Bmp-2 and HoxD members

the polarising region is found at the position where *Shh*, *Fgf-4* and *Wnt-7a* signals are present, in the posterior-distal mesenchyme (Fig. 1.4; Yang and Niswander, 1995).

1.1.6 *Hox* genes

Once the limb has been initiated and the axes of the limb have been established providing positional information, target genes acting in response to the signals from the three axes control growth, differentiation and pattern. Examples of such target genes include the *Hox* genes which are homeobox containing genes, of which some are also involved in axial specification as well as later morphogenesis.

Hox genes encode transcription factors containing a conserved DNA binding domain consisting of 61 amino-acids. *Hox* genes are homologues of the *Drosophila Homeotic* complex (*Hom-C*) which is made up of two parts; the *Antennapaedia* complex (*Antp-C*) and the *Bithorax* complex (*Bx-C*; for review see Duboule and Morata, 1994; Krumlauf, 1994). The *Hom-C* complex in *Drosophila* controls cell and segment identity and fate. Mutations in such genes can lead to homeotic transformations (for review see Krumlauf, 1994).

Hox genes, of which there are around 40, are clustered in four complexes termed *HoxA*, *HoxB*, *HoxC* and *HoxD* (for review see Krumlauf, 1994). Each cluster contains 9-11 genes, spaced around 200 base pairs apart. When the clusters are aligned, sequence similarities can be seen between paralogous genes, where the paralogues are more related than the neighbouring gene in the cluster i.e. *Hoxd-13* and *Hoxa-13* are more related than *Hoxd-13* and *Hoxd-11*. It has been suggested that gene duplication and cluster duplication events from a single ancestral cluster occurred in vertebrates to produce the four complexes, and thus allowed increased developmental complexity (Ruddle et al., 1994; Duboule, 1994; but also see Meyer, 1998).

Activation and expression of *Hox* genes within a cluster follows the rules of temporal and spatial colinearity (Duboule, 1992, 1994; Duboule and Tabata, 1994; Krumlauf, 1994). Temporal colinearity is when the genes are expressed in the order of their position in the *Hox* complex such that 3' (anterior) located genes are activated before their more 5' (posterior) neighbour. Spatial colinearity is the phenomenon in which 3' (anterior) positioned genes are expressed up to more anterior positions in the embryo than 5' (posterior) genes, such that 5' gene expression domains are nested within the 3' gene expression domains, hence their are large areas of overlap between *Hox* genes (Duboule, 1992, 1994; Duboule and Tabata, 1994; for example see Fig. 1.5). *Hox* genes show dynamic patterns of expression, particularly in the limb where *Hox* genes have a characteristic early phase of expression followed by a later phase of

expression. The pattern of the late expression phase can be very different to the early expression domain (Nelson et al., 1996). Another important consideration in interpreting patterns of *Hox* gene expression is that a 5' (posterior) *Hox* gene is dominant over its more 3' (anterior) neighbour i.e. 5' genes repress 3' genes, so that, despite the overlapping expression domains, different *Hox* genes are dominant in different positions within the embryo or limb. This is termed 'posterior prevalence' (Duboule, 1994; see also van der Hoeven et al., 1996; Goff and Tabin, 1997).

1.1.6.1 *HOXD* genes

Members at the 5' end of the *HoxD* complex, *Hoxd-9*, *d-10*, *d-11*, *d-12* and *d-13*, follow the rules of temporal and spatial colinearity and are expressed across the antero-posterior axis of the vertebrate limb (Dolle et al., 1989; Izpisua-Belmonte et al., 1991; Nelson et al., 1996). In the chick wing bud, the expression of the 5' *HoxD* genes is centered around the posterior of the limb and *Hoxd-9* is the first to be expressed around stage 16. Over the next 3 hours expression of *Hoxd-10* to *Hoxd-12* are activated sequentially in progressively restricted domains and *Hoxd-13* expression is first observed restricted to posterior distal mesenchyme from stage 18/19, tightly nested within the expression domains of the other 5' *HoxD* gene expression domains (Fig. 1.5A; Izpisua-Belmonte et al., 1991; Nelson et al., 1996). As development proceeds, the expression of the 5' *HoxD* genes is elaborated such that by stage 26 *Hoxd-13* expression fills the majority of the prospective hand plate, and is not detected elsewhere; expression of *Hoxd-10*, *d-11* and *d-12* occupy most of the forearm and handplate. The genes no longer remain in nested domains in the hand plate as *Hoxd-13* has the most anterior distal extent of expression. *Hoxd-10*, *-11* and *-12* transcripts all occupy the same spatial domain within the hand plate and share an anterior distal limit of expression just posterior to that of *Hoxd-13* (Fig. 1.5A; Nelson et al., 1996). However in the forearm *Hoxd-10*, *-11* and *-12* transcripts remain expressed in nested domains i.e. *Hoxd-12* within that of *Hoxd-11* (Fig. 1.5A). The areas of overlap between the expression domains of *HoxD* genes may be important for their functioning. For example, in the early distal forelimb bud, the expression domain of *Hoxd-13* is within that of *Hoxd-12* which is within that of *Hoxd-11*. According to posterior prevalence where overlap of all three genes occurs, *Hoxd-13* will be dominant. Likewise, more proximally in the early forelimb bud where overlap occurs between *Hoxd-12* and *Hoxd-11*, *Hoxd-12* will be dominant. In this manner differential growth of the limb elements could be achieved (Duboule, 1994, 1995). Moreover, the overlapping of the *HoxD* genes may confer some redundancy between *HoxD* genes. Consistent with this idea loss of *Hoxd-11* only results in minor defects

Figure 1.5

A) 5' *HoxD* genes are expressed in nested domains in the early limb bud, where the more 'posterior' gene is nested within that of its 'anterior' neighbour. Hence at stage 20 *Hoxd-13* is restricted to posterior-distal mesenchyme and is within the *Hoxd-12* domain which is nested within that of *Hoxd-11*. As development proceeds *HoxD* gene expression changes so at stage 26 in the hand plate the *HoxD* genes are no longer in nested domains. *Hoxd-13* now fills the majority of the prospective hand plate and the anterior-distal limit of *Hoxd-13* expression is now more anterior than the anterior distal limit of expression of *Hoxd-10*, *-11*, *-12* which occupy the same spatial domain in the hand plate. However *Hoxd-10*, *Hoxd-11* and *Hoxd-12* remain in nested expression domains in the forearm. **B**) At stage 21 5' *HoxA* genes, like the 5' *HoxD* genes, are initially expressed in nested domains. At stage 26, *Hoxa-13* is expressed throughout the entire prospective hand plate and is no longer nested within the expression domains of *Hoxa-10* and *Hoxa-11* which are both restricted to the prospective forearm region.

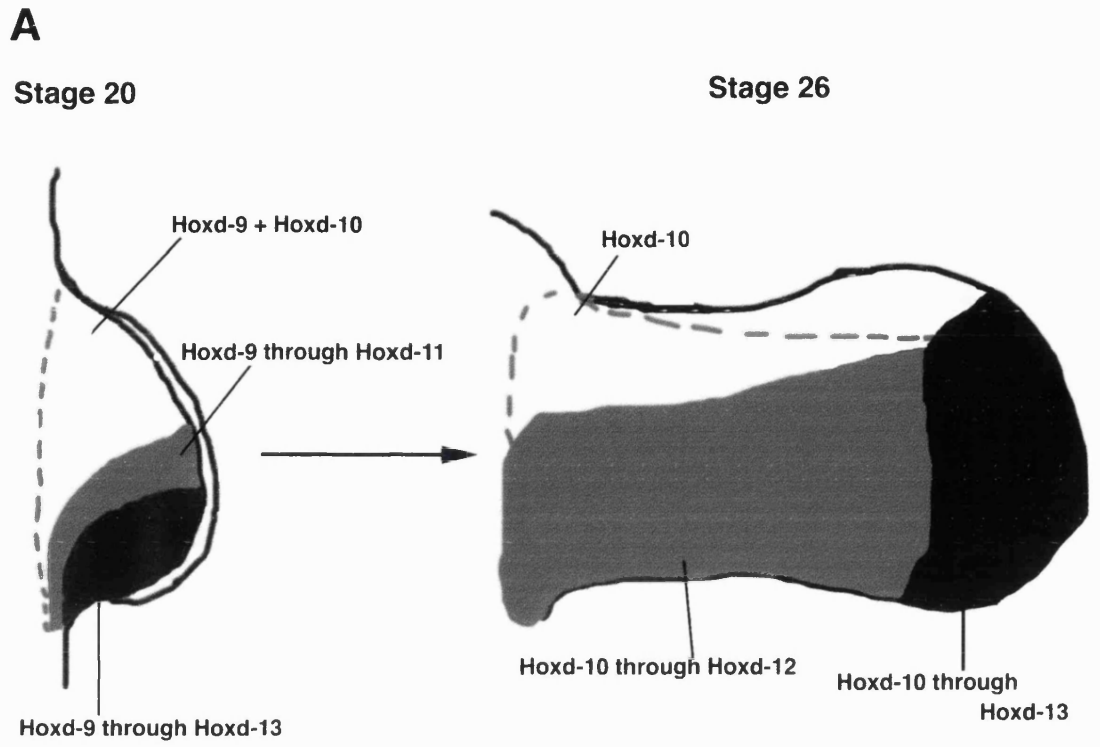
A
Stage 20
Stage 26
Hoxd-9 + Hoxd-10
Hoxd-9 through Hoxd-11
Hoxd-9 through Hoxd-13
Hoxd-10
Hoxd-10 through Hoxd-12
Hoxd-10 through
Hoxd-13

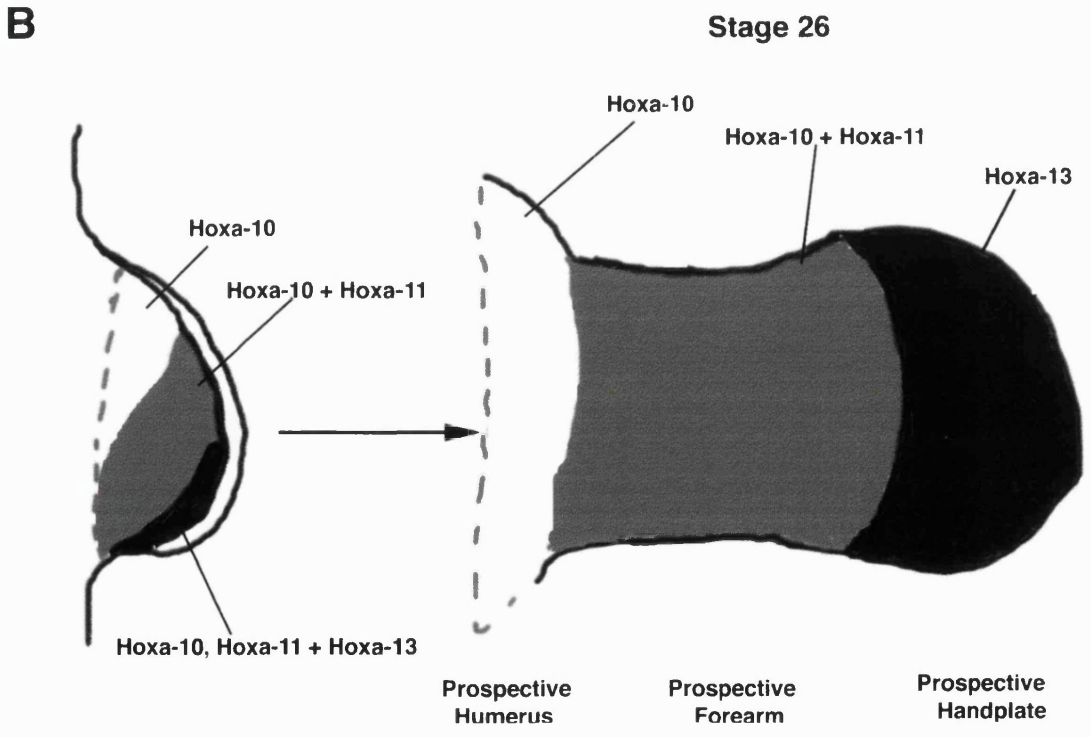
B
Stage 26
Hoxa-10
Hoxa-10 + Hoxa-11
Hoxa-10, Hoxa-11 + Hoxa-13
Hoxa-10
Hoxa-10 + Hoxa-11
Hoxa-13
Prospective
Humerus
Prospective
Forearm
Prospective
Handplate

in forearm pattern, despite the expression domain of *Hoxd-11* being throughout the forearm (Davis and Capecchi, 1994), suggesting that other *Hox* genes may functionally replace *Hoxd-11*. Indeed loss of both *Hoxa-11* and *Hoxd-11* results in the loss of the forearm, suggesting that redundancy actually exists between paralogous *Hox* genes and that, in the *Hoxd-11* knockout, *Hoxa-11* was able to compensate (Davis et al., 1995; for review see Ruji and Chambon, 1997).

Activation of 5' *HoxD* genes can occur in response to a signal(s) from the polarising region as shown by ectopic *HoxD* gene expression following polarising region grafts (Izpisua-Belmonte et al., 1992a, b), as well as following retinoic acid beads and grafts of *Shh* expressing cells which are known to induce pattern duplications (Izpisua-Belmonte et al., 1991; Nohno et al., 1991; Riddle et al., 1993). Furthermore an apical ridge signal is also essential for *HoxD* gene activation as ectopic *HoxD* gene expression induced by a retinoic acid bead is distal to the bead, adjacent to the ridge and not all around the bead (Izpisua-Belmonte et al., 1991; Nohno et al., 1991). When a retinoic acid bead was implanted following apical ridge removal although some apparent *HoxD* gene expression was observed elaboration of the domains was not (Izpisua-Belmonte et al., 1992b). Furthermore a recent study shows that, following ridge removal, *Hoxd-13* expression is lost (Hayamizu et al., 1994; Vogel et al., 1995a). This suggests that polarising region and apical ridge signals together have roles in the regulation, elaboration and maintenance of *HoxD* gene expression. However, it is unlikely that *Shh* initiates expression of *HoxD* genes as *Hoxd-9* and *Hoxd-10* are expressed before *Shh* expression is observed (Nelson et al., 1996). Moreover, the early but not late patterns of *Hoxd-11* and *Hoxd-13* expression are present in the *limbless* mutant, despite no *Shh* expression, suggesting the initial expression patterns of *HoxD* genes at least, are activated by another mechanism (Ros et al., 1996; Normaly et al., 1996; Grieshammer et al., 1996). Retinoic acid initiates *HoxD* gene expression when applied to the anterior margin of the limb bud and could drive initial *HoxD* gene expression, particularly as some *Hox* genes including *Hoxd-10* and *Hoxd-11* (Gerard et al., 1996) contain retinoic acid response elements within their regulatory regions (for review see Tabin, 1991; Tickle and Eichele, 1994; Krumlauf, 1994). However in embryos treated with retinoid antagonists no limbs form but it is claimed that expression of *Hoxd-11* and *Hoxd-13* is still observed (Lu et al., 1997). An alternative mechanism for initiation of early *HoxD* and perhaps *Hox* gene expression may involve cell division and some as yet unknown intrinsic nature of proliferating mesenchyme (Duboule, 1994).

Another possibility is that *HoxD* gene initiation is controlled by *Polycomb* group and *Trithorax* group genes. These genes in *Drosophila,* are necessary to

maintain the expression of homeotic genes in segments and loss of function mutants lead to homeotic transformation and ectopic expression of *Hom-C* genes (for review see Paro, 1990; Gaunt and Singh, 1990; Krumlauf, 1994; Pirrotta, 1997; Gould, 1997). *Polycomb* group genes are negative regulators of transcription and *Polycomb* group products form large protein complexes (heterochromatin) preventing transcriptional activation of gene targets. *Trithorax* genes are positive regulators (for review see Pirrotta, 1997; Gould, 1997). Hence temporal colinearity and the ordered sequential activation of the *HoxD* genes could be controlled by changes in heterochromatin regulated by *Polycomb* and/or *Trithorax* genes (for review see Gaunt and Singh, 1990; Paro, 1990; Duboule, 1994; Pirrotta, 1997; Gould, 1997). Sequential expression of the *HoxD* genes depends upon repression of the heterochromatin, by signals such as *Trithorax* family members allowing access to a specific *HoxD* gene which could then be activated and maintained via *Shh*, retinoic acid, FGFs etc. Hence this prevents the more 5' posteriorly located genes from being initiated before the 3' anteriorly located genes. Recent work supports this theory. Mice in which murine homologues of *Polycomb* group genes, namely *M33* (Core et al., 1997), *mel-18* (Akasaka et al., 1996) and *Bmi-1* (van der Lugt et al., 1996) have been functionally inactivated show posterior homeotic transformation, greatly retarded growth and limb malformations and anterior shifting of expression of some *Hox* genes (for review see Gould, 1997). Moreover, Core et al (1997) suggest that *M33* may play a role in limiting access to retinoic acid response elements within the regulatory regions of some *Hox* genes, thereby controlling the activation of the *Hox* genes until a specific time.

The expression patterns of the 5' *HoxD* genes in developing limb buds together with studies investigating gain or loss of function suggest that *HoxD* genes have at least two roles in limb development (for review see Morgan and Tabin, 1994); an early role in determining structures and the timing of proliferation and differentiation (Dolle et al., 1993; Morgan and Tabin, 1994; Davis et al., 1995; Duboule, 1995; Goff and Tabin, 1997); and a late role controlling condensation formation, organisation of the condensation and growth rates of individual elements as shown by changes in the length and shape of skeletal elements in *Hoxd-13* and *Hoxd-11* viral misexpression and knockout mice (Morgan and Tabin, 1994; Davis et al., 1995; Duboule, 1995; Yokouchi et al., 1995; Goff and Tabin, 1997; see also Knezevic et al., 1997). Moreover, *Hoxd-12* may act to maintain *Shh* expression during limb outgrowth (Knezevic et al., 1997). Furthermore the *HoxD* genes may also play a role in cartilage bifurcation events as condensations form (Yokouchi et al., 1991b). An

outstanding question, receiving lots of attention, is the nature of the target genes that the *Hox* genes activate to co-ordinate these activities.

1.1.6.2*HOXA* genes

Not much is known about the regulation and activation of the *HoxA* genes. *The 5' HoxA* genes (*Hoxa-10, a-11, a-13)* are expressed in the chick limb (Yokouchi et al., 1991b) and mouse limb (Haack and Gruss, 1993) and *Hoxa-11* expression has also been described in the fins of the Zebrafish embryo (Sordino et al., 1995). The 5' *HoxA* genes follow the rules of temporal and spatial colinearity and of posterior prevalence. Like the *HoxD* genes, the *HoxA* genes show restricted domains of expression but along the proximo-distal axis rather than the antero-posterior axis (Fig. 1.5B). Initially all the gene expression domains overlap and *Hoxa-13* expression is found restricted to the posterior distal mesenchyme nested within the expression domains of *Hoxa-11* and *Hoxa-10* (Fig. 1.5B; Yokouchi et al., 1991b). As development proceeds, *Hoxa-13* expression expands to fill the hand plate and *Hoxa-11* expression is lost from distal mesenchyme so that no overlap in expression of *Hoxa-11* is observed with *Hoxa-13* (Fig. 1.5B; Yokouchi et al., 1991b). *Hoxa-11* expression is strong in the prospective forearm region of the limb and *Hoxa-10* expression is strong in the prospective humerus and forearm region (Fig. 1.5B; Yokouchi et al., 1991b; Haack and Gruss, 1993). Hence, it is suggested that the 5' *HoxA* genes are involved in the proximo-distal segmentation of the limb and the specification of the stylopod (humerus), zeugopod (forearm) and autopod (digits; Yokouchi et al., 1991b; Haack and Gruss, 1993). Furthermore recent work suggests that *HoxA* and *HoxD* genes co-operate to produce various elements of the limb. This is supported, for example, by the fact that when either *Hoxa-11* or *Hoxd-11* is knocked out, only mild defects to the zeugopod occur (Small and Potter, 1993; Davis and Capecchi, 1994). However when a double knockout of *Hoxa-11* and *Hoxd-11* is produced no zeugopod forms (Davis et al., 1995). When either *Hoxa-13* or *Hoxd-13* is knocked out only mild defects are observed in the hand plate (Dolle et al., 1993; Fromental-Ramain et al., 1996) but when *Hoxa-13* and *Hoxd-13* are both knocked out, no autopod forms (Fromental-Ramain et al., 1996; for review see Ruji and Chambon, 1997). These results suggest that *Hoxa-11* and *Hoxd-11* are involved in forearm patterning and *Hoxa-13* and *Hoxd-13* involved in hand plate patterning. They also show that combinations of paralogous *Hox* genes co-ordinate limb patterning, adding further evidence to the theory that vertebrate *Hox* clusters underwent several duplication events (Ruddle et al., 1994).

1.1.7 Muscle formation in limb development

As outgrowth of the limb proceeds under the control and regulation of ectodermal-mesenchymal interactions, other tissues besides cartilage condensations are also patterned and produced, such as muscle and the vasculature. Mechanisms that control the patterning and regulation of muscle and vascular formation are still far from clear, however in Chapter Five, I outline a signalling pathway that may play a role in the formation of the musculature and vasculature.

The musculature of the limb arises from migration of myogenic precursors from the somites into the limb between stages 13-18, as shown via quail-chick somite grafting experiments (Christ et al., 1977; Jacob et al., 1978; Chevallier et al., 1977, 1978). The migrating myogenic precursor cells, which express *Pax-3*, depend upon signals within the limb environment to control and regulate muscle differentiation, preventing premature differentiation (Robson and Hughes, 1996). Moreover muscle patterning is controlled by the connective tissue. For example, when thoracic mesoderm is transplanted in place of a brachial somite, the resulting myogenic cells form brachial musculature (for review see introduction Robson et al., 1994). Furthermore following polarising region grafts or the application of retinoic acid soaked beads which produce mirror-image cartilage duplications, muscle masses are also duplicated producing symmetrical muscle patterns, and posterior muscles form in the anterior part of the wing (Shellswell and Wolpert, 1977; Robson et al., 1994). The cellular pattern of fast and slow fibres in the duplicated muscle is the same as the corresponding normal posterior muscle suggesting that connective tissue or the environment of connective tissue controls muscle pattern and the cellular constitution of the muscle (Robson et al., 1994). Muscle pattern is also controlled to some extent, by dorsal-ventral ectoderm signalling, as rotation of the ectodermal jacket by 180° results in reversed dorsal-ventral muscle polarity in the distal limb (see earlier; MacCabe et al., 1974; Shellswell and Wolpert, 1977; Geduspan and MacCabe, 1987, 1989; Akita, 1996). Muscle formation occurs in a proximal to distal sequence where myogenic precursor cells, when committed to myogenesis express *MyoD* or *Myf-5* and later the dividing committed myoblasts will differentiate and form myotubes, expressing muscle contractile proteins (for review see introduction Robson and Hughes, 1996). Signals involved in the localisation of myoblasts to muscle masses are unknown, but signals involved in the differentiation of myoblasts into myotubes include FGFs, PDGF and TGFβ family members (for review see introduction Robson and Hughes, 1996).

1.1.8 Vascularisation

In order for limb development to proceed successfully, a vascular system is required which must increase in size and complexity as limb outgrowth proceeds. Vascularsiation of the limb has occurred by the time limb outgrowth is initiated and can be seen and studied either by Indian ink injection (for example see Feinberg and Saunders, 1982; Wilson, 1983; Feinberg and Noden, 1991) or by the use of Quail grafts (for example see Wilson, 1983; Pardanaud et al., 1989). The limb possesses a rudimentary vascular system at the proximal base of the limb from stage 17, no vasculature is present in distal tissue. The vascular bundle present is thought to arise by angiogenesis (where new blood vessels sprout from existing vessels via proliferation, migration and differentiation of endothelial cells) from the dorsal aorta or cardinal veins (see Wilson, 1983; Pardenaud et al., 1989; Feinberg and Noden, 1991). As limb outgrowth continues the subclavian artery carries blood into the limb and radiates into a network of smaller capillaries, formed by the proliferation and migration of pre-existing capillaries (angiogenesis), which drain into the anterior and posterior marginal veins (Wilson, 1983; Pardenaud et al., 1989). This was shown by exchanging the avascular distal limb tip of a chick with a similar staged quail distal limb tip. The resulting vasculature in the distal limb tip was of host origin only, showing that the limb vasculature arises through angiogenesis, that is the proliferation and migration of pre-existing capillaries (Wilson, 1983). More recent work suggests that the process of limb angiogenesis may also incorporate populations of endogenous limb endothelial cells present in the limb from pre-limb stages (Feinberg and Noden, 1991). A vascular pattern resembling that of the adult wing bud is established by stage 25, however the distal mesenchymal tissue beneath the apical ridge is avascular (see Feinberg and Saunders, 1982; Feinberg and Noden, 1991), perhaps due to increased proliferation in subapical mesenchyme (Summerbell and Wolpert, 1972). The signals involved in initiating and maintaining angiogenesis and maintaining a proliferating supply of endothelial cells in the limb bud is not fully understood, but recent work suggests VEGF (vascular endothelial growth factor) may be an important factor (for review see Risau, 1997). Moreover apical ridge signalling also has a role, as vascularisation is prevented following ridge removal (Feinberg and Saunders, 1982).

1.2 Work described in this thesis

The aims of this thesis are three-fold: First, to make a detailed fate map and to relate this directly to patterns of gene expression; Second, to investigate cell fate in regulating and regenerating limbs and also in limbs with excess tissue induced by polarising region signals to gain further insight into mechanisms of limb morphogenesis; Third, to investigate the expression of members of the *Notch* signalling pathway in the developing limb and in tissue formation and vascularisation and then to suggest functions of this pathway by comparison to the known functions of these genes in *Drosophila*.

CHAPTER TWO

Materials and Methods

2.1 Handling and preparing chick embryos

Fertilised White Leghorn chicken embryos were purchased from J. K. Needle and Co. Ltd, Poyndon Farm, Silver Street, Goffs Oak, Herts., UK and stored for up to one week in a cooled incubator at 12°C. For experimentation, embryos were incubated at 37°C. The eggs were windowed, see below, staged according to Hamburger and Hamilton (1951) and replaced in the incubator until the desired stage was reached.

To make a window in the egg shell, to allow operations to be carried out upon the embryo, each egg was rotated 180° and swabbed with 70% alcohol. A hole was made in the blunt end of the egg using a pair of forceps. A further hole was made midway along the long axis of the egg in the upper surface and the shell membrane pierced so that the embryo drops down. The hole was covered with sellotape and then a small circle of egg shell cut away, being careful not to cut the underlying embryo or yolk sac. The embryo was staged and then a further piece of sellotape applied over the window. Embryos were then replaced into the incubator and development monitored until the appropriate experimental stage was obtained. Embryos could be left at room temperature, to slow development down, if embryos were developmentally advanced, then replaced into the incubator to obtain the desired stage.

Following surgical manipulation (see later for outline of such manipulations) or for embryos required as controls, embryos were dissected from the egg using forceps to hold the vitelline membrane and surrounding tissues, and scissors were used to cut out the embryo out of the egg. The embryos were placed into a dish of phosphate buffered saline (PBS). Following removal of any excess unwanted tissue, embryos were either; 1) fixed in 4% paraformaldehyde (4g paraformaldehyde in 100ml sterile distilled water heated to 70°C and pH to 7.5 with 1M Sodium hydroxide (NaOH), when cool 1ml 10X PBS added) and stored at 4°C before being processed for either fluorescence photography or whole mount in situ hybridisation; or 2) fixed in 5% Trichloroacetic acid (in sterile distilled water), before being processed and stained for cartilage (see later).

2.2 Iontophoretic application of DiI and DiA

DiI (1,1-dioctadecyl-3,3,3',3'-tetramethylindo-carbocyanine perchloride, Molecular Probes, D-282) is a vital dye and member of the carbocyanine dye family. DiI is highly fluorescent and lipophilic and labels the cell membrane and has been widely used for studying cell fate. It is passed on to progeny of labelled cells but does not leak to neighbouring cells and is not toxic (Honig and Hume, 1986, 1989). DiI (3mg/ml in dimethylformamide) was used to investigate cell lineage in the limb, cell lineage in relation to gene expression and also to mark the vasculature (see later). DiI was administered, by pressure-injection using a picospritzer (General Valve), via a micro-pipette, that has a tip opening of 1-2μm made using a thin walled 1mm diameter borosilicate capillary pipette in a Flaming Brown Micro-pipette puller (Model P-87). The micro-pipette was mounted in a Newport MX110R micromanipulator, and was manoeuvred into position such that the tip pierced the dorsal ectoderm and mesenchyme or the apical ridge, where a small dot of DiI was delivered by one to four 10msec pulses (50 pounds psi) from the picospritzer. For double labelling experiments, a second member of the carbocyanine dye family, DiA (4-Di-16-Asp, Molecular Probes D-3883) was used. When investigating mesenchymal or ectodermal cell lineage, application of DiI and/or DiA into the limb bud was carried out using the somites as reference points. When the relationship between cell lineage and gene expression domains was investigated, the perimeter of the gene expression domain (as outlined initially in high power photographs of whole mounts showing expression of a specific gene) was used as a reference for DiI injection. The accuracy of the position of DiI label (on, within or above the perimeter of gene expression) was confirmed by whole mount in situ hybridisation (see later) for the specific gene in limbs fixed immediately after DiI injection.

In these experiments, cells in the right limb bud were labelled, and measurements were taken of the DiI dot size and position at the time of administration and after the incubation period. The average initial size of the DiI injected dot was 25-50μm (n=35). The limbs were incubated for 48 or 96 hours when they were fixed in 4% paraformaldehyde for 24 hours before being processed for fluorescence photography.

Photography

1. When a DiI labelling experiment was carried out just to investigate fate of labelled cell populations in mesenchyme and/or apical ridge, limb buds were removed from embryos and mounted whole onto glass slides, under a coverslip with a solution

of 70% glycerol/29% PBS/1% Dabco. Limb buds were viewed within one/two days after fixation using a Nikon Optiphot 2 microscope with fluorescence attachment. Whole mounts were photographed either in black and white using Ilford HP5 film rated at 400ASA. The film was developed using Ilford Microphen Film Developer and printed using a Rapidoprint DD3700 printing machine (Agfa-Gevaert), or using colour slide film Kodak EPY400 and developed at CPL Laboratories, London. **2.** When cell populations were DiI labelled to study the relationship between cell lineage and gene expression, limbs were removed from the embryo and mounted onto glass slides, under a coverslip with a fresh solution of 4% paraformaldehyde. Wholemounts were photographed in black and white (as above) and then prepared for whole mount in situ hybridisation which visualises a specific gene expression domain (see later) where upon photographs of the gene expression domain could be compared to photographs of patterns of labelled cell populations.

'Archimedes' analysis of DiI spread and of areas of gene expression

Detailed analysis of DiI labelled limb buds, 48 hours and 96 hours after injection and also of the areas of *Hoxa-13* gene expression in response to different concentrations of FGF-4 (see Chapter Three) was carried out using the computer program 'DIGIT' on a BBC Archimedes 310 computer. Outlines of the DiI labelled cell population or gene expression domain were incorporated into the computer and subsequent analysis allowed measurement of the area (and subsequent percentage value) for each DiI labelled cell population (see Chapter Three) and for the area of ectopic gene expression in response to FGF-4 (see Chapter Three).

2.3 Labelling of the vasculature

Indian Ink (No. 951, Windsor and Newton Ink) or DiI, was administered into the vitelline vein, by pressure-injection using a picospritzer, via a micro-pipette with a tip opening of 3μm to investigate the extent of the limb vasculature (see Chapter Five). The micro-pipette, mounted in a Newport MX110R micromanipulator, was manoeuvred into a position just below the heart of the stage 20-21 embryo such that the tip pierced the vitelline vein which enters the embryo in midflank. Ink was delivered into the vein by 15-20 20msec bursts (50 pounds psi) from the picospritzer, which stained the entire vascular system of the embryo.

Embryos labelled with Indian Ink were fixed immediately in 5% trichloroacetic acid and left overnight, whereupon they were dehydrated through alcohols and then cleared in Methyl salicylate (BDH). Limbs were photographed using a Yashica 108 camera attached to a Zeiss Stemi SV6 binocular dissecting

microscope using black and white Ilford PanF film rated at 50ASA or using Kodak 64T tungsten colour slide film and processed and printed as discussed earlier in Section 2.2. Limbs were then wax sectioned (see later). Embryos labelled with DiI, were fixed in 4% paraformaldehyde overnight. The limbs were then removed from the embryo and mounted in fresh 4% paraformaldehyde and photographed using a fluorescence microscope (as described earlier), and then processed for frozen sectioning (see later).

2.4 Surgical procedures

All operations upon the chick embryo were carried out on the right limb. All operations were performed using a Zeiss binocular dissecting microscope and a Schott KL1500 fibre optic lamp for illumination. The windowed egg was placed beneath the microscope and the sellotape removed and the embryo made accessible by tearing away the vitelline and amniotic membranes using two pairs of fine forceps.

In order to remove tissue and/or graft tissue or beads into the limb, the limb tissue was cut with sharp tungsten needles.

Apical ridge removal

The apical ridge is a clear thickened epithelial structure around the rim of the limb bud. To remove the apical ridge, a sharpened needle was used to gently score tissue between the apical ridge and mesenchyme starting from the posterior of the bud and working up to the anterior, being careful to try and remove as little mesenchyme with the apical ridge as possible. Then the scored tissue was cut deeply starting from the posterior and the apical ridge gently prised away from the underlying mesenchyme. The apical ridge was then cut away from the limb. Further experimentation, if required, could then proceed, for example DiI injection. Limbs were incubated for between 6 hours and 7 days, depending on the experiment carried out and either fixed in 4% paraformaldehyde overnight before being processed according to the protocol for DiI injection or for whole mount in situ hybridisation (see later), or fixed in 5% trichloroacetic acid and then processed for alcian green cartilage staining.

Mesenchyme removal

Mesenchyme was removed from stage 21/2 wing buds (Hamburger and Hamilton, 1951) by gently scoring the outline of a square of the desired size onto the dorsal surface of the limb bud with a sharp tungsten needle. Care was taken to leave the apical ridge intact. The outline of the square was then cut deeply so that the

tungsten needle pierced through to the ventral surface. The block of mesenchyme was then removed, leaving a limb with an area of central mesenchyme missing. In some experiments the apical ridge was removed before the removal of the mesenchyme block (see Chapter Four). DiI injection of mesenchyme around the wound margin could then carried out, if desired. Embryos were incubated for either 24 hours, 48 hours or 7 days, before fixation, depending on the experiment carried out, and processed according to the protocol for DiI injection or whole mount in situ hybridisation (see later) or for alcian green cartilage staining (see later).

Preparation and application of FGF-4 soaked beads

Heparin acrylic beads with a diameter of 200-250μm were soaked in a 2μl volume of recombinant FGF-4 protein (a kind gift from Prof. John Heath) in 9mm sterile petri dishes. Up to 15 beads were placed in the FGF-4 protein solution, at either full concentration (0.7mg/ml) or dilutions of the full concentration in PBS (phosphate buffered saline). Beads were soaked for one hour minimum at room temperature. Beads were placed in stage 20/21 limb buds either in slits made in proximal posterior mesenchyme or in place of the apical ridge pinned to apical mesenchyme by pins made from platinum wire (25μm thick; Goodfellows, Cambridge, UK). Limb buds were then left to develop for varying time periods up to 48 hours, when they were fixed in 4% paraformaldehyde and processed for whole mount in situ hybridisation (see later). Some limb buds were left to develop for 7 days, when they were fixed in 5% trichloroacetic acid, for cartilage staining.

Preparation and application of retinoic acid soaked beads

AG1-X2 beads between 150-200μm in diameter were soaked in 0.1mg/ml all-*trans*-retinoic acid (obtained from Sigma, UK) in dimethylsulphoxide (DMSO) for 30 minutes at room temperature in 9mm petri dishes in the dark. Beads were then briefly washed in Minimum Essential Medium (MEM, Gibco, UK) containing 10% foetal calf serum (Gibco, UK) and 1/100 antibiotic/antimycotic solution (Gibco, UK) to remove the retinoic acid solution and then placed in fresh MEM in the dark for 30 minutes at 37°C. Beads were then kept in the dark at room temperature and placed in limb buds in slits made in mesenchyme beneath the anterior apical ridge. Limb buds were then incubated either for 48 or 96 hours, following subsequent experimental manipulations i.e. DiI injection and fixed in 4% paraformaldehyde, or for 7 days to investigate the cartilage pattern and fixed in 5% trichloroacetic acid.

2.5 Processing and staining for cartilage

The protocol used was as follows:

a) Embryos fixed in 5% trichloroacetic acid overnight.
b) Rinse in 70% alcohol for 5 minutes.
c) Wash in acid alcohol (1% concentrated Hydrochloric acid in 70% alcohol) for 10minutes, twice.
d) Stain with Alcian green (0.1% in acid alcohol) for between 3 hours and overnight.
e) Differentiate the tissue in acid alcohol, overnight.
f) Dehydrate in absolute alcohol for 1 hour, twice.
g) Clear in Methyl salicylate.

Specimens were analysed and photographed using Ilford PanF black and white film or Kodak 64T tungsten colour film using a Yashica 108 camera attached to a Zeiss Stemi SV6 dissecting microscope.

2.6 Whole mount in situ hybridisation

The whole mount in situ hybridisation method described was kindly provided by Dr. Ketan Patel, UCL and is a modification of the protocol of Nieto et al (1996).

Probe production

DIG labelled RNA probes between 0.8 and 1.2kb in length were generated from a DNA template in Bluescript plasmids to detect transcripts of *Hoxa-10* to *-13* (gift from Prof. Cliff Tabin; Nelson et al., 1996); *Hoxd-13* (gift from Prof. Denis Duboule; Dolle et al., 1993); *Fgf-4* (gift from Dr. L. Niswander; Niswander et al., 1993); *Notch 1*, *Serrate 1*, *Serrate 2* and *Delta 1* (gift from Dr. J. Lewis and Dr. D. Henrique; Myat et al., 1996).

The DNA to produce the probes was prepared according to the following protocol:

Between 50-100µg of plasmid containing the probe DNA was linearised using a gene specific endonuclease together with 10µl of reaction buffer made up to a 100µl final volume in autoclaved distilled water and incubated overnight at 37°C. An aliquot was run on a 0.8% agarose gel to check the plasmid was linearised (Agarose gel: agarose dissolved in 1X TAE (Tris-Borate-EDTA) with 0.5mg/ml Ethidium bromide; DNA sample loaded onto the gel mixed with loading buffer containing 0.25%

bromophenol blue, 25mM EDTA, 50% glycerol and run at 80-100V. DNA was visualised on an ultraviolet transilluminator). The linearised plasmid DNA was then cleaned, to remove any excess uncut DNA by phenol-chloroform extraction, then precipitated in 3M sodium acetate and ethanol and incubation at -70°C for 1 hour. The solution was then centrifuged and following an aliquot of ethanol to wash the pellet, was air dried and resuspended in autoclaved distilled water and stored at -20°C until required to produce the probe.

RNA probes were made as follows:

In a reaction tube were placed: linearised DNA (to give approximately 1µg), 5µl 5X transcription buffer, 1µl of 10mM UTP, 2µl of 10mM ATP, 2µl of 10mM CTP, 2µl of 10mM GTP, 1µl of DIG-11-UTP, 9µl of autoclaved distilled water then 1µl RNase inhibitor and 2µl of either T7 or T3 RNA polymerase (depending on the probe being produced i.e. *Delta-1, Hoxa-13* and *Hoxd-13* require T3 RNA polymerase, all others require T7 RNA polymerase which produce the single strand RNA probe). The mixture was incubated for 2-3 hours at 37°C. To check the probe had been synthesised a 1µl aliquot was then removed and electrophoretically run on a 0.8% agarose gel (shown by the presence of an RNA band at the appropriate size marker for the transcript insert). If the probe has been successfully produced then 2µl of DNase and 1µl of RNase inhibitor was added to the reaction tube and incubated for a further 30 minutes at 37°C to stop the reaction and remove the linearised DNA. The RNA probe was then precipitated with 3M sodium acetate, ethanol and 1µl glycogen (20µg/µl) at -70°C until required for use.

The probe, when required, following centrifugation at 13000rpm at 4°C was washed in 70% ethanol, air dried and resuspended in 50-100µl of autoclaved distilled water and stored at -20°C until use. 1-2µl of the probe was used per ml of hybridisation mix.

Embryo processing

DiI labelled limbs to be used for whole mount in situ hybridisation following fluorescence photography were placed in fresh 4% paraformaldehyde in plastic screw top tubes. Embryos to be used for whole mount in situ hybridisation were following removal from the egg, decapitated and cleaned of all extra-embryonic membranes including stomach, lungs, heart. The embryos were fixed in 4% Paraformaldehyde in plastic screw top tubes overnight before being washed and dehydrated successively for 10 minutes in 25% Methanol:PBST (PBS + 0.1% Tween 20); 50% Methanol:PBST; 75% Methanol:PBST and finally 100% Methanol twice and stored at -20°C until required.

The whole mount in situ hybridisation process is carried out over 5 days

Pretreatments

Embryos were rehydrated and washed for 10 minutes each through a graded series of methanol solutions from 100% methanol, through 75% methanol:PBST, 50% methanol:PBST; 25% methanol:PBST and finally in PBST three times.

Embryos were then incubated in Proteinase K (20mg/ml in PBST) which causes pores to form in the membranes covering the limb, which will allow probe access into limb tissue. Incubation in Proteinase K depends on age of the specimen and experiment to be carried out, for example, 7 minutes for stage 20 embryos, 20 minutes for stage 28 embryos. Embryos were then rinsed in PBST and refixed in 4% paraformaldehyde for 20 minutes. Following a further rinse in PBST embryos were placed in prehybridisation buffer overnight at 65°C (50ml volume of prehybridisation solution contained 25ml deionised formamide (Fluka Chemicals), 12.5ml 20X SSC (3M NaCl, 0.3M Sodium citrate to pH4.5 with citric acid), 1g Blocking reagent (Boehringer Mannheim), 100µl Triton X-100 (Sigma), 0.5ml 10% CHAPS (3[(3-Chloamidopropyl)dimethylammonion]-1-propane-sulfonate; Sigma), 50µl Heparin (50mg/ml), 0.5ml EDTA pH8, 125µl t-RNA (20mg/ml stock to make 50µl/ml final), sterile double distilled water to 50ml). The prehybridisation buffer prepares the limb tissue for the probe.

Hybridisation and post-hybridisation treatments

Embryos were placed in fresh pre-hybridisation solution containing 1-2µg digioxygenin labelled probe. Embryos were left at 65°C overnight.

All post-hybridisation steps were carried out on rotating rocking platforms, unless otherwise stated. Embryos were washed twice in 2XSSC containing 0.1% CHAPS for 1 hour at 65°C and then washes in 0.2XSSC containing 0.1% CHAPS for 45 minutes at 65°C. Embryos were then rinsed at room temperature in KTBT buffer (50mM Tris/HCl pH75.5, 150mM NaCl, 10mM KCl in sterile distilled water and 1% Triton X-100). Embryos were then placed in 20% lamb serum in KTBT buffer at 4°C for 4 hours before being placed in fresh 20% lamb serum in KTBT buffer containing 1/2000 anti-digioxygenin antibody (Boehringer Mannheim) and incubated overnight at 4°C. The antibody binds only to the DIG labelled probe. To visualise the pattern of transcripts as shown by the probe, a colour reaction which identifies the antibody bound to the probe is carried out. Embryos were placed in Colour reaction buffer (50ml stock solution made from 5ml 1M Tris pH9.5, 2.5ml 1M $MgCl_2$, 1ml 5M NaCl, 200µl Triton X-100 and sterile double distilled water to 50ml)

for 10 minutes twice, at room temperature. Embryos were then placed in Colour reaction buffer containing 3µl NBT per ml (75mg/ml Nitroblue tetrazolium salt in 70% dimethylformamide; Boehringer Mannheim) and 2µl BCIP per ml (50mg/ml 5-bromo-4-chloro-3-indolyl-phosphate in 100% dimethylformamide; Boehringer Mannheim) to effect the colour reaction and detect the transcript pattern. The colour reaction was carried out in the dark and colour allowed to develop until the required colour intensity was obtained. The colour reaction was stopped by rinsing in PBS three times and the embryos were then stored in PBS:0.02% Sodium azide. Embryos were analysed and photographed using a Yashica 108 camera attached to a Zeiss Stemi SV 6 binocular dissecting microscope using colour 64T tungsten slide film on 1% agar plates.

2.7 Sectioning

Frozen sectioning

Embryos following whole mount in situ hybridisation or DiI labelling of the vasculature following photography were frozen sectioned using one of two methods: **1**) embryos were refixed in 4% paraformaldehyde at 4°C for 1 hour to overnight. Embryos were then placed in 30% sucrose in PBS overnight at 4°C. Embryos after being placed in O.C.T (Tissue-Tek; Miles Inc.) for 1 hour were embedded in O.C.T and then frozen using liquid nitrogen or dry ice. Blocks were stored at -20°C for up to one week and then sectioned at 10µm on a Leica CM1900 Cryostat and placed on glass slides, allowed to air dry and then mounted with glycerol; **2**) Embryos were fixed in 4% paraformaldehyde containing 4% sucrose at 4°C overnight. Embryos were then embedded in 1.5% Bacto-agar (DIFCO, Detroit, USA; 0140-01) containing 5% sucrose, made in water and left for 1 hour. The agar blocks were then placed in 30% sucrose in PBS overnight at 4°C. The agar blocks were then coated in O.C.T and frozen in dry ice before being sectioned as above. The sectioned whole mount in situ hybridisation limbs were analysed and photographed using Kodak 64T tungsten colour film within 2 days and stored at 4°C. The sectioned DiI labelled limbs were analysed and photographed using a fluorescence microsope immediately, as the fluorescent DiI signal is lost rapidly following sectioning.

Wax sectioning

Embryos that been injected with Indian ink were wax sectioned. Embryos following fixing, dehydrating and clearing were placed in 100% molten wax three times for one hour each. The embryo was then embedded in 100% wax and allowed to set. Wax blocks were then sectioned on a '820' Spencer wax microtome (American

Optical Corporation) at 15μm and placed onto glass slides, allowed to dry and then mounted in glycerol before being viewed under a microscope a photographed using Ilford HP5 ASA50 black and white film.

2.8 Thesis figure production

Photographs contained within this thesis were scanned onto a 230MB Optical disc using a Kodak slide scanner. Figures were organised and produced using Adobe Photoshop 4.0 on a Power Macintosh. Summary diagrams and figures were generated using Adobe Photoshop 4.0.

CHAPTER THREE

Cell fate in the chick limb bud and relationship to gene expression

3.1 Introduction

In spite of considerable progress in understanding the cellular and molecular nature of the interactions involved in patterning the limb (see Chapter One), basic parameters of limb development remain unclear. While several fate maps exist (Saunders, 1948; Stark and Searls, 1973; Lewis, 1975; Summerbell, 1976; Bowen et al., 1989), they are not always consistent with one another and detailed information on the fate of small groups of cells is not available either for the mesenchyme or, in particular, for the apical ectodermal ridge. Several methods have been used to produce fate maps including carbon particle labelling (Saunders, 1948; Muneoka et al., 1989; Bowen et al., 1989), tritiated thymidine (Stark and Searls, 1974), quail/chick chimaera (Bowen et al., 1989) as well as theoretical fate maps (Lewis, 1975). The fate maps show that the majority of the limb elements arise from the posterior half of the limb bud and the digits from subapical posterior mesenchyme. These maps also show complex cell interactions occurring as limb development proceeds, such as posterior cell populations displacing anterior cell populations. The fate maps obtained are reasonably accurate but are not highly detailed, in that not every area or region of mesenchyme was labelled. A reliable fate map of the mesenchyme would be valuable for dealing with a number of issues: First, to show exactly what part(s) of the bud give rise to specific structures, e.g. the digits. Second, to compare cell fate with gene expression. This is a relatively new area requiring accurate fate maps to interpret dynamic patterns of gene expression to see how populations of cells maintain or alter expression of genes. Finally, a detailed fate map would show exactly how the bud expands, which could be relevant to evolutionary ideas about the origin of amniote limbs (Shubin and Alberch, 1986; Coates, 1991, 1995; Sordino et al., 1995).

I have constructed fate maps of the limb bud using the lipophilic dyes DiI and DiA. These dyes can be administered easily in a minimally-invasive way and this allows a detailed, comprehensive and accurate fate map to be produced. I have used this technology to update existing fate maps and ask questions that it has not been possible to address previously. I have investigated, for example, the relationship between the gene expression domains of *Fgf-4*, *Hoxd-13* and *Hoxa-13* and cell behaviour. The results are also relevant to evaluating the proposal that an anterior bending of the primitive

vertebrate limb was central to the evolution of digits in limbs of higher vertebrates. Furthermore the results of this study also suggest that *Hoxd-13* and *Hoxa-13* expression may be regulated by different mechanisms. Rather little is known about the regulation and initiation of expression of *HoxA* genes within the developing limb bud in comparison with the *HoxD* genes. Therefore, I have started to investigate the role of FGF signalling in the initiation and maintenance of *Hoxa-13* expression and examine whether a dose-dependent mechanism is involved.

3.2 Results

3.2.1 Fatemaps

3.2.1.1 *Mapping mesenchymal fate*

DiI was injected into mesenchyme, using a picospritzer, at different antero-posterior levels in wing buds using the somites and somite boundaries as reference points and the fate of labelled mesenchyme cells followed for either 48 or 96 hours. The wing was divided into thirds (Fig. 3.1A). The distance between each injection position was 150μm and the amount of DiI injected was approximately the same each time, giving a small patch 25-50μm in diameter, containing approximately 150 cells, as shown by sections of specimens fixed immediately after DiI injection.

After 48 hours incubation, a dense region of labelled mesenchyme cells was observed, with a minority of brighter scattered cells lying outside this main region. The identity of these scattered cells is unknown. They could be macrophages engulfing dead or dying DiI labelled cells or they could be a population of more mobile mesenchyme cells, which, as they appear to be brighter than cells in the main core, divide less. These scattered cells appeared to be more numerous anterior to the main region of labelled cells irrespective of the position in which cells were labelled. However in 96 hour specimens, their numbers were reduced. The position, size and shape of the core of labelled cells was used to produce the fate maps (Fig. 3.1). My results are compiled from 450 wing and 75 leg buds labelled at stage 20.

Subapical wing mesenchyme

A marked difference was found, after 48 hours incubation, between behaviour of populations of cells labelled directly beneath the apical ridge at stage 20, in the anterior third of the bud compared to the middle and posterior thirds (Fig. 3.1B). Average expansion for each site of injection at 48 hours is shown in Fig. 3.2A and at 96 hours in Fig. 3.2B.

Figure 3.1

A). Diagram of a stage 20 wing bud showing positions at which DiI was injected. Dashed lines indicate, with reference to the somites, anterior (A), middle (M) and posterior (P) thirds used for analysis. Each labelled somite position is colour coded for easy reference to each map. Asterisks indicate these cell populations were labelled at 450μm from the apical ridge rather than at 500μm. Scale bar represents 300μm.

B-F Representative stage 28 wing buds, 48 hours after DiI labelling showing a typical example of the result for each injection site studied. **B**) Subapical mesenchyme populations. Note marked anterior shift of cells labelled on a level with somite 18 (asterisk). **C**) Mesenchyme labelled 500μm from the somites. **D**) Mesenchyme labelled 250μm from the somites. Note extensive overlap of labelled cell populations. **E**) Mesenchyme labelled 50-75μm from the somites. Note proximo-distal displacement of posterior populations. **F**) Apical ectodermal ridge populations. Extent of apical ridge indicated by arrowheads. Scale bar represents 500μm. **G**) Summary map of representative results obtained in chick wings at 96 hours for populations of cells labelled subapically with DiI at stage 20. The map shows contributions to digits and also that posterior cell populations do not bend anteriorly. Numbers indicate digit identity. Scale bar represents 1500μm. **H**) Summary map of representative results obtained in chick leg buds at 48 hours for populations of cells labelled subapically with DiI at stage 20. Note anterior shift of apical populations, between somite 28 and somite 29, towards the anterior tip and posterior shift of posterior populations. Scale bar represents 500μm. Numbers indicate the somite position at which the labelled cell population was initially labelled at stage 20. **I**) Summary of relative rates of cell population expansion in stage 20 wing bud over 48 hours. Blue colour indicates low expansion and this region occupies a small percentage of the limb bud at 48 hours. Red colour indicates the highest expansion and this region comes to occupy the majority of the limb bud. White colour indicates intermediate expansion. Scale bar represents 250μm.

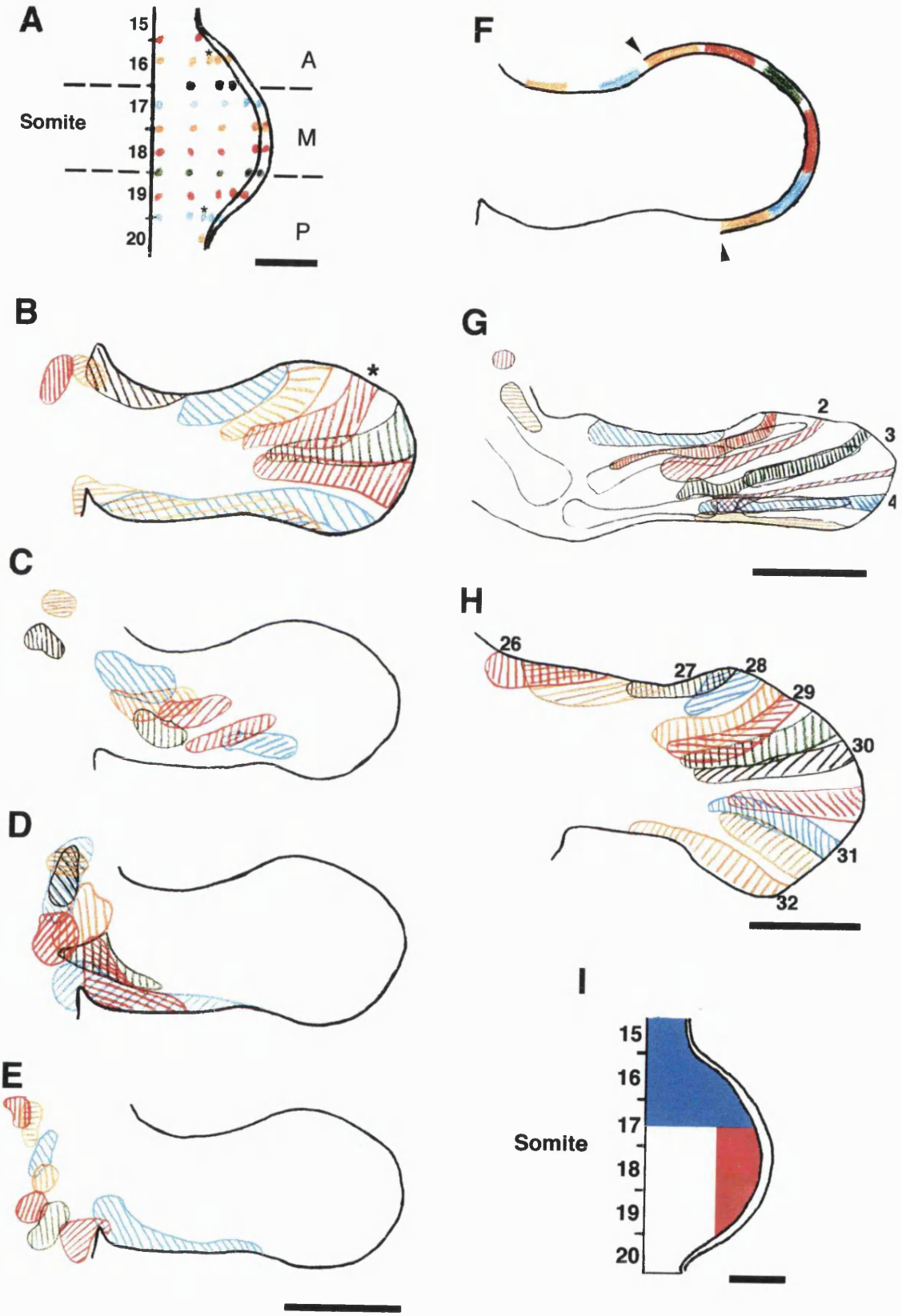
A
15
16
17
18
19
20
Somite
A
M
P
B
*
C
D
E
F
G
2
3
4
H
26
27
28
29
30
31
32
I
15
16
17
18
19
20
Somite

Figure 3.2

A-C Histograms showing the expansion of labelled cell populations in chick wing bud at different positions with respect to the somites. Expansion was measured as the increase in area of labelled cells (measured in arbitrary units) from time of injection to time of analysis 48 or 96 hours later. **A**) mesenchyme at 48 hours showing a general increase in expansion from anterior to posterior and more expansion subapically than proximally. **B**) subapical mesenchyme at 96 hours. **C**) apical ridge at 48 hours, note that posterior ridge expands more than anterior ridge.

A

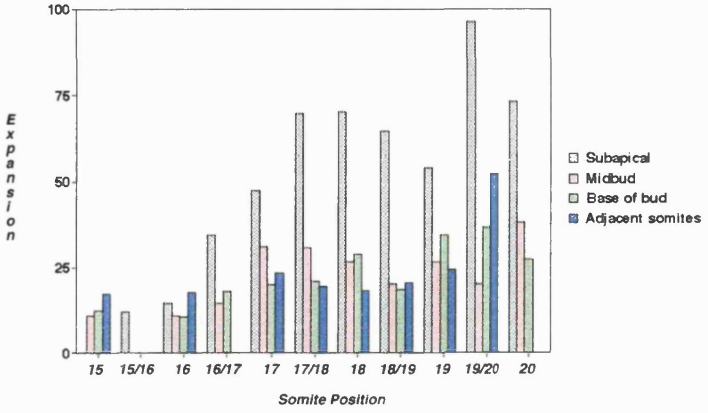
100
75
50
25
0
Expansion
15
15/16
16
16/17
17
17/18
18
18/19
19
19/20
20
Somite Position
Subapical
Midbud
Base of bud
Adjacent somites

B

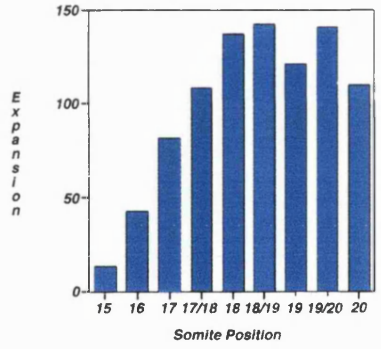
150
100
50
0
Expansion
15
16
17
17/18
18
18/19
19
19/20
20
Somite Position

C

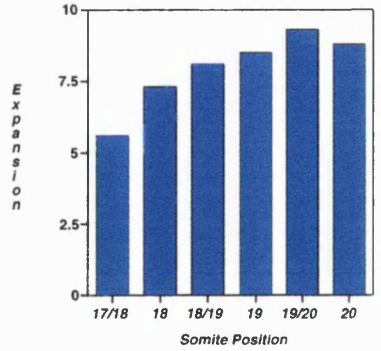
10
7.5
5
2.5
0
Expansion
17/18
18
18/19
19
19/20
20
Somite Position

The most anterior cell populations (opposite somite 15, 15/16, 16) remained in proximal positions, expanded little compared to other regions and remained adjacent to the ectoderm occupying 2% of the limb area (n=7, Fig. 3.1B, 3.3A). For cells opposite somite 16/17, expansion was greater and the label was distributed beneath the ectoderm in a proximo-distal direction, occupying 3% of the limb area (n=2). In the middle third, the labelled cells formed wide streams running proximo-distally between apical ridge and proximal regions of the bud, occupying around 20% of the limb area (n=35); moreover in the distal limb these labelled streams fanned out in an anterior direction towards the anterior tip (see asterisk Fig. 3.1B, 3.3B). In the posterior third, the labelled cells formed long, wide proximo-distal streams running from the apical ridge proximally, occupying 22% of the limb area (n=23), but no anterior shift was observed (Fig. 3.1B, 3.3C,D,E). Thus, although the posterior third produces a greater proportion of the total area, it is the middle third that fills the anterior tip of the wing bud and contributes to much of the handplate (Fig. 3.1B, 3.2A). The 96 hour fatemaps (Fig. 3.1G, 3.4G-K) show that digit **2** arises from subapical cells on a level with somite 17/18 (Fig 3.4H), digit **3** from subapical cells on a level with somite 18/19 (Fig. 3.4J) and digit **4** from subapical cells on a level with somite 19/20 (Fig. 3.4K). Note that an anterior shift of cells into the anterior handplate was also observed at 96 hours (Fig. 3.4I).

To test directly the amount of cell mixing within the wing bud, two different subapical mesenchyme populations were labelled within the bud and their fate followed. The main domains did not intermingle when labelled populations were 150μm apart initially (Fig. 3.5E). Thus, when populations of cells were labelled subapically at, for example, somite 18 with DiI, which fluoresces red, and at somite 18/19 with DiA, which fluoresces green, densely labelled cells occupied distinct non-overlapping territories particularly clear in distal regions. Some mingling of cells occurred between scattered cells lying outside the main domain of each labelled cell population proximally (Fig. 3.5E).

Proximal wing mesenchyme

DiI was injected into mesenchyme at three proximal locations in stage 20 embryos; Mid-bud (500μm from the somites; Fig. 3.1A,C); Base of bud (250μm from the somites; Fig. 3.1A,D) and adjacent to the somites (50-75μm from the somites; Fig. 3.1A,E). Average expansion for each site of injection is shown in Fig. 2A.

i) Labelled mesenchyme midway between apical ridge and bud base (500μm from the somites) at stage 20, was generally found within the limb bud, 48 hours later (Fig. 3.1C). Cell populations labelled within anterior third, showed some expansion, occupied 2% of the limb area (n=2) and remained in a proximal position (Fig. 3.2A, 3.3F). Cell

Figure 3.3

Fatemaps of wing bud mesenchyme.

Examples of DiI labelled wing buds 48 hours after injection at different antero-posterior levels with reference to the somites (see somite numbers) and at different positions along the proximo-distal axis of the bud.

A-E Subapical injections **A)** labelled cells have remained proximal and ended up anterior to wing bud, **B)** labelled cells have expanded forming a stream between apical ridge and proximal regions which bend towards anterior tip, **C)** and **D)** labelled cells form a wide stream of cells between apical ridge and proximal regions, no anterior bending seen, **E)** labelled cells spread along posterior margin of the wing but not right up to tip.

F-H Proximal mesenchyme injections midway in the limb bud (500μm from somites) **F)** labelled cells remain proximal, end up anterior to humerus head, **G)** and **H)** labelled cells expand and occupy prospective forearm region, note cells are not touching the apical ridge. **I)** is an example of a subapical mesenchyme injection labelled at somite 17/18, fixed and photographed at time zero.

J-M Proximal mesenchyme injections at base of the bud (250μm from somites) **J)** labelled cells remain anterior and end up anterior to limb, **K)** labelled cells expand and are at base of limb, **L)** labelled cells are at base of limb and expand toward posterior margin, **M)** labelled cells form a stream between proximal regions and prospective forearm.

N-P Proximal mesenchyme injections adjacent to the somites (50-75μm from somites) **N)** labelled cells remain proximal, end up next to somites, proximal and anterior to scapula (arrow) and humerus, **O)** labelled cells end up outside the limb, **P)** labelled cells remain proximal, end up in flank posterior to the limb. Scale bar represents 500μm. Anterior: up; Posterior: down; Distal: right; proximal: left.

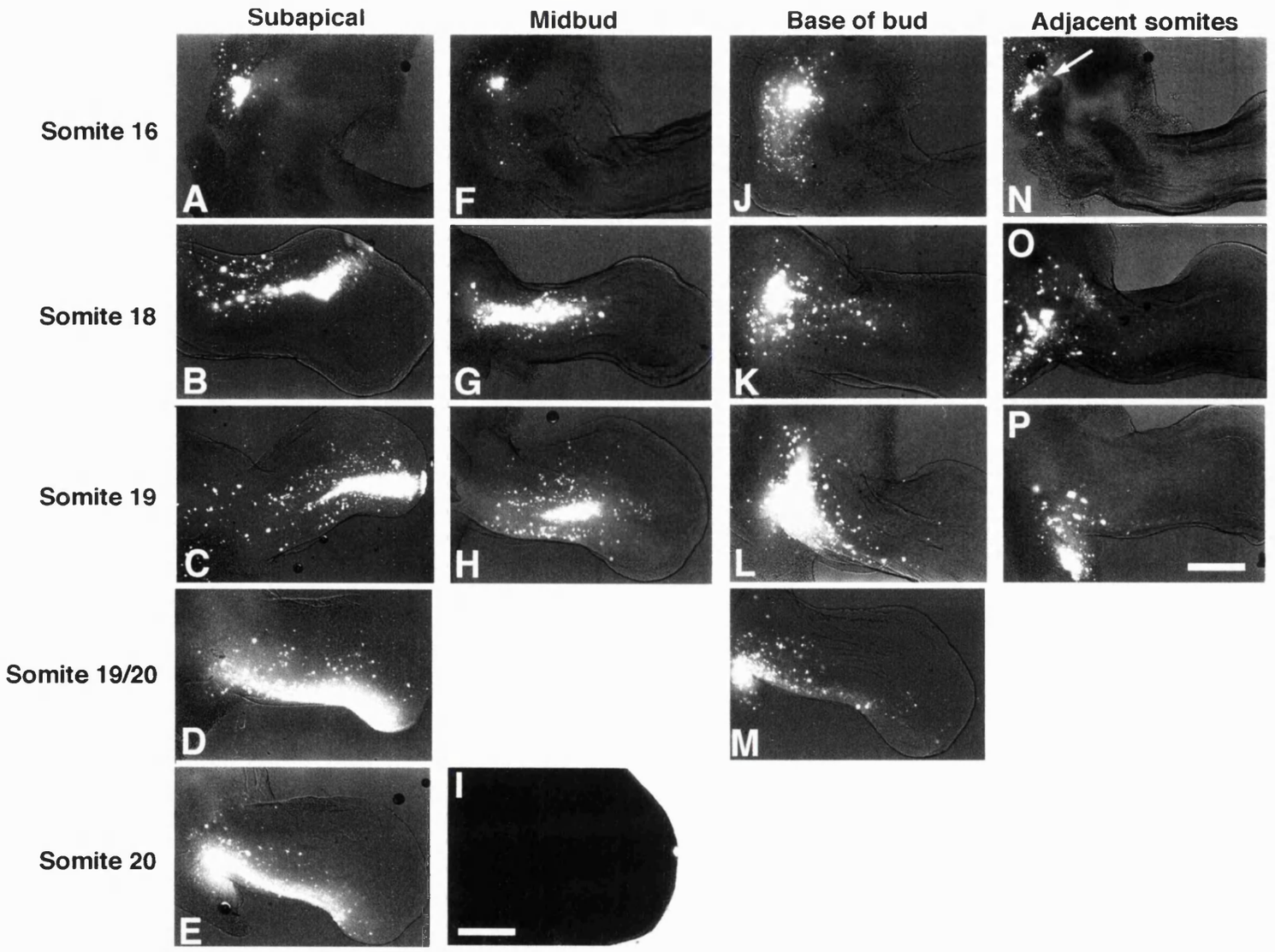
Subapical
Midbud
Base of bud
Adjacent somites
Somite 16
Somite 18
Somite 19
Somite 19/20
Somite 20
A
B
C
D
E
F
G
H
I
J
K
L
M
N
O
P

Figure 3.4

Fatemaps of apical ectodermal ridge and subapical mesenchyme.

(A-E) **Apical ectodermal ridge** labelled wing bud. **A**) control time zero injection into apical ridge opposite somite 17/18. **B-E** Examples of wing buds incubated for 48 hours after injection of DiI into apical ectodermal ridge at different antero-posterior levels with reference to somites, **B**) opposite somite 17. Note labelled cells are no longer in apical ridge but in non-ridge ectoderm, arrowheads indicate extent of apical ridge, **C**) opposite somite 17/18. **D**) opposite somite 19. Note a little DiI was also injected into non-ridge ectoderm in this specimen. **E**) opposite somite 19/20. Note in **D** and **E** long thin ribbons of labelled cells (compare with spot of labelled cells in anterior injections; Fig. 3.4B). Scale bar represents 500μm.

(F and L) **Leg bud mesenchyme**. Examples of legs incubated for 48 hours after injection of DiI into subapical mesenchyme at stage 20: **F**) opposite somite 28/29, note anterior shift, **L**) opposite somite 31/32, note no anterior shift. Scale bar represents 500μm.

(G-K) **Wing bud mesenchyme**. Examples of wing buds incubated for 96 hours after injection of DiI into subapical mesenchyme at stage 20: **G**) opposite somite 17; labelled cells anterior to digit **2**, **H**) opposite somite 17/18; labelled cells contributing to digit **2**, **I**) opposite somite 18; note labelled cells fanning out towards anterior tip and ending up between digit **2** and **3** (asterisk), **J**) opposite somite 18/19; labelled cells contributing to digit **3**, **K**) opposite somite 19/20; labelled cells contributing to digit **4**. Scale bar represents 650μm. Anterior: top; posterior: bottom; Distal: right; Proximal: left.

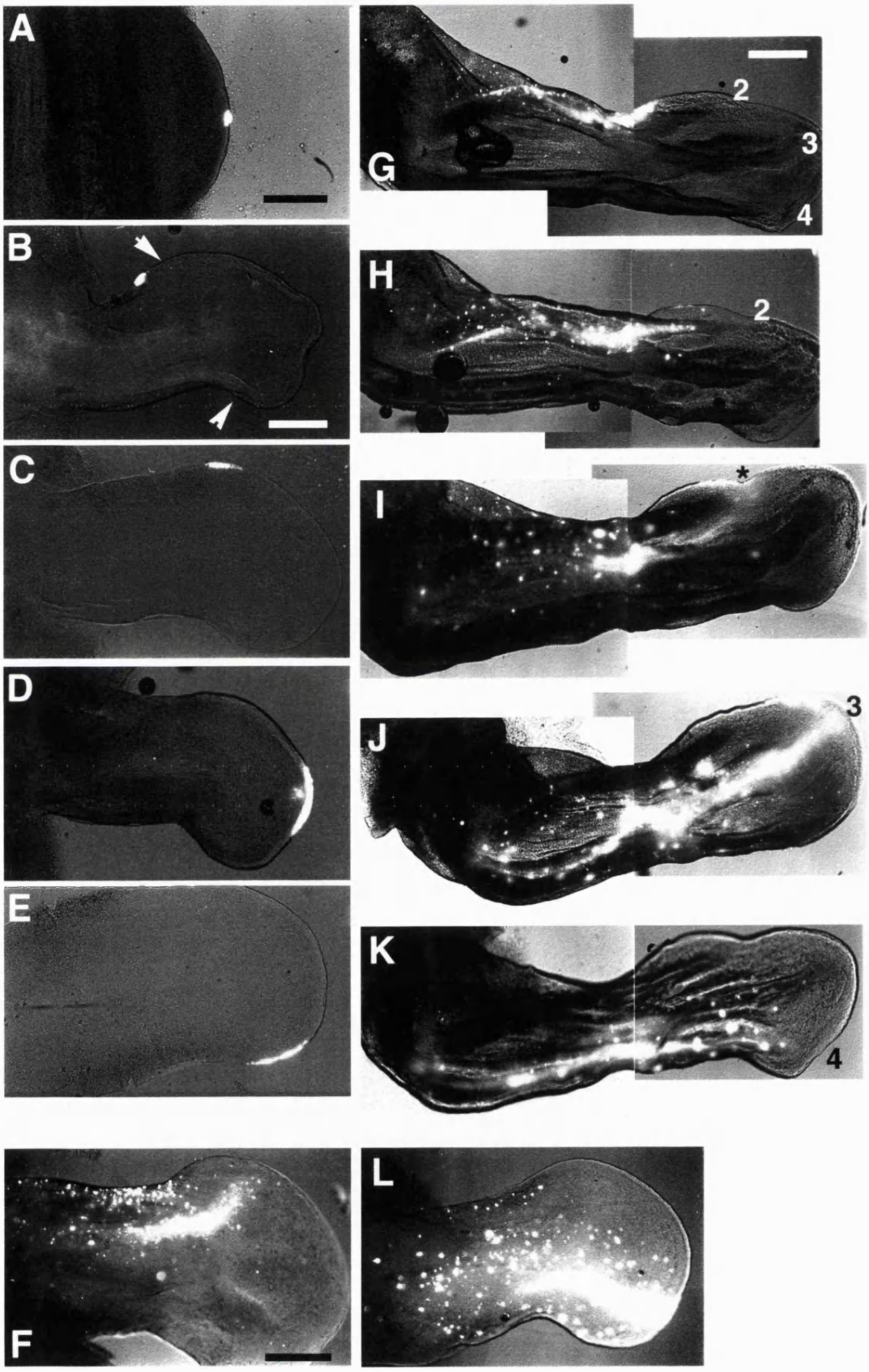
A
B
C
D
E
F
G
2
3
4
H
2
I
*
J
3
K
4
L

Figure 3.5

Wing buds in which two cell populations were labelled at stage 20 to assess relative displacements and cell mixing after 48 hours. **A)** Subapical mesenchyme (DiI) and apical ridge (DiA) were both initially labelled opposite somite 18. Labelled ridge cells come to lie anterior to labelled mesenchyme. **B)** Relative displacement of subapical mesenchyme and apical ectodermal ridge. Left is a diagram of a stage 20 wing bud showing positions in which apical ridge and mesenchyme were labelled at same antero-posterior levels. Positions are numbered 1-6 so that positions where labelled cells end up can be matched to original positions. Right, resulting limb 48 hours later showing positions of labelled cells in mesenchyme in relation to position of labelled cells in apical ridge. Note that apical ridge ends up anterior to mesenchyme except opposite somite 17 where apical ridge and mesenchyme remain in register and opposite somite 16 where mesenchyme is proximal to apical ridge. Scale bar represents 500μm. Numbers in μm indicate average displacement between labelled mesenchyme and apical ridge (between 2 and 8 cases for each value). **C)** Apical ridge labelled on a level with somite 17/18 with DiA and somite 18 with DiI, 48 hours after labelling; Note populations are still discrete. **D)** Higher magnification of **C**, photographed under fluorescence only, showing intermingling of labelled cells with non-labelled cells in apical ridge. Arrow indicates some labelled cells in non-labelled cell territory. Scale bar represents 100μm. **E)** Subapical mesenchyme populations with DiI opposite somite 18/19 and with DiA opposite somite 19, 48 hours after labelling. Note distinct separate domains, distally, but overlapping and intermingling of scattered cells proximally. **F)** Proximal mesenchyme, 50-75μm from somites labelled with DiI on a level with somite 18/19 and DiA on a level with somite 19, 48 hours after labelling. Note overlap and that DiA cells now lie mostly distal to DiI cells. Scale bar represents 500μm in A, C, E and F.

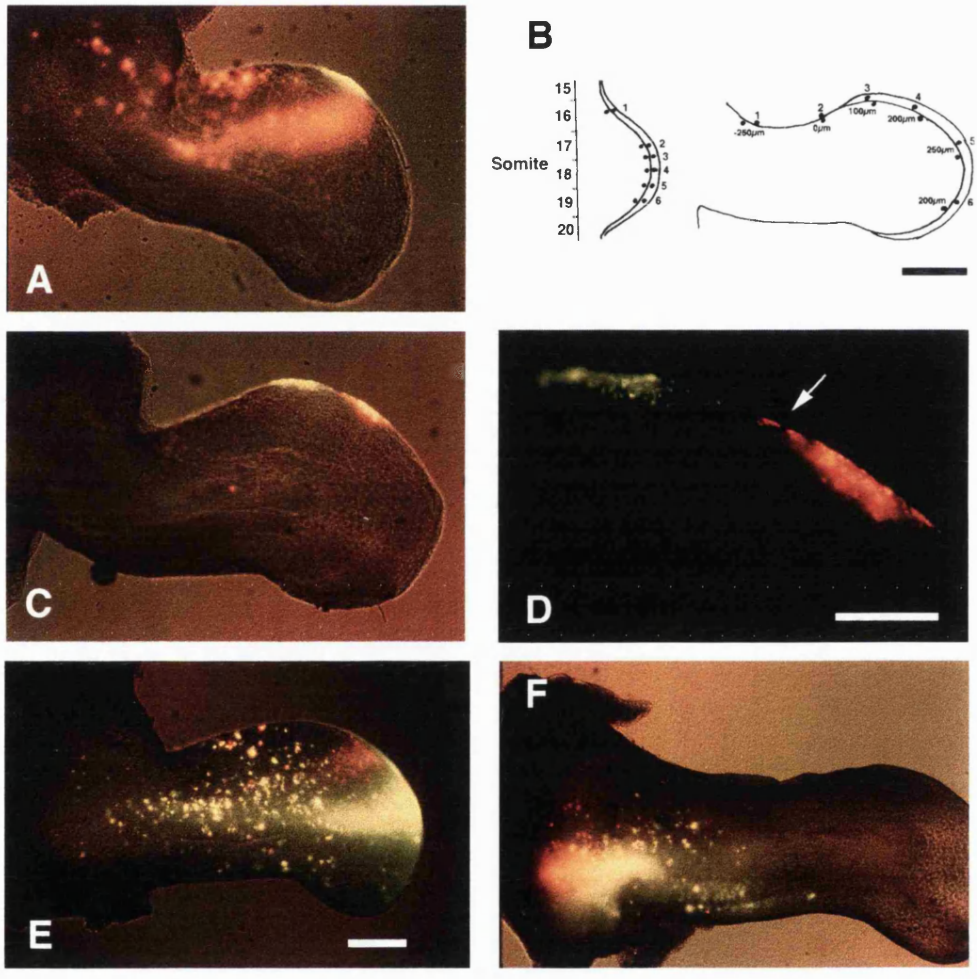
A
B
Somite
15
16
17
18
19
20
1
2
3
4
5
6
-250µm
0µm
100µm
200µm
250µm
200µm
C
D
E
F

populations labelled in the middle third showed greatest expansion, occupying 10% of the limb area (n=15) and form streams of cells in the central region of the limb, lying in the prospective forearm region (Fig. 3.2A, 3.3G). In the posterior third, labelled cell populations showed large expansion occupying 8.5% of the limb area (n=7) and formed streams running into the prospective wrist area (Fig. 3.3H).

ii) Labelled mesenchyme at the base of the bud (250μm from the somites) at stage 20, was generally found at the base of the limb 48 hours later (Fig. 3.1D). Cell populations labelled within the anterior third remained proximal and did not expand much, occupying 2.5% of the limb area (n=3; Fig. 3.2A, 3.3J). Labelled cell populations in the middle third also remained proximal but showed greater expansion than anterior cell populations occupying 8% of the limb area (n=18; Fig. 3.3K). Posterior populations of labelled cells formed streams running along the posterior margin into presumptive forearm and occupied 9.5% of the limb area (n=8; Fig. 3.2A, 3.3L,M). There was a large amount of overlap and intermingling between neighbouring labelled populations of cells, and the labelled populations did not always keep in the same relative positions.

iii) Labelled mesenchyme adjacent to the somites, in the body wall (50-75μm from the somites), at stage 20, remained more or less next to the somites, outside the limb, 48 hours after injection (Fig. 3.1E). In the anterior third, labelled populations ended up proximal and anterior to humerus and scapula and expanded almost uniformly over the 48 hour incubation period, occupying 2.5% of the total limb area (n=3; Fig. 3.2A, 3.3N). Cell populations labelled more posteriorly, in the middle third, underwent greater expansion, which was still fairly uniform and were found proximal to the humerus, occupying 7% of the limb area (n=17; Fig. 3.3O,P). Very posterior populations of cells formed short proximo-distal streams running from the somites along the posterior margin into the central region of the limb, occupying 8.5% of the limb (n=11). The labelled cell populations overlapped. Populations in middle and posterior thirds in particular do not stay in the same relative positions as when initially labelled. For example, a population of cells labelled on a level with somite 18/19, ended up in a proximal position adjacent to cells labelled opposite somite 19 (Fig. 3.1E, 3.5F).

Leg mesenchyme

DiI was injected subapically into the stage 20/21 chick leg, again using the somites and somite boundaries as reference points. As in the wing, populations of cells labelled in the anterior third (i.e.: opposite somite 26, 26/27, 27, 27/28) expanded to form short stripes of labelled cells which remained proximal (Fig. 3.1H). In contrast populations of cells labelled in the middle third of the leg bud (i.e. opposite somite 28,

28/29, 29, 29/30) expanded considerably, remained distal and their progeny formed streams of labelled cells running between apical ectodermal ridge and proximal regions of the leg. An anterior bending of cell populations labelled in the middle third was observed toward the anterior tip of the leg, although the shift did not appear to be as great as in the wing (Fig. 3.4F). Populations of labelled cells in the posterior third of the leg bud (i.e. opposite somite 30, 30/31, 31, 31/32 and 32) also expanded, fanning out posteriorly and forming streams running from apical ridge into prospective foreleg region (Fig. 3.4L). Mesenchyme cells on a level between somites 28 and 29 give rise to digit **1**, somite 29/30-30 for digit **2**, somite 30/31 for digit **3** and somite 31 for digit **4**.

Mesenchymal cell fate and apical ridge signalling

In order to investigate how the apical ridge affects the expansion of mesenchyme cell populations, the apical ridge was removed from stage 20 wing buds. Small populations of mesenchyme were labelled with DiI in subapical and proximal positions using the somites as reference points and development allowed to proceed for 48 hours (n=24). Cell populations labelled subapically were grossly affected by apical ridge removal. Populations labelled on a level with somite 16/17 (Fig. 3.6A) appeared to behave as normal as shown in fate maps, but subapical populations posterior to somite 17 (Fig. 3.6B) did not expand much and did not form the wide long streams stretching between proximal regions and the apical ridge (Fig. 3.6C, D, E, F) as shown in the normal fatemaps. In essence the mid limb and posterior subapical populations following apical ridge removal behaved like anterior populations with or without an apical ridge. The apical ridge therefore controls subapical mesenchyme cell behaviour. In contrast, the behaviour of labelled proximal mesenchyme populations (Fig. 3.7) following apical ridge removal is generally unchanged, except in very posterior proximal positions (Fig. 3.7B; compare with Fig. 3.1, 3.3); the cell populations do not expand and remain proximal. As expected the apical ridge has little affect on proximal cell behaviour.

3.2.1.2 *Fate map of the apical ectodermal ridge*

Cells in the apical ridge of a stage 20 wing bud were DiI labelled at different antero-posterior positions, using somites as reference points. Both basal cells and periderm cells were probably labelled. The labelled cells were initially in a patch 25μm in diameter (Fig. 3.4A) containing 50-75 cells, and after 48 hours incubation, these formed a fairly compact ribbon of labelled cells in the ridge. It was also noted that cells labelled in the apical ridge, remained in the apical ridge or ectodermal layer at all times; none were found in the mesenchyme. Average expansion for each site of injection is shown in Fig. 2C.

Figure 3.6

The effect of apical ridge removal on subapical mesenchymal cell behaviour

To investigate the effect of the ridge on subapical mesenchyme cell behaviour, the ridge was removed at stage 20/21 and mesenchyme populations labelled with DiI using the somites as reference positions. After 48 hours, all the limbs (A-F) were truncated and considerably smaller than contralateral limbs, see **G**). Cell populations labelled in anterior subapical mesenchyme **A**), on a level with somite 16/17; **B**), on a level with somite 17 had similar patterns of DiI spread as when compared to normal fate maps (see Fig. 3.1, 3.3) suggesting the apical ridge does not have much influence upon anterior subapical populations. Cell populations labelled in more posterior apical positions following apical ridge removal had very different patterns of DiI spread as compared to normal fate maps (see Fig. 3.1, 3.3); **C**) cell populations labelled on a level with somite 17/18 which normally form a long stream between the apical ridge and central regions of the limb, forms a small stream; **D**) populations labelled on a level with somite 18, which normally forms a long stream between central mesenchyme and the distal tip which shifts anteriorly into the anterior tip of the limb, remains in the position it was labelled and does not expand a great deal, see also **E**), populations labelled on a level with somite 18/19 and **F**), somite 19/20. This suggests that the apical ridge is essential for regulating subapical mesenchyme fate and cell movement. **G**) is an example of a contralateral limb with apical ridge intact. Scale bar represents 500μm. **H**) On the right, an example of the cartilage pattern of a limb following apical ridge removal at stage 21, note no distal structures present and on the left a normal, contralateral limb. Scale bar represents 2000μm.

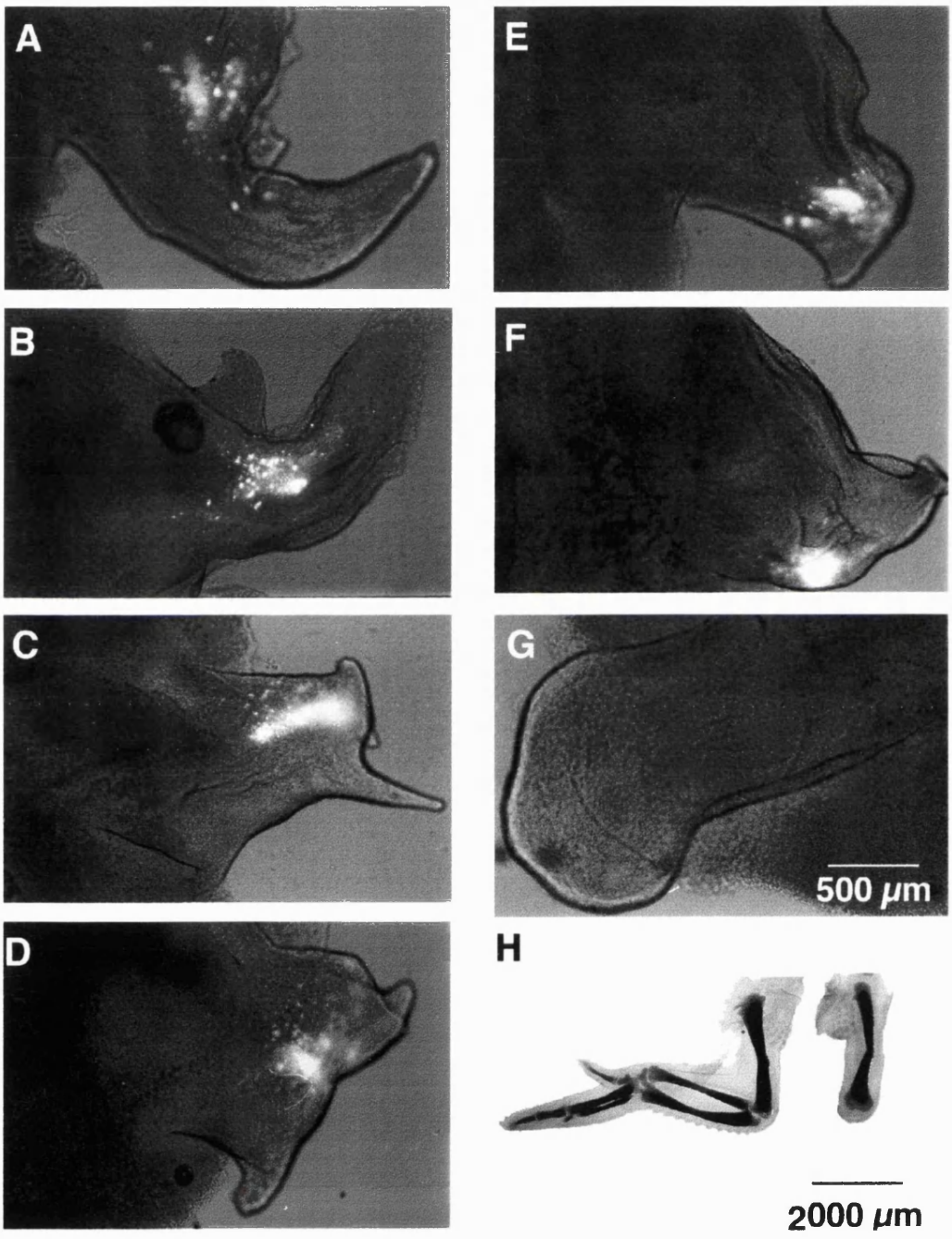
A
B
C
D
E
F
G
500 μm
H
2000 μm

Figure 3.7

The effect of apical ridge removal on proximal mesenchymal cell behaviour

Following apical ridge removal in stage 20/21 wing buds, populations of mesenchyme were DiI labelled in proximal mesenchyme positions as shown in **A'**), to investigate the effect of the apical ridge upon proximal populations, scale bar represents 150μm. The limbs are all truncated. **A**) Proximal anterior mesenchyme remains in proximal anterior mesenchyme and do not expand a great deal, as for normal fate maps. **B**) Proximal posterior mesenchyme and **C**) posterior mesenchyme labelled 200μm from the apical tip remain where labelled and do not expand a great deal. These results are different to normal fate maps where at position B, a long stream of label is normally observed running along the posterior margin and at position C, a stream of label is within the prospective forearm region (see Fig. 3.1, 3.3), however the limb is truncated and distal area is missing; **D**) Mesenchyme labelled 200μm from the apical tip on a level with somite 18 and **E**) anterior mesenchyme labelled 200μm from the tip on a level with somite 16/17 all remain where they were originally labelled, not expanding much. This shows that proximal mesenchyme is not influenced by the apical ridge. Scale bar represents 250μm in A, B, C, D and E.

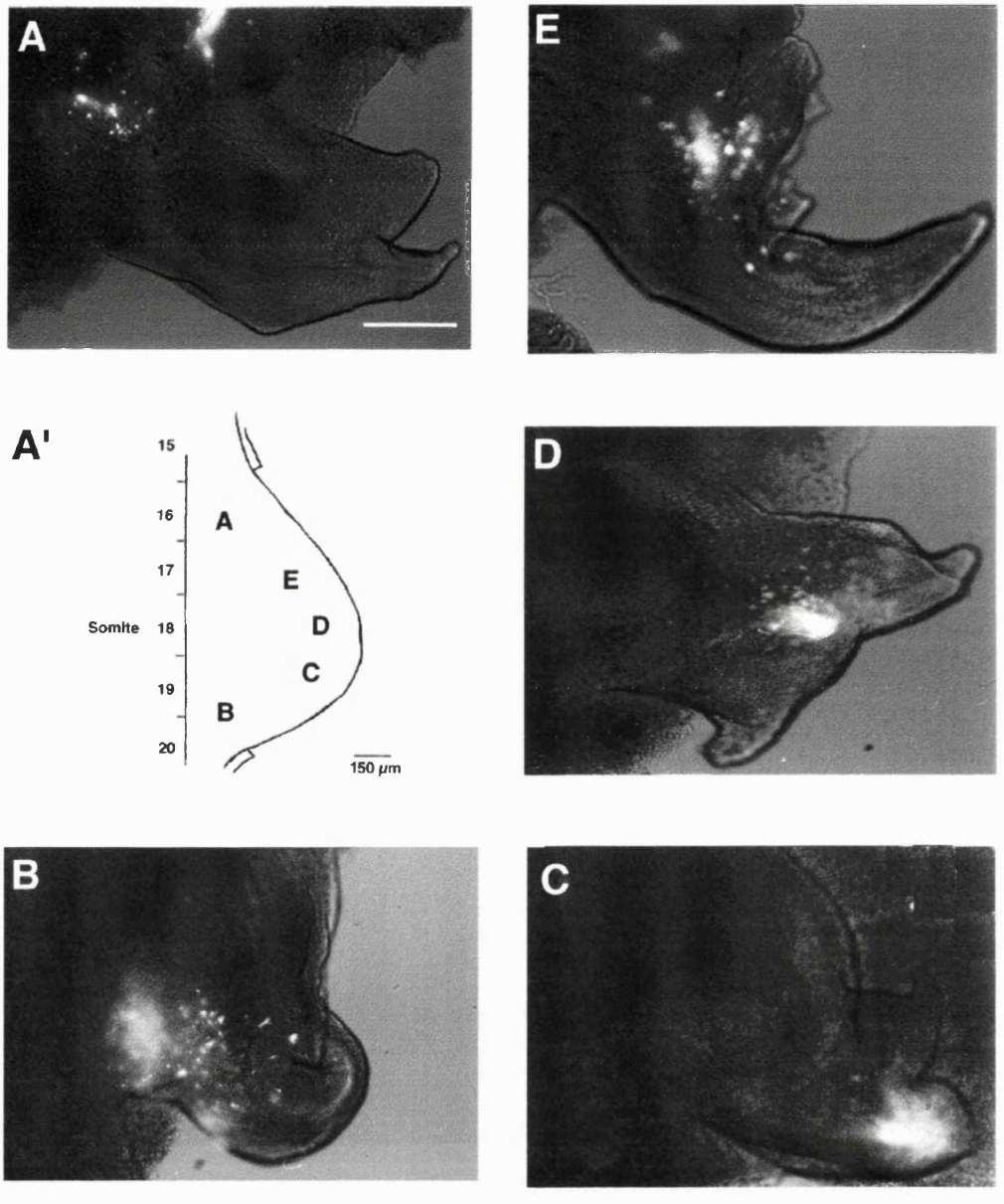
A
E
A'
15
16
17
Somite 18
19
20
A
E
D
C
B
150 μm
D
B
C

Labelled cells in anterior third and anterior part of the middle third of the ridge showed some expansion and remained proximal (Fig. 3.4B). Moreover by 48 hours, these labelled cells appeared to have moved out of the apical ridge, into non-apical ridge ectoderm on the anterior margin of the wing bud (Fig. 3.4B). The cell population labelled in the middle apical ridge (i.e. opposite somite 17/18 and 18) showed greater expansion, over the 48 hour incubation period, remaining within and occupying approximately 25% of the final total length of the apical ridge (Fig. 3.4C). Posterior populations of labelled ridge cells showed the greatest expansion (Fig. 3.4D) coming to occupy approximately 50% of the final total area of the apical ridge (Fig. 3.2C) suggesting a posterior bias in proliferation as in the mesenchyme. At the borders of the labelled populations, it was noted that some labelled cells could be seen outside the main labelled domain, appearing to intermingle with cells in the non-labelled area of apical ridge (see also Fig. 3.5C).

To investigate specifically the extent of cell mixing within the apical ectodermal ridge, two populations of apical ridge cells were labelled and the distance between them measured immediately after injection and again after 48 hours incubation. When the apical ridge was labelled with DiI at somite 18 and DiA on a level with somite 18/19, the spots were found on average to be 153μm apart at time zero (n=6). After 48 hours incubation the labelled populations had expanded as expected from the fate map, and individual domains were easily visible, and were still around 100μm apart (Fig. 3.5C). Although some cells were observed intermingling with unlabelled cells (Fig. 3.5D). This suggests that there is some local but no widespread translocation of cells within the apical ridge.

In order to examine relative movements of apical ridge and underlying mesenchyme, populations of apical ridge cells were labelled on a level with a particular somite with DiI and cells in the mesenchyme at the same somite level labelled with DiA and the relative positions of labelled cells in mesenchyme and apical ridge examined 48 hours later (Fig. 3.5B). When mesenchyme and apical ridge were labelled at the same level at different positions between somite 17/18 and somite 19/20, the labelled apical ridge ended up further anterior than the mesenchyme, by up to 250μm (Fig. 3.5A). For injections on a level with somite 17, there was no anterior displacement of the ridge and mesenchyme and ectoderm appeared to stay in register, but at somite 16 the mesenchyme remained more proximal than labelled ectoderm. Thus the apical ridge does not stay in register with the mesenchyme but generally shifts anteriorly (Fig. 3.5B).

3.2.2 Cell lineage and the relationship to gene expression

DiI labelling can be used to mark populations of cells within gene expression domains and investigate the relationship between cell fate and gene expression. FGF-4 is

an important ridge signal and *Hoxd-13* and *Hoxa-13* have important roles in hand plate development.

3.2.2.1 *Fgf-4*

Fgf-4 transcripts are found in the posterior of the apical ridge at stage 20/21 and the anterior limit of expression is on a level with somite 17/18 (Fig. 3.8H). *Fgf-4* appears to be expressed throughout the apical ridge at stage 24 but at around stage 26 expression disappears (Niswander and Martin, 1992; Duprez et al., 1996b). To investigate the relationship between *Fgf-4* expression and cell lineage, populations of apical ridge cells were labelled with DiI on the anterior boundary of the *Fgf-4* expressing part of the ridge and both just inside and just outside the domain of expression at stage 20/21 (Fig. 3.8G). The accuracy of the labelling was confirmed by observing the fluorescence pattern followed by whole mount in situ hybridisation and the labels were found in the appropriate locations in 10/12 cases. Limbs were incubated for 24 hours, the position of labelled cells recorded and then whole mount in situ hybridisation for *Fgf-4* was carried out to compare the relationship between expression and the labelled cells. Cells labelled on the *Fgf-4* expression border remained on the *Fgf-4* expression border 24 hours later (n=3; Fig. 3.8J). Cells, labelled just anterior to the expression domain, remained anterior to the expression domain (n=3; Fig 3.8I) and cells labelled within the expression domain (n=3) remained within the domain 24 hours later (Fig. 3.8K). This data suggests that *Fgf-4* expression expands throughout the apical ridge as development proceeds due to cell movement, not by induction of *Fgf-4* expression in previously non-expressing cells.

3.2.2.2 *Hoxd-13*

Hoxd-13 transcripts are initially observed restricted to the posterior distal region of the wing mesenchyme at stage 19. By stage 20/21, the anterior limit of expression is on a level with somite 18 (Fig. 3.8B), but 48 hours later *Hoxd-13* transcripts are found in prospective distal hand plate (Fig. 3.8F). The relationship between expression of *Hoxd-13* and cell lineage was investigated by marking cells in stage 20 wing buds outside the expression domain, at the boundary of the expression domain and within the domain. For each set of labelled positions relative to the perimeter of the *Hoxd-13* domain, cells were marked at distal end, at proximal end and midway along the perimeter boundary (Fig. 3.8A). The accuracy with which these marks were placed was confirmed by whole mount in situ hybridisation immediately after observing the fluorescence pattern (Fig. 3.8A). In such time zero specimens, labelled cells were found to be respectively on the border (3/4 cases), above (3/3 cases) or within (3/3 cases) the *Hoxd-13* expression

Figure 3.8

Relationship between cell lineage and gene expression.

(A-F) ***Hoxd-13*** **A)** Example of stage 20/21 wing with DiI label applied in 3 positions in non-expressing cells just outside the perimeter of the expression domain of *Hoxd-13* and fixed immediately. **B)** Same wing bud as in **A)** after whole mount in-situ hybridisation to show pattern of *Hoxd-13* expression. Arrowhead indicates anterior boundary of *Hoxd-13* expression on a level with somite 18. Scale bar represents 650μm. **C)** Wing bud incubated for 48 hours after DiI labelling in 3 positions outside expression domain of *Hoxd-13* at Stage 20. None of the labelled cells lie within expression domain of *Hoxd-13* (compare with **F** whole mount showing *Hoxd-13* expression at stage 28. Note *Hoxd-13* expression fills most of the handplate; see arrowhead). **D)** Wing bud 48 hours after DiI labelling in 3 positions on boundary of expression domain of *Hoxd-13* at stage 20. Labelled cells on proximal boundary are now a long way from region of *Hoxd-13* expression; labelled cell population on anterior boundary is still associated with boundary and also extend proximally (compare with **F**). **E)** Wing bud 48 hours after DiI labelling in 3 positions just within the perimeter of the expression domain of *Hoxd-13* at stage 20. Cells initially labelled proximally within the domain are now well outside the domain. Cells which were labelled in an anterior position within the domain are still found within the region of expression and extend proximally. Scale bar represents 500μm.

(G-L) ***Fgf-4*** **G)** Example of stage 20/21 wing bud DiI labelled on anterior boundary of expression domain of *Fgf-4* and fixed immediately (same scale as A,B). **H)** Same wing bud as in **G** after whole mount in situ hybridisation. Arrow head indicates anterior boundary of *Fgf-4* expression in apical ridge on a level with somite 17/18. **I)** Wing bud 24 hours after DiI labelling anterior to *Fgf-4* expression domain at stage 20. Labelled cells (arrowhead) lie anterior to anterior boundary of *Fgf-4* expression (compare with **L**, whole mount showing *Fgf-4* expression at stage 25. *Fgf-4* expression switches off at around stage 26. Note arrowhead indicating anterior boundary of *Fgf-4)*. **J)** Wing bud 24 hours after DiI labelling on anterior border of *Fgf-4* expression domain at stage 20. Labelled cells remain on border (see arrowhead). **K)** Wing bud 24 hours after DiI labelling within the expression domain of *Fgf-4* at Stage 20. Labelled cells remain within domain (see arrowhead). Scale bar represents 200μm.

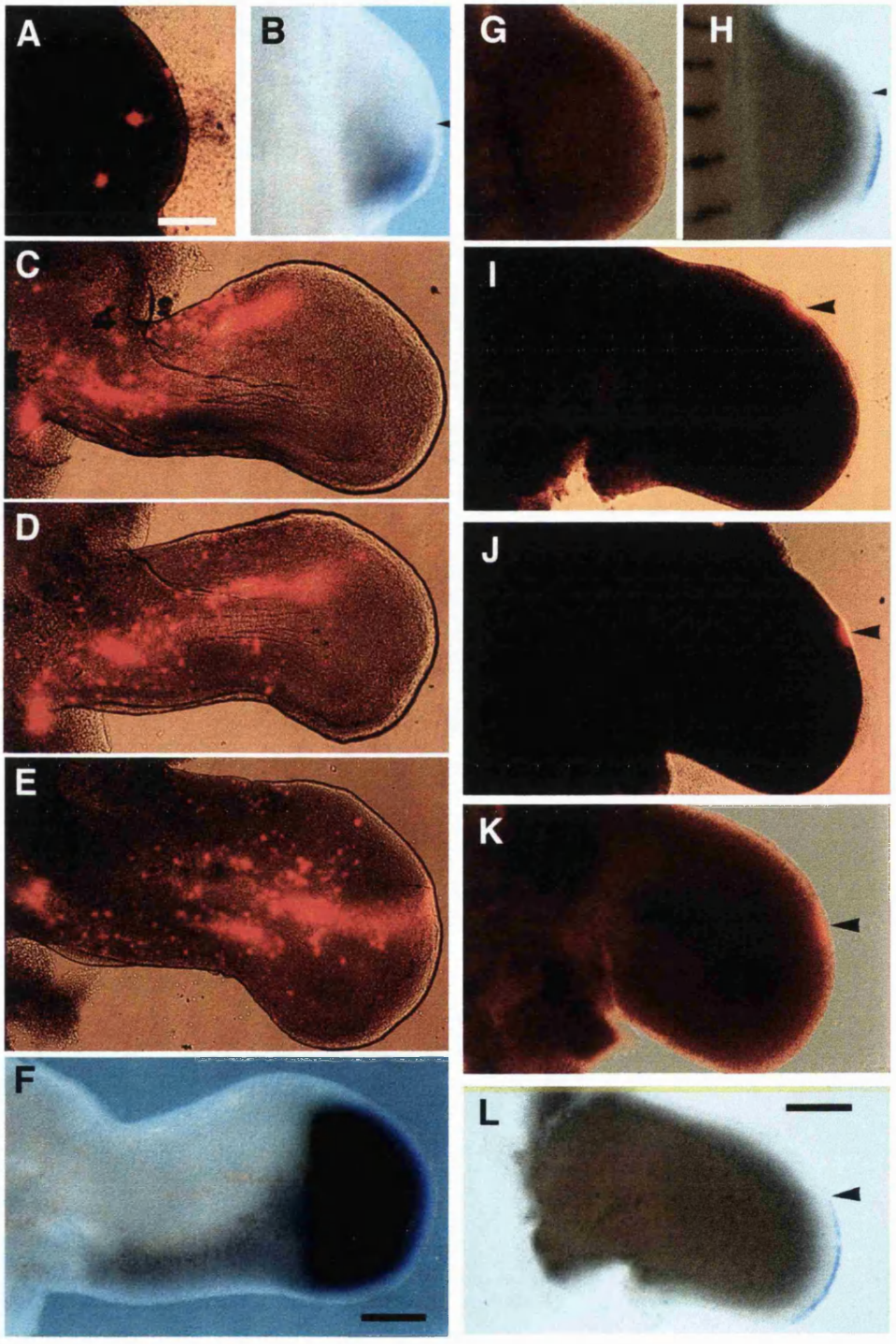
A
B
G
H
C
I
D
J
E
K
F
L

domain (Fig. 3.8A,B). Limbs were incubated for 48 hours after labelling, the position of the labelled cells recorded and then whole mount in situ hybridisation was carried out for *Hoxd-13*. Cells labelled at stage 20 just outside the perimeter of the *Hoxd-13* domain were not incorporated into the domain (n=5; Fig. 3.8C,F). Cells labelled at perimeter boundary of *Hoxd-13* domain at stage 20 remained on the boundary distally 48 hours later but proximally fell out of the domain (n=5; Fig. 3.8D,F). Distally, cells labelled just inside the perimeter of the *Hoxd-13* domain remained in the domain but proximally ended up outside the domain (n=4; Fig. 3.8E,F). This result shows that expansion of *Hoxd-13* expression is due largely to cell movement and proliferation and not induction of previously non-expressing cells.

3.2.2.3 *Hoxa-13*

Hoxa-13 transcripts are initially observed at stage 21 and are restricted to postero-distal mesenchyme but 48 hours later, at stage 28, they occupy the entire handplate. Elaboration of the *Hoxa-13* expression domain in relation to cell lineage was investigated by DiI labelling populations of cells on, above or below the anterior distal domain of expression at stage 21/2 and following their fate over 48 hours (as above). The anterior distal boundary of *Hoxa-13* at stage 21/22 is on a level with somite 18 (Fig. 3.9A). Populations of cells were labelled with DiI above (on a level with somite 17) just above (on a level with somite 17/18), on (somite 18) or below (somite 18/19) the anterior distal boundary of *Hoxa-13* expression at stage 21/22 (Fig. 3.9A). The accuracy of injections was confirmed by whole mount in-situ hybridisation performed upon limbs fixed immediately after injection for *Hoxa-13* which showed the injections in the correct positions in relation to the expression domain (n=6 for each position). Experimental embryos were incubated for 48 hours and the limbs then observed using a fluorescence microscope to monitor the position of labelled cells. The position of mesenchyme labelled cells was compared to the position of *Hoxa-13* expression by whole mount in situ hybridisation (Fig. 3.9F). Populations of cells labelled on or just above the anterior distal boundary at stage 21/22 were 48 hours later within the expression domain of *Hoxa-13* (Fig. 3.9B, C). Populations of cells labelled within the domain at stage 21/22 remained associated within the expression domain although some cells had fallen out of the expression domain proximally and ceased expressing *Hoxa-13* (Fig. 3.9E). Cell populations labelled above the domain, on a level with somite 17 at stage 21/22 come to be at the anterior boundary of *Hoxa-13* 48 hours later (Fig. 3.9B). This result shows that the expression pattern of *Hoxa-13* expands anteriorly as development proceeds by the induction of expression and incorporation of previously non-expressing cells. Similar results were achieved by Nelson et al. (1996). This result is in contrast to that obtained

Figure 3.9

Relationship between cell lineage and *Hoxa-13* expression

A) Example of stage 21/2 wing bud after whole mount in-situ hybridisation to show *Hoxa-13* expression. Arrowhead marks anterior boundary of *Hoxa-13* expression on a level with somite 18. Scale bar represents 600μm. **B)** Wing bud 48 hours after being DiI labelled above the domain of *Hoxa-13* expression on a level with somite 17 at stage 21/2. The labelled cells lie close to or on the anterior limit of *Hoxa-13* expression (compare with **F**.). **C**) Wing bud 48 hours after being DiI labelled just above the anterior limit of *Hoxa-13* expression on a level with somite 17/18 at stage 21/2. Note the cells lie within the *Hoxa-13* domain (compare with **F**.). **D**) Wing bud 48 hours after being DiI labelled on the anterior limit of *Hoxa-13* expression, on a level with somite 18, at stage 21/2. Note the cells are within the *Hoxa-13* expression domain. **E**) Wing bud 48 hours after being DiI labelled within the *Hoxa-13* expression domain, on a level with somite 18/19 at stage 21/2. Note the cells are well within the expression domain of *Hoxa-13*. **F**) Whole mount showing a stage 28 limb following whole mount in-situ hybridisation for *Hoxa-13*. Scale bar represents 500μm.

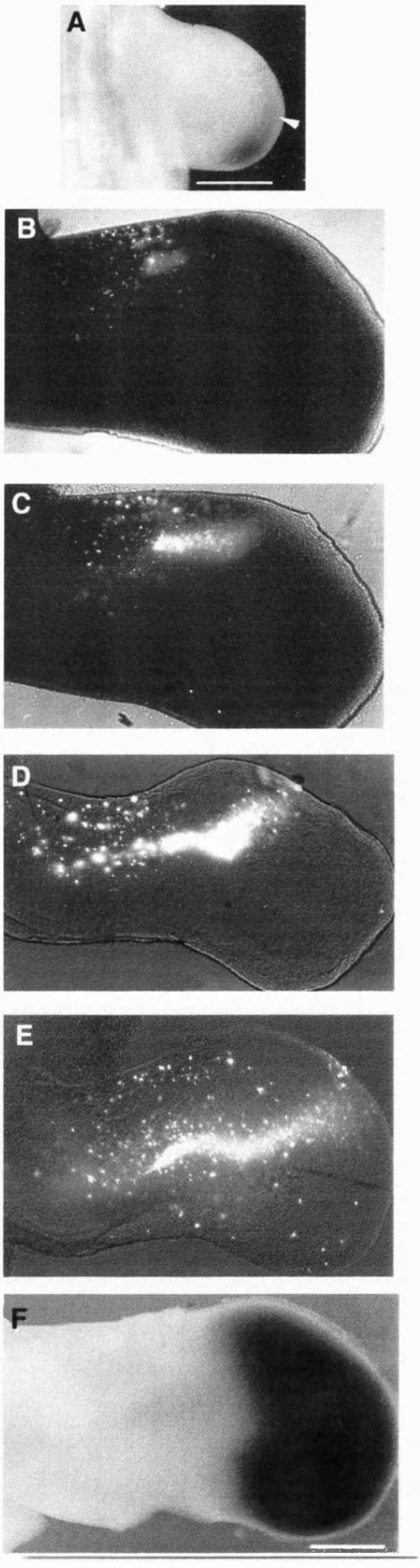
A
B
C
D
E
F

for *Hoxd-13* where the expansion of early *Hoxd-13* expression from postero-distal mesenchyme to end up across the antero-posterior axis of the hand plate appears to be due to expansion of the original domain of expressing cells. Thus, elaboration of expression of genes of the *HoxA* and *HoxD* complexes may be controlled by different mechanisms. It should be noted that *Hoxa-13* expression is activated 8-12 hours after that of *Hoxd-13* which further suggests that activation and elaboration of *Hoxa-13* is not regulated by the same signals as for *Hoxd-13* expression (Nelson et al., 1996).

3.2.3 Initiation of *HoxA* gene expression

Relatively little is known about the way in which *HoxA* gene expression is initiated and maintained in developing limbs. The 5' *HoxA* genes are expressed along the proximo-distal axis of the limb bud following the rules of temporal colinearity like the *HoxD* genes. The 5' *HoxA* genes are thought to be involved in the segmentation of the proximo-distal axis and the morphogenesis of limb cartilage elements where *Hoxa-10* specifies humerus, *Hoxa-11* forearm and *Hoxa-13* hand plate and digits (Yokouchi et al., 1991b, 1995). *Hoxa-13* expression, together with that of *Hoxd-13,* is important for digit development as in double knockout mice digits are lost (Fromental-Ramain et al., 1996). *HoxD* gene expression has been extensively studied and initiation appears to require a polarising region signal and an apical ridge signal, for example retinoic acid and FGF or *Shh* and FGF or *Bmp-2* and FGF-4 (Izpisua-Belmonte et al., 1992b; Niswander et al., 1994; Laufer et al., 1994; Duprez et al., 1996b). Here, I begin to examine how initiation and expansion of the *Hoxa-13* expression domain is controlled and how *Hoxa-13* expression is related to apical ridge FGF signalling.

3.2.3.1 *Expression patterns of 5' HoxA genes*

The expression patterns of *Hoxa-10*, *Hoxa-11* and *Hoxa-13* in the developing limb bud have previously been characterised for the chick (Yokouchi et al., 1991b; Nelson et al., 1996) and mouse (Haack and Gruss, 1993).

Expression of *Hoxa-10* in the chick wing bud is first observed at stage 19 (Nelson et al., 1996) and by stage 21 is observed strongly in central mesenchyme and faintly in distal mesenchyme (Fig. 3.10A). As development proceeds, expression almost fills the limb bud but is stronger proximally (Fig. 3.10B, C) until around stage 25 when fainter expression is restricted to proximal central mesenchyme (Fig. 3.10D). By stage 28 expression is restricted to proximal regions of the limb, stretching from the proximal base of the limb which will produce the distal part of the humerus and elbow joint (stylopod)

Figure 3.10

Expression patterns of *Hoxa-10*, *Hoxa-11* and *Hoxa-13*

A-E Whole mount limbs showing various stage limbs following whole mount in situ hybridisation for *Hoxa-10*. **A)** Stage 21, transcripts throughout the posterior two-thirds of the bud. **B)** Expression of *Hoxa-10* by stage 23 has expanded to fill the majority of the limb bud. **C)** Stage 24, expression appears to be restricted to central proximal mesenchyme and is faint in distal regions. **D)** Stage 25/6, *Hoxa-10* expression is no longer detectable in distal regions, but is expressed throughout the proximal region, strongly near the posterior margin. Scale bar represents 500μm in A, B, C and D. **E)** Stage 28, expression is seen throughout the prospective humerus and forearm regions, particularly clearly along the anterior margin and posterior margin. Scale bar represents 550μm. F-J Whole mount limbs showing various stage limbs following whole mount in situ hybridisation for *Hoxa-11*. **F)** *Hoxa-11* expression appears throughout the central and distal regions of the limb at stage 21. **G)** and **H)** Stages 23 and 24, expression is throughout the distal mesenchyme up to the apical ridge. Note expression domain of *Hoxa-11* by comparison appears to be within domain of *Hoxa-10* expression. **I)** From stage 25/6, expression of *Hoxa-11* is reduced in distal domains but maintained in the prospective forearm regions. No expression is observed proximally but expression overlaps with that of *Hoxa-10* in central mesenchyme. Scale bar represents 500μm in F, G, H and I. **J)** Stage 28, expression is restricted to the forearm region particularly along anterior and posterior margins. Note no expression proximally or distally. Scale bar represents 550μm. K-O Whole mount limbs showing various stage limbs following whole mount in situ hybridisation for *Hoxa-13*. **K)** Stage 21, expression of *Hoxa-13* is first detected in the posterior distal mesenchyme. **L)** Stage 23, *Hoxa-13* expression still restricted to posterior-distal mesenchyme but domain has started to expand across distal antero-posterior axis. Note no expression proximally. **M)** Stage 24, expression of *Hoxa-13* has spread across most of the distal antero-posterior axis of the prospective hand plate. Note that by comparison *Hoxa-13* expression domain is within domain of *Hoxa-11*expression. **N)** From stage 25/6, *Hoxa-13* expression expands to fill the prospective hand plate and is no longer within or overlapping with the domain of *Hoxa-11*. Scale bar represents 500μm in K, L, M and N. **O)** *Hoxa-13* expression is throughout the hand plate from the base of the prospective wrist to the apical ridge. Expression of *Hoxa-13* is starting to be reduced in digit condensation areas. Scale bar represents 550μm.

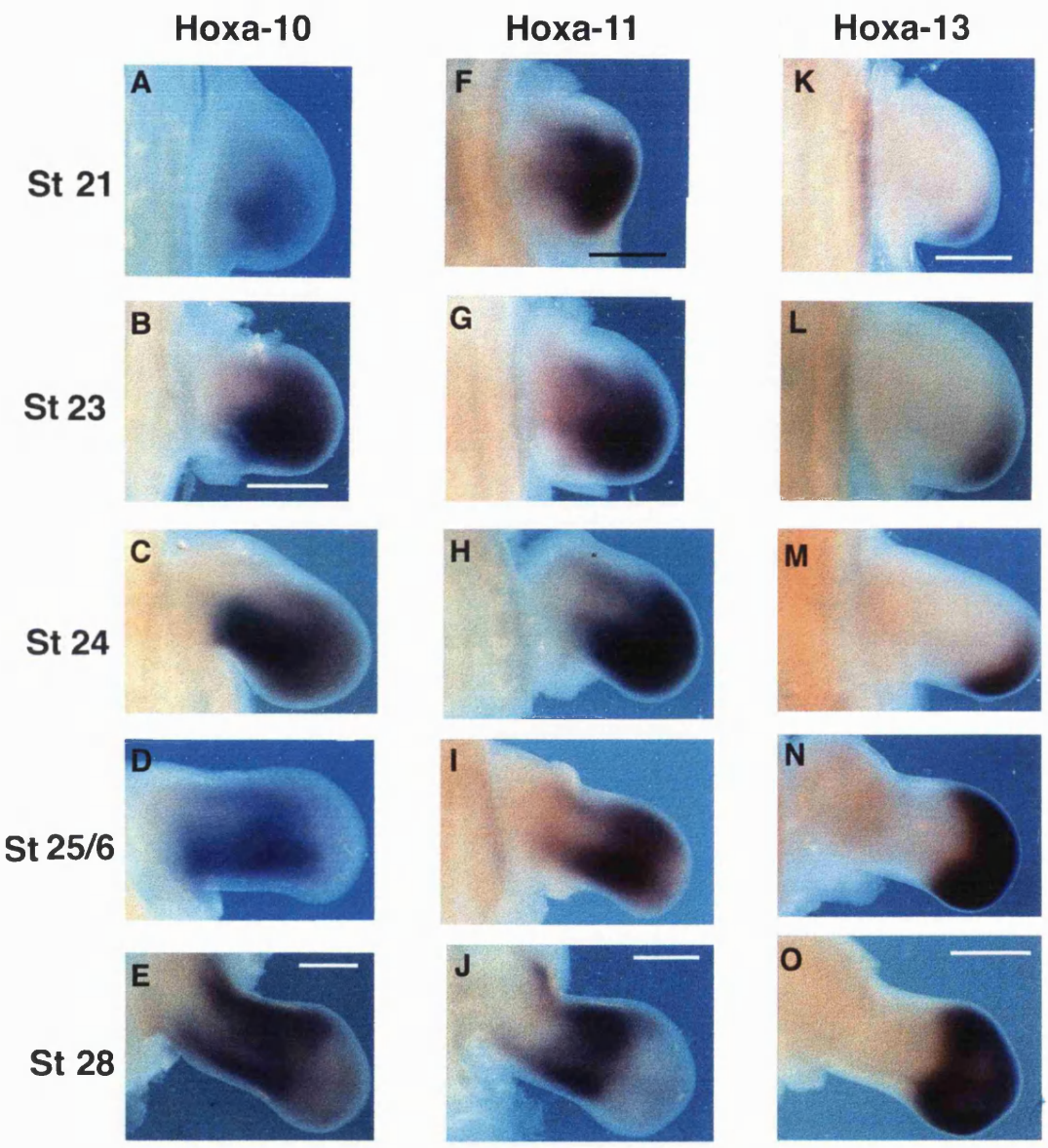
Hoxa-10
Hoxa-11
Hoxa-13
St 21
St 23
St 24
St 25/6
St 28
A
B
C
D
E
F
G
H
I
J
K
L
M
N
O

up to the forearm region (zeugopod) but is not present distally (Fig. 3.10E; Yokouchi et al., 1991b; Haack and Gruss, 1993).

Hoxa-11 expression is observed at late stage 19 along the posterior distal margin of the chick wing bud (Nelson et al., 1996). By stage 21, expression is observed across the distal antero-posterior axis of the bud (Fig. 3.10F). As development proceeds, expression remains across the distal antero-posterior axis and is faintly found in proximal regions (Fig. 3.10G, H, I). From stage 24, expression decreases in the hand plate, which coincides with the increase in expression of *Hoxa-13* (see below), but is maintained strongly in the prospective forearm region (zeugopod), so that by stage 28 expression of *Hoxa-11* is found only in the zeugopod (forearm; Fig. 3.10J). Thus, the expression domain of *Hoxa-11* at stage 28, overlaps with that of *Hoxa-10* in proximal regions of the limb (Yokouchi et al., 1991b; Haack and Gruss, 1993).

Hoxa-13 is the most 5' *HoxA* gene and expression is first detected at stage 21 in a very small region of posterior distal mesenchyme in the chick wing bud, within the expression domains of *Hoxa-11* and *Hoxa-10* (Fig. 3.10K; Nelson et al., 1996). This expression domain changes considerably as development proceeds (Fig. 3.10L). The anterior distal boundary of the expression domain moves towards the anterior tip of the bud and by stage 25, the *Hoxa-13* domain extends across the distal part of the antero-posterior axis of the hand plate (Fig. 3.10M, N). Moreover, from stage 25 onwards, the expression of *Hoxa-13* hardly overlaps with that of *Hoxa-10* or *Hoxa-11* (see also Yokouchi et al., 1991b; Haack and Gruss, 1993; Nelson et al., 1996). Expression then expands proximo-distally to fill the entire hand plate, the proximal boundary of expression lying at the junction between the hand plate and the forearm (Fig. 3.10O). By stage 28 expression is starting to become weaker in areas of cell condensation which will give rise to the digit cartilage (Fig. 3.10O).

3.2.3.2 *Initiation of Hoxa-13 expression is apical ridge dependent*

In order to ascertain if expression of the 5' *HoxA* genes depends on apical ridge signalling, the apical ridge was removed from stage 20-21 limb buds which results in limb truncations and 24 hours later the expression patterns of the genes were examined.
Expression of *Hoxa-10* and of *Hoxa-11* in mesenchyme cells showed different responses to the apical ridge. Twenty-four hours after ridge removal at stage 20/21, expression of both genes is clearly observed in the truncated wing bud but expression is not as extensive as in the contralateral limb (n=7 each; Fig. 3.11A, B). However, when the expression patterns of the truncated wings are compared to those at the time of apical ridge removal *Hoxa-10* expression seems normal if not stronger in expression (Fig. 3.10A, 3.11A), suggesting that maintenance of *Hoxa-10* is independent of the apical

ridge. In contrast, *Hoxa-11* expression levels seem reduced 24 hours following apical ridge removal as compared to a normal stage 20/21 limb (Fig. 3.10F; 3.11B) suggesting that expression of *Hoxa-11* may to some extent be maintained by the apical ridge. *Hoxa-11* expression can still be detected 48 hours following apical ridge removal (data not shown). The apical ridge was removed at stage 20/21 in these experiments when the expression domains of *Hoxa-10* and *Hoxa-11* are well established. To find out whether the ridge may be required to initiate expression of these genes earlier in development, the apical ridge was removed at stage 17, before *Hoxa-11* expression is normally seen. Twenty-four hours later, *Hoxa-11* expression is still observed in the truncated wing bud (n=2). This result suggests that initiation of expression of *Hoxa-11* does not require the apical ridge.

In contrast to these results for *Hoxa-10* and *Hoxa-11*, initiation and maintenance of expression of *Hoxa-13,* the most 5' gene in the complex does depend on the apical ridge. Expression of *Hoxa-13* is not seen either 24 or 48 hours after removal of the apical ridge at stage 20 (Fig. 3.12A, B; n=6). As expression of *Hoxa-13* is not normally observed until stage 21, initiation of expression of *Hoxa-13* thus appears to depend upon the ridge. Moreover when the apical ridge is removed at stage 22, after *Hoxa-13* is normally seen, 24 hours later *Hoxa-13* is not observed (n=2). This suggests that expression of *Hoxa-13* depends on the apical ridge for initiation, maintenance and elaboration of expression.

3.2.3.3 *FGF-4 and Hoxa-13 expression*

The results above show that *Hoxa-13* expression is dependent on the apical ridge. The apical ridge is essential for continued limb outgrowth and patterning as removal of the apical ridge at different stages in development gives different degrees of limb truncation (Saunders, 1948; Summerbell, 1974; see Chapter One). Recent work has shown that FGFs are involved in apical ridge signalling as an FGF-4 loaded bead can rescue limb outgrowth following ridge removal (Niswander et al., 1993). How is FGF signalling related to expression of *HoxA* genes?

When beads soaked in a high concentration of FGF-4 protein (0.7mg/ml) were pinned to the posterior distal mesenchyme in place of an apical ridge at stage 20/21, the limb buds show some outgrowth 24 hours later (n=21). Expression of *Hoxa-10* and *Hoxa-11* transcripts were still present in the limb. The patterns of expression were unchanged and appeared normal as compared to the contralateral limb i.e. no increase in gene expression even in the rescued tissue (Fig. 3.11C, D; Table 3.1). Expression of *Hoxa-13* was also clearly observed but only around the bead in the posterior distal mesenchyme (Fig. 3.12C; Table 3.1), whereas in the contralateral limb (now at stage 24)

Figure 3.11

Apical ridge removals and application of beads soaked in different concentrations of FGF-4 have little effect upon expression of *Hoxa-10* and *Hoxa-11*

Examples of limbs 24 hours after the apical ridge was removed at stage 21/2 and replaced with a bead soaked in different concentrations of FGF-4. **Hoxa-10**. **A**) Following apical ridge removal at stage 22, the limb is truncated and *Hoxa-10* expression is still present and not reduced, compare with expression in normal stage 22 bud (see Fig. 3.10B). **C**) Expression of *Hoxa-10* in response to a full concentration FGF-4 (0.7mg/ml) soaked bead. Limb outgrowth has occurred but no marked increase in *Hoxa-10* expression is observed. Note no expression in distal most part of limb or of contralateral limb. Expression of *Hoxa-10* appeared unaffected for all other concentrations of FGF-4 tested; **E**) 1/2 dilution of the full concentration stock. **G**) 1/10 dilution. **I**) 1/50 dilution. **K**) 1/100 dilution; **Hoxa-11**. **B**) Following apical ridge removal at stage 21/2, the limb is truncated, but *Hoxa-11* still expressed particularly in posterior of limb. When compared to a stage 21/2 control wing, expression is, however, reduced particularly in anterior limb bud (Fig. 3.10F). **D**) Expression of *Hoxa-11* in response to FGF bead soaked in 0.7mg/ml. Outgrowth of the limb has occurred and *Hoxa-11* expression is normal (compare with contralateral). For all other concentrations of FGF tested *Hoxa-11* expression is also unaffected; **F**) 1/2 dilution of full concentration stock. **H**) 1/10 dilution. **J**) 1/50 dilution. **L**) 1/100 dilution. All experiments were performed upon the right limb. Scale bars represent 300μm.

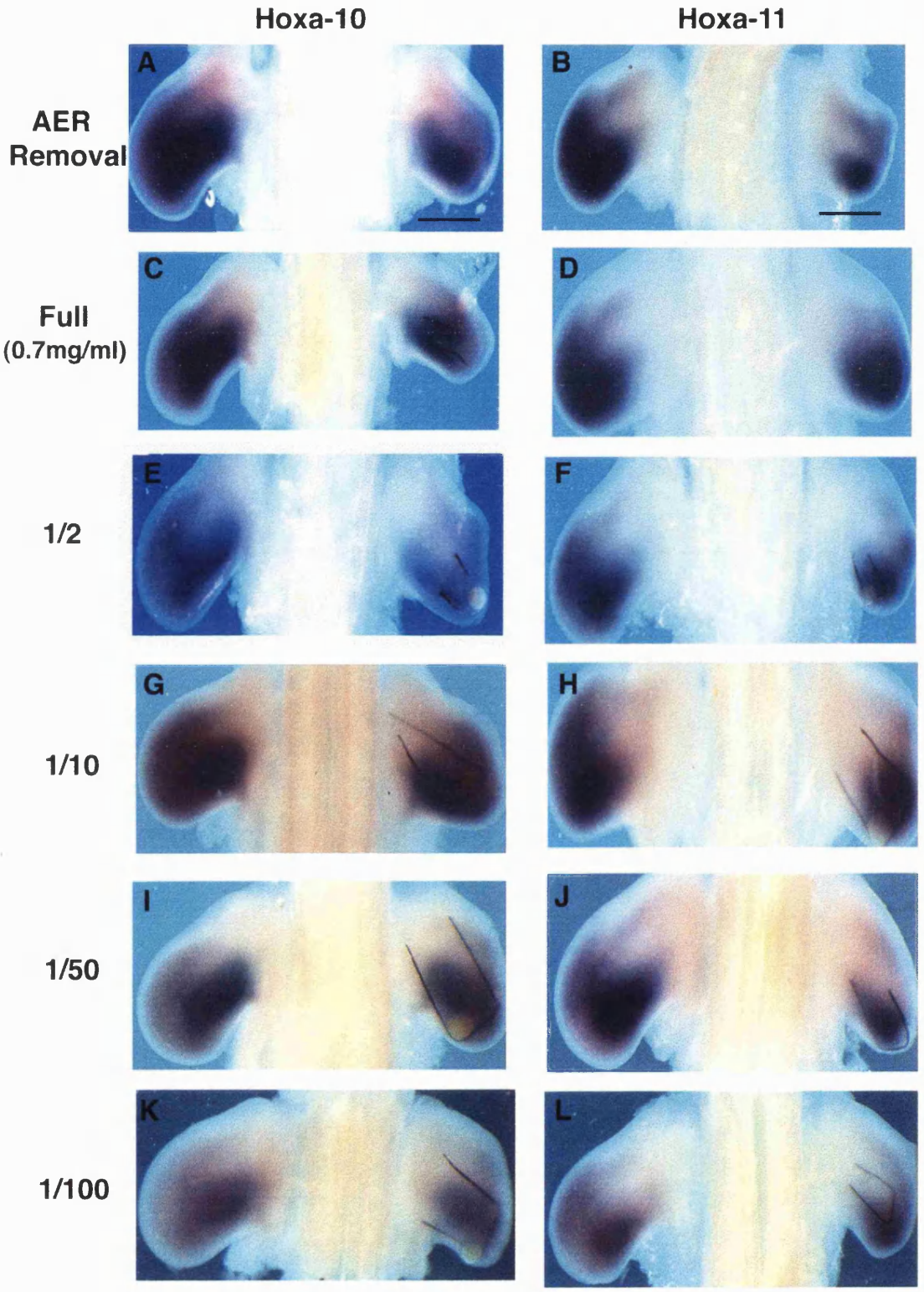
Hoxa-10
Hoxa-11
AER Removal
Full (0.7mg/ml)
1/2
1/10
1/50
1/100
A
B
C
D
E
F
G
H
I
J
K
L

Figure 3.12

Effects of apical ridge removal and application of beads soaked in different concentrations of FGF-4 upon expression of *Hoxa-13*

A-B Expression of *Hoxa-13* was analysed 24 and 48 hours following apical ridge removal at stage 21/2. **A**) 24 hours after the ridge was removed no expression of *Hoxa-13* is observed and the limb is truncated, while expression of *Hoxa-13* in contralateral limb (now stage 24/5) is across the antero-posterior axis. **B**) Expression of *Hoxa-13* is not observed 48 hours after ridge removal, now at stage 28/9, whereas in the contralateral limb, expression is throughout the hand plate and reduction of expression in regions of condensing digits can be observed. C-N *Hoxa-13* expression at 24 and at 48 hours following removal of the apical ridge and application of beads soaked in different concentrations of FGF-4.

24 hours **C**) Expression of *Hoxa-13* was observed around the bead in response to full concentration FGF-4 (0.7mg/ml). Expression of *Hoxa-13* was also observed around the bead for all lower concentrations tested; **E**) 1/2 dilution of the full concentration stock; **F**) 1/10 dilution; **I**) 1/50 dilution; **K**) 1/100 dilution; **M**) 1/200 dilution. However the extent of the amount of expression seen adjacent to the FGF bead appears larger at high concentrations than at low concentrations of FGF-4, for example compare **C**) with **M**). A bead soaked in PBS was applied in place of an apical ridge at stage 21/2 and incubated for 24 hours, see **N**). No expression of *Hoxa-13* was observed around the PBS bead, indicating that the application of a bead itself is not capable of inducing expression of *Hoxa-13*. Scale bar represents 500μm.

48 hours - **D**) Expression of *Hoxa-13* was observed around the bead in response to full concentration FGF-4 and has a much wider domain of expression that at 24 hours. As for the 24 hour studies *Hoxa-13* expression was observed adjacent to the FGF bead for all dilution's of the full concentration stock tested; **F**) 1/2 dilution. **H**) 1/10 dilution. **J**) 1/50 dilution. **L**) 1/100 dilution. Scale bar represents 650μm. Note that as observed after 24 hours there appears to be a dose response in that lower concentrations do not have as large a domain of expression around the bead as high concentrations. Note however that at 24 and 48 hours *Hoxa-13* expression is seen at very low FGF concentrations despite hardly any rescued outgrowth.

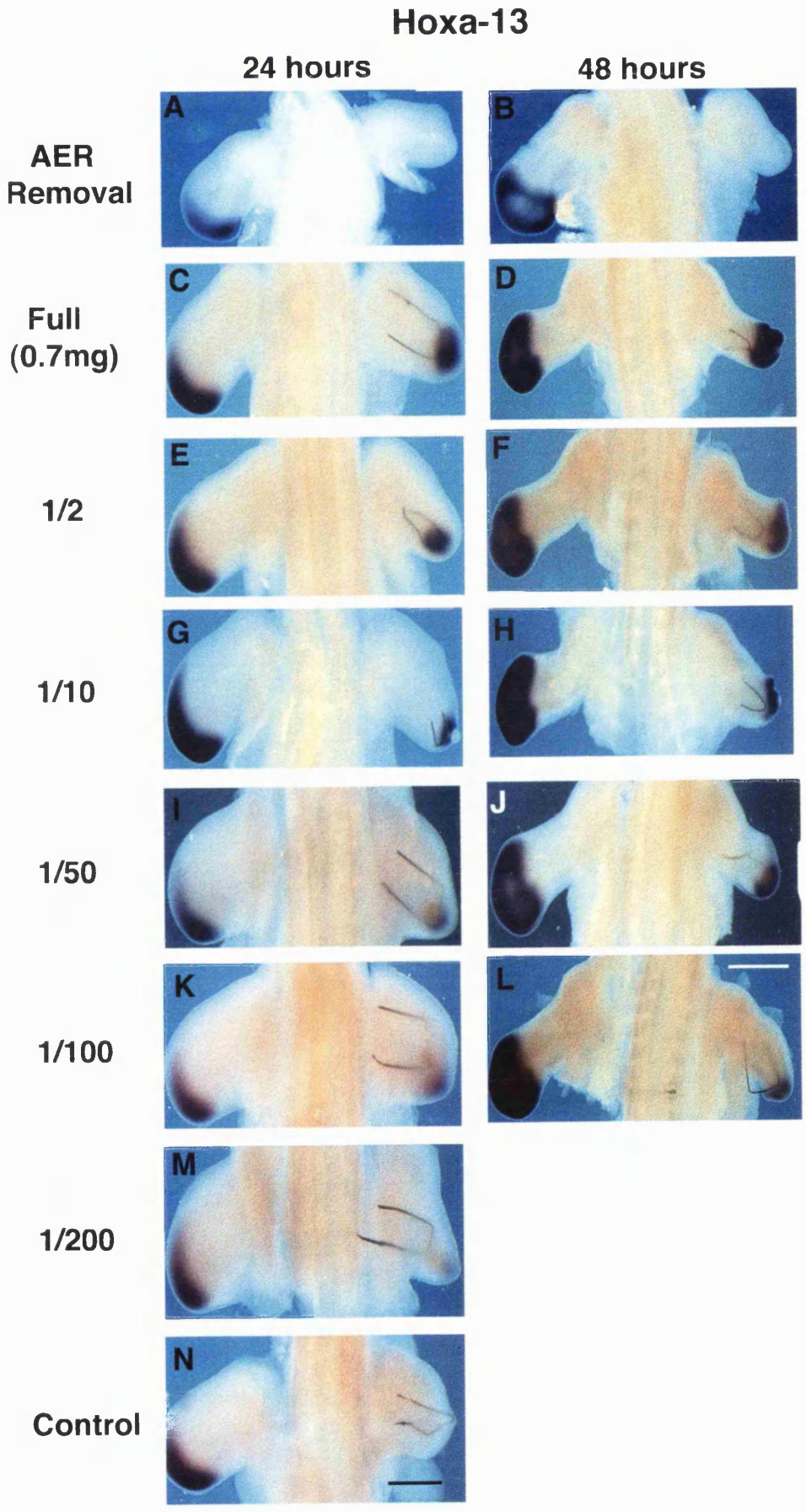
Hoxa-13
24 hours
48 hours
AER Removal
Full (0.7mg)
1/2
1/10
1/50
1/100
1/200
Control
A
B
C
D
E
F
G
H
I
J
K
L
M
N

Table 3.1

The effect of different doses of FGF replacing the apical ectodermal ridge at stage 20 upon HoxA gene expression 24 hours later.

	Hoxa-10		Hoxa-11		Hoxa-13	
Conc'n (FGF-4)	Expression upregulated	No ectopic expression	Expression upregulated	No ectopic expression	Expression upregulated	No ectopic expression
Full	0	2	0	3	8	1
1/2	0	1	0	1	2	0
1/4	0	2	0	2	1	0
1/10	0	2	0	3	2	0
1/25	0	1	0	3	2	0
1/50	0	2	0	2	3	1
1/100	0	3	1	3	5	0
1/200	-	-	-	-	1	0

Numbers represent total numbers of examples.

Table indicating the effect of different FGF-4 doses upon expression of *HoxA* gene expression, showing all FGF concentrations rescue/activate *Hoxa-13* expression but *Hoxa-10* and *Hoxa-11* expression are not rescued or upregulated by any FGF-4 concentration.

Hoxa-13 was expressed in distal mesenchyme all the way across the antero-posterior axis. However, expression of *Hoxa-13* could not be induced prematurely 24 hours after replacing the apical ridge with a bead soaked in 0.7mg/ml FGF-4 at stage 17 (see Fig. 3.13Q; n=2). As a control a bead soaked in PBS (phosphate buffer solution) was pinned onto the posterior distal mesenchyme in place of an apical ridge at stage 20. No expression of *Hoxa-13* was observed in this limb 24 hours later (Fig. 3.12N). This result shows that FGF signalling has no effect upon expression of *Hoxa-10* and *Hoxa-11* but can initiate and maintain *Hoxa-13* expression.

3.2.3.4 *Effects of beads soaked in different concentrations of FGF-4 on expression of HoxA genes*

What is the mechanism by which FGF signalling regulates *HoxA* gene expression? One possibility is that the amount of FGF seen by cells in the limb initiates sequential *HoxA* gene expression. A recent theoretical model (Papageorgiou and Almirantis, 1996) suggested that FGF-4, secreted from the apical ridge, initiates expression of members of the 5' *HoxA* complex at a series of different concentration thresholds. Low concentrations of FGF-4 would initiate *Hoxa-10* and *Hoxa-11* expression early in limb development and a higher concentration of FGF-4 would activate *Hoxa-13* later in development. I have already shown that *Hoxa-10* and *Hoxa-11* are not responsive to FGF-4 at stage 20 and appear to be apical ridge independent however the model may explain the activation of *Hoxa-13*.

To test how *HoxA* gene expression responds to different concentrations of FGF-4, I removed the apical ridge of stage 20 limb buds, pinned beads soaked in different concentrations of FGF to the posterior distal mesenchyme and then analysed the expression patterns of 5' *HoxA* genes over a 24 hour time period. A prediction of the model is that if initiation of *Hoxa-13* is due to the amount of FGF seen, then below a certain concentration threshold *Hoxa-13* expression would no longer be rescued.

When beads soaked in a range of FGF-4 concentrations from a 1:2 dilution (0.35mg/ml) to a 1:100 dilution (7μg/ml) of the concentrated stock (0.7mg/ml; Table 3.1) were applied to the limb in place of an apical ridge, no increase or decrease in expression was observed for *Hoxa-10* (Fig. 3.11E-K) or *Hoxa-11* (Fig. 3.11F-L) as expected. In contrast, *Hoxa-13* expression was observed around the bead, at 24 hours, at every concentration of FGF-4 used from a 1:2 dilution all the way down to a 1:200 dilution (0.35mg/ml to 3.5μg/ml; Fig. 3.12E-M; Table 3.1). However the size of the *Hoxa-13* domain at 24 hours and at 48 hours following the operation, appeared smaller at lower FGF-4 doses, although the abundance of transcripts within the domains appeared to be

relatively similar (Fig. 3.12D-L). These results show that *Hoxa-13* expression can be initiated over a wide range of FGF concentrations.

According to the model, proximal cells do not express *Hoxa-13* because they have not been exposed to sufficient amounts of FGF. Therefore to investigate whether supplementing the amount of FGF-4 seen by proximal cells could initiate expression of *Hoxa-13* proximally, beads soaked in different concentrations of FGF-4 were placed in posterior proximal positions in stage 20/21 limbs (with the apical ridge intact) for 24 hours. With a bead soaked in the highest concentration of FGF-4 (0.7mg/ml) faint expression of *Hoxa-13* could be detected around a bead after 24 hours (Fig. 3.13G; n=5) but at lower concentrations, *Hoxa-13* expression was not observed around the bead (Fig. 3.13H, I; Table 3.2). As expected, no effect upon expression of *Hoxa-10* and *Hoxa-11* was observed following application of beads soaked in different concentrations of FGF-4 into proximal tissue (*Hoxa-10* Fig. 3.13A-C; *Hoxa-11* Fig. 3.13D-F; Table 3.2). By placing two beads soaked in the high concentration of FGF-4 in posterior proximal mesenchyme, a high level of *Hoxa-13* expression was observed posterior and distal to the posterior of the two beads 24 hours later (Fig. 3.13K) but this was then reduced at 48 hours (Fig. 3.13L, N). Interestingly, if a bead soaked in high concentration FGF-4 was placed at stage 20/21 in the polarising region of the limb, high expression of *Hoxa-13* was observed around the bead 24 hours later (Fig. 3.13J; Table 3.2). After 48 hours incubation a new outgrowth from the posterior margin was evident and expression of *Hoxa-13* was throughout the induced structure (Fig. 3.13M; n=1).

The model of Papageorgiou and Almirantis (1996) was also proposed to account for the initiation of *Hoxa-13* expression. Therefore I applied FGF-4 soaked beads at the tip of early limb buds (with the apical ridge intact) to investigate if *Hoxa-13* can be prematurely activated. Beads soaked in 0.7mg/ml FGF-4 were placed in apical mesenchyme beneath the apical ridge at stage 17 and incubated for 18 hours till stage 20 (Fig. 3.13P; n=2). In neither case was *Hoxa-13* expression detected around the bead. Thus, supplying early limbs with additional FGF does not activate *Hoxa-13* prematurely.

3.2.3.5 *Dose of FGF-4 and limb patterning*

All concentrations of FGF-4 tested initiate *Hoxa-13* expression when applied following apical ridge removal, however the size of the *Hoxa-13* domain appears smaller at lower FGF doses. As *Hoxa-13* expression is correlated with digit formation (Fromental-Ramain et al., 1996; this study) it is interesting to examine how the different sizes of the expression domains of *Hoxa-13* induced by different concentrations of FGF

Figure 3.13

Proximal application of FGF-4 and effect upon expression of 5' HoxA genes Beads soaked in either full strength FGF-4 (0.7mg/ml), a 1/50 or 1/100 dilution of the full strength concentration were placed in posterior proximal positions in limb buds at stage 21, with the apical ridge intact to investigate the effect upon *HoxA* gene expression. In all cases some outgrowth of tissue adjacent to the position of the bead was observed. A-C *Hoxa-10* expression 24 hours after bead insert. Expression of *Hoxa-10* was not affected at all by **A**) full strength FGF-4 (Scale bar represents 500μm). **B**) 1/50 dilution or **C**) a 1/100 dilution. D-F *Hoxa-11*expression 24 hours after bead insert. Expression of *Hoxa-11* was not affected at all by **D**) full strength FGF-4. **E**) 1/50 dilution or **F**) a 1/100 dilution. G-Q *Hoxa-13*expression. **G**) In contrast to the results of *Hoxa-10* and *Hoxa-11*, full strength (0.7mg/ml) FGF-4 induced faint expression of *Hoxa-13* posterior to the bead in proximal positions, 24 hours later (arrowed). However when investigated after 48 hours, **L**) expression though present was very faint (arrowed; Scale bar represents 500μm). 24 hours after application of lower concentrations of FGF-4, **H**) and **I**) to proximal positions no *Hoxa-13* expression was observed around the bead (arrowed).Full strength FGF-4 soaked beads placed in the polarising region at stage 21, **J**) 24 hours later expression of *Hoxa-13* is observed strongly posterior and distal to the bead. Scale bar represents 500μm in J and K. **M**) 48 hours later a new secondary axis has formed and *Hoxa-13* expression is observed throughout this second axis. Scale bar represents 500μm in M and N. Two full strength FGF-4 soaked beads placed in posterior proximal mesenchyme at stage 21, **K**) 24 hours later expression is observed posterior to the posterior of the 2 beads. **N**) 48 hours after application, ectopic expression of *Hoxa-13* is practically non-existent. In both cases the distal pattern of *Hoxa-13* expression appears normal. To investigate if *Hoxa-13* expression can be induced prematurely a bead of full strength FGF-4 was placed into posterior proximal mesenchyme with the ridge intact at stage 17, **P**), 24 hours later no *Hoxa-13* expression was observed in the limb or around the bead (marked by asterisk). **Q**) A full strength FGF-4 bead (marked by asterisk) replaced an apical ridge from a stage 17 limb, 24 hours later, no *Hoxa-13* expression was observed. Scale bar represents 500μm.

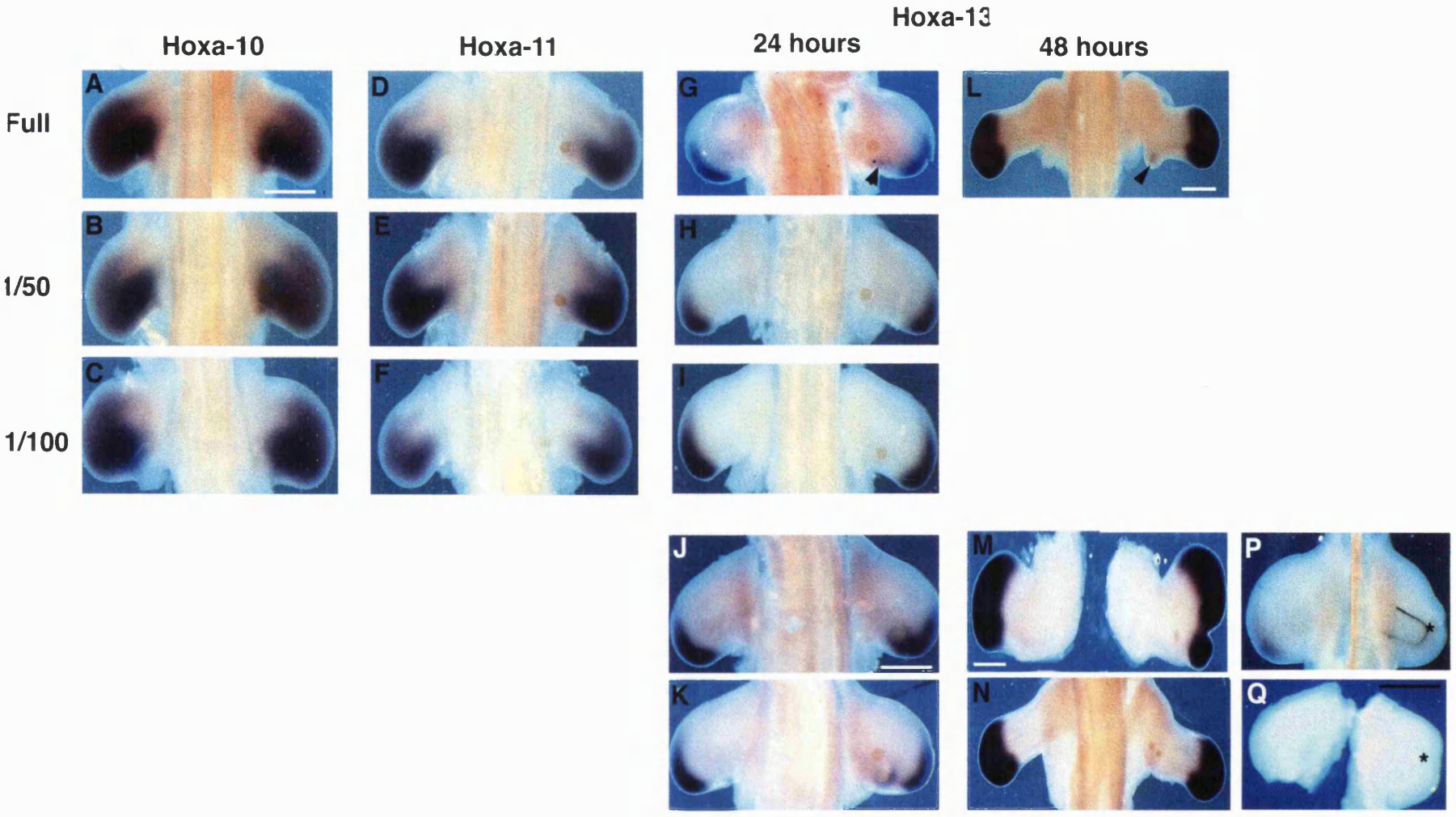
Hoxa-10
Hoxa-11
Hoxa-13
24 hours
48 hours
Full
1/50
1/100
A
B
C
D
E
F
G
H
I
J
K
L
M
N
P
Q

Table 3.2

The effect of different doses of FGF placed in proximal mesenchyme at stage 20 upon *HoxA* gene expression 24 hours later.

	Hoxa-10		Hoxa-11		Hoxa-13	
Conc'n	Expression upregulated	No ectopic expression	Expression upregulated	No ectopic expression	Expression upregulated	No ectopic expression
Full	0	2	1	2	7	3
1/2	0	1	0	1	0	1
1/4	0	2	-	-	0	1
1/10	0	4	0	2	0	3
1/25	0	3	0	3	0	5
1/50	0	2	0	2	0	3
1/100	0	3	0	3	0	3
1/200	-	-	-	-	-	-

Numbers represent cases examined

Table showing that expression of*Hoxa-10* and *Hoxa-11* is not induced following the application of beads soaked in any FGF concentration to posterior proximal mesenchyme at stage 21. Table also shows that *Hoxa-13* expression is induced around a bead placed in posterior proximal mesenchyme soaked in the highest FGF concentration (0.7 mg/ml) but that all other concentrations of FGF fail to induce *Hoxa-13* in posterior proximal tissue.

are related to the final observed cartilage pattern. Hence I investigated how proximo-distal patterning of the limb and digit formation is related to the dose of FGF-4 applied.

Beads soaked in different concentrations of FGF were stapled to the posterior margin of the bud after ridge removal at stage 20/21 and left for 7 days. Beads soaked in 0.7mg/ml rescued the limb pattern, producing a humerus, forearm and hand plate rudiments although the digits were not clearly distinguishable (Fig. 3.14B; n=4). When this stock is diluted 100X, some rescue was obtained but only a very small part of the radius and ulna is observed (Fig. 3.14C; n=2). Beads soaked in a 1:200 dilution of the stock 0.7mg/ml FGF-4 concentration do not appear to rescue the limb as the resulting limb was very similar to a limb that had no FGF-4 bead replacing the apical ridge (Fig. 3.14D; n=2; compare with Fig. 3.14A). Thus the amount of pattern laid down appears to be related to the concentration of FGF in which beads are soaked. High concentrations of FGF allow the full extent of limb pattern to be laid down whereas low concentrations, despite initiating expression of *Hoxa-13,* allow very little patterning to take place. This suggests that a specific size of *Hoxa-13* expression is required to pattern limb elements.

3.3 Discussion

3.3.1 Fate maps

I have produced detailed fate maps for small groups of cells in stage 20 chick wing bud mesenchyme and apical ectodermal ridge. A fate map for the apical ridge has not previously been constructed and the fate map for the wing mesenchyme is more comprehensive than previous fatemaps. At stage 20, the majority of cells that will make up the humerus are not in the protruding part of the limb bud. In contrast, radius and ulna arises from mesenchyme 250μm to 500μm from the somites; digits and handplate arise from subapical mesenchyme, specifically digit **2** from cells on a level with somite 17/18, digit **3** from cells on a level with somite 18/19 and digit **4** from cells on a level with somite 19/20 (Fig. 3.1G, 3.4G-K).

My fate map for chick limb buds (see also Vargesson et al., 1997) is in reasonable agreement with previous fatemaps (Saunders, 1948; Stark and Searls, 1973; Bowen et al., 1989) in that it shows that limb elements arise from the posterior two-thirds of the early limb bud. The anterior third of the bud does not expand very much and is destined to form parts of the shoulder joint and upper humerus (see also Bowen et al., 1989). There are some differences between my conclusions and those of Stark and Searls (1973), who followed mesenchyme implants labelled with tritiated thymidine and concluded that the majority of the humerus arises from inside the stage 20 limb bud. They also suggested that the digits arise in a slightly more anterior position than our data would suggest.

Figure 3.14

Rescue of cartilage pattern depends on concentration of FGF-4 in which beads are soaked

A) Example of the cartilage pattern of a wing, 7 days after apical ridge removal at stage 20. Only a full length humerus is observed following such an operation, no distal structures can be seen. Scale bar represents 2000μm. **B**) Cartilage pattern can be practically rescued by the addition of a bead soaked in full concentration FGF-4 (0.7 mg/ml) after apical ridge removal at stage 20. A normal humerus, ulna and radius are observed, the short rudiments of two digits (arrowed) can be observed in the high power image, as can the bead (asterisk; Mag. X50; scale bar represents 500μm). Dilution's of the full concentration FGF-4 stock result in less substantial rescue of cartilage elements as shown in **C**) where a 1/100 dilution produces a normal humerus and a small proximal piece of ulna and radius articulating with the base of the distal humerus. **D**) a 1/200 dilution of the full strength FGF-4 concentration results in a short stump of cartilage articulating with the base of the humerus. There is not any real significant rescue of cartilage elements at this concentration, suggesting the cartilage shows a dose response to FGF-4 concentration (compare with A, B).

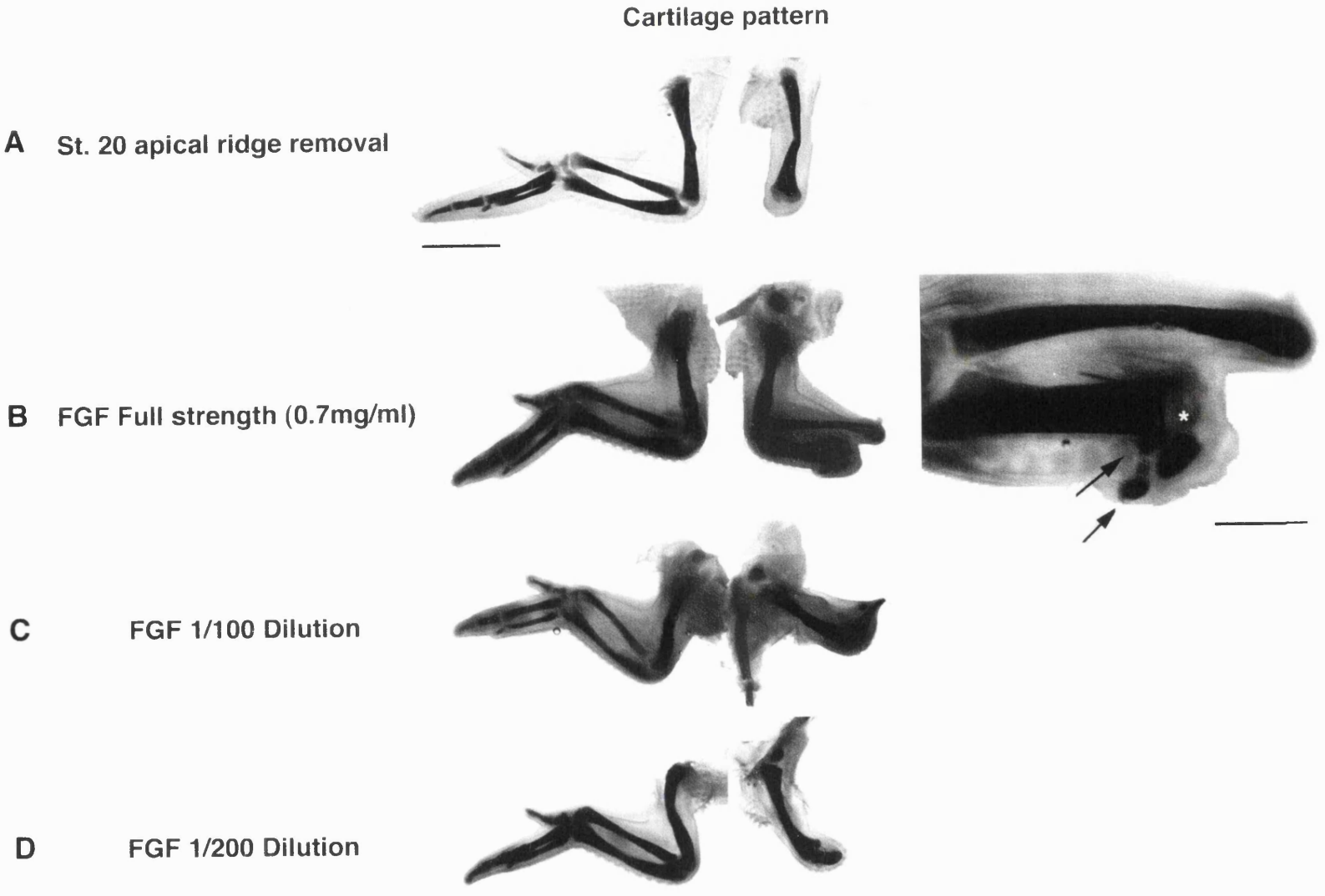
Cartilage pattern
A St. 20 apical ridge removal
B FGF Full strength (0.7mg/ml)
C FGF 1/100 Dilution
D FGF 1/200 Dilution

Rowe and Fallon (1981) however, arrived at the same conclusion as this study about the levels at which cells give rise to the digits, based on a quite different approach in which most of the apical ridge was removed and specific small segments of ridge were left in place. The only available fate map of a mouse hindlimb bud suggests several features in common with our chick limb fatemaps (Muneoka et al., 1989). Most of the distal limb parts come from the posterior of the mouse hindlimb bud and the femur region arises from the body wall (Muneoka et al., 1989).

3.3.1.1 *Expansion of labelled mesenchymal cell populations*

Populations of mesenchyme cells labelled subapically show greater expansion and occupy a greater percentage of the limb bud after 48 hours than proximally labelled mesenchyme (Fig. 3.1I). Hornbruch and Wolpert (1970) showed that the mitotic index was high for distal regions of the limb bud but considerably lower for proximal regions. Expansion of distal mesenchyme on a level with somite 18 is 70 fold over the initial injection size (Fig. 3.2A). If cells double each time they divide, then this amount of expansion can be produced from 6 cell divisions in 48 hours, hence 8 hours per cell cycle. Other workers have shown cell cycle times of between 8 and 13 hours for the mesenchyme (Janners and Searls, 1970; Hornbruch and Wolpert, 1970; Searls and Janners, 1971; Cooke and Summerbell, 1980). I found that cell populations labelled subapically remained in contact with the apical ridge and extended proximally into the limb bud. Both Saunders (1948) and Bowen et al. (1989) noted in some cases that cell populations labelled near the apical ridge were found in proximal positions which we did not find, but they both used carbon particles which may not remain associated with the cells initially labelled.

There are marked differences in expansion of subapical mesenchyme at different antero-posterior levels across the limb bud. Posterior and apical mesenchyme expands much more than anterior mesenchyme. It seems unlikely that local cell death can account for this differential expansion since there are necrotic zones both anteriorly and posteriorly in the developing bud (Saunders et al., 1962). Cooke and Summerbell (1980) have shown that there tends to be a higher S phase labelling index posteriorly in the bud suggesting a higher proliferation rate posteriorly (Fig. 3.1I). This could be due to influences from polarising region and posterior apical ridge. Posterior ridge expresses high levels of FGFs and in particular *Fgf-4*. Li et al. (1996) recently reported altered patterns of expansion of posterior proximal cell populations in response to FGF-2 in chick wing buds and Kostakopoulou et al. (1997) found that labelled posterior cell populations expanded distally in amputated limb buds when a source of FGF-4 was applied. My results also show a striking differential expansion of subapical mesenchyme

across the antero-posterior axis. Cells labelled subapically in the middle third of the limb bud fan out into the anterior tip (Fig. 3.1B). Bowen et al. (1989) also observed anterior fanning out of marked cells in a similar position at stages 22 and 24. This anterior shift could be due to the fact that the posterior third expands considerably while the anterior part of the limb expands very little causing overgrowth of the middle third. Cell populations in the posterior third of the limb bud give rise to wide, straight tracts of cells with no anterior bending.

The expansion of the middle and posterior third subapical mesenchyme populations is dependent upon the apical ridge. Apical ridge removal results not only in limb truncation but also the labelled populations do not expand but instead remain in the position initially labelled i.e. behaving like anterior subapical or proximal mesenchyme (Fig. 3.8). This suggests an apical ridge signal, such as FGF-2 and/or FGF-4 (see also Li et al., 1996; Kostakopoulou et al., 1996, 1997), is directly affecting subapical mesenchymal cell fate, perhaps by controlling rates of proliferation. Ridge removal has little effect upon proximal mesenchyme cell behaviour except at the very posterior (Fig. 3.9).

I also noted that subapical cell populations in the bud keep in register (Fig. 3.1B), whereas proximal cell populations show more overlap and relative displacements (Fig. 3.1D). Relative displacements of proximal cell populations may be allowed because patterning of these cells may already have been specified irreversibly. Generally, I find no evidence for compartments in chick limb mesenchyme from stage 20.

3.3.1.2 *Dynamics of the Apical Ectodermal Ridge*

My fate map of the apical ridge shows that cells in the posterior two-thirds at stage 20 make up the entire apical ridge later in development, and that labelled cells fall out of the apical ridge anteriorly. Cell death appears to be evenly distributed throughout the ridge at stage 20 (Todt and Fallon, 1984). When limb duplications are induced by placing beads soaked in retinoic acid underneath the apical ridge at stage 20, the apical ridge is longer than normal and covers the induced structure (Lee and Tickle, 1985). It seems likely that the longer apical ridge is due to the maintenance of cells in the apical ridge that normally leave. This is consistent with the idea that the apical ridge is produced from a finite population of cells early in development. Experiments in which quail apical ridge was grafted in place of chick apical ridge show that the apical ridge behaves autonomously and cells are not recruited from either dorsal or ventral ectoderm (Saunders et al., 1976).

I have shown that the apical ridge does not keep in register with the underlying mesenchyme. This disparity appears to be due to differences in expansion between mesenchyme and apical ridge, with the apical ridge generally expanding more in an

anterior direction. We observed intermingling of labelled and unlabelled cells, but only at the borders of the labelled domain, suggesting that local cell rearrangements may occur as the ridge expands. This suggests that the ridge, as for the mesenchyme, is not compartmentalised between the stages of this study.

3.3.2 Relationship between cell lineage and gene expression

3.3.2.1 *Fgf-4*

Fgf-4 is expressed in posterior cells of the apical ridge at stage 20 but is expressed more widely throughout the apical ridge as development proceeds. Cells labelled anterior to the expression domain at stage 20 are not incorporated into the *Fgf-4* domain after 24 hours incubation. Therefore no new cells are induced to express *Fgf-4* and it is the original population of expressing cells in the posterior two-thirds of the apical ridge that expand and fill the apical ridge in late development. The expansion of *Fgf-4* throughout the apical ridge is probably due to proliferation of the *Fgf-4* expressing cells, which causes the posterior cell populations to overgrow the anterior populations. This could be due to FGFs being present in the apical ridge which are known to increase proliferation, but also due to the SHH-FGF-4 feedback loop acting between posterior mesenchyme and posterior apical ridge which may cause a higher proliferation rate in the posterior mesenchyme and apical ridge (Niswander et al., 1994; Laufer et al., 1994).

3.3.2.2 *Hoxd-13*

Hoxd-13 has a dynamic expression pattern and initially transcripts are restricted to posterior distal mesenchyme and later appear throughout most of the prospective hand plate, the most anterior limit of expression ending up in between prospective digit **2** and digit **3** (see also Yokouchi et al., 1991b). I have found by labelling populations of wing cells and following their fate over 48 hours, that proximal cells that were expressing *Hoxd-13* at stage 20/21, switch off *Hoxd-13* and no longer express it as development proceeds. *Hoxd-13* can be reactivated in proximal cells by locally applying FGF-4 (K. Kostakopoulou, unpublished observations). Thus it seems likely that cells are left proximally and stop expressing *Hoxd-13* because they are too far away from the influence of apical ridge or progress zone signals as the bud grows out. Interestingly in the mouse mutant *Ulnaless* in which proximal cells do not switch off *Hoxd-13* expression, proximal forelimb defects, including the loss of the ulna, were observed; probably due to *Hoxd-13* down regulating *Hoxd-11* expression (Peichel et al., 1997; Herault et al., 1997).

I have also shown that the anterior shift in *Hoxd-13* expression to occupy most of the hand plate, up to the inter-digit region between digit **2** and digit **3**, is in concert with the fate map and can be accounted for by the way that the limb bud grows. Thus, there appears to be no initiation of *Hoxd-13* expression in anterior, previously non-expressing cells. This argues against the idea that *Hoxd-13* gene expression in the hand plate represents a distinct separate phase of *Hoxd-13* initiation (Morgan and Tabin, 1994; Sordino et al., 1995; Nelson et al., 1996). However these results do not rule out the possibility that *Hoxd-13* expression in distal wing cells might be maintained by different signals at different times in development, where one signal acts at an early time and a different signal acts at a later time.

My findings also do not preclude the possibility that *Hoxd-13* has different functions throughout development, an early phase involved in growth, patterning and identity (Morgan and Tabin, 1994; Nelson et al., 1996; Zakany and Duboule, 1996) and a late phase involved in growth and differentiation later (Morgan and Tabin, 1994; Duboule, 1995; Yokouchi et al., 1995; Goff and Tabin, 1997) especially as *Hoxd-13* is expressed on its own initially, but later in concert with *Hoxa-13*.

What controls the anterior expansion of cell populations and *Hoxd-13* expression in the wing? The apical ridge is the obvious candidate for a potential activator of the mechanism controlling the anterior shift of cells and hence the extension of *Hoxd-13* expressing cells into the anterior tip of the limb. The anterior shift of subapical cell populations is abolished following ridge removal, showing that subapical mesenchymal population fate and behaviour is apical ridge dependent. Apical ridge signals, notably FGFs, have been shown to increase proliferation and direct limb outgrowth (Niswander and Martin, 1992; Niswander et al., 1993). Between stage 20 and stage 24 the mesenchymal *Hoxd-13* domain is overlapped by the apical ridge *Fgf-4* expression domain (anterior limit of *Hoxd-13* is on a level with somite 18, anterior limit of *Fgf-4* is on a level with somite 17/18, at stage 20). Mesenchyme cells have been shown to move towards an FGF source (Li et al., 1996; Kostakopoulou et al., 1997) and it is possible that *Fgf-4* signalling to the mesenchyme may contribute to the expansion of *Hoxd-13* expressing cells into the hand plate to produce the late expression pattern of *Hoxd-13* by increasing the proliferation of *Hoxd-13* expressing cells which overgrow anterior cell populations.

3.3.2.3 *Hoxa-13*

Hoxa-13 has a dynamic expression pattern. Like *Hoxd-13*, transcripts are initially restricted to posterior distal mesenchyme and later appear throughout the

prospective hand plate. By labelling populations of cells above, on and within the distal boundary of expression I found that the expansion of *Hoxa-13* across the handplate involves the incorporation of previously non-expressing cells (see also Nelson et al., 1996). This contrasts with my analysis of *Hoxd-13* and thus, it appears that elaboration of *HoxA* and *HoxD* expression patterns occur by different mechanisms, possibly due to different enhancers within each *Hox* complex (Nelson et al., 1996) and/or different activating and maintenance signals.

3.3.3 Initiation and maintenance of *Hoxa-13* in the limb bud

I have shown that the apical ridge is necessary for *Hoxa-13* initiation and maintenance. In contrast *Hoxa-10* and *Hoxa-11* do not appear to require an apical ridge for initiation of expression especially as *Hoxa-11* expression is still observed despite removing the apical ridge before normal endogenous expression is initiated. Furthermore beads soaked in high concentrations of FGF-4, an apical ridge signal, initiate *Hoxa-13* expression, but have no effect upon expression of *Hoxa-10* and *Hoxa-11.* These results argue against the idea that different *HoxA* gene expression domains represent responses to different concentrations or thresholds of FGF-4 as proposed in the model by Papageorgiou and Almirantis (1996). However other FGF members are expressed in presumptive limb tissue well before the expression of FGF-4 is observed, for example FGF-8 and FGF-10 which could have roles in *HoxA* gene initiation (Mahmood et al., 1995; Ohuchi et al., 1997). Interestingly Nikbacht and McLachlan (1997) recently proposed the existence of a proximo-distal gradient of FGF in the limb mesenchyme. However this gradient was only detected in established limb buds, from stage 21, when all the *HoxA* genes are already initiated and not looked for in earlier limb buds.

Even if FGF-4 is not involved in the initiation of *Hoxa-10* and *Hoxa-11*, it is still possible that the amount of FGF-4 seen by cells controls the initiation of *Hoxa-13.* However a wide range of doses of FGF-4 all led to initiation of *Hoxa-13* expression in the absence of the ridge. This argues against the amount of FGF-4 controlling the initiation of *Hoxa-13.* It is possible however that at the stage the experiments were carried out, cells had already seen almost sufficient endogenous FGF-4 to activate *Hoxa-13.* Thus, the lowest FGF concentration was sufficient to activate a small domain of *Hoxa-13* expression. The dose response experiment should be repeated using stage 17 limbs where cells will have seen less endogenous FGF-4. The finding that *Hoxa-13* expression can not be activated prematurely in limbs by addition of FGF-4 also argues that the amount of FGF seen does not control initiation of *Hoxa-13.* However it is possible that the limb bud has a buffering capacity. Thus, when FGF-4 is added, endogenous FGF-4 levels may drop, so that *Hoxa-13* activation still occurs on schedule.

The size of the domain of *Hoxa-13* varied in response to different FGF-4 concentrations where high concentrations of FGF appear to activate a larger domain of *Hoxa-13* expression around the bead than lower concentrations. However only the highest concentration rescues limb pattern. This dose response of the extent of *Hoxa-13* expression in response to FGF-4, suggests that a diffusion mechanism might operate. This raises the question of whether FGF-4 itself is diffusing and directly activating *Hoxa-13* throughout the domain or whether another signal is induced. Dose dependency argues against a simple relay mechanism which predicts that all activating concentrations should activate the same amount of a target gene (Papageorgiou and Almirantis, 1996). Thus, initiation of *Hoxa-13* might require not only FGF-4 but other signal(s) collaborating to initiate *Hoxa-13* expression, as is the case in initiation of *Hoxd-13* expression. Co-operating signals could come from the polarising region. When beads soaked in 0.7mg/ml FGF-4 are placed in the polarising region, a secondary axis is formed which expresses *Hoxa-13* throughout. Moreover, beads soaked in 0.7mg/ml FGF-4 placed in posterior proximal mesenchyme do appear to activate weak *Hoxa-13* expression. This result could be explained by the fact that FGF-4 is signalling to cells that may have been in the polarising region earlier in development and seen SHH and/or BMP-2. FGF-4 then initiates a feedback loop by activating SHH which then together with FGF-4 initiates *Hoxa-13*. This hypothesis may explain the relationship between the size of the *Hoxa-13* domain in response to FGF-4 and digit development, where only the highest FGF concentration rescues limb and digit pattern. All the lower FGF-4 concentrations, despite activating *Hoxa-13* expression, can not rescue limb and digit development, suggesting that the FGF present was not sufficient to diffuse far enough to activate secondary signals necessary for the expansion of the *Hoxa-13* domain.

The timing of *Hoxa-13* initiation is difficult to alter experimentally and I was not able to prematurely initiate expression of *Hoxa-13* by altering the concentration of FGF-4. This suggests that initiation of *Hoxa-13* expression is not simply due to the amount of FGF-4 seen. Furthermore a different mechanism or signalling pathway must be involved in initiation of *Hoxa-10* and *Hoxa-11*. The *Hox* complexes are activated in a 3' to 5' manner. It has been suggested that the 5' genes are prevented from being expressed before the 3' genes due to complexes of heterochromatin preventing inducers and enhancers access to the genes (Duboule, 1994; for review see Paro, 1990; Singh and Gaunt, 1990; Pirrotta, 1997). The heterochromatin complex is controlled by several gene products including those of *Polycomb* genes and*Trithorax* genes (for review see Singh and Gaunt, 1990; Paro, 1990; Pirrotta, 1997; Gould, 1997). It is possible that initiation of *Hoxa-13* (and of *Hoxd-13*) is prevented until the complex is opened by the repression of heterochromatin, which occurs following activation of *Hoxa-11*, hence controlling the timing and activation of the 5' *HoxA* genes. Once heterochromatin has been repressed,

FGF-4 or another FGF member, perhaps in conjunction with other signals, can initiate expression of *Hoxa-13*. This explains why premature activation of *Hoxa-13* could never be induced by FGF-4. Thus, initiation of expression of *Hoxa-13* and *Hoxd-13* may be by similar mechanisms. However, the differences in timing of expression and elaboration of expression domains is probably due to different enhancers within each *Hox* complex (see also Nelson et al., 1996) and perhaps via different combinations of signalling molecules.

3.3.4 Fatemaps and evolutionary theories

The fatemaps together with their relationship to gene expression domains has implications for evolutionary theories of the origin of the hand plate. It has been suggested that evolution of the hand plate is due to an anterior bending of the metapterygial axis of the limb at the level of the digital arch and digits then arising from the distal side of the arch i.e. the original posterior side (Shubin and Alberch, 1986; Coates, 1991, 1995). Coates (1991, 1995) noted that the late expression pattern of *Hoxd-13* looked very similar to the proposed axis bending. Sordino et al (1995) showed that, early in development Zebrafish fin and mouse limb buds both display similar *HoxD* and *HoxA* gene expression patterns. Fin buds however do not display the late limb bud *HoxD* gene expression pattern which, in amniotes, corresponds to most of the prospective handplate. They suggest therefore that the developing hand/foot plate of the amniote limb has no homologous structures in the Zebrafish fin and conclude that evolution of the autopod (hand plate) depended on a second phase of *Hox* gene expression which was brought about by bending of the metapterygial axis. I find that subapical populations in the middle third of the wing and in the leg fan out antero-distally into the anterior tip (see also Bowen at al., 1989). I also find that digits arise from separate unrelated streams of subapical mesenchyme in wing and leg. Furthermore I find no evidence for a second phase of *Hoxd-13* induction in wing. This does not appear to be consistent with the model of Shubin and Alberch (1986), which suggests that mesenchyme at the posterior margin should expand across the antero-posterior axis of the handplate and contribute to each of the digits and should therefore be linearly related.

CHAPTER FOUR

Cell lineage in pattern regulation and duplication in developing limb buds

4.1 Introduction

The DiI technique was used in Chapter Three to follow normal wing development. Here I have used the technique to investigate the behaviour of cells in regulating or regenerating limb buds and in limb duplications in which cell fate changes occur. Regulation is the process by which the limb replaces deficiencies or incorporates excesses after experimental procedures, producing a normal pattern. Regeneration is the process by which a specific structure which has been lost is re-placed and also involves regulative processes. A knowledge of how cells behave in such manipulated limbs may help to elucidate further the mechanisms of limb development.

The regulative powers of the chick limb have been shown in studies in which tissue was removed or extra tissue added to the limb bud. Previous studies have shown that the limb bud can pattern normally and regulate for loss of some of the distal mesenchyme (Zwilling, 1956; Barasa, 1964; Stark and Searls, 1974; Hornbruch, 1980; Hayamizu et al., 1994). Furthermore the limb bud appears to lose its regulative ability as development proceeds since when similar sized blocks of mesenchyme were removed at various stages between stage 20 and stage 25, defects in pattern were more apparent in the older limbs (Stark and Searls, 1974). Similarly with experiments in which transverse slices of mesenchyme were excised from the limb bud, for example, the middle third of the bud, and the distal tip pinned back onto the stump, some regulation was observed in limbs up to stage 22. Up to this stage, limb pattern was reasonably normal but the length of the limb was shorter (Summerbell, 1977; Hornbruch, 1980). After stage 22, limbs did not regulate well for the missing tissue and limb defects were apparent along the proximo-distal axis (Summerbell, 1977; Hornbruch, 1980; see also Summerbell and Lewis, 1975). Likewise, the limb is also able to regulate for excess mesenchymal tissue placed in the anterior of the bud, producing a normal pattern, but only up until stage 22 (Yallup and Hinchliffe, 1983). After this stage, skeletal defects are observed, such as loss of radius or ulna (Yallup and Hinchliffe, 1983). X-irradiation experiments have also demonstrated the regulative powers of the limb bud. Cells are killed by the X-irradiation and here too,

early limbs are more complete following X-irradiation than those after X-irradiation at a later stage (Wolpert et al., 1979). The loss of regulative powers with increasing age is probably due to the fact that cells by now are irreversibly determined and cannot be reprogrammed; hence regulation is involved in replacement of undifferentiated tissue.

The ability of the limb to regulate must involve changes in cell fate. What is the origin of cells that are involved in regulation? DiI labelling and accurate fate maps (see Chapter Three; Vargesson et al., 1997) can be used to address this question.

Recent work shows that regeneration can be induced in chick embryonic limb buds if beads soaked in FGF are applied to the amputated surface of the limb bud (Kostakopoulou et al., 1996; Taylor et al., 1994). No regeneration is seen at all in chick embryos without addition of FGF. This is probably due to the inability of the chick to reform an apical ridge which directs outgrowth of the limb (Muneoka and Sassoon, 1992). Some regeneration is observed in embryonic and fetal stages of mice where amputated digit tips can regenerate (Chan et al., 1991; Reginelli et al., 1995). Urodele amphibians are the only adult vertebrate group that can spontaneously regenerate lost or amputated limbs. Following the amputation of the tail, jaw or limb, a blastema forms at the amputated site. The blastema is a mass of undifferentiated mesenchyme cells, covered by thick epithelium which re-generates the missing tissue (for review see Brockes, 1997). The same questions as those posed about limb regulation arise when investigating the regeneration of tissue/structures; which cells contribute to the regenerated tissue? In amphibians, cells that contribute to the blastema have local origins. Here I examine the origin of cells that give rise to distal structures when FGF-4 is applied to amputated chick wing buds.

In addition to regulation and restoration of normal pattern, chick limbs can respond to grafts of polarising region signals and form additional structures. Where do these come from? The DiI technique can also be used to investigate the origin of cells in duplicated limbs in response to polarising signals, such as retinoic acid and Sonic hedgehog (*Shh*). This may give some insight into the distance over which these molecules exert their effects. This is particularly important for *Shh* as it is unclear whether *Shh* acts as a long range signal/morphogen or acts locally inducing secondary signals which mediate the effect of the polarising region (for review see Johnson and Tabin, 1997).

4.2 Results

4.2.1 Cell fate and regulation of limb bud pattern

In this set of experiments, blocks of mesenchyme tissue and dorsal and ventral ectoderm, were cut out from the stage 21-22 limb bud, leaving the apical ridge intact, to investigate the effect upon pattern and to see how these manipulations affected cell fate. Small blocks up to 400μm in length and 400μm in width in central mesenchyme, and large blocks up to 600μm in length and 1000μm in width in central and distal mesenchyme were removed from the wing bud (see Fig. 4.4, 4.5). The mesenchymal blocks were initially scored on the dorsal surface of the wing bud to outline the tissue to be removed. Then deeper cuts through dorsal ectoderm and mesoderm through to the ventral surface were made and the blocks of mesenchyme removed. Holes were healed within 24 hours and limbs were left to develop to investigate the effect upon pattern.

4.2.1.1 *Changes in limb pattern and limb length with increasing areas of mesenchyme removed from the early limb bud.*

I found that, following the removal of small blocks of mesenchyme (with dorsal and ventral ectoderm) the limb had regulated very well after 7 days development. The limbs were normally patterned although slightly smaller in length (Table 4.1A, B; Fig. 4.4). In contrast, limbs that had large squares of mesenchyme removed, although displaying some regulation, have severe patterning defects, in some cases having a hand plate only which is reduced in length (Table 4.1A, C; Fig. 4.5). These results suggest although the early chick limb bud has regulative powers it regulates poorly following the removal of large mesenchymal blocks.

Regulation occurs when small areas of mesenchyme are removed and the limbs that form have an almost perfect limb pattern. Blocks of mesenchymal tissue up to 400μm^2 were removed from the centre of a stage 21/22 bud leaving the apical ridge intact with approximately 350μm of mesenchyme attached to the ridge (see Fig. 4.4E). The excised mesenchyme (see Chapter Three) would normally have contributed to the radius and ulna, whereas the mesenchyme tissue left behind would normally contribute to the humerus and the digits. The resulting limbs have a normal cartilage pattern (Fig. 4.1A). However, despite being normally patterned, the limb itself and the cartilage elements are slightly smaller than the contralateral limb. Measurements of the experimental limb cartilage elements, after 7 days incubation, as compared to the contralateral limb show that these are reduced in length by up to

Table 4.1

A. Control limb lengths after 7 days incubation

Skeletal element	Left limb μm	Right limb μm	Percentage difference
Whole Limb	8300 +/-224	8300 +/-224	0
Humerus	4856 +/-101	4825 +/-112	0.7
Ulna	4675 +/-130	4631 +/-141	0.9
Radius	4043 +/-102	4075 +/-158	0.8
Digit 2	1975 +/-176	1975 +/-176	0
Digit 3	4568 +/-110	4631 +/-123	1.4
Digit 4	3175 +/-102	3175 +/-102	0

B. Limb and skeletal element lengths following small mesenchyme removals at stage 21/2

Skeletal element	Contralateral limb μm	Experimental limb μm	Percentage reduction
Whole Limb	8490 +/-187	7835 +/-290	8
Humerus	5325 +/-130	4625 +/-125	14
Ulna	5125 +/-135	3700 +/-155	20
Radius	4455 +/-110	4125 +/-100	17
Digit 2	1800	1805 +/-100	0
Digit 3	5150 +/-100	4350 +/-135	16
Digit 4	3050 +/-150	2950 +/-100	4

n=3

C. Limb and skeletal element lengths following large mesenchyme removals at stage 21/2

Skeletal element	Contralateral limb μm	Experimental limb μm	Percentage reduction
Whole Limb	8040 +/-212	3210 +/-182	60
Humerus	4608 +/-207	1816 +/-502	61
Ulna	4400 +/-217	1191 +/-488	63
Radius	4175 +/-217	1000 +/-359	76
Digit 2	1650 +/-169	978 +/-350	40
Digit 3	4196 +/-277	3000 +/-505	29
Digit 4	2709 +/-171	1533 +/-427	43

n=6

Tables comparing the left (contralateral) limb and skeletal element lengths with the right (operated) limb and skeletal lengths. Note there is a slight reduction in size in the right limb as compared the left in the normal, unoperated limb, but with increasing mesenchyme loss, increasing reductions in lengths of limb and limb elements is seen.

Figure 4.1

Wings that developed after removal of blocks of mesenchyme

All wholemounts stained with alcian green to show cartilage pattern. In all cases contralateral wing on the left, operated wing on the right. Scale bar represents 3000μm.

A) Wing that developed after removing a small block of mesenchyme from a stage 21/2 bud, leaving the apical ridge intact. Operated wing has normal pattern but is slightly shorter than contralateral (n=2); B and C Wings that developed following removal of large blocks of mesenchyme from stage 21/2 bud; **B)** Hand plate has developed but no proximal structures. The hand plate is short, a digit **3** is present together with 2 unidentifiable digits (n=3); **C)** A very small wing, containing a very shortened humerus, thin and short ulna, no radius but almost normal hand plate (n=2); **D)** Wing that developed following removal of a large block of mesenchyme and removal of apical ridge. The only cartilage element observed is a very severely truncated humerus. The humerus is even more truncated than that seen when just the ridge is removed (see Fig. 3.6H), suggesting that the apical ridge has an essential role in regulation.

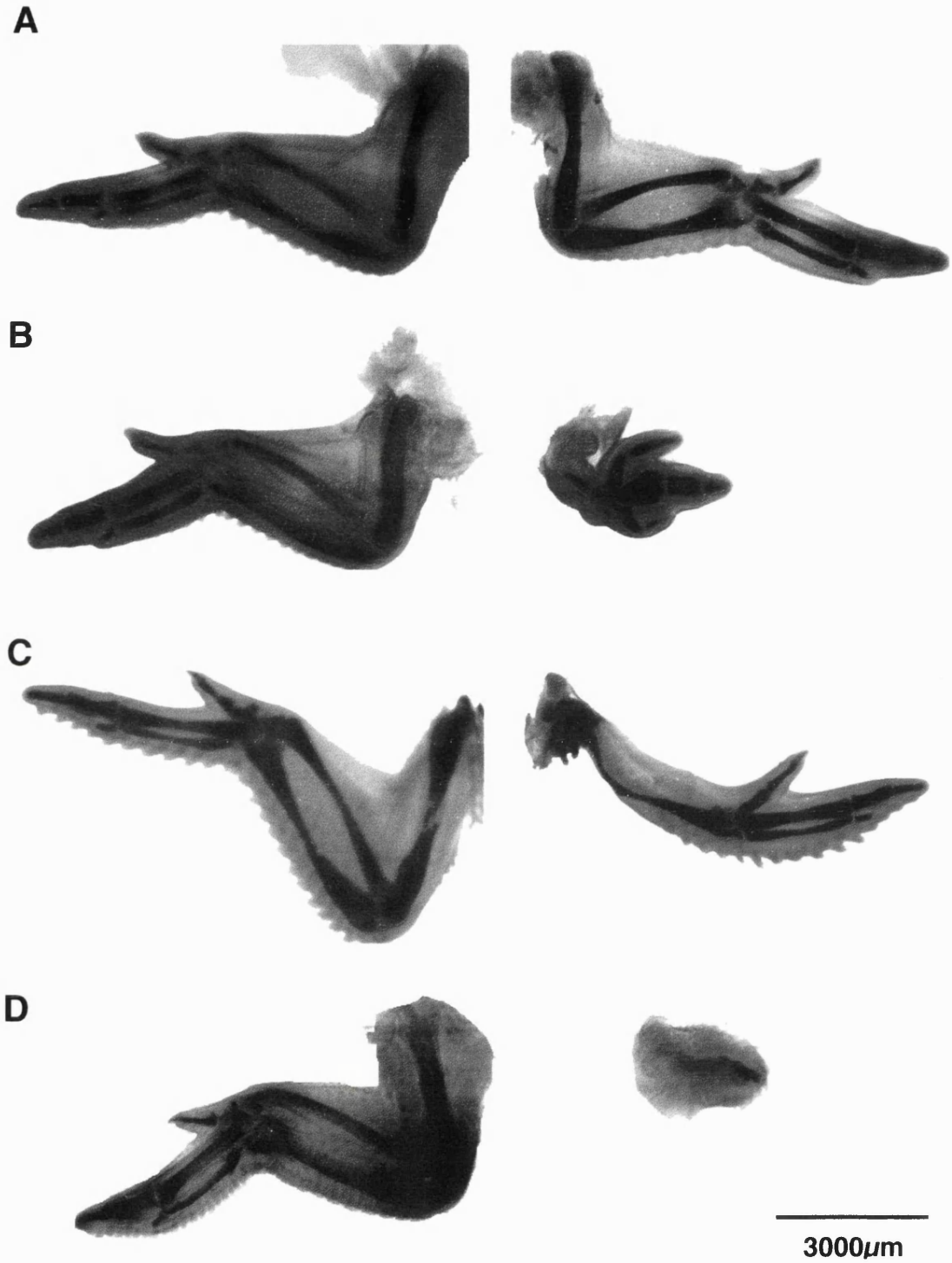
A
B
C
D
3000μm

20% (Fig. 4.1A, 4.2A, 4.3; Table 4.1B). In these experiments, the most affected elements are the ulna and digit **3** while the rest of the hand plate is relatively normal (Fig. 4.1A, 4.3; Table 4.1B). That the limb is patterned and has a radius and an ulna suggests the limb regulated for the loss of tissue very well in both antero-posterior and proximo-distal directions.

Removal of large blocks of mesenchyme causes severe patterning defects. Large blocks of tissue (600μm X 1000μm) were removed from a stage 21-22 bud, removing practically all the central and distal mesenchyme leaving the apical ridge intact with less than 100μm mesenchyme attached to the ridge. The mesenchyme removed would have made the distal part of the humerus, radius, ulna and the wrist, whereas the mesenchyme left would be predicted, from fate maps, to produce part of the humerus and the digits (see Chapter Three). Within 2 hours of the operation, the apical ridge and underlying mesenchyme had contracted onto the proximal mesenchyme and the hole completely healed in most cases within 24 hours. These limbs were left to develop for a further 48 hours or 7 days (Fig. 4.1, 4.5). After 7 days incubation the resulting limb pattern, in 3/5 cases, was that of a hand plate only, which had defects and was considerably shorter than normal (Fig. 4.1B; Table 4.1C). In two cases, a limb was present but the hand plate was shorter than normal and the forearm and humerus were severely shortened (Fig. 4.1C, 4.2B, 4.3; Table 4.1C). Thus, following large mesenchyme removals severe pattern defects are observed; little if any regulation is seen but a hand plate is always formed. Thus, the defects observed after large amounts of mesenchyme were removed were more severe than those observed after the removal of small amounts of mesenchyme where pattern was normal.

4.2.1.2 *DiI analysis to investigate the origins of tissue involved in regulation of the excised mesenchyme*

The DiI labelling technique was used to investigate the origins of cells that restore normal pattern after removal of small blocks of mesenchyme. Populations of cells in specific positions around the wound margin were labelled with DiI and their subsequent fate followed. The limbs were incubated for 48 hours and then observed under fluorescence microscopy to analyse the patterns of cell movement.

Cells from the distal wound margin were involved in the regulation of pattern following removal of small blocks of mesenchyme. Populations of cells were DiI labelled in four areas on the margin of the wound; along posterior margin of the wound proximally, distally and midway between these two positions; and a

Figure 4.2

Mean length of limbs and of individual skeletal elements following removal of blocks of mesenchyme compared with the mean lengths of unoperated contralateral limbs and their individual skeletal elements. **A**) removal of small blocks of mesenchyme; note small changes in lengths of the skeletal elements. **B**) removal of large blocks of mesenchyme; note large changes in length of skeletal elements. Scale bars represent standard error. Note with removal of both small and large blocks of mesenchyme, the digits seem least affected. H = humerus, U= ulna, R = radius, 2 = digit **2**, 3 = digit **3**, 4 = digit **4**.

A

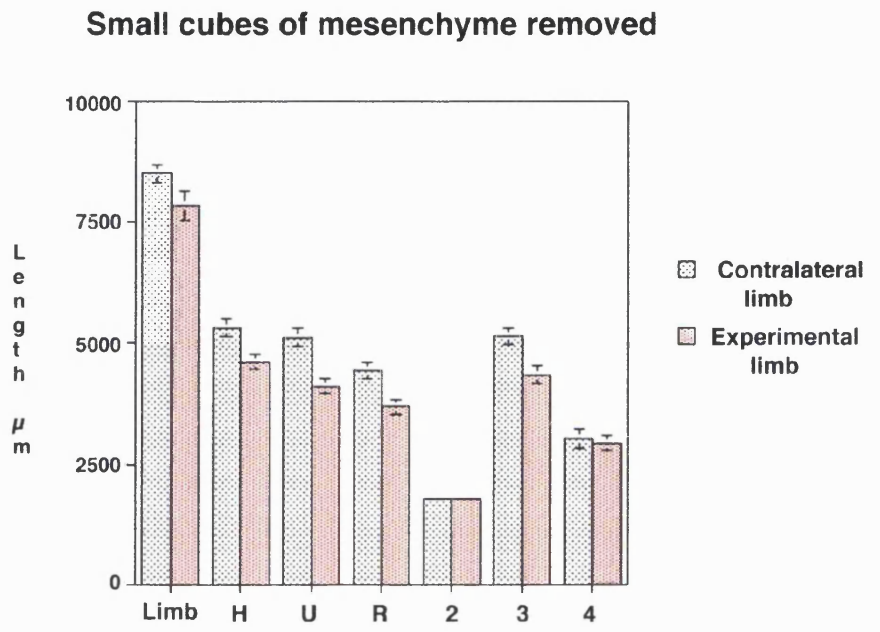
Small cubes of mesenchyme removed
10000
7500
5000
2500
0
Length μm
Limb
H
U
R
2
3
4
Contralateral limb
Experimental limb

B

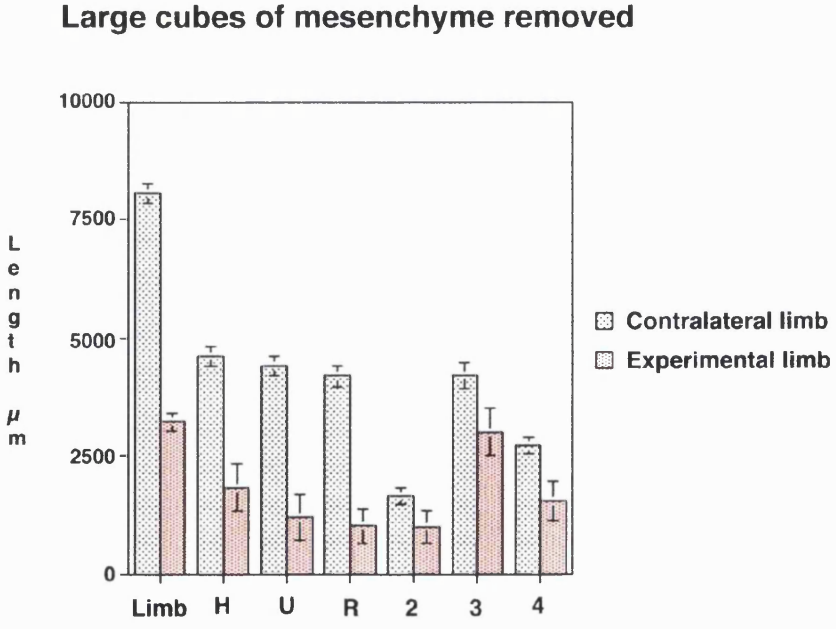
Large cubes of mesenchyme removed
10000
7500
5000
2500
0
Length μm
Limb
H
U
R
2
3
4
Contralateral limb
Experimental limb

Figure 4.3

Percentage reduction of limb length and of each length of the skeletal elements following removal of small and of large blocks of mesenchyme as compared to the control lengths of the limb and skeletal elements. Note the effect of removal of small blocks of mesenchyme is considerably less than that of large blocks of mesenchyme and that in both cases the hand plate seems to generally be less affected than the rest of the limb. H = humerus, U= ulna, R = radius, 2 = digit **2**, 3 = digit **3**, 4 = digit **4**.

Comparision of the percentage reduction in skeletal element size after removal of large mesenchyme cubes and after removal of small mesenchyme cubes

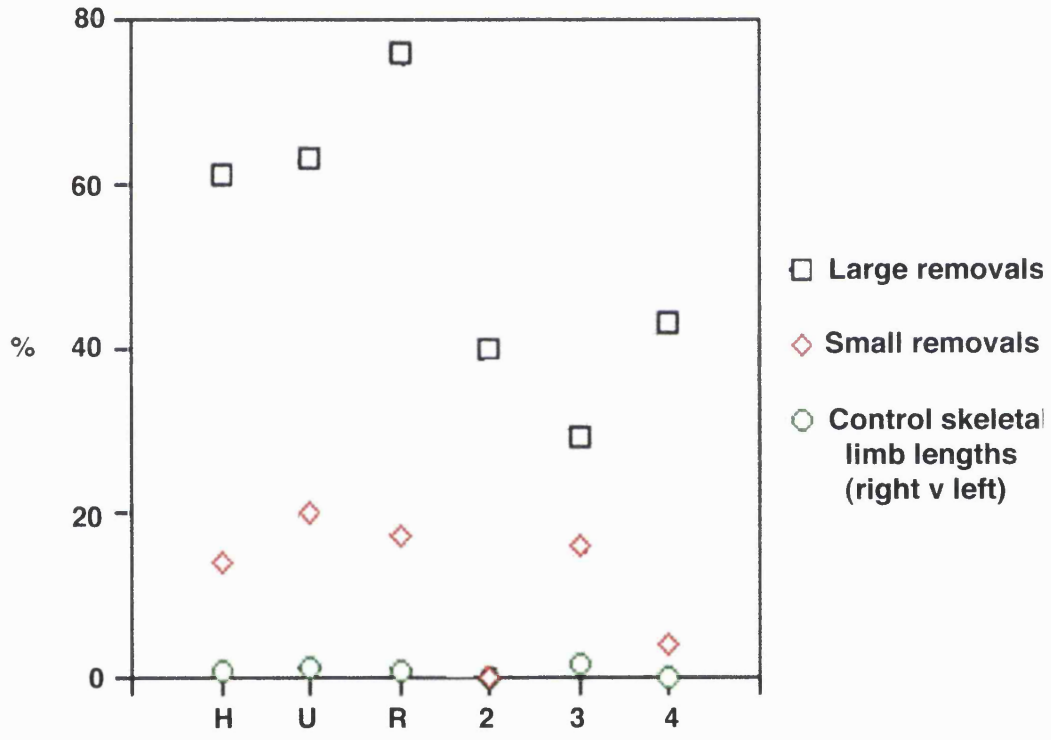

Figure 4.4

DiI investigation into behaviour of cells after removal of small blocks of mesenchyme

Small blocks of mesenchyme containing cells normally fated to form the fore-arm were removed from wing buds at stage 21/2 and DiI was injected into positions around the wound margin as shown in **E**), positions marked A, B, C, D. Scale bar represents 300μm. 48 hours later, the position of the labelled cell populations was investigated; Mesenchyme labelled in posterior proximal corner of the wound (**A**) behaves as in normal fate maps and does not contribute to the regulated structure. Labelled cells are found in prospective elbow region and not in the forearm region; Mesenchyme labelled half way along the posterior margin of the wound (**B**) behave normally as shown in fate maps (see Chapter Three) and are not found contributing to the forearm region; Cells labelled at the distal corner of the posterior margin of the wound (**C**) do not contribute to the regulated forearm tissue, ending up, as predicted from fate maps (see Chapter Three), around the prospective elbow region of the limb; (**D**) Mesenchyme labelled on the distal margin in a position on a level with somite 18, contributes to the forearm region suggesting these cells have changed fate to regulate for the missing tissue. Scale bar represents 500μm.

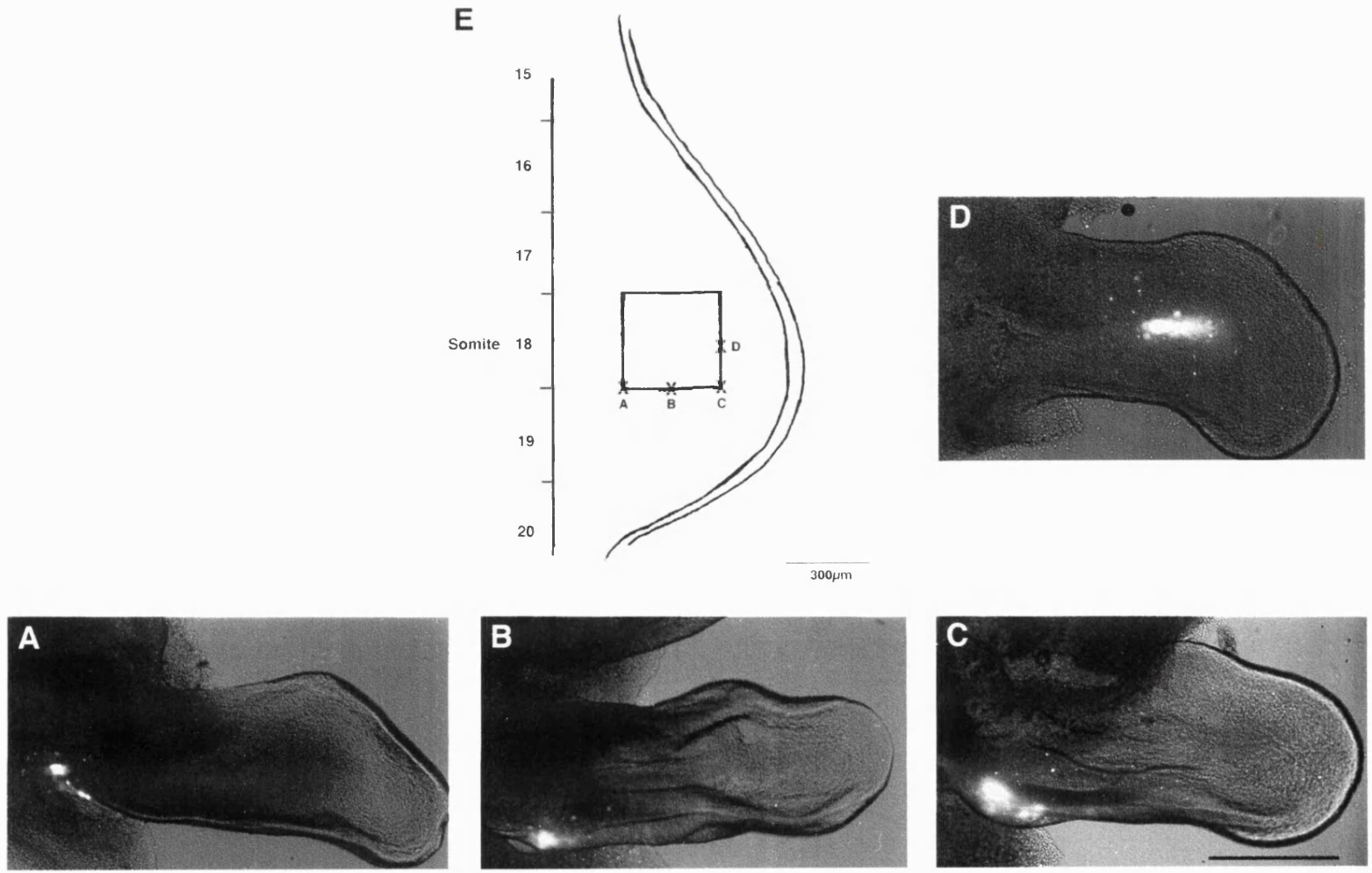
E
15
16
17
Somite 18
19
20
D
A
B
C
300μm
D
A
B
C

Figure 4.5

DiI investigation into behaviour of cells after removal of large blocks of mesenchyme

Large blocks of mesenchyme were removed from a stage 21/2 limb, apical ridge left intact with a rim of mesenchyme attached (75-100μm thick) beneath the ridge. Cells are fated normally to form distal humerus, forearm and proximal hand plate. Small populations of mesenchyme around the perimeter of the wound margin were labelled with DiI in positions as shown in **H**), scale bar represents 150μm. Following DiI labelling, limbs were left to develop for a further 48 hours. In all cases, the resulting limbs were shorter than normal. In contrast to the removal of small blocks of mesenchyme, tissue contributing to the resulting structure following large mesenchyme loss, the hand plate, originates from distal, posterior margin and proximal posterior cell populations. **A**) Populations labelled at anterior proximal corner of wound, remain proximal, and do not appear to contribute to the regulated structure, the hand plate. Populations labelled midway along the proximal wound margin **B**), may be a little more posteriorly located than in normal fate maps and contribute to proximal parts of the regulated structure (Chapter Three; Fig. 3.3; Table 4.2A, B). **C**) populations labelled on the proximal posterior margin of the wound behave very similarly to equivalent positions in normal fate maps (Chapter Three; Fig. 3.3), however a small proportion of these cells do contribute to the regulated area (Table 4.2A, B). Populations labelled midway along the posterior margin of the wound contribute to the regulated area as cells are found within the regulated area as shown in **D**). Cell populations labelled on the distal corner of the posterior wound margin, **E**) and midway along the distal wound margin (on a level with somite 18), **F**), both contribute to the hand plate as labelled cells are found throughout the middle of the operated limb. Measurements of all the DiI labelled streams suggest that these populations make up a greater proportion of the limb than the DiI labelled streams which result when cell populations are labelled in similar positions in normal limb buds. **G**) Represents a whole mount of a contralateral limb to compare with the experimental limbs to show the effect of the mesenchyme removal. Scale bar represents 500μm.

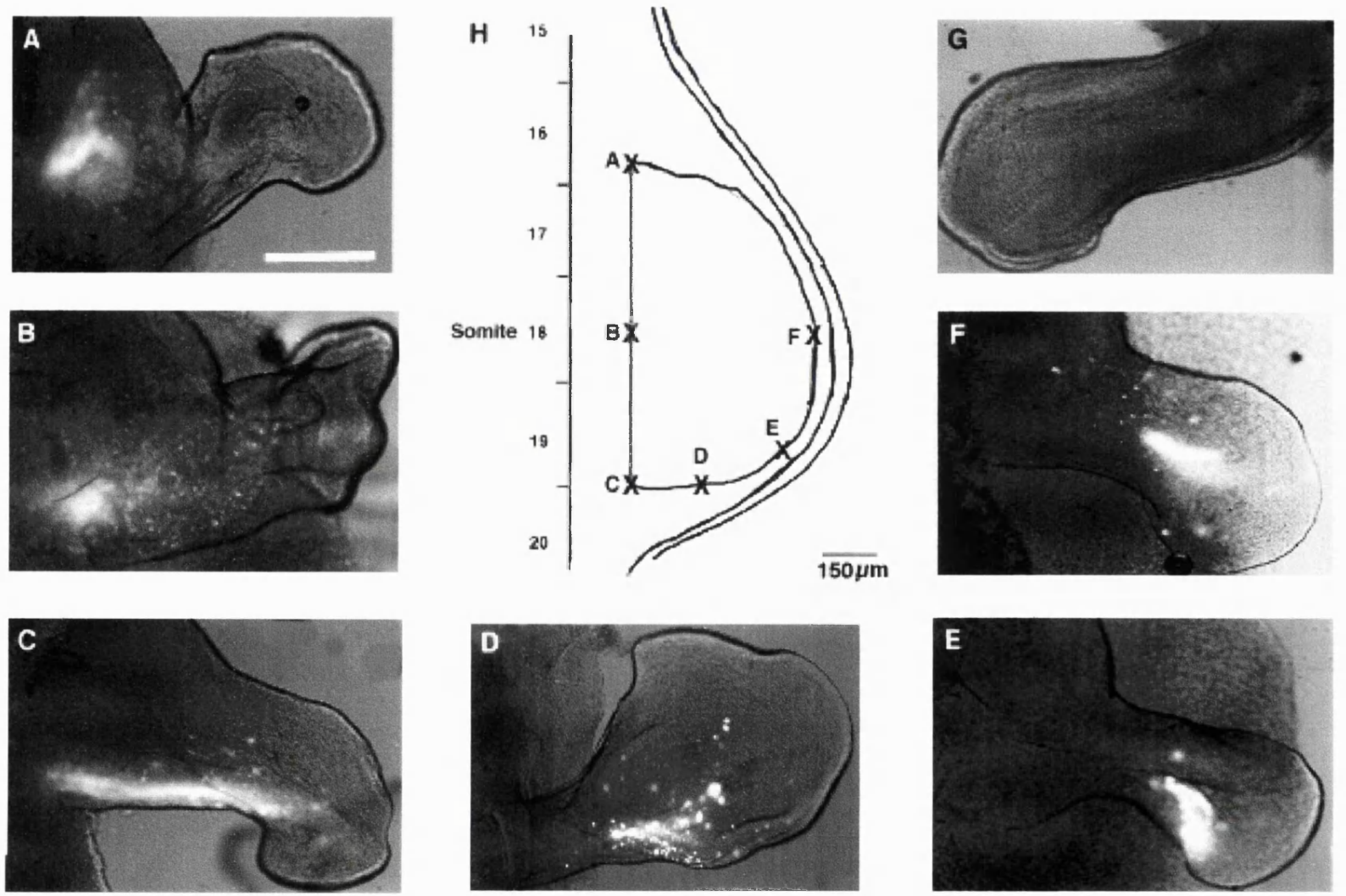
A
B
C
D
E
F
G
H
15
16
17
Somite 18
19
20
A
B
C
D
E
F
150μm

population at the midpoint of the distal border of the wound was also labelled (Fig. 4.4). Only cells from the population labelled distally were seen within the area that will give rise to the forearm (Fig. 4.4D). Proximal populations of mesenchyme cells remained proximal and behaved as in normal limbs (Fig. 4.4A, B, C) i.e. not expanding and not contributing to the forearm region. Thus, following removal of small blocks of mesenchyme, cells from the distal wound margin appear to change fate to contribute to the forearm (Fig. 4.6A)

Following removal of large blocks of mesenchyme, populations of mesenchyme were labelled with DiI in several positions along the posterior, distal and proximal margins of the wound (Fig. 4.5). After 48 hours incubation, posterior proximal, posterior distal and distal cell populations were observed within the central region of the limb bud (Fig. 4.5C, D, E, F); proximally labelled populations remain proximal (Fig. 4.5A, B). When the proximo-distal lengths of the DiI domains were measured, these were found to be shorter in length than domains in comparable positions in normal limbs (see Chapter Three; Table 4.2A, B). However the entire limb is shorter. If cell behaviour was affected only distally as appears to be the case following small mesenchyme removal, than the entire regulated area should come from distal cells. However following large mesenchyme removal, the distal DiI labelled cell populations do not completely fill the regulated area. This result suggests that both distal and proximal tissue contribute to the structures formed. When the proximally labelled populations are measured and compared to patterns of spread within a normal un-operated limb, these populations do indeed show increased expansion and domain sizes (Table 4.2A, B). Thus, following large mesenchyme removal, cell populations labelled along the distal, posterior distal and posterior proximal margin all contribute to the limb structures observed (Fig. 4.6B).

4.2.1.3 *Expression of Hoxa-10, Hoxa-13 and Hoxd-13 after large mesenchyme removal*

In order to see if expression patterns of genes involved in hand plate development are disrupted when large blocks of mesenchyme are removed, the expression patterns of the genes *Hoxa-10*, *Hoxa-13* and *Hoxd-13* were assessed within limbs (Fig. 4.7). These genes were chosen as they are expressed in the regions of mesenchyme that were removed at stage 22. Hence most of the expression domain of *Hoxa-10* i.e. proximal and central mesenchyme and faintly beneath the apical ridge will be removed. In addition most of the early expression domains of *Hoxa-13* and *Hoxd-13* which are both found in posterior distal mesenchyme beneath the apical

Table 4.2

A. DiI comparison analysis 48 hours - Mesenchyme removal with apical ridge intact

Position	Limb length μm	Contralateral limb length μm	% Reduction in limb length	Length DiI μm	Proportion limb
A	750	1250	40	250	0.33
B	625	1250	50	142	0.22
C	725	1225	41	625	0.83
D	600	1225	51	250	0.40
E	650	1275	50	250	0.40
F	800	1350	40	312	0.41

B. Control DiI labelled limbs in similar positions to the experimental positions (see Chap.3)

Position	Limb length μm	Length DiI μm	Proportion limb
A	1250	177	0.14
B	1625	177	0.11
C	1375	750	0.54
D	1500	312	0.21
E	1500	562	0.37
F	1500	500	0.33

Tables showing that removal of large blocks of mesenchyme reduces the length of the limb as compared to the contralateral limb, but that DiI labelled populations make up a larger proportion of the operated limb than in normal unoperated limbs in similar labelled positions. This suggests that proximal and distal populations contribute to regulate for the missing tissue.

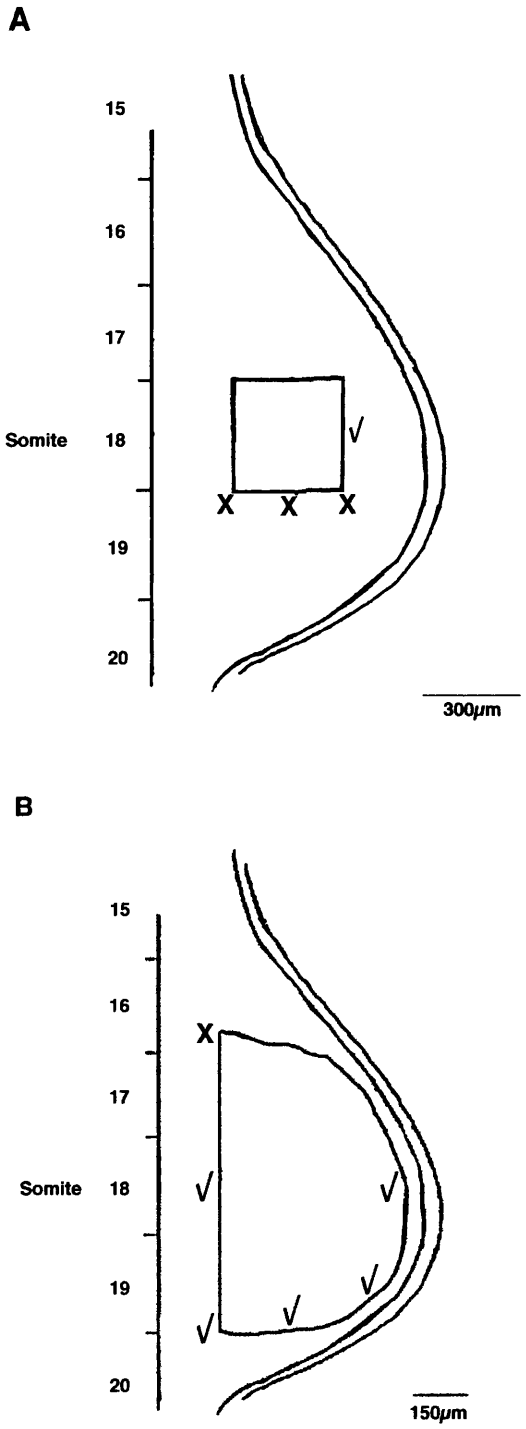

Figure 4.6

Summary of the mapping experiments showing origin of cells involved in regulation of small and large mesenchyme losses

A) Following removal of small cubes of mesenchyme, only cells from the distal margin were found to be involved in regulation of the lost tissue to produce a relatively normal limb (√). Cells in all other positions tested (X) did not contribute to the regulated area and cell fate was normal (compared with normal fate maps; see Chapter Three; Scale bar represents 300μm); B) Shows cells at distal margin, posterior distal and posterior proximal margins contribute to structures formed following removal of large cubes of mesenchyme (√). Scale bar represents 150μm

Figure 4.7

***Hox* gene expression following removal of large blocks of mesenchyme**

Hoxa-10 A-B; *Hoxa-13* C-D and *Hoxd-13* E-F. Despite removal of most of the expression domain at stage 21/2, *Hox* gene expression was re-established in the prospective hand plate 24 and 48 hours later, although limbs were truncated and smaller and narrower than normal. In all cases contralateral normal limb on left and operated limb on right. Following removal of large blocks of mesenchyme: *Hoxa-10* expression was found in proximal tissue, **A)** 24 hours and **B)** 48 hours later; **C)** After 24 hours *Hoxa-13* expression in posterior distal tissue; but expression domain is smaller than that in contralateral limb but makes up a larger proportion of the limb; **D)** after 48 hours expression of *Hoxa-13* at tip of operated limb now more extensive that at 24 hours. Note the operated limb is truncated and narrower than normal limbs. **E)** After 24 hours *Hoxd-13* expression is found faintly in posterior mesenchyme. **F)** After 48 hours extensive *Hoxd-13* expression is seen in very small narrow bud. Note expression is almost throughout this small bud. Scale bars represent 500μm.

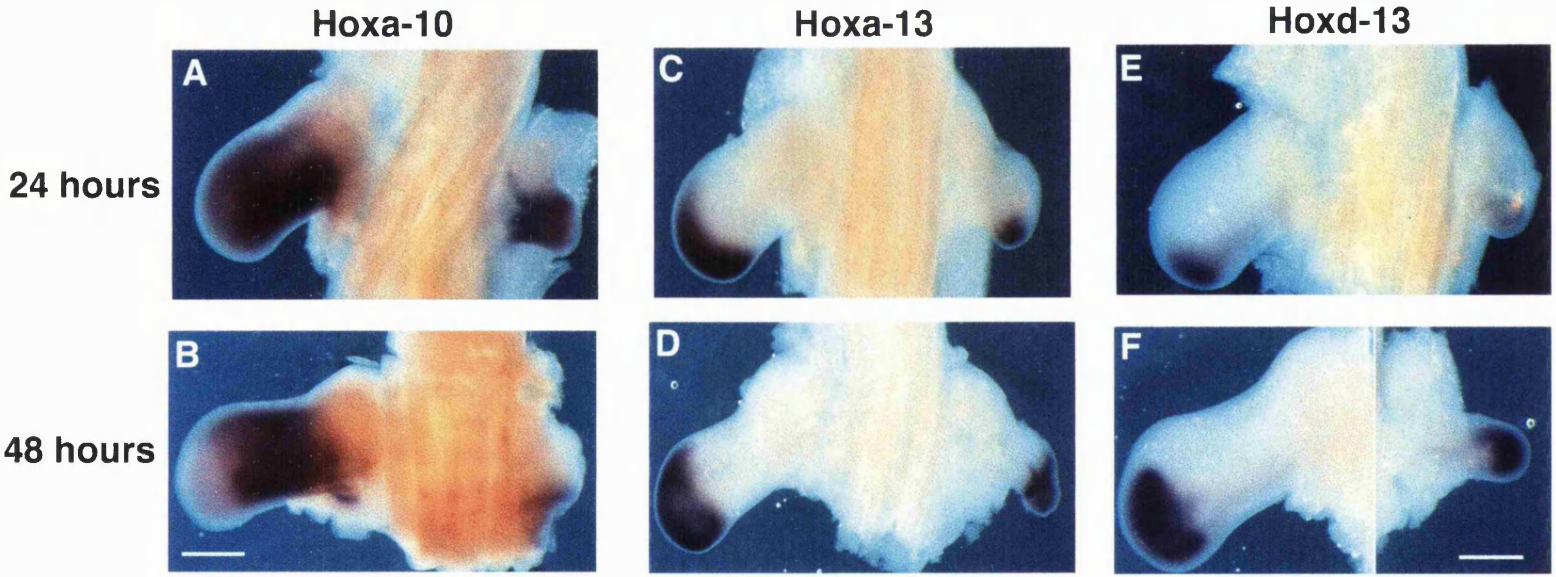
Hoxa-10
Hoxa-13
Hoxd-13
24 hours
48 hours
A
B
C
D
E
F

ridge would be removed (Fig. 3.8A, 3.10G, L), except for the small amount of mesenchyme that expresses these genes which will be left attached directly beneath the apical ridge.

Expression of all these genes was detected in the manipulated limbs 24 and 48 hours after the operation (Fig. 4.7). The expression domains of the genes appear to be more extensive (Fig. 4.7A, C, E). For example, the expression domains of *Hoxa-13* and *Hoxd-13* 48 hours after mesenchymal removal extend throughout the majority of the limb which is however, much shorter and narrower than normal. This extended expression may be the result of incorporation of proximal cells that would not normally express these genes to contribute to the formation of distal structures. This may be the reason why the hand plate is always seen after such manipulations and why in many cases only the hand plate is observed. (Fig. 4.7B, D, F).

Apical ridge removal affects regulation of removed mesenchyme

To test the effects of the apical ridge upon the limbs regulative capacity, the apical ridge was removed and large blocks of mesenchyme were then removed. Cell populations were labelled with DiI around the distal, proximal and posterior margins of the wound (Fig. 4.8). After 48 hours, the labelled populations of cells had not expanded and remained where they had been originally labelled (Fig. 4.8; Table 4.3) and the limbs were very severely truncated. Furthermore, limbs left for 7 days gave rise to part of a humerus only (Fig. 4.1D). Thus the presence of the apical ridge appears to be necessary for replacement and regulation of missing tissue. Earlier, I showed that ridge removal had no affect on proximal cells (see Chapter Three) but in apical ridge intact regulating limbs these cells do show increased expansion. This increase in expansion is inhibited if the ridge is removed. Thus, regulation and change in behaviour of proximal cell populations appears to depend on apical ridge signalling.

4.2.1.4 *Regeneration of limb stumps in response to FGF-4*

The results just described show that the apical ridge is important in regulation and the recruitment of proximal cells to contribute to distal structures producing a normal pattern. Recently it has been shown that the apical ridge, specifically an apical ridge signal - the FGFs can lead to regeneration of chick wing stumps (Taylor et al., 1994; Kostakopoulou et al., 1996) where again proximal cells are induced to form the regenerated distal structures. In order to define which proximal cells are able to contribute to the 'regenerate' I used the DiI labelling technique to study the effect of FGF upon cell fate (Kostakopoulou et al., 1996). Distal tips of stage 24 limb buds were

Figure 4.8

DiI investigation into behaviour of cells after removal of large blocks of mesenchyme accompanied by apical ridge

Large blocks of mesenchyme and apical ridge were removed from stage 21/2 limbs and populations of mesenchyme around the wound perimeter were labelled in positions as shown in (**I**). At 48 hours, all limbs showed truncation and all labelled populations do not expand and remain where they were initially labelled. **A**) Example of a contralateral limb. **B**) Cell populations labelled proximally on a level with somite 18 remain proximal, not expanding much and their behaviour appears normal as compared to normal fate maps. **C**) Cell populations labelled on the posterior proximal corner of the wound remain proximal and do not expand. **D**) Cell populations labelled in the middle of the posterior margin of the wound end up at the base of the prospective elbow. Populations labelled on the distal margin of the wound in the posterior **E**), middle **F**) or anterior **G**), all remain where labelled and do not expand much. Note the area of non-labelled mesenchyme distal to the DiI label. Scale bar represents 250μm in A, B, C, D, E, F and G. **H**) Example of a limb fixed immediately following mesenchyme and ridge removal and after labelling with DiI in position B, scale bar represents 450μm.

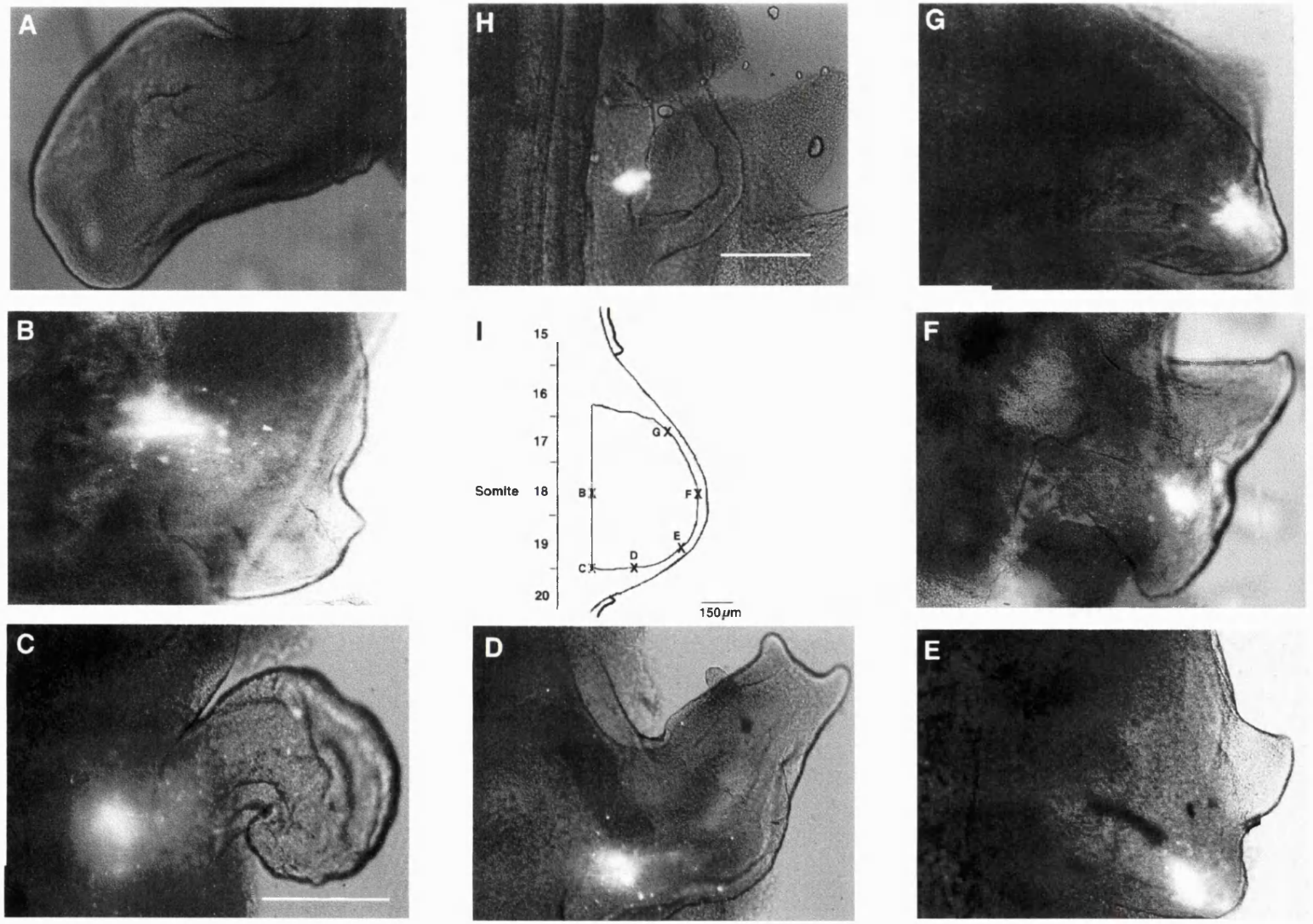
A
H
G
B
I
15
16
17
Somite 18
19
20
G
B
F
E
D
C
150μm
F
C
D
E

Table 4.3
Mesenchyme removal following apical ridge removal

Position	Limb length μm	Contralateral limb length μm	% Reduction	Length DiI μm	Proportion limb
A					
B	375	1150	68	162	0.43
C	400	1200	66	87.5	0.21
D	475	1200	60	62.5	0.13
E	375	1175	68	87.5	0.23
F	375	1200	69	87.5	0.23

Table showing that limb length and length of streams of DiI are severely reduced following removal of large blocks of mesenchyme and the apical ridge.

amputated and beads of FGF-4 stapled to the distal posterior surface. The DiI technique was then used to elucidate the origin of the cells that make up the regenerated structures and by comparison with fatemaps (see Chapter Three; Vargesson et al., 1997) to elucidate if cell fate and behaviour has been altered.

Small populations of mesenchyme were labelled with DiI in positions anterior, posterior and proximal to the FGF-4 bead pinned at the posterior distal margin of a limb bud that had 300μm of the distal tip amputated, carried out by K. Kostakopoulou (Fig. 4.9). Only cell populations in the immediate vicinity of the FGF-4 bead were found 48 hours later to be contributing to the regenerated structure (Kostakopoulou et al., 1997; Fig. 4.9; Fig. 4.10). This regions extends 200μm proximally along the posterior margin of the bud and up to 100μm anteriorly in distal mesenchyme above the bead (Fig. 4.9; Fig. 4.10C-H). Cells within these regions located proximal to the bead were observed to move distally towards the bead (Fig. 4.10C, D). Anterior populations over 100μm anterior to the bead remain anterior and do not expand or contribute to the regenerated structure (Fig. 4.10F, G, H).

Beads soaked in FGF-4 were also pinned to the anterior distal margin of amputated wing buds and populations of mesenchyme labelled with DiI in positions anterior, posterior and postero-distal to the bead. However no outgrowth of the limb was observed (Kostakopoulou et al., 1997) and subsequently the labelled DiI populations remained anterior in small domains and behaved as shown in fatemaps (Chapter Three; Vargesson et al., 1997). This result shows that like the large mesenchyme removal experiments, posterior cell populations have the potential to generate distal structures but to realise this potential they need a source of FGF. These results also show that this potential does not appear to be present in the anterior of the bud.

4.2.2 Cell fate in pattern duplications

The polarising region can induce digit duplications if grafted to the anterior margin of the wing (Saunders and Gasseling, 1968). This effect can be mimicked by retinoic acid and also by the proposed polarising region signal, *Shh* (Tickle et al., 1982; Riddle et al., 1993). DiI technology can be used not only to investigate the origin of cells that contribute to duplicated structures in response to polarising signals but also elucidate the potential distances over which these molecules may signal.

Figure 4.9

Summary of origins of cells that contribute to limb outgrowth in response to FGF-4 following distal limb tip amputation

Following the amputation of the distal wing tip and the application of an FGF-4 soaked bead, mesenchyme populations were DiI labelled in various positions around the bead and at different distances. Black circle indicates where all labelled cells end up in FGF-4 induced outgrowth. Stippled circles indicate some labelled cells were found in the FGF-4 induced outgrowth. Clear circle indicate no cell contribution to the FGF-4 induced outgrowth. Cells directly posterior to the bead contribute to the outgrowth and cells up to 200μm proximal posteriorly and anteriorly can also contribute all other positions.

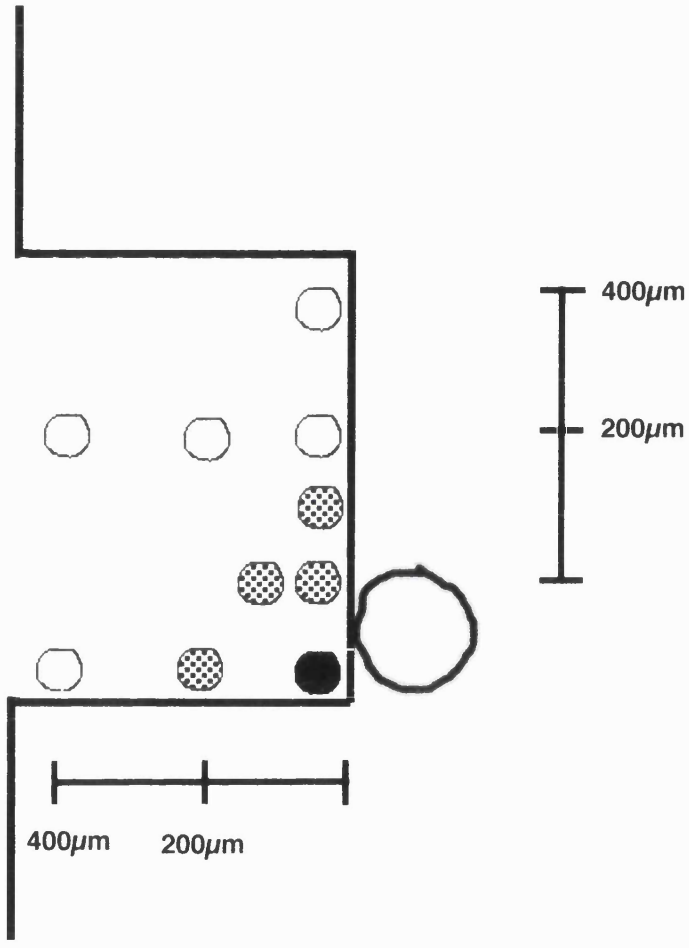
400μm
200μm
400μm
200μm

Figure 4.10

Origin of cells contributing to regenerating chick wing buds after amputating 300μm from the tip of the bud at stage 23-24, application of FGF-4 and injection of DiI

Following amputation of distal 300μm of stage 23/4 limb tip, an FGF-4 soaked bead was stapled to posterior stump. DiI was injected into positions proximal, anterior and posterior to the bead at various distances, in order to ascertain the origin of cells that produce the FGF-4 induced outgrowth. **A)** Limb fixed after FGF-4 bead application and DiI injection proximal to bead on the posterior margin. Scale bar represents 500μm. **B)** Limb fixed 48 hours after application of PBS soaked bead and DiI injected 50μm proximal to the bead (arrowed) on the posterior margin. Note not much spread of DiI. C-H Limbs fixed 48 hours after FGF bead application and DiI injection. Arrowhead denotes position of bead. Regions distal to the dotted lines indicate the amount of outgrowth induced by the FGF-4 bead. **C)** 0-50μm proximal to bead on posterior margin. Note all labelled cells within the induced outgrowth area; **D)** 200μm proximal to bead on the posterior margin. Note some cells seen in the outgrowth; **E)** 400μm proximal to the bead on the posterior margin; **F)** 0-50μm anterior to the bead on the plane of amputation. Note cells in the induced outgrowth; **G)** 200μm anterior to the bead along the plane of amputation; **H)** 400μm anterior to the bead along the plane of amputation. Scale bar represents 500μm.

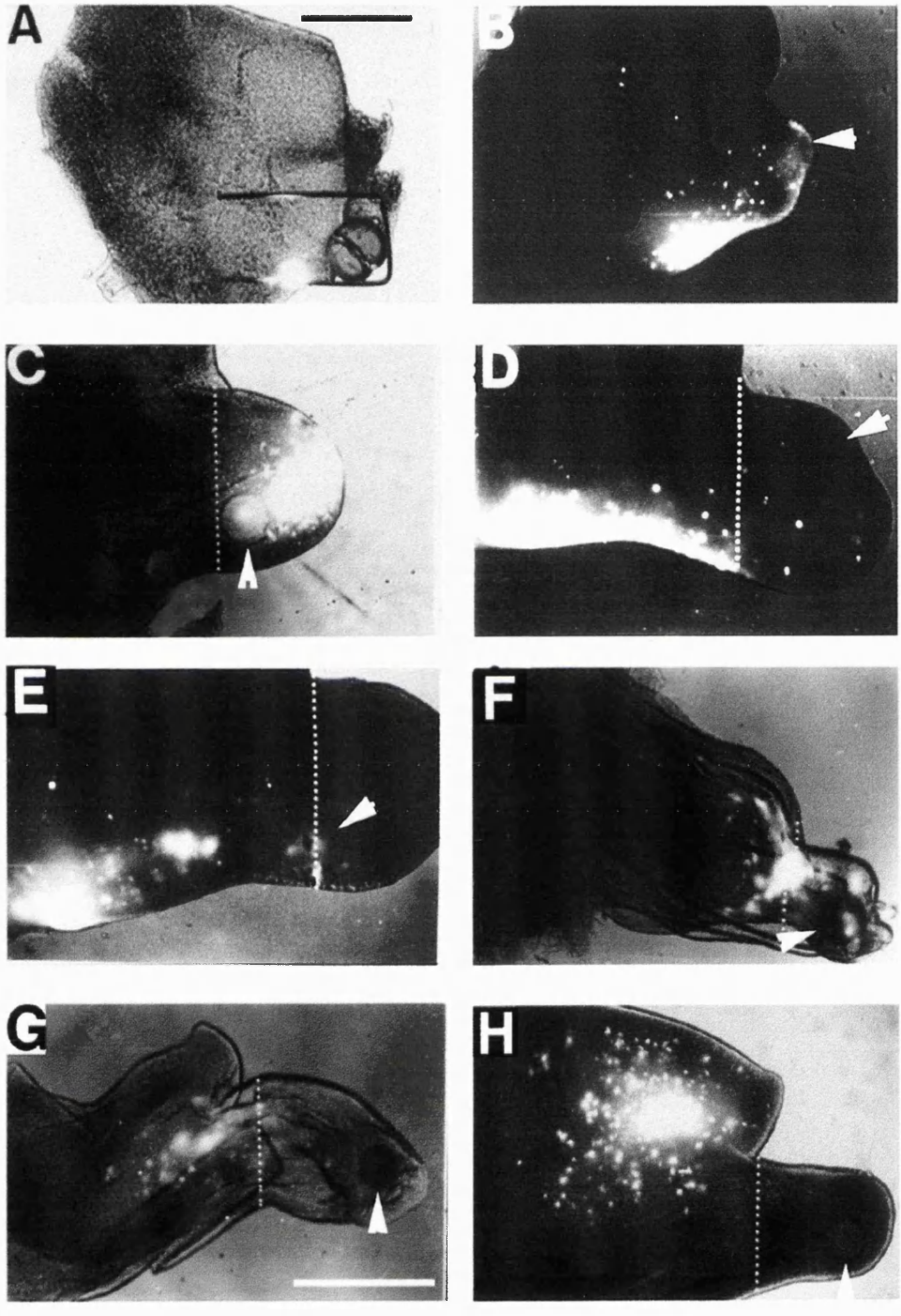
A
B
C
D
E
F
G
H

Retinoic acid

Beads soaked in 0.1mg/ml retinoic acid were placed beneath the anterior apical ridge of stage 20 limb buds on a level with somite 17 and allowed to develop for a further 96 hours to 7 days, so that the resulting skeletal pattern of the limbs could be seen. The majority of limbs had one or two extra digits. The most common pattern of digits was **4-3-3-4** (n=12), but **4-3-2-3-4** (n=2) was also seen (Fig. 4.11B). In normal limb buds, cells labelled subapically opposite somite 17 do not contribute to the digits and remain proximal. Do these cells give rise to the additional digits when retinoic acid is applied?

Small populations of mesenchyme cells in positions anterior, posterior and postero-distal to the retinoic acid bead (Fig. 4.12) were labelled. 96 hours later when the pattern of digits could be made out, it could be seen that cell populations postero-distal to the bead contribute to the additional digits but not cell populations in anterior and proximal positions (Fig. 4.12). By carefully labelling cell populations at set distances from the bead in mesenchyme postero-distal to the bead, I deduced that only a small region of postero-distal mesenchyme, up to 250μm away from the bead contributed to the additional digits (Fig. 4.11; Table 4.4). Populations of cells labelled 125μm from the bead form streams running from the bead into the anterior part of the duplication (Fig. 4.11D). Mesenchyme populations labelled 200μm from the bead form streams running into the duplicated part of the limb into the additional digit **4** (Fig. 4.11E). Whereas cell populations labelled 225-250μm from the bead form streams running into a potential duplicated digit **3** (Fig. 4.11F). Any cell population labelled over 250μm from the bead did not contribute to the duplicated structure and behaved as shown for normal fatemaps (Fig. 4.11G; Chapter Three) i.e. populations labelled over 300μm away from the bead, on a level with somite 18, form a wide stream of labelled cells running from proximal regions towards the apical ridge, in between the host limb digit **3** and the additional digit **3**.

This work shows that retinoic acid induces additional structures from a small region of postero-distal mesenchyme. Under the influence of retinoic acid the behaviour of anterior cell populations, which normally remain proximal and do not expand or contribute to digit formation, is changed so that they behave like posterior populations producing streams of labelled cells which contribute to the additional digits.

Sonic hedgehog (*Shh*)

Using the DiI technique, I labelled populations of mesenchymal cells in various positions around a bead soaked in *Shh* protein, implanted by G. Drossopoulou, beneath the anterior apical ridge on a level with the boundary between

Figure 4.11

Origins of cells contributing to duplicated digits following application of retinoic acid to the anterior margin

Following application of retinoic acid soaked beads beneath anterior apical ridge populations of mesenchyme cells were DiI labelled at different distances from the bead in postero-distal mesenchyme, adjacent to the apical ridge, to investigate the origins of the duplicated tissue and duplicated digits. **A)** Stage 20/21 limb fixed immediately after retinoic acid bead application (arrowed) and DiI injection postero-distal to bead adjacent to the ridge. Scale bar represents 500μm. **B)** Cartilage stained whole mount of a limb left for 7 days following the application of a retinoic acid bead at stage 20/21 showing the typical cartilage pattern obtained, **4-3-3-4**. Scale bar represents 3000μm. C-G Examples of limbs fixed 96 hours after retinoic acid application and DiI injection at stage 20/21; **C)** labelled 100μm postero-distal to bead. Note labelled cells at the anterior margin of the duplicated tissue. **D)** 125μm postero-distal to bead. Note labelled cells streaming along anterior margin of duplicated structure; **E)** 200μm postero-distal to the bead. Note labelled cells streaming into the middle of the duplicated tissue, into prospective duplicated digit **4**; **F)** 250μm postero-distal to the bead. Note labelled cells streaming into a prospective duplicated digit **3**; **G)** 300μm postero-distal to the bead. Note labelled cells not in duplicated structure but stream into posterior part of limb (see Chapter Three). Scale bar represents 1000μm in C, D, E, F and G.

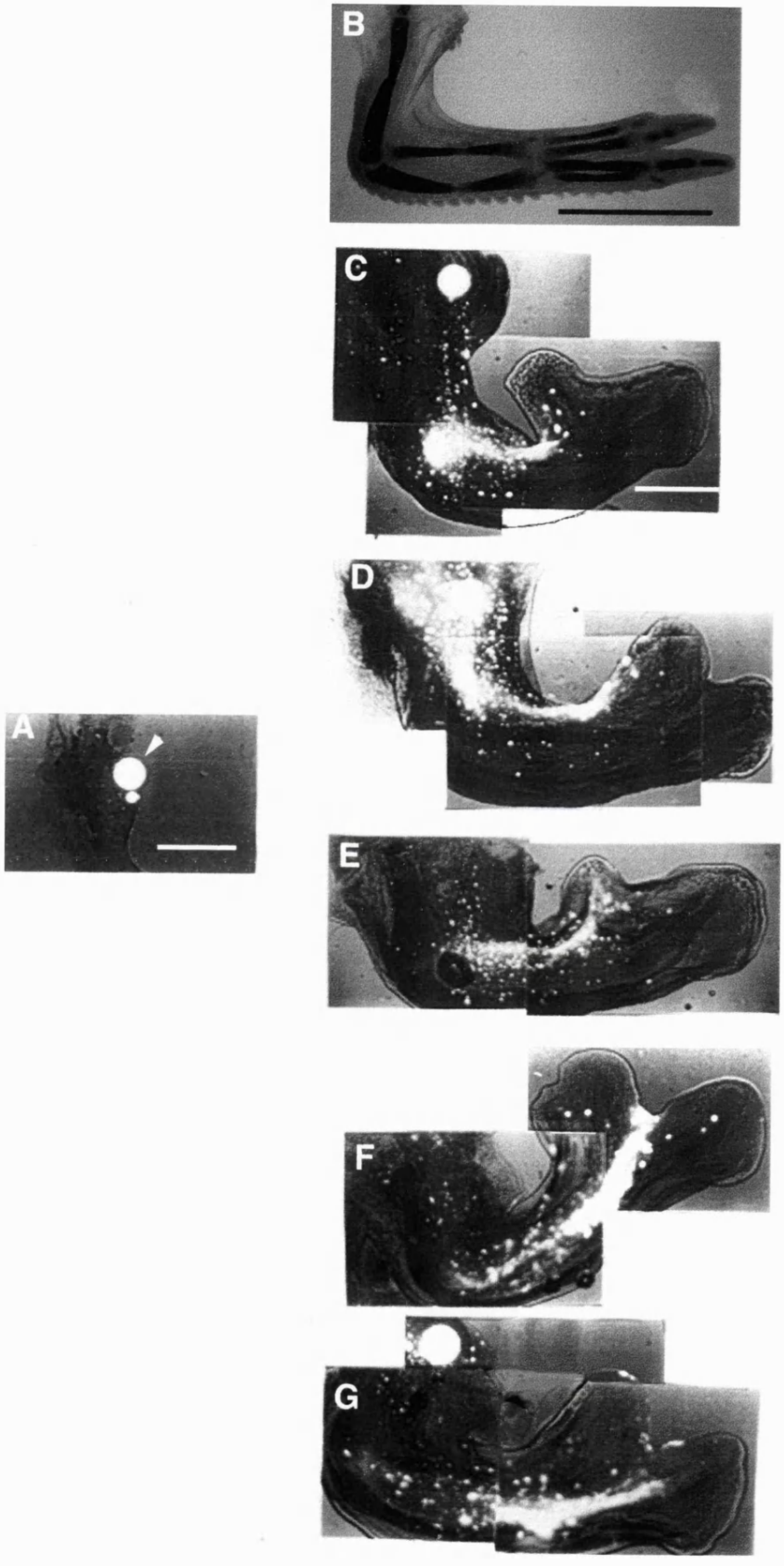
A
B
C
D
E
F
G

Figure 4.12

Summary diagram showing origin of cells contributing to duplicated digits induced by retinoic acid

To deduce the origins of cells that are induced to produce duplicated digits following retinoic acid treatment to the anterior margin of stage 20/21 limbs, populations of mesenchyme were DiI labelled in various positions around the bead. Only populations postero-distal to the retinoic acid bead up to 250μm from the bead, contributed to the duplicated digits 96 hours later; populations proximal or anterior to the bead remained in the position they were labelled and did not contribute to the duplicated structure. • represents positions at which DiI label was injected; X = no contribution; √ = contribution. Scale bar represents 200μm.

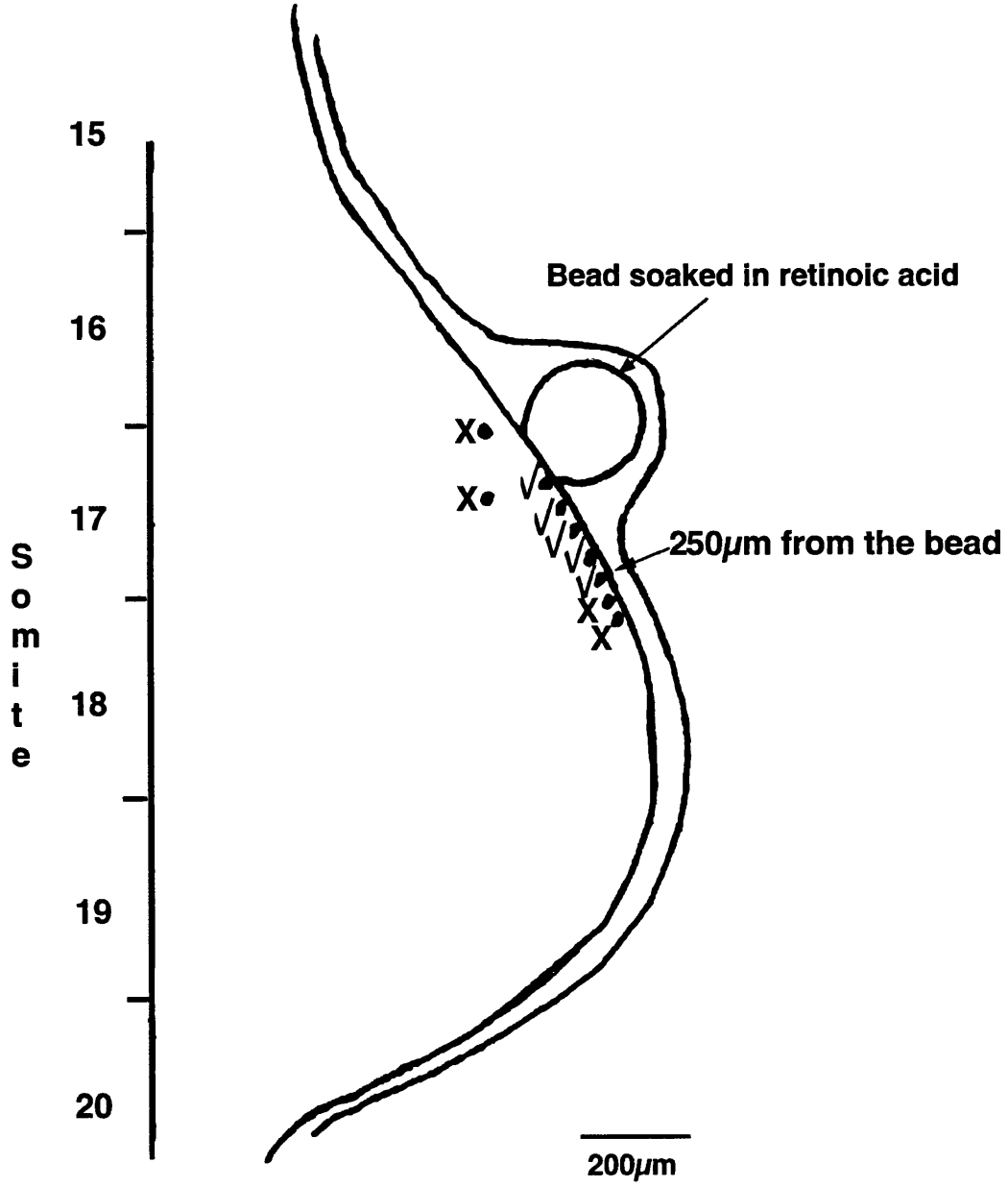
15
16
17
18
19
20
Somite
Bead soaked in retinoic acid
250μm from the bead
200μm

Table 4.4

Summary of the distances from the retinoic bead which are induced to contribute to the additional structures.

Distance from bead (μm)	n	Result
100	5	}
125	5	}
150	6	} in duplication
175	1	}
200	7	⇒ dup. digit **4**
225	6	}
250	6	⇒ dup. digit **3**
275	5	}
300	5	} not in duplication

The distance from the bead is calculated as being from the centre of the bead to the centre of a DiI labelled population. As the retinoic acid bead was usually 200μm in diameter, this means that the nearest mesenchyme population is 100μm from the centre of the bead.

somites 16 and 17. The majority of limbs had one or two extra digits, the common digit patterns being **3-3-3-4** and **4-3-3-4** (Yang and Drossopoulou et al., 1997). As found with retinoic acid, only a small amount of tissue posterior-distal to the *Shh* bead is induced to contribute to the duplicated structures. A duplicated digit **4** arose from mesenchyme labelled within a 90μm radius of the bead; a duplicated digit **3** forms from cells initially between 90μm and 300μm away from the bead (Yang and Drossopoulou et al., 1997; Figure 4.13D, E). Cell populations labelled over 300μm away from the bead contributed to the normal limb pattern and not the duplicated structures. The streams of labelled cells ran toward the apical ridge, posterior to the duplicated digits and anterior to the host digit **3** which forms opposite somite 18/19, approximately 480μm from the bead (see Chapter Three; Fig. 4.13A, E). As in the retinoic acid studies, anterior mesenchyme populations which normally do not contribute to digits and do not expand have been induced to contribute to duplicated digits and behave like posterior located populations (see Chapter Three).

Experiments with *Shh* in which the bead soaked in *Shh* is removed at varying times after implantation, show that the length of time cells are exposed to *Shh* affects the particular duplicated structures that form. For example, by implanting a bead soaked in a concentration of *Shh* that induces full duplications but removing the bead 16 hours after implantation, an extra digit **2** only is induced and not a full duplication (Yang and Drossopoulou et al., 1997). In this case, cells labelled 90μm to 250μm away from the bead which would have contributed to the extra digit **3** if the *Shh* bead was left in place, now contribute to the duplicated digit **2** (Yang and Drossopoulou et al., 1997). Therefore the same cells can give rise to either a digit **2** or a digit **3** depending on the length of time the *Shh* bead has been in place (Yang and Drossopoulou et al., 1997; Fig. 4.13F).

4.3 Discussion

4.3.1 Regulation of limb pattern following mesenchyme manipulations

4.3.1.1 *Mesenchyme removal*

My work confirms previous studies (Hayamizu et al., 1994; Stark and Searls, 1974; Barasa, 1964; Zwilling, 1956; Saunders, 1948) showing that limbs with an intact apical ridge can regulate well after removal of small blocks of mesenchyme, producing normally patterned limbs. However I find that limbs do not regulate well after large mesenchyme removal and parts of the final limb pattern are missing. It is

Figure 4.13

Origin of cells contributing to duplicated digits following *Shh* application at anterior margin

Beads soaked in 16mg/ml *Shh* protein were placed beneath the anterior apical ridge of a stage 20/21 limb bud and populations of cells were labelled with DiI or DiA at different distances postero-distal to the bead to deduce the origins of duplicated digits. **A**) Cells up to 300μm postero-distal to the bead, contribute to the duplicated digits as shown in the columns on the right part of the upper figure. The columns show data for extended treatment (i.e. bead left in place for 96 hours), 16 hour treatment (i.e. bead removed after 16 hours) and following a control PBS bead. Lower part of the figure shows examples of labelled wing buds. **B**) Wing bud fixed immediately after *Shh* bead implanted and mesenchyme populations labelled with DiI 90μm (arrowhead) and DiA 300μm (small arrow) from the bead in a postero-distal domain. Scale bar represents 500μm. C-F Examples of limbs left 96 hours following bead implant and DiI and DiA injection. **C**) Control (PBS) bead; cells marked with DiA 90μm from the bead did not contribute to distal structures (arrowhead), while cells marked with DiI 375μm end up in the normal digit **2** (small arrow). **D**) Cells marked with DiI at 90μm (arrowhead) and with DiA at 300μm (small arrow) from the implanted bead end up in the prospective duplicated structures. **E**) Cells marked with DiA at 90μm away from the bead contribute to extra structures (arrowhead), while cells marked with DiI at 340μm from the bead do not (small arrow). Scale bar represents 1000μm in C, D and E. **F**) When a *Shh* bead was removed 16 hours after being implanted, a digit pattern of **2234** results. Cells marked initially 90μm from the bead with DiI (arrowhead) contribute to duplicated digit **2**, while cells marked initially 300μm from the bead with DiA (small arrow) contribute to the normal digit **2** (normal and extra digit **2** indicated by asterisks). Scale bar in F, represents 500μm.

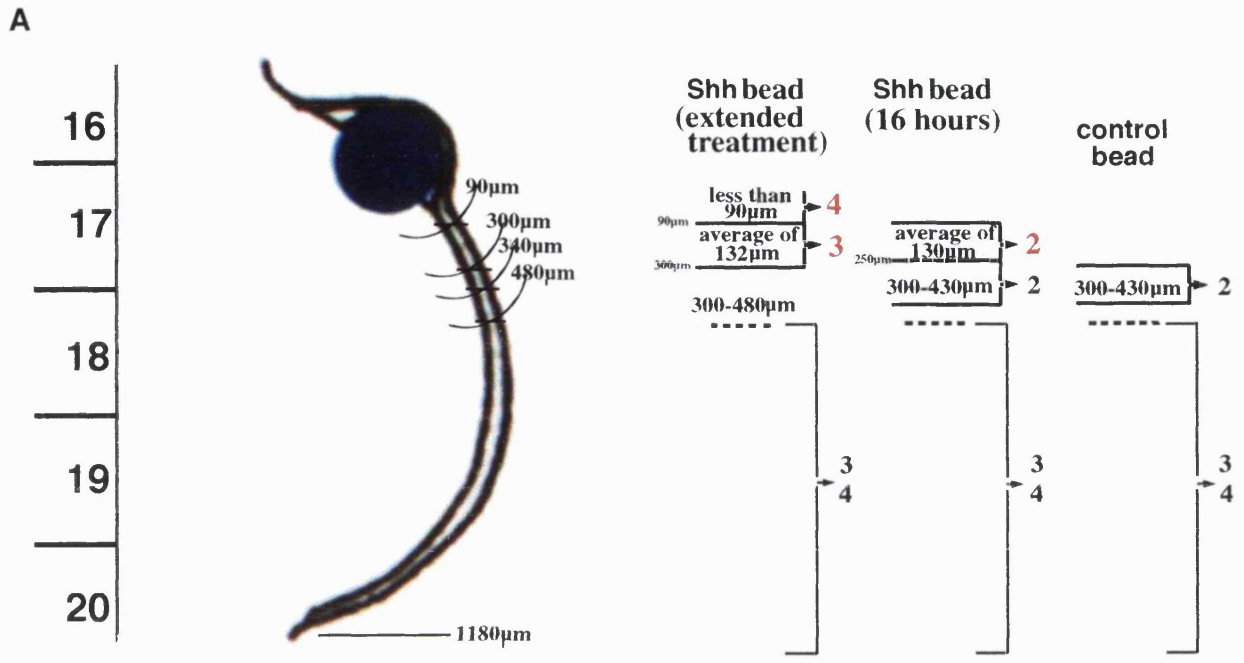
A
16
17
18
19
20
90µm
300µm
340µm
480µm
1180µm
Shh bead (extended treatment)
Shh bead (16 hours)
control bead
less than 90µm
average of 132µm
average of 130µm
300-430µm
300-480µm
300-430µm
4
3
2
2
3
4
3
4
3
4

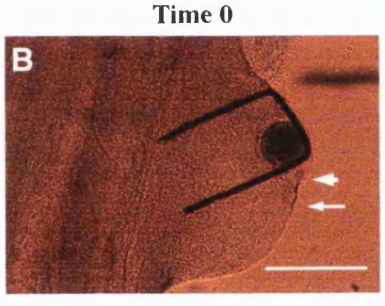
Time 0
B

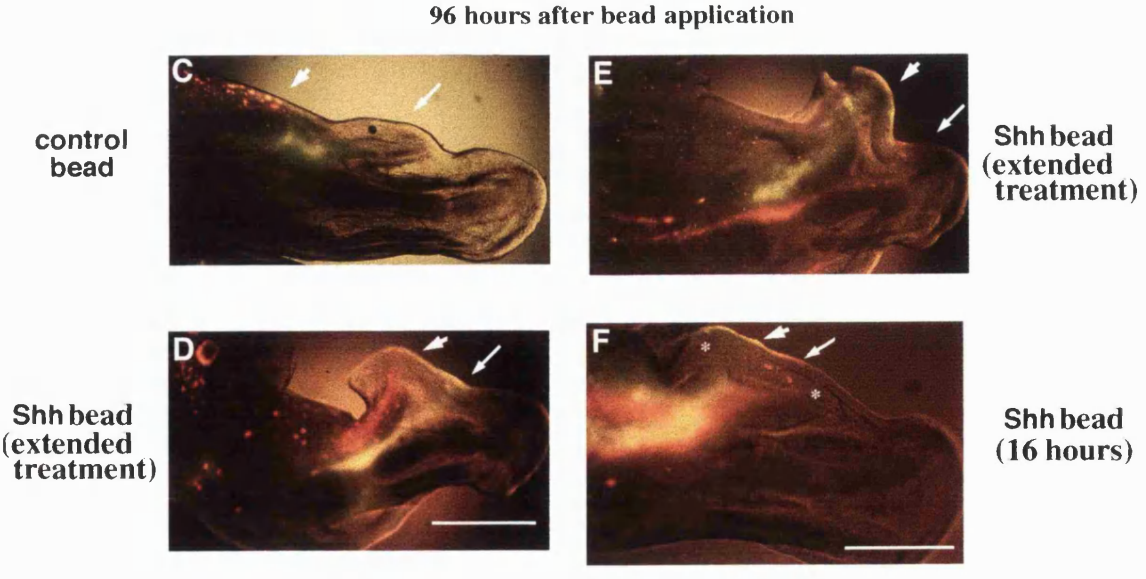
96 hours after bead application
control bead
C
E
Shh bead (extended treatment)
Shh bead (extended treatment)
D
F
Shh bead (16 hours)

striking that distal structures are present while proximal structures are absent. Following removal of small blocks of mesenchyme, the cells that mediate regulation appear to arise from the distal margin of the wound, whereas cells that contribute to regulated structures following large mesenchyme removal arise not only from the distal but also from proximal posterior margin. Thus, when large blocks of mesenchyme are removed, proximal cells contribute to distal structures, as shown via DiI labelling, and expression of *Hoxa-13* and *Hoxd-13* appears to be extended along the proximo-distal axis of the limb buds which give rise to distal structures.

Regulation of mesenchymal removal

I have applied two criteria to determine how well the limb has regulated. Firstly skeletal pattern after 7 days, and secondly, measurement of lengths of individual elements. Fatemaps suggest that the small blocks of mesenchyme removed at stage 20/21 would normally have contributed to a radius and ulna, as central mesenchyme only is removed. If no regulation occurred, then no forearm should form. However I find a limb with normal pattern but which is shorter than normal. In contrast, following removal of a large block of mesenchyme (that would have contributed to proximal hand plate, forearm and distal humerus) only a hand plate, with well formed digits develops. This suggests that some regulation has occurred, in that cells have contributed to produce the hand plate. This is the expected result if the apical ridge contracts onto the proximal tissue and then redirects and re-specifies growth allowing proximal cells to be incorporated into the distal structures, thus altering cell fate (see also Hayamizu et al., 1994; Stark and Searls, 1974; Barasa, 1964; Zwilling, 1956; Saunders, 1948). Moreover, when the apical ridge is stripped off following removal of a large area of mesenchyme, only a very short, small humerus develops. The proximal humerus is the part of the pattern that would have been predicted to be left proximally after removal of a large block of mesenchyme. When the apical ridge is removed these cells are not reprogrammed to form distal structures.

As removing small areas of mesenchyme gives considerably different results to those for large removals I shall discuss these two results separately.

Regulation of removal of small blocks of mesenchyme

After removing a small block of mesenchyme, the limb regulates and repopulates the excavated area from the distal margin of the wound site; no proximal cells contribute. The limb has a normal pattern after acquiring the appropriate new positional information, but is slightly smaller than unoperated limbs. There are several theories about how this could be achieved:

The polar co-ordinate model (French et al., 1976; Bryant et al., 1977) is based on cells being assigned positional information in terms of a two dimensional co-ordinate system. The main feature of this model is the ability of cells to intercalate to replace the missing tissue. Cells at wound edges would recognise that they are no longer next to cells with the normally adjacent positional values. This would induce growth to fill in the deficiency, resulting in normal pattern. This model requires there to be an increase in proliferation to generate cells with the appropriate positional values. I have not looked for an increase in proliferation directly, but patterns of DiI spread look normal when compared to normal fatemaps. However this does not rule out local increases in proliferation not detected by DiI. Hence it is difficult to say whether or not intercalation is involved in regulation of the chick limb.

Another hypothesis to explain how normal pattern is obtained is via a gradient of some chemical. The gradient model (Wolpert, 1969; Tickle et al., 1975), suggests that within the limb bud cells are acted upon and given positional information by morphogens, which are present in a graded fashion. Each cell is exposed to a set concentration of morphogen and differentiates accordingly. Perhaps after removal of tissue the gradient would be re-established and this could re-programme cells to form the missing structures. Thus, for example, anterior cells would be respecified to produce posterior structures and proximal cells respecified to contribute to distal structures. This model may work in conjunction with mechanical properties of the limb, where due to loss of small amounts of tissue the cells contract toward each other to re-establish cell contact and the morphogen then respecifies positional information.

Following removal of small blocks of mesenchyme distal cells contribute to the regulated pattern (rather than proximal cells), however, I find that the radius and ulna are considerably shortened, as is digit **3** which suggests that these elements contain fewer cells than normal due to a delay in development. As digit **3** is shortened this argues against the intercalation model, as tissue near the hand plate area was not removed and hence the hand plate should be normal. It is possible that following mesenchyme removal, a gradient of morphogen(s) had to be re-established which organised a normal skeletal pattern. The elements are slightly shorter due to the delay in re-establishing the gradient.

Regulation of removal of large blocks of mesenchyme

In contrast to small mesenchyme removals, large pattern defects are observed after large blocks of mesenchyme are removed which contain practically all the distal mesenchyme leaving just 75-100μm (approximately 10 cell diameters) still attached

to the apical ridge. Severe defects were observed in the skeletal pattern but also changes in the developing limb bud shape occurred which could clearly be seen after 48 hours. This may be due to the apical ridge contracting back onto the proximal base of the bud, which would shorten the limb bud as compared to the contralateral. The most appropriate model to explain the formation of distal structures at the expense of proximal structures is the progress zone model (Summerbell et al., 1973; Wolpert et al., 1979). This model hypothesises that positional information along the proximo-distal axis is specified by the amount of time that cells spend in the progress zone, a zone of proliferating, undifferentiated distal mesenchyme directly beneath the apical ridge (Summerbell and Wolpert, 1972). Cells that spend a long time in the progress zone form distal structures, those that spend a shorter time in the progress zone form proximal structures (Summerbell et al., 1973). In the large mesenchyme removal experiments, I removed a large proportion of the progress zone as well as most of the central mesenchyme. Thus, there is a decrease in the number of cells in the progress zone and cells cease to leave it. The progress zone is then repopulated due to proliferation and recruitment of cells from proximal regions. Only when the progress zone is back to normal size, would cells start to leave the progress zone and differentiate according to the time they spent in the progress zone. Thus with larger removals, mesenchyme cells would spend longer in the progress zone and distal structures would be formed at the expense of proximal structures i.e. cells that should have made proximal structures will contribute to distal structures. At stage 21/22, the time when these experiments were carried out, the humerus is already patterned (as shown by apical ridge removal experiments, Summerbell, 1974; Saunders, 1948), but in the majority of cases I do not see a humerus. This suggests that the cells that were specified to be humerus were reincorporated into the progress zone once the apical ridge contracted onto the proximal base and then contributed to the digits. Furthermore the DiI analysis carried out suggests no large widespread increase in proliferation occurred and that proximal cell populations do indeed contribute to distal structures (Fig. 4.5). Earlier studies involving mesenchyme removal, leaving the apical ridge intact were interpreted in the same way (Hayamizu et al., 1994; Stark and Searls, 1974; Zwilling, 1956). Moreover, an apical ridge placed onto the proximal stump of a limb induces proximal mesenchyme to produce a new limb (Saunders, 1948). The limbs which develop following large mesenchyme removal are similar to those obtained by X-irradiating the progress zone of chick limbs (Wolpert et al., 1979). X-irradiation kills cells and with increasing doses of X-irradiation proximal structures are progressively lost, but the digits are normal (Wolpert et al., 1979). Wolpert et al, (1979) deduced that there is a threshold number of cells required to produce a skeletal element. If the number of cells falls below this threshold then the

element does not form. Large removals of mesenchyme could therefore reduce the threshold number of cells so that proximal elements do not form.

The difference in the origin of cells in regulation of small mesenchyme removals to large mesenchyme removals, could be due to being inside or outside the progress zone. Large mesenchyme removals include most of the progress zone and following ridge retraction onto the proximal base, the progress zone is reestablished and thus, incorporates proximal cells which contribute to distal structures. However small blocks of mesenchyme were removed from the edge of the progress zone, proximal cells are too far away from the ridge to be incorporated into a reestablished progress zone and hence do not contribute to distal structures. Thus, regulation occurs mostly from distal cells via mechanisms outlined earlier.

Gene expression and regulation

Expression of *Hoxa-13* and *Hoxd-13* is required for proper development of the hand plate. Therefore I investigated expression of *Hoxa-13* and *Hoxd-13* in limbs following removal of large blocks of mesenchyme where distal structures form at the expense of proximal structures. I also investigated the effect of large mesenchyme removals upon the expression of *Hoxa-10*, a gene normally expressed in the forearm. The majority of the progress zone was removed bar about 100-150μm of mesenchyme left attached to the apical ridge, hence most of the mesenchyme expressing *Hoxa-10, Hoxa-13* and *Hoxd-13* will have been removed.

The results are quite striking in that all 3 genes are expressed within the operated limb but *Hoxa-13* and *Hoxd-13* expression domains appear to have expanded and seem to occupy more of the limb than normal. However the limb is smaller and narrower than contralateral, normal limbs. It is quite likely that due to the large loss of mesenchyme, the progress zone is re-established but can not replace all the cells hence proximal structures are lost and only the hand plate forms. Proximal cells are re-incorporated into the progress zone, and induced to express *Hoxa-13* and *Hoxd-13* and produce the hand plate. Extended domains of *Hoxa-13* and *Hoxd-13* are consistent with the fact that distal structures form at the expense of proximal structures. Interestingly the expression of *Hoxa-10* is present in proximal limb regions, despite the fact that proximal structures will be missing. Due to the principle of 'posterior prevalence' (for review see Duboule and Morata, 1994) it is possible that *Hoxa-10* transcripts are present but are being repressed by the increased domains of expression of *Hoxa-13* and *Hoxd-13* in the operated limb which are normally involved in patterning the hand plate.

The results discussed suggest that a signal from the apical ridge and/or the progress zone is directly or indirectly involved in regulation of large mesenchyme removals. Several important genes involved in growth control are expressed in the progress zone including *Msx-1* (for review see Tickle and Eichele, 1994). The apical ridge is a source of FGFs which are known to be involved in controlling proliferation and outgrowth of the limb (Niswander and Martin, 1992; Niswander et al., 1993, 1994; Vogel and Tickle, 1993; Fallon et al., 1994; Crossley et al., 1995). In particular FGF-4 which is expressed in the posterior apical ridge can functionally replace the apical ridge after apical ridge removal (Niswander et al., 1993). It seems likely that FGFs (including FGF-4) may play a role in regulation of limb pattern, although the distance over which FGFs can signal is unclear.

4.3.1.2 *Distal tip regeneration following amputation*

I have proposed that regulation and formation of distal structures after removing large regions of mesenchyme is due to contraction of the apical ridge back onto the proximal stump which re-establishes a progress zone. When the distal tip of a chick limb bud, including the apical ridge is amputated, outgrowth is lost but can be rescued by the addition of an FGF bead (Kostakopoulou et al., 1996). Amputated limbs that are not treated with FGF do not regenerate and are severely truncated. Chick limb buds can undergo regeneration after distal tip amputation in response to beads soaked in either FGF-4 or FGF-2 stapled to the posterior distal margin of the stump (Kostakopoulou et al., 1996; Taylor et al., 1994). This suggests that as in mesenchyme removal, proximal cell populations are incorporated into a re-established progress zone which re-patterns and controls limb outgrowth/regerneration in response to apical ridge signalling producing a shorter but normally patterned limb.

By labelling populations of mesenchyme cells with DiI in various positions around an FGF-4 soaked bead, placed on the posterior-proximal stump following amputation, I have traced the origin of cells that contribute to the 'regenerated' distal structures. Cells from posterior proximal tissue and tissue just anterior to the bead contribute to the FGF-4 induced outgrowth (Fig. 4.9; Fig. 4.10). Furthermore beads soaked in FGF-4 pinned onto the amputated stump in anterior positions did not induce limb outgrowth and behaviour of cells around the bead as shown by DiI labelling was not altered.

These results show that only cells located close to an FGF-4 source contribute to the outgrowth of amputated limb bud stumps. This finding may reflect an inability of proximal cells to respond and participate in regeneration. However it is more likely that proximal cells cannot respond due to the limited range of influence of

the FGF signal (Kostakopoulou et al., 1996). This finding is similar to the amphibian limb where amputation leads to a blastema formed from local cell populations. Furthermore this result indicates that like the mesenchyme removal experiments, proximal cells are induced to contribute to distal structures in response to a ridge signal. Taken together all these results show that posterior and posterior proximal mesenchyme has the potential to regenerate lost or missing structures but anterior populations do not.

Role of Msx-1

An important gene that could be involved in the regulation process and regeneration following mesenchyme removal and distal tip amputation is *Msx-1*. *Msx-1* is expressed in the progress zone and is thought to control proliferation and differentiation and thus could be involved in initiating the regenerative response (Robert et el., 1989; Hill et al., 1989; Davidson et al., 1991; Muneoka and Sassoon, 1992). Expression of *Msx-1* is apical ridge dependent (for review see Muneoka and Sassoon, 1992) and is increased in areas of regeneration in mouse limbs after digit tip amputation (Reginelli et al., 1995) and chick limbs in response to FGF-4 after distal tip amputation (Kostakopulou et al., 1996). However *Msx-1* is not expressed in proximal areas where regeneration does not occur after distal limb amputation (Kostakopoulou et al., 1996; Reginelli et al., 1995). It will be important to look at the expression of *Msx-1* in limbs following removal of large blocks of mesenchyme to see whether expression of this gene is increased and if it is reactivated in proximal tissue which is incorporated into the progress zone and respecified to form distal structures. Another gene that could be important in the regulation and regeneration process is *Slug*, which also has been suggested to keep cells in an undifferentiated state and is expressed in distal mesenchyme beneath the apical ridge until late stages of limb development (Buxton et al., 1997; Ros et al., 1997).

4.3.2 Pattern duplication

Retinoic acid and *Shh* (*Sonic hedgehog*) lead to mirror image duplications of the hand plate when placed at the anterior margin of the limb bud. In order to deduce the distance over which these molecules exert their effects, I labelled populations of mesenchyme with DiI in various positions around a retinoic acid soaked or *Shh* loaded bead. Anterior mesenchyme does not normally give rise to digits, and remains proximal, not expanding greatly (see Chapter Three; Vargesson et al., 1997). I found that a small domain of anterior mesenchyme postero-distal to the implanted bead expanded a great deal and produced streams of labelled cells that contributed to the

duplicated digits that were induced. The distance over which cells are recruited to form the extra digits following the application of the polarising signal was between 250μm (retinoic acid) and 300μm (*Shh*), around 25 to 30 cell diameters (Fig. 4.11, 4.12, 4.13). Thus, retinoic acid and *Shh* have changed the behaviour and fate of a substantial anterior mesenchyme population into that of posterior-like mesenchyme. More importantly, the result suggests that retinoic acid and *Shh* have a similar range of influence and it is known that retinoic acid initiates expression of *Shh* in the cells adjacent to the retinoic acid bead (Riddle et al., 1993). Thus, the *Shh* expressing cells may initiate a cascade of secondary signalling molecules, such as *Bmp-2* (Laufer et al., 1994) in adjacent cells which mediate long range patterning.

In the case of *Shh*, this work has also shown directly that cell fate changes with length of exposure to *Shh*. Cells form an extra digit **2** if the *Shh* bead is removed within 16 hours but an extra digit **3** if the *Shh* bead is left in place (Yang and Drossopoulou et al., 1997). Thus, cells, in response to *Shh*, are promoted to produce posterior digits after initially being induced to produce anterior digits (see Tickle, 1995). This suggests that cells may be continuously interpreting the morphogen signal (Yang and Drossopoulou et al., 1997). Thus, early after *Shh* application an additional digit **2** is induced in mesenchyme next to the bead, as development proceeds this is promoted to a digit **3** and later to a digit **4**. The digit **2** could arise further away from the bead as the morphogen(s) diffuses further into the limb tissue (see scheme in Tickle, 1995).

Retinoic acid and Sonic hedgehog and the polarising region

Inhibiting retinoic acid synthesis in prelimb embryos disrupts limb initiation and abolishes *Shh* expression (Stratford et al., 1996; Helms et al., 1996; Lu et al., 1997), while *Shh* inactivation does not prevent limb initiation as a truncated limb is observed (Chiang et al., 1996). Beads soaked in retinoic acid can activate *Shh* in a dose dependent fashion (Yang and Niswander, 1995). Moreover, in mouse forelimbs where *Hoxb-8* is misexpressed anteriorly, an ectopic polarising region forms, including *Shh* expression resulting in a duplicated forelimb (Charite et al., 1994). Retinoic acid applied to the anterior wing margin induces *Hoxb-8* expression (Stratford et al., 1997; Lu et al., 1997) as well as activating *Shh* expression which results in duplicated digits. Taken altogether, this suggests retinoic acid is involved in limb initiation (see also Stratford et al., 1996).

Shh appears to mediate the effect of the polarising region and via a positive feedback loop with FGF-4 is involved in maintaining limb outgrowth (Riddle et al., 1993; Niswander et al., 1994; Laufer et al., 1994). Moreover, *Shh* has a dose dependent effect upon cells, where high concentrations induce full digit duplications

and low concentrations induce a digit **2** only (Yang and Drossopoulou et al., 1997). However *Shh* is not directly acting upon cells at a distance, as a duplicated limb pattern was still obtained when *Shh* was tethered to cells to prevent diffusion. This suggests that *Shh* acts over a short range activating secondary signals which mediate polarising activity (Yang and Drossopoulou et al., 1997). Furthermore other evidence indicates that *Shh* may only be required for a short period of time and is not required continuously, as the distal hand plate elements are not patterned at the time of a *Shh* bead removal, yet still form (Yang and Drossopoulou et al., 1997).

In summary, the replacement and regulation of excised undifferentiated mesenchyme, and regeneration of amputated structures both require a progress zone. Furthermore duplicated digits, formed in response to polarising region signals, are induced from a quite small population of mesenchyme postero-distal to the source of the signal. That retinoic acid and *Shh* appear to act over a short range suggests that *Shh* might normally act short range and induce signalling cascades to mediate antero-posterior pattern.

CHAPTER FIVE

The *Notch* signalling pathway in chick limb development

5.1 Introduction

Signalling pathways are essential for the controlled development of organisms and their appendages. Signalling molecules can be divided into six main groups (FGF, TGFβ, *Hedgehog*, *Wingless*, *Notch* and the ephrins) each controlling diverse developmental processes some of which may be interdependent (for review see Wolpert et al., 1998). These pathways provide developmental signals in vertebrates and invertebrates. Members of these six families are either secreted or expressed on cell membranes (for review see Wolpert et al., 1998). The focus of this chapter is on the *Notch* signalling pathway which has well documented roles in *Drosophila* neurogenesis (for review see Muskavitch, 1994; Artavanis-Tsakonas et al., 1995) and wing development (for review see Brook et al., 1996). Recently this signalling pathway has been suggested to have many diverse functions in vertebrate development particularly in vertebrate neurogenesis (for review see Lewis, 1996; Robey, 1997) and more importantly for this chapter, also in limb development (for review see Irvine and Vogt, 1997; see also Laufer et al., 1997; Rodriguez-Esteban et al., 1997).

Notch was so named due to the mutant phenotype in *Drosophila* where notches or scalloping were observed in mutant *Drosophila* wings. *Notch* is a transmembrane receptor, produced in the Golgi apparutus and then transported to the cell membrane and is made up of an extracellular domain and a linked transmembrane-intracellular domain. The extracellular domain contains 36 Epidermal Growth Factor (EGF) repeats as well as several different motifs within its extracellular domain that mediate ligand binding (for review see Artavanis-Tsakonas et al., 1995; Nye et al., 1997). When the *Notch* receptor is activated, the intracellular domain of *Notch* translocates to the nucleus and binds to *Suppressor of Hairless* (*Su(H)*), a transcription factor, although this may occur in the cytoplasm. The *Notch-Su(H)* complex then activates downstream genes such as *Enhancer of split* (*Espl*) which control cell fate (for review see Artavanis-Tsakonas et al., 1995; Robey, 1997; Nye, 1997). *Notch* is activated by ligands containing the DSL motif, *Delta*, *Serrate* and *Lag-2*. *Delta* and *Serrate* are so named due to the phenotypes they induce in the *Drosophila* wing if mutated and *Lag-2* is a ligand of *Notch* in *C. elegans*. *Delta* causes

the wing veins at the distal part of the wing blade to thicken and merge (Vassin et al., 1987; see also de Celis et al., 1996) and *Serrate* causes nicks around the rim of the *Drosophila* wing blade and small wings (Fleming et al., 1990; Thomas et al., 1991; see also de Celis et al., 1996). *Delta* and *Serrate* are structurally very similar to *Notch*, being transmembrane proteins, and contain EGF repeats in their extracellular domains. These repeats aid binding to the 11^{th} and 12^{th} EGF repeats of *Notch* (Rebay et al., 1991; for review see Artavanis-Tsakonas et al., 1995). Evidence that *Delta* and *Serrate* are ligands for *Notch* in *Drosophila* comes from the ability of both ligands to bind to *Notch* expressing cells in cell adhesion assays (Rebay et al., 1991). Furthermore, when *Delta-1* is overexpressed in Xenopus and in mouse this disturbs neurogenesis (Chitnis et al., 1995; de la Pompa et al., 1997). Moreover, *Jagged-1*, the rat *Serrate-1* homologue, inhibits differentiation of a muscle cell line in culture, mimicking the effects of an activated form of *Notch* (Lindsell et al., 1995).

Notch plays a key role in many cell fate decisions in *Drosophila* and particularly has been shown to have essential roles in wing development such as in dorsal-ventral margin formation, proliferation and wing vein differentiation (de Celis and Garcia-Bellido, 1994; for review see Brook et al., 1996). Most investigations of *Notch* function and signalling have centred around the role of *Notch* in neurogenesis (for review see Artavanis-Tsakonsas et al., 1995; Lewis, 1996). Recently several vertebrate homologues of *Notch* (4 known; Uttendaele et al., 1996), *Serrate* (2 known; Myat et al., 1996; Hayashi et al., 1996) and *Delta* (3 known; Henrique et al., 1995; Dunwoodie et al., 1997) have been identified in chick, rat, mouse, Xenopus and human. These *Notch* homologues have been implicated in many diverse developmental functions ranging from, for example, limb development (for review see Blair, 1997; Irvine and Vogt, 1997), lateral inhibition in the nervous system (for review see Lewis, 1996), T-cell determination (for review see Robey, 1997) and somite segmentation and polarity (Hrabe de Angelis et al., 1997). Moreover, *Notch* signalling is also associated with disease and cancer (for review see Robey, 1997). Hence *Notch* signalling functions in many different tissues controlling cell fate and differentiation.

Notch signalling in Drosophila wing development

The wing of *Drosophila* develops from the wing imaginal disc which initially consists of 20-40 cells and will eventually consist of 50000 cells (for review see Blair, 1995, 1997). As development proceeds, an anterior-posterior compartment boundary forms across the imaginal disc followed by a dorsal-ventral wing margin forming at the boundary of the dorsal and ventral ectoderm. Signalling between cells in adjacent compartments at the compartment boundaries establishes organising regions

controlling cell fate, differentiation and wing development allowing the eventual development of the wing blade. The wing blade is ectodermal, containing no mesodermal structures (for review see Blair, 1995, 1997; Brook et al., 1996).

The dorsal-ventral wing margin forms after the antero-posterior compartment boundary and acts as an organiser controlling growth and specifying spatial pattern along the dorsal-ventral axis (Fig. 5.1). *Notch*, *Serrate* and *Delta* have essential functions in maintaining the wing margin and wing outgrowth. *Serrate* is initially expressed throughout the dorsal compartment but becomes restricted to dorsal cells at the dorsal-ventral margin (Couso et al., 1995; de Celis et al., 1996). Expression of *Delta* is found throughout the ventral compartment and then becomes restricted to ventral cells at the dorsal-ventral margin (Fig. 5.1A, B; de Celis et al., 1996; Doherty et al., 1996). *Serrate* and *Delta* establish a positive feedback loop, where *Serrate* signals to ventral cells to activate *Notch* and *Delta*. *Delta* then signals to dorsal cells to activate *Notch*, *Serrate* and *Delta* (Fig. 5.1A; for review see Irvine and Vogt, 1997). *Fringe* expression in the dorsal compartment prevents *Serrate* signalling to other dorsal cells, hence *Serrate* can only signal to ventral cells, but attentuates *Delta* signalling to dorsal cells, hence positioning the wing margin and restricting the *Serrate-Delta* positive feedback loop and *Notch* activation to the wing margin only (Fig. 5.1A, B; Irvine and Wieschaus, 1994; Kim et al., 1995; de Celis et al., 1996; Yuan et al., 1997; Panin et al., 1997; Fleming et al., 1997).

Once *Notch* expression is established throughout the wing margin the expression of *Serrate* and *Delta* becomes restricted to cells flanking the wing margin and are inhibited in the wing margin itself (de Celis and Bray, 1997; Micchelli et al., 1997), thus producing a *Notch*-ligand boundary, thus activation of *Notch* now depends upon a positive feedback loop with *Serrate* and *Delta* between margin and margin flanking cells which further maintains and positions *Notch* expression to the wing margin (Fig. 5.1B; de Celis and Bray, 1997; Micchelli et al., 1997; Fleming et al., 1997; for review see Irvine and Vogt, 1997). *Notch* then directs wing outgrowth activating amongst others *Vestigial*, which is essential for cell proliferation and wing outgrowth (Couso et al., 1995; de Celis et al., 1996; Kim et al., 1996; for review see Brook et al., 1996). Loss of *Notch*, *Serrate* or *Delta* results in wing defects, whereas ectopic expression of *Serrate* induces ectopic wing structures and wing overgrowth. Moreover addition of ectopically activated *Notch* induces expression of *Serrate* and *Delta* and induces an ectopic wing (Speicher et al., 1994; Couso et al., 1995; de Celis et al., 1996; de Celis and Bray, 1997; Panin et al., 1997; see Irvine and Vogt, 1997).

Figure 5.1

A) The *Drosophila* wing dorsal-ventral compartment (anterior-posterior compartment not shown) showing a summary of gene expression across the established dorsal-ventral wing margin. *Apterous* and *Fringe* are expressed throughout the dorsal compartment. At the juxtaposition of *Fringe* expressing and *Fringe* non-expressing cells, *Serrate* expression is activated on the dorsal part of the margin. *Delta* is expressed on the ventral part of the wing margin and both activate *Notch* throughout the wing margin which activates downstream targets such as *Wingless*, *Cut* and *Vestigial* regulating wing outgrowth. The interactions across the wing margin as marked by the highlighted box are explained in B.

B) A model for *Notch* activation at the dorsal-ventral margin. Adapted from de Celis and Bray (1997). In early wing discs (Top) *Serrate* (Ser), in dorsal cells, activates *Notch* (N) and *Delta* (Dl) in adjacent ventral cells and ventral *Delta* (Dl) then activates *Notch* and *Serrate* in adjacent dorsal cells. This *Serrate-Delta* feedback loop is positioned by the activity of *Fringe*, which prevents *Serrate* signalling to dorsal cells, only to ventral cells, but potentiates *Delta* signalling to dorsal cells. This leads to the accumulation of *Notch* and *Wingless* (Wg) across the dorsal-ventral boundary. As the dorsal-ventral wing margin is established (Bottom), *Serrate* and *Delta* are eliminated from the margin by the expression of *Cut* (Ct) throughout the margin. The presence of *Wingless* induces (and restricts) *Serrate* and *Delta* expression in flanking cells abutting the dorsal-ventral wing margin. This enables *Serrate* and *Delta* to continue to activate *Notch* in the adjacent wing margin in a positive feedback loop. Furthermore high levels of *Serrate* and *Delta* together inhibit activation of *Notch* expression in the flanking cells which enables a stripe of *Notch* across the wing margin to be established and maintained.

A

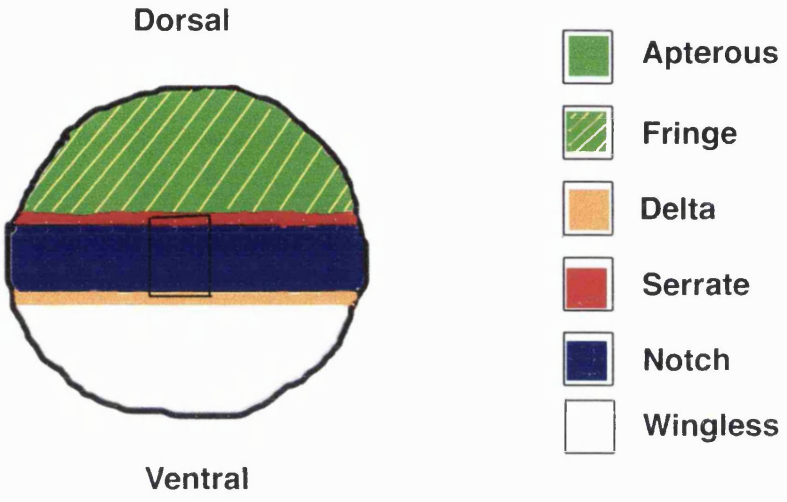
Dorsal
Ventral
Apterous
Fringe
Delta
Serrate
Notch
Wingless

B

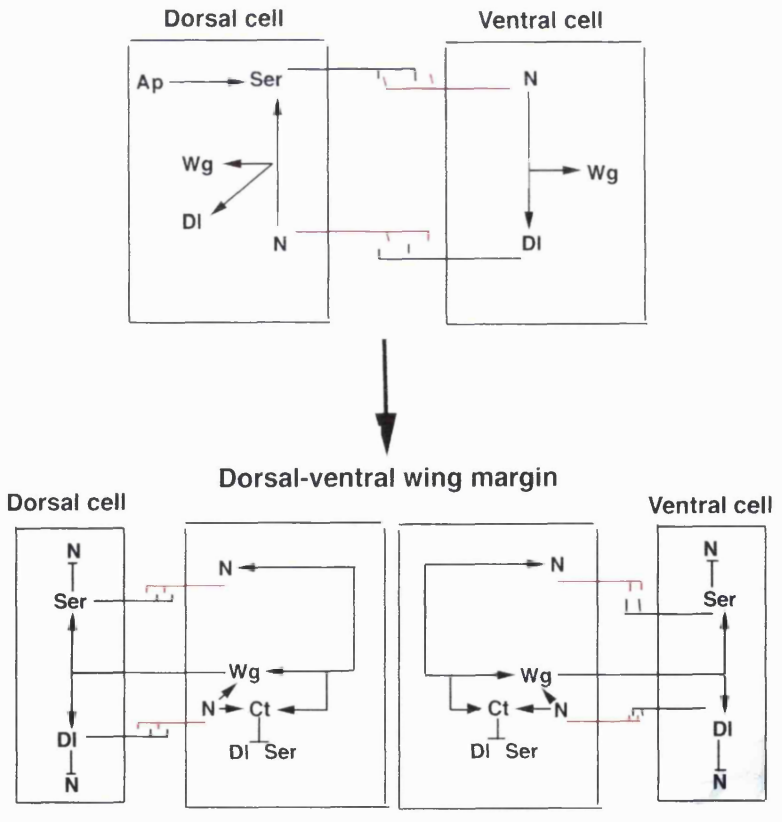
Dorsal cell
Ventral cell
Ap
Ser
N
Wg
Dl
N
Wg
Dl
Dorsal-ventral wing margin
Dorsal cell
Ventral cell
N
Ser
Dl
N
N
Wg
N
Ct
Dl
Ser
N
Wg
Ct
N
Dl
Ser
N
Ser
Dl
N

The *Notch* pathway also has a role in positioning the wing vein and extent of the wing vein competent tissue (Huppert et al., 1997; de Celis, 1997; see also de Celis and Garcia-Bellido, 1994). Wing veins develop from proveins which are partitioned into veins and intervein tissue. *Notch* is expressed in intervein cells directly adjacent to a vein which expresses *Delta* - no overlap of expression of *Notch* and *Delta* is observed, hence *Notch* generates a boundary between cell populations, as for the dorsal-ventral margin (Huppert et al., 1997; de Celis, 1997). Where *Delta* expression abuts with *Notch* expression, *Delta* signals to *Notch* which inhibits lateral intervein cells from adopting the vein fate until proper numbers of intervein cells are produced, hence controlling the position of the vein via a lateral inhibition mechanism. This was shown in *Delta* mutant wings, where wing veins are very thick as cells are not inhibited from the vein fate and in *Notch* gain-of-function wings veins are lost in distal wing blade region as cells were inhibited from producing vein structures (Huppert et al., 1997). The full differentiation of the vein requires other additional factors such as *Decapentaplegic* which appears to interact with the *Notch* pathway (de Celis, 1997).

Notch signalling in vertebrate wing development

Homologues of members of the *Notch* signalling pathway are also expressed in vertebrate wing development however their functions are far from certain. As in *Drosophila*, the meeting of dorsal and ventral ectoderm forms a signalling region, the apical ridge, which controls and maintains proximo-distal outgrowth of the wing. The recent discovery of *Radical fringe*, vertebrate homologue of *Drosophila Fringe*, suggests that the formation, positioning and maintenance of the apical ridge could be via the same mechanism that initiates and positions the wing margin in *Drosophila*. *Radical fringe* is expressed in dorsal ectoderm and the boundary of expression, as in *Drosophila*, demarcates the position of a signalling centre, in this case the apical ridge (see Fig. 1.3A; Laufer et al., 1997; Rodriguez-Esteban et al., 1997). *Serrate 2* and *Notch 1* have recently been suggested to mediate the action of *Radical fringe,* as both these genes are expressed in the chick apical ridge (for review see Blair, 1997; Irvine and Vogt, 1997). Furthermore, an induced mutation in *Serrate 2* leads to syndactylism in mice where the apical ridge is hyperplastic leading to digit tip fusions (Sidow et al., 1997). In loss of function *Notch 1* mouse mutants, embryos die early, before limb outgrowth can be properly observed. However there are severe defects in somite segmentation and a lot of cell death suggesting the *Notch* pathway in vertebrates may be involved in growth and differentiation control (Conlon et al., 1995; Swiatek et al., 1994). Expression patterns of some other vertebrate homologues

of the *Notch* signalling pathway potentially involved in limb development are now becoming known. *Serrate 1* is initially expressed in hindlimb posterior distal mesenchyme at stage 21 and by stage 26 across the entire footplate, but is not expressed in the apical ridge (Myat et al., 1996) unlike mouse *Serrate 1* (*Jagged 1*) which is expressed in both mesenchyme and apical ridge (Mitsiadis et al., 1997). *Serrate 2* is expressed in dorsal ectoderm and along with *Notch 1* is expressed in the apical ridge of the early chick wing bud (Hayashi et al., 1996; Myat et al., 1996; as is rat *Jagged 2*, Shawber et al., 1996). However, the exact function of *Serrate, Notch* and *Delta* in the chick wing bud is presently unclear, but it is likely that each different gene could have several different functions as expression of some of these genes are found in the mesenchyme as well as the ectoderm.

As briefly discussed (see above) it is known that some vertebrate homologues of *Notch*, *Serrate* and *Delta* are expressed in developing vertebrate limbs, although our knowledge is rather limited (Bettenhausen et al., 1995; Myat et al., 1996; Hayashi et al., 1996; Laufer et al., 1997; Rodriguez-Esteban et al., 1997). For example *Serrate 1* is expressed in early chick limb mesenchyme (Myat et al., 1996) and *Notch 1* and *Serrate 2* are expressed throughout the apical ridge at early limb bud stages (Myat et al., 1996; Laufer et al., 1997; Rodriguez-Esteban et al., 1997). However, the expression patterns of genes in the vertebrate *Notch* signalling pathway have not been fully analysed/elucidated. Hence, there are gaps in the expression pattern data of *Notch*, *Serrate* and *Delta* in the vertebrate limb. In order to try and understand and identify the roles of the *Notch* signalling pathway in vertebrate limb development it is initially important to elucidate the full expression patterns of all the genes in the *Notch* signalling pathway throughout limb development. Once the full expression patterns of these genes is known, further work to identify exact functions of the *Notch* signalling pathway in vertebrate limb development, can be carried out.

I have used whole mount in-situ hybridisation to document the expression patterns of *Notch 1*, *Serrate 1*, *Serrate 2* and *Delta 1* in chick limb development. I have concentrated on mesenchymal expression of these genes as apart from early mesenchyme expression of *Serrate 1* little is known about the expression patterns of other members of the *Notch* signalling pathway in mesenchyme. I have not investigated in great detail expression patterns of members of the *Notch* signalling pathway in the apical ridge, as earlier studies have previously outlined expression of *Notch 1* and *Serrate 2* in the early apical ridge and suggested *Notch-Serrate* signalling is central to apical ridge formation and maintenance (Laufer et al., 1997; Rodriguez-Esteban et al., 1997).

I will describe the mesenchymal expression patterns of *Notch 1*, *Serrate 1*, *Serrate 2* and *Delta 1* throughout chick limb development as well as experiments

investigating how expression of these genes in the mesenchyme may be initiated and controlled. I propose that the complex mesenchymal expression patterns of *Notch 1*, *Serrate 1*, *Serrate 2* and *Delta 1* throughout limb development are suggestive of multiple roles for these genes at different stages in limb development: in limb outgrowth, in myogenesis, vascularisation and in digit spacing. However these proposals are based entirely on expression data only and further work will be required to confirm and extend these results, which can be based upon this expression data, for example gene misexpression studies, gene inactivation studies.

5.2 Results

Expression patterns of *Notch 1*, *Serrate 1*, *Serrate 2* and *Delta 1* were documented in both wing bud and leg bud of chick embryos up to stage 30 (Hamburger and Hamilton, 1951). Detailed information is shown in Table 5.1A, B. These patterns are complex and dynamic and it seems likely that different phases of expression may fulfill different functions during limb bud development.

Table indicating the presence or absence of expression of *Notch 1*, *Serrate 1*, *Serrate 2* and *Delta 1* in wing mesenchyme and apical ridge

Table 5.1A

Stage	15		16		17		18		19		20		21		22	
	Mes	AER	Mes	AER	Mes	AER	Mes	AER	Mes	AER	Mes	AER	Mes	AER	Mes	AER
Ser 1	- (3)		- (1)		- (2)		- (2)		- (2)		- (7)		- (7)		- (7)	
Ser 2																
Not 1	- (1)	- (1)			- (3)	- (3)	- (2)	- (2)	- (3)	- (3)	+/7 -/4	+/3 -/4	+/14 -/2	+/3 -/7	+ (18)	+/4 -/4
Del 1															+/1 -/3	

Stage	23		24		25		26		27		28		29		30	
	Mes	AER	Mes	AER	Mes	AER	Mes	AER	Mes	AER	Mes	AER	Mes	AER	Mes	AER
Ser 1	+/3 -/9		+/11 -/3		+ (26)		+ (29)		+ (26)		+ (27)		+ (7)		+ (3)	
Ser 2			+ (2)	+ (1)	+ (2)		+ (5)		+ (2)	+ (1)	+ (4)		+ (1)		+ (1)	
Not 1	+ (8)	+/4 -/2	+ (14)	+/5 -/9	+ (13)	- (7)	+ (11)	- (8)	+ (25)	- (12)	+ (20)	- (15)	+ (6)	- (6)	+ (5)	- (4)
Del 1	+/6 -/3		+ (8)		+ (8)		+/5 -/1		+ (9)		+/14 -/1		+ (5)			

- = no expression observed + = expression observed ( ) = number of cases

WING

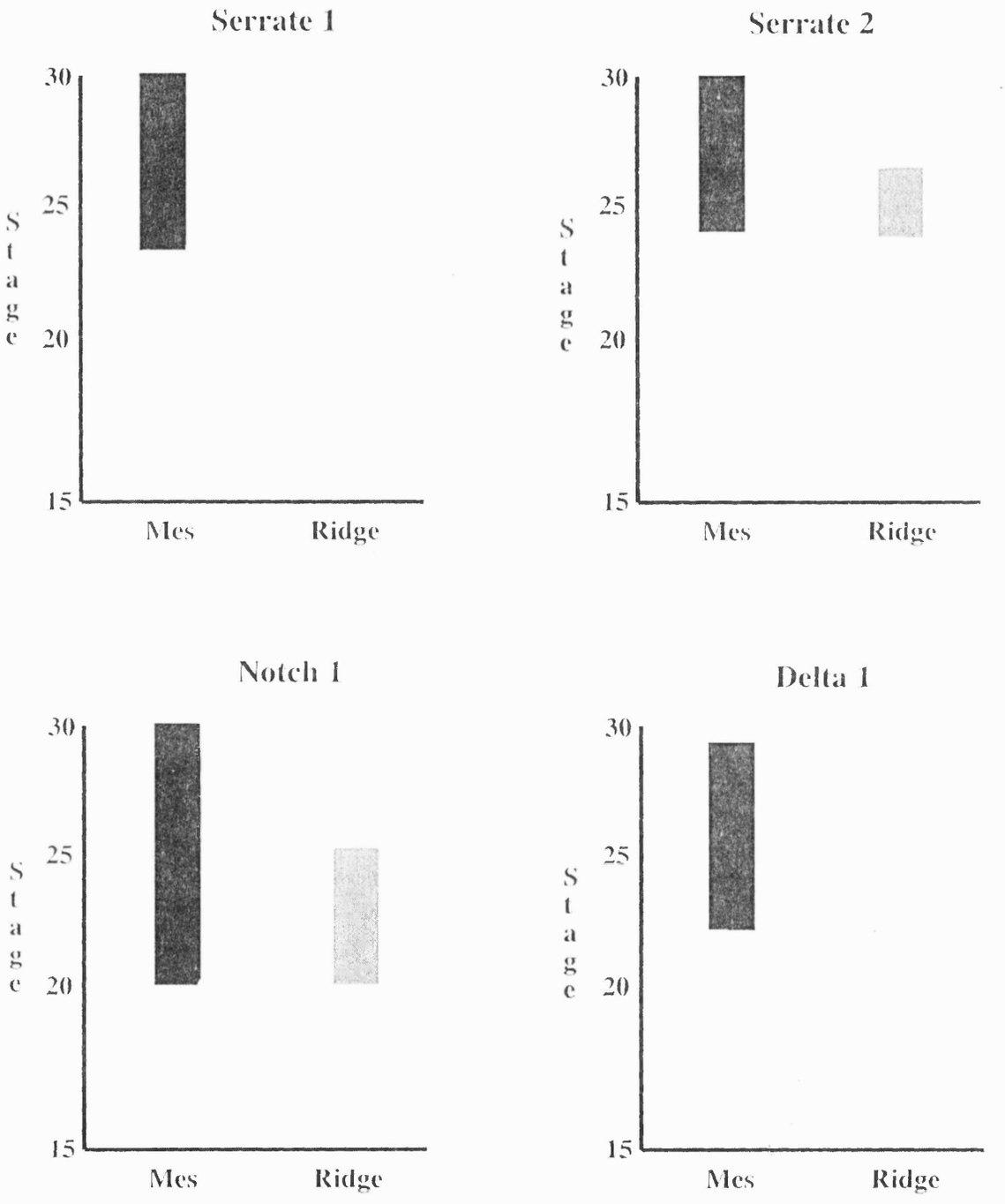

Figure summarising expression of Serrate 1, Serrate 2, Notch 1 and Delta 1 in wing mesenchyme and apical ridge in this study.

Mes= mesenchyme Ridge= apical ectodermal ridge

Table indicating the presence or absence of expression of *Notch 1*, *Serrate 1*, *Serrate 2* and *Delta 1* in leg mesenchyme and apical ridge.

Table 5.1B

Stage	15		16		17		18		19		20		21		22	
	Mes	AER	Mes	AER	Mes	AER	Mes	AER	Mes	AER	Mes	AER	Mes	AER	Mes	AER
Ser 1	- (3)		- (1)		- (2)		- (2)		- (2)		- (6)		+/3 -/2		+ (6)	
Ser 2																
Not 1	- (1)	- (1)			- (3)	- (3)			+ (1)	- (1)	+/3 -/1	+/4 -/2	+ (13)	+/7 -/6	+/11 -/2	+/4 -/7
Del 1															+/1 -/3	

Stage	23		24		25		26		27		28		29		30	
	Mes	AER	Mes	AER	Mes	AER	Mes	AER	Mes	AER	Mes	AER	Mes	AER	Mes	AER
Ser 1	+/3 -/1		+ (13)		+ (20)		+ (24)		+ (20)		+ (23)		+ (7)		+ (6)	
Ser 2			+ (2)		+ (2)		+ (5)		+ (2)		+ (4)		+ (1)		+ (1)	
Not 1	+/7 -/2	+/3 -/5	+ (14)	+/2 -/11	+ (12)	- (8)	+ (11)	- (8)	+ (20)	- (13)	+ (20)	- (11)	+ (7)	- (6)	+ (5)	- (4)
Del 1	+/6 -/2		+ (8)		+/7 -/1		+/5 -/1		+ (8)		+/11 -/1		+ (5)			

- = no expression observed + = expression observed ( ) = number of cases

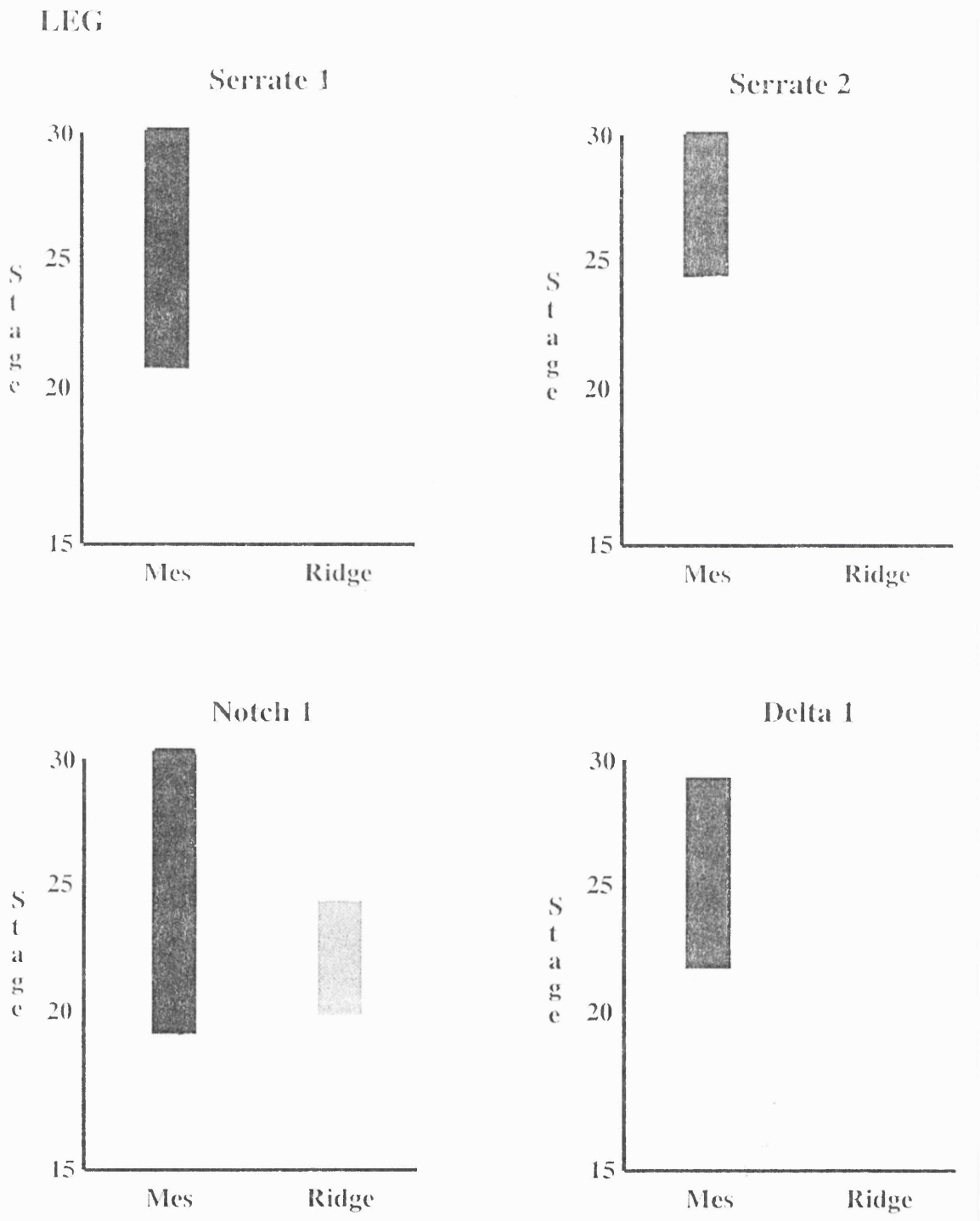

Figure summarising expression of Serrate 1, Serrate 2, Notch 1 and Delta 1 in leg mesenchyme and apical ridge in this study.

Mes= mesenchyme Ridge= apical ectodermal ridge

5.2.1 Early expression during limb bud outgrowth.

In the early bud, at stage 20, *Notch 1* is expressed in the mesenchyme (Fig. 5.2A). *Notch 1* is also expressed throughout the apical ridge (see also Myat et al., 1996) up until stage 24 (Fig. 5.2B, see arrow). *Notch 1* expression in the mesenchyme is extensive in the anterior two-thirds of the bud. The posterior third of the bud does not express the gene (Fig. 5.2A see arrow, Fig. 5.2B). There is a zone of mesenchyme immediately beneath the apical ridge where no transcripts of *Notch* 1 can be detected (Fig. 5.2A). Over the next 24 hours the bud elongates considerably. At stage 23/4, *Notch 1* is expressed strongly in the mesenchyme of the anterior two-thirds of the bud, particularly in a central domain, but not posteriorly nor in the strip of cells immediately beneath the apical ridge (Fig. 5.2B).

Transcripts of *Serrate 1*, *Serrate 2* and *Delta 1* are first detected in the mesenchyme at stage 23/4 (Fig. 5.2D, G, I). *Serrate 1* expression is detected in a restricted postero-distal domain in mesenchyme but not immediately beneath the apical ridge (Fig. 5.2D, E). *Serrate 1* transcripts are not observed in proximal tissue. *Serrate 2* is expressed proximally in the limb in central mesenchyme in a faint band but no expression is observed in distal regions (Fig. 5.2G). *Delta 1* is expressed dorsally in centrally located proximal mesenchyme but also in a discrete posterior domain, near the bud tip (arrowed Fig. 5.2I, J).

During the next 8 hours as the limb takes on a paddle shape (stage 25), the general expression of most of these genes is unchanged (Fig. 5.2C, F, H, K). *Notch 1* expression is still restricted to distal anterior two thirds mesenchyme and the central patch expression becomes stronger (Fig. 5.2C). *Serrate 1* expression however now extends across most of the handplate (Fig. 5.2F). *Serrate 2* expression has broadened in the central mesenchyme and faint expression between proximal regions and the central mesenchyme is apparent (arrowed Fig. 5.2H). In addition although the posterior domain of *Delta 1* is still present, it will disappear shortly afterwards. Thus the posterior domain of *Delta 1* is a transitory patch of expression lasting around 20 hours (arrowed Fig. 5.2I-K).

5.2.1.1 *Expansion of Serrate 1 expression involves incorporation of cells previously not expressing Serrate 1*

Serrate 1 expression expands across the antero-posterior axis of the prospective hand plate and eventually fills it (as just described). The relationship between this expansion and cell lineage was investigated by labelling small populations of mesenchyme with DiI on (Fig. 5.3C), within (Fig. 5.3D) or above

Figure 5.2

Early expression patterns of *Notch 1* (A-C), *Serrate 1* (D-F), *Serrate 2* (G-H) and *Delta 1* (I-K) in chick wings from stage 20 to stage 25.

Notch 1: **A**) stage 20 mesenchymal expression, note the lack of expression in the posterior third of bud (arrow). Scale bar represents 500μm in A, D and I. **B**) stage 24. Mesenchymal expression still restricted to anterior two-thirds of the bud and does not abut the apical ridge, note expression in streak in central mesenchyme; arrow indicates expression in the apical ridge. **C**) stage 25. Anterior two-thirds of bud mesenchyme expresses *Notch 1*and central mesenchyme streak expression is more pronounced. No expression detected within the ridge. Scale bar represents 500μm.

Serrate 1: **D**) Stage 23/4 limb bud. Small patch of expression of *Serrate 1* near posterior-distal tip of bud. **E**) Stage 24. Posterior distal domain of *Serrate 1* clearly defined. **F**) Stage 25. Note that expression has expanded anteriorly but strip of cells immediately beneath the apical ridge does not express *Serrate 1*.

Serrate 2: **G**) Proximal streak of transcripts at stage 24. **H**) stage 25. Proximal streak of expression is stronger and also note weak expression of *Serrate 2* between proximal tissue and the central mesenchyme expression (arrow).

Delta 1: **I**) Stage 23. Expression can be seen in central and in postero-distal mesenchyme (postero-distal domain arrowed); these two domains are clearly visible at later stages, **J**) stage 24, **K**) stage 25.

Anterior is up; posterior down; in figures showing one bud, distal is to the right.

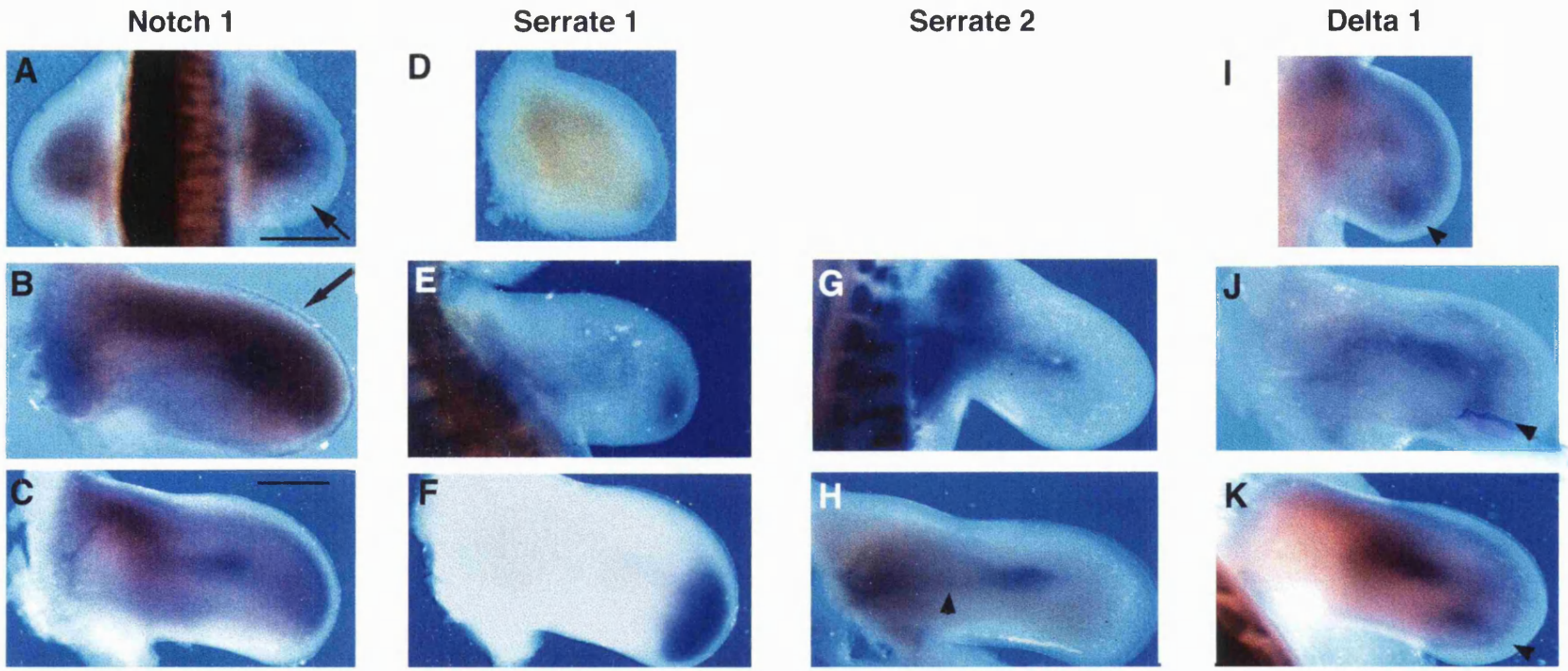
Notch 1
Serrate 1
Serrate 2
Delta 1
A
B
C
D
E
F
G
H
I
J
K

Figure 5.3

Expansion of *Serrate 1* expression incorporates cells previously not expressing *Serrate 1*

A) Stage 23/4 whole mount limb showing expression of *Serrate 1*. Note the anterior limit of expression is on a level with somite 17/18 (arrowed). B-D Examples of limbs fixed immediately after DiI injection. **B)** DiI labelled cells on a level with somite 17, above the anterior limit of *Serrate 1*. **C)** DiI labelled cells on a level with somite 17/18. **D)** Labelled cells on a level with somite 18, within the anterior limit of *Serrate 1* expression. Scale bar represents 250μm in A, B, C and D. **E)** Example of a stage 26 limb showing the expression pattern of *Serrate 1*, 20-24 hours after initial expression observed. F-H examples of limbs 24 hours after DiI injection at stage 23/4; **F)** above the anterior limit of *Serrate 1* expression. Note the labelled cells are still above the anterior limit of *Serrate 1* expression, compare with **F. G)** on the anterior limit of *Serrate 1*expression. Note labelled cells appear to still be associated with the anterior limit. **H)** within the anterior limit of *Serrate 1* expression. Note labelled cells are still within the labelled domain. Scale bar represents 300μm in E, F, G and H. **I)** Stage 28 whole mount limb showing the expression of *Serrate 1*, 40-48 hours after initial expression seen. J-L examples of limbs 48 hours after DiI injection at stage 23/4; **J)** above the anterior limit of *Serrate 1* expression. Note labelled cells now appear to be associated with the anterior limit of *Serrate 1* expression, compare to I. **K)** on the anterior limit of *Serrate 1* expression. Note labelled cells are within the *Serrate 1* expression domain. **L)** within the anterior limit of *Serrate 1* expression. Note labelled cells are now well within the *Serrate 1* expression domain. Scale bar represents 500μm in I, J, K and L.

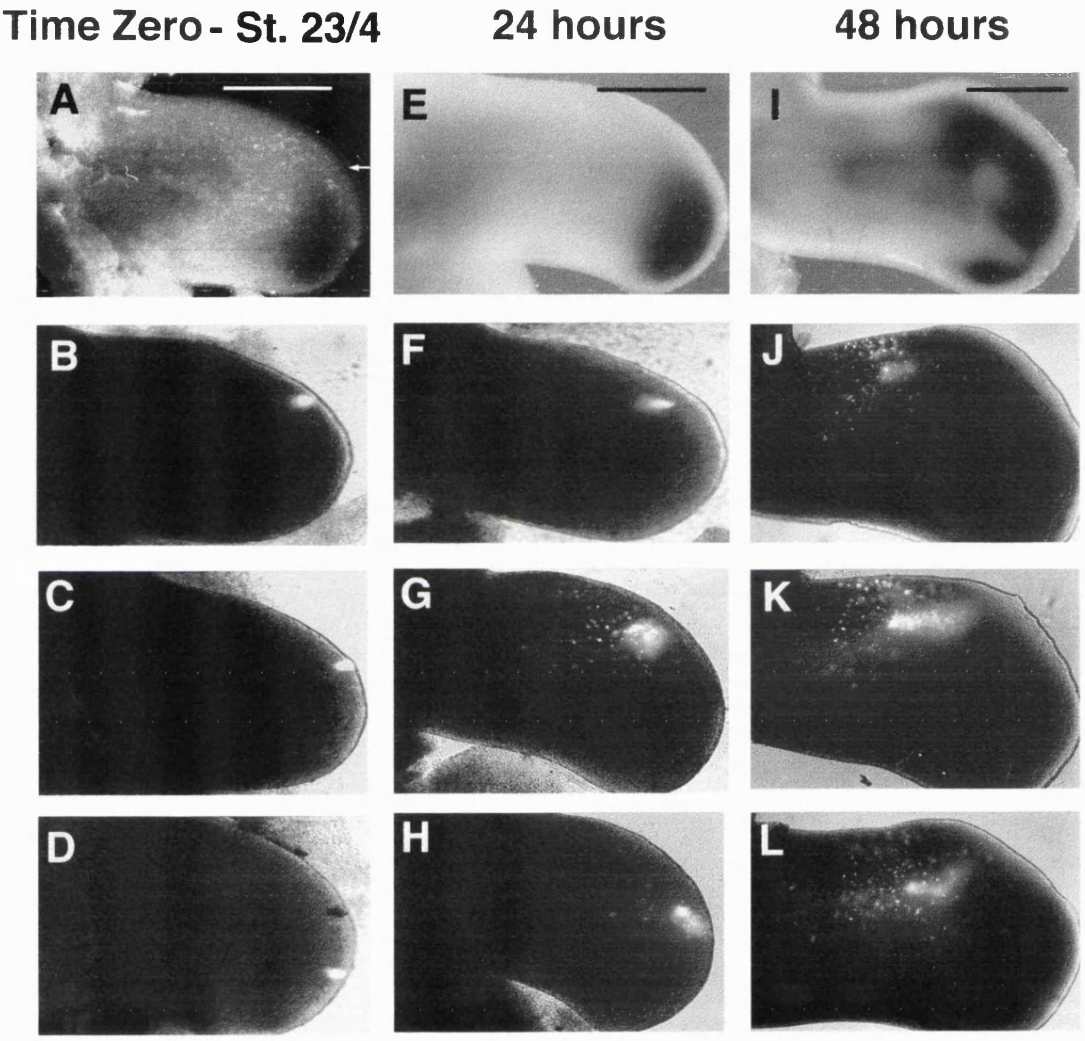
Time Zero - St. 23/4
24 hours
48 hours
A
E
I
B
F
J
C
G
K
D
H
L

(Fig. 5.3B) the anterior distal limit of *Serrate 1* expression in stage 23/24 limb buds and following cell fate over 48 hours (Fig. 5.3). The anterior distal limit of *Serrate 1* expression at stage 23/24 is on a level with somite 17/18 (Fig. 5.3A). Cell populations labelled on the anterior distal limit of *Serrate 1*, were now found to be within the expression domain 24 and 48 hours later (Fig. 5.3H, I, M, N). Similarly, cell populations labelled just above the anterior distal limit of *Serrate 1* at stage 23/24 (in subapical mesenchyme on a level with somite 17), were found, 24 and 48 hours later, to be on the anterior distal limit of *Serrate 1* expression (Fig. 5.3G, L). This result shows that expansion of the *Serrate 1* expression domain requires incorporation of previously non-expressing cells.

5.2.2 Experimental manipulations and effects on *Notch 1, Serrate 1, Serrate 2* and *Delta 1* expression

5.2.2.1 *Apical ridge removal*

To begin to explore how activation and/or maintenance of expression of these genes is mediated during early limb bud outgrowth, the apical ectodermal ridge was removed from stage 20 and from stage 24 wing buds. Following removal of the apical ectodermal ridge in stage 20 wing buds, *Notch 1* is still expressed (see for example Fig. 5.4B) but *Serrate 1* and *Delta 1* expression distally does not occur in the truncated buds (see for example Fig. 5.4A; Table 5.2). When the apical ridge is removed at stage 24, expression of *Notch 1* persists in the truncated wing buds (Table 5.2 and data not shown) but again no expression of *Serrate 1* is observed and neither is the posterior-distal domain of *Delta 1*, 24 hours later. The central proximal domain of *Delta 1* and proximal *Serrate 2* expression remain whether the apical ridge is removed at stage 20 or at stage 24. These data indicate that activation and maintenance of mesenchymal expression of *Serrate 1* at the tip of the limb bud and the posterior-distal domain of *Delta 1* are dependent upon the presence of an apical ridge but *Notch 1* expression can be maintained in the absence of the apical ridge.

5.2.2.2 *Notch 1, Serrate 1 and Delta 1 are FGF responsive*

Apical ridge signalling has been shown to be mediated by FGFs (Niswander et al., 1993). To test whether FGF signalling is involved in activation of expression of *Serrate 1* and *Delta 1* expression in posterior distal mesenchyme, and how FGF affects expression of the other genes, the apical ridge was removed and replaced with FGF-4 loaded heparin beads (see also *Hoxa-13* activation investigation in Chapter

Table 5.2.

Apical ridge removals

	Stage 20		Stage 24	
	24 hours	48 hours	24 hours	48 hours
Serrate 1	- (6)	- (10)	- (7)	- (6)
Serrate 2	+ (3)	+ (4)	+ (3)	+ (4)
Notch 1	+ (8) - (1)	+ (7) - (1)	+ (4)	+ (2) - (1)
Delta 1-.....distal	- (1)	- (4)	- (3)	- (3)

+ designates expression remaining. - designates expression not present

Numbers in brackets indicate total number of embryos

Figure 5.4

Effects of manipulations on early wing buds upon gene expression.

A) 24 hours after apical ridge removal at stage 20. *Serrate 1* transcripts not detectable in truncated limb bud (right). **B**) *Notch 1* transcripts can still be detected 24 hours after apical ridge removal at stage 20 in anterior and distal mesenchyme. **C**) and **D**) 24 hours after FGF bead stapled in place of apical ridge at stage 20. *Serrate 1* is activated around bead (see arrow) and *Notch 1* expression maintained (asterisk marks the position of the FGF bead). **E**) No activation of *Serrate 1* in proximal cells after implantation of an FGF bead proximally at stage 20 (bead arrowed). **F**) *Notch 1* expression activated in posterior-proximal mesenchyme 24 hours after an FGF bead placed proximally (arrow denotes position of FGF bead). **G**) and **H**), show *Serrate 1* and *Notch 1* expression (respectively) around and up to an FGF bead 48 hours after ridge was removed at stage 20 and an FGF bead stapled in its place.

When embryo torso is shown, manipulated limb is on the right; control limb on the left; Anterior is up; posterior down; For single buds shown, distal is to the right. Scale bar represents 500μm.

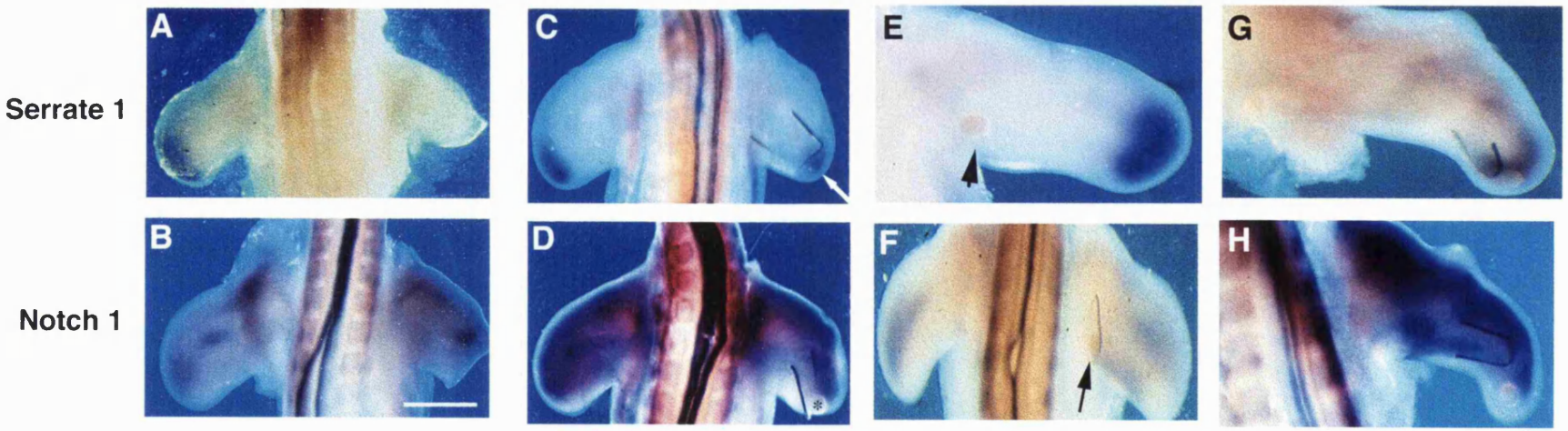
Serrate 1
Notch 1
A
B
C
D
E
F
G
H

Three). In addition, FGF-4 beads were placed proximally in the wing buds. In limbs, where the apical ridge was removed at stage 20 or stage 24 and an FGF-4 bead pinned to posterior mesenchyme, outgrowth appeared normal and *Serrate 1* expression was observed around and up to the bead at 24 hours and 48 hours later (Fig. 5.4C see arrow, 5.4G; Table 5.3). *Notch 1* was expressed in the limb mesenchyme up to the FGF bead (Fig. 5.4D, H). Expression of *Delta 1* is also enhanced by FGF at 24 hours, and the transitory distal domain of *Delta 1* appears as normal (Data not shown). Thus, expression of *Serrate 1* and *Delta 1* in distal regions appears to be mediated by apical ridge FGF signalling. In contrast to the similarities in the response to FGF of *Serrate 1* and *Delta 1* expression in distal mesenchyme, when FGF beads were placed proximally, *Delta 1* is activated but *Serrate 1* is not (Fig. 5.4E). *Notch 1*expression is also increased (Fig. 5.4F) even though *Notch 1* is not normally expressed in the posterior part of the bud. Thus, *Notch 1*and *Delta 1* can be activated in proximal cells in response to FGF.

5.2.3 Expression in relation to digit formation.

At stage 27/28, *Serrate 1*and *Notch 1*are expressed in the handplate but no *Serrate 2* and *Delta 1* transcripts can be detected in this region (see later). *Notch 1* expression fills the anterior two-thirds of the handplate and is interdigital at stage 28 (Fig. 5.5A, B). As condensations form, a reduction in transcript abundance occurs in the condensing digit. Then later, further reduction in transcript abundance occurs interdigitally, leaving expression around the digits (compare Fig. 5.5A, B, C). By stage 30, *Notch 1* transcripts are restricted to the edges of digit **2** and **3** and are seen faintly along the anterior edge of digit **4** (Fig. 5.5C). *Notch 1* is also expressed in dorsal and ventral ectoderm from stage 28 (data not shown). *Serrate 1* transcripts are restricted interdigitally. The interdigital boundaries of *Serrate 1* sharpen but expression in the anterior and posterior edges of the handplate has gone by stage 30 (Fig. 5.5F). This late expression of *Serrate 1* appears complementary to that of *Notch 1*. Thus, for example, *Serrate 1* transcripts are present in the interdigital space between digits **2** and **3** (as well as between digits **3** and **4**) and this interdigital domain appears to be bordered by expression of *Notch 1* (compare Fig. 5.5C and Fig. 5.5F, see asterisk). However it should be noted that in a thin strip of mesenchyme directly beneath the apical ridge no transcripts of either *Serrate 1* or *Notch 1* were found (Fig. 5.5C, F).

Table 5.3.
FGF-4 experiments

	Stage 20		Stage 24	
	24 hour	48 hour	24 hour	48 hour
Proximal				
Serrate 1	- (4)	+ (2) - (5)	+ (1) - (3)	+ (2) - (3)
Notch 1	+ (5)	+ (6) - (2)	- (1)	+ (1)
Delta 1- .....distal	+ (1)	+ (2)	+(1)	+ (1)
No AER				
Serrate 1	+ (4) - (3)	+ (5) - (2)	+ (2)	
Serrate 2	- (1)	+ (1) - (2)		
Notch 1	+ (2) - (1)	+ (4) - (2)		
Delta 1	+ (2)	- (2)		

+ designates expression present/maintained - designates no expression present

Numbers in brackets indicate total number of embryos

Figure 5.5

Expression patterns of *Notch 1* and *Serrate 1* in late buds between stages 27 and 31

Wing buds at stages 27 (top row), stage 28 (middle row) and stage 30/31 (bottom row).

Notch 1 (A-C), **A)** *Notch 1* expression in central proximal mesenchyme and throughout anterior distal handplate, note no expression observed in posterior third. **B)** *Notch 1* expression confined to hand plate. Reduction in *Notch 1* transcript levels in the area of digit **3** condensation, note no expression in posterior third of handplate; **C)** Further reduction in the level of *Notch 1* transcripts in regions of both digit **2** and **3** condensations and a reduction in the level of transcripts interdigitally; expression outlines digit **2** and **3**, note the asterisk in interdigital regions between digit **2** and **3** not expressing *Notch 1* and compare with **F**.

Serrate 1 (D-F). **D)** transcripts are confined to the handplate; 3 broad areas where transcripts are absent represent the forming digits; **E)** expression is further interdigitally restricted - anterior to digit **2**, in between digit **2** and **3** and in between digit **3** and **4** and posterior to digit **4**. A wide gap of non expressing mesenchyme separates the main domains and the apical ridge; **F)** expression is interdigital between digits **2** and **3** and also **3** and **4** and the boundaries of expression domains are sharper. Expression anterior to digit **2** and posterior to digit **4** is no longer present. Note the asterisk in between digit **2** and **3** and compare to **C**, illustrates apparent complementary expression pattern between *Notch 1* and *Serrate 1*.

Anterior is up; Posterior down; Distal to the right. Scale bar represents 650μm.

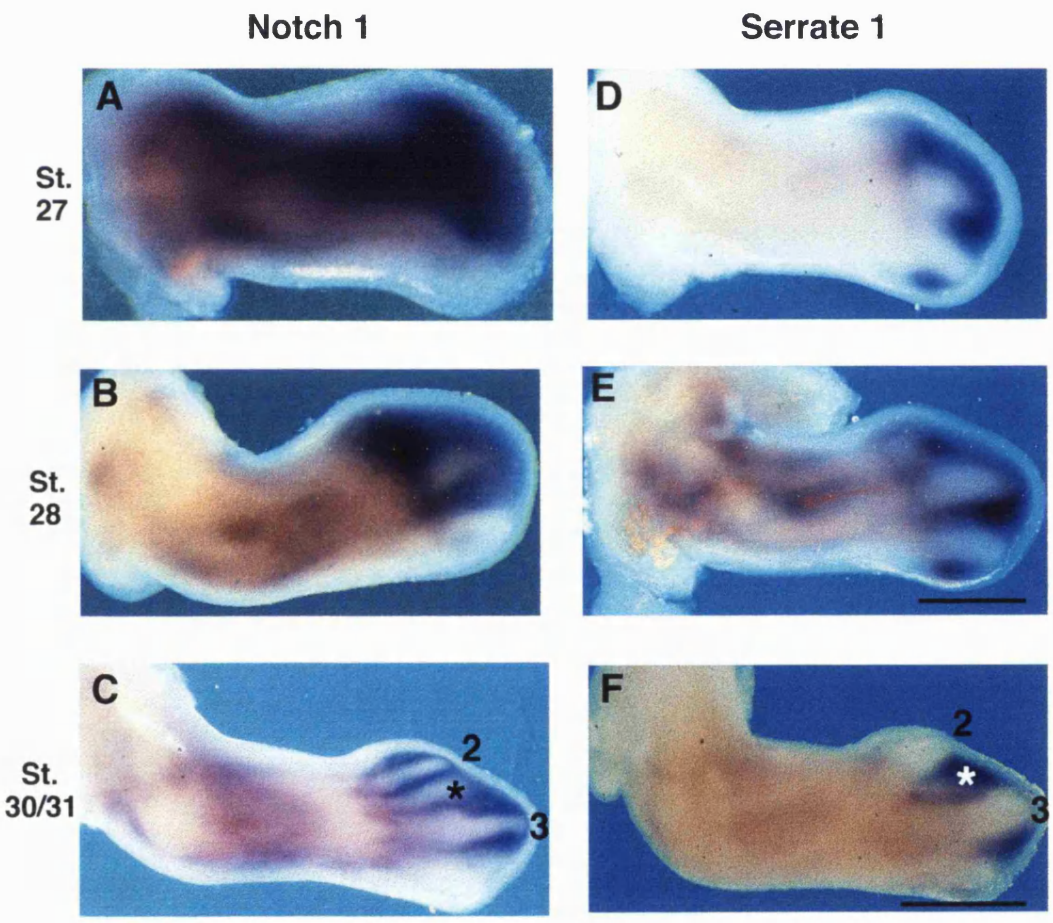
Notch 1
Serrate 1
A
D
St.
27
B
E
St.
28
C
F
2
*
3
St.
30/31

5.2.4 Expression in the vasculature.

At stage 24 (when limb bud is elongated), *Serrate 2* transcripts are confined to a streak in the proximal regions of the developing limb bud (Fig. 5.6D). Similarly one can see a proximal streak of high level *Notch 1* expression in the centre of the limb at similar stages (Fig. 5.6B). Outwardly a similar proximal patch of expression is observed for *Delta 1*, but this turns out to mark developing muscle (Fig. 5.2M; see later). From around stage 25, *Serrate 2* expression is apparent initially faintly, then in two streams, between proximal regions and the central streak (Fig. 5.6D). The central streak of *Serrate 2* and of *Notch 1* expression in whole mounts can be seen until at least stage 27 and is in the same position as the major artery supplying the limb (Fig. 5.6A). This suggests that *Notch 1* and *Serrate 2* might be expressed in the main artery and vasculature. When stage 24 limbs are sectioned, expression of *Serrate 2* is observed strongly in and around blood vessels in proximal and forearm tissue (Fig. 5.6F, I), as is *Notch 1* (Fig. 5.6E, G) and *Serrate 1* (Fig. 5.6C, H; see also Myat et al., 1996). As development proceeds it is clear, from sections that other parts of the vasculature in addition to the major limb artery also express *Notch 1*, *Serrate 1* and *Serrate 2*. For example *Serrate 2* transcripts are associated with blood vessels, presumably marking endothelial cells, in ventral muscle masses at stage 30 (Fig. 5.7E, F). Furthermore expression patterns of *Notch 1, Serrate 1* and *Serrate 2* are very similar to the vasculature pattern as demonstrated by injection of India Ink or DiI, a lipophilic, fluorescent compound, for example see Fig. 5.6J which is an Indian ink labelled stage 21/2 limb showing ink in the main artery and compare to Fig. 5.6K a section of a stage 21/2 limb after whole mount in situ hybridisation for *Notch 1* showing *Notch 1* expression in the main artery. These data suggest that *Serrate 2*, *Serrate 1* and *Notch 1* are expressed in the developing vasculature.

5.2.5 Myogenesis.

The expression patterns of *Serrate 2*and *Delta 1*, as limb development proceeds, suggest roles for both genes in myogenesis. *Serrate 2* transcripts are first observed in potential muscle precursors, as well as in and around blood vessels, from stage 25 (Fig. 5.7A, B). Fig. 5.7C shows *Serrate 2* expression at stage 30 in discrete patches of expression. Sections show that these patches of expression mark developing muscles (Fig. 5.7E, G). Both dorsal and ventral muscles express *Serrate 2* (Fig. 5.7E). Moreover from high magnification analysis, *Serrate 2* seems to be expressed in myotubes (Fig. 5.7D) and in blood vessels within the muscle (Fig. 5.7E, F). *Serrate 2* is expressed in the majority but not all muscle condensations in the limb

Figure 5.6

Expression of *Notch 1*, *Serrate 2* and *Serrate 1* in the vasculature.

A) DiI injection into the vasculature marking central artery of a limb bud of a stage 24/5 embryo. B-D Examples of stage 24 whole mount limb showing expression of **B**) *Notch 1*; **C**) *Serrate 1*; **D**) *Serrate 2;* suggesting *Notch 1* and *Serrate 2* genes are expressed in the central artery early in development. Scale bar represents 300μm.

Mid limb sections of st24/5 limb buds expressing:

Notch 1; **E**), transverse section; Mag. X6 (scale bar 150μm) and **G**) higher power of E; Mag. X40 (scale bar 35μm). ***Serrate 2***; **F**), transverse section; Arrows denote expression in and around blood vessels; Mag. X6 (scale bar 125μm) and **I**), higher power of F; Mag. X16 (scale bar 50μm); **L**) higher power of F; Mag. X40 (scale bar 35μm); ***Serrate 1***; **H**) transverse section; expression within a blood vessel (Mag. X16; scale bar 50μm). **J**) Example of the vasculature at mid limb level after India Ink was injected into the umbilical vein of a stage 24 limb and fixed immediately and then wax sectioned. Mag. X6. Scale bar represents 150μm; **K**) shows the complementary expression of *Notch 1* in blood vessels in mid limb bud section after whole mount in situ hybridisation; Mag. X40. Scale bar represents 35μm.

For A-D Distal is to the right and anterior to the top.

For E-F and J dorsal is to the top; Ventral to the bottom and anterior to the right. All sections were cut in the transverse plane.

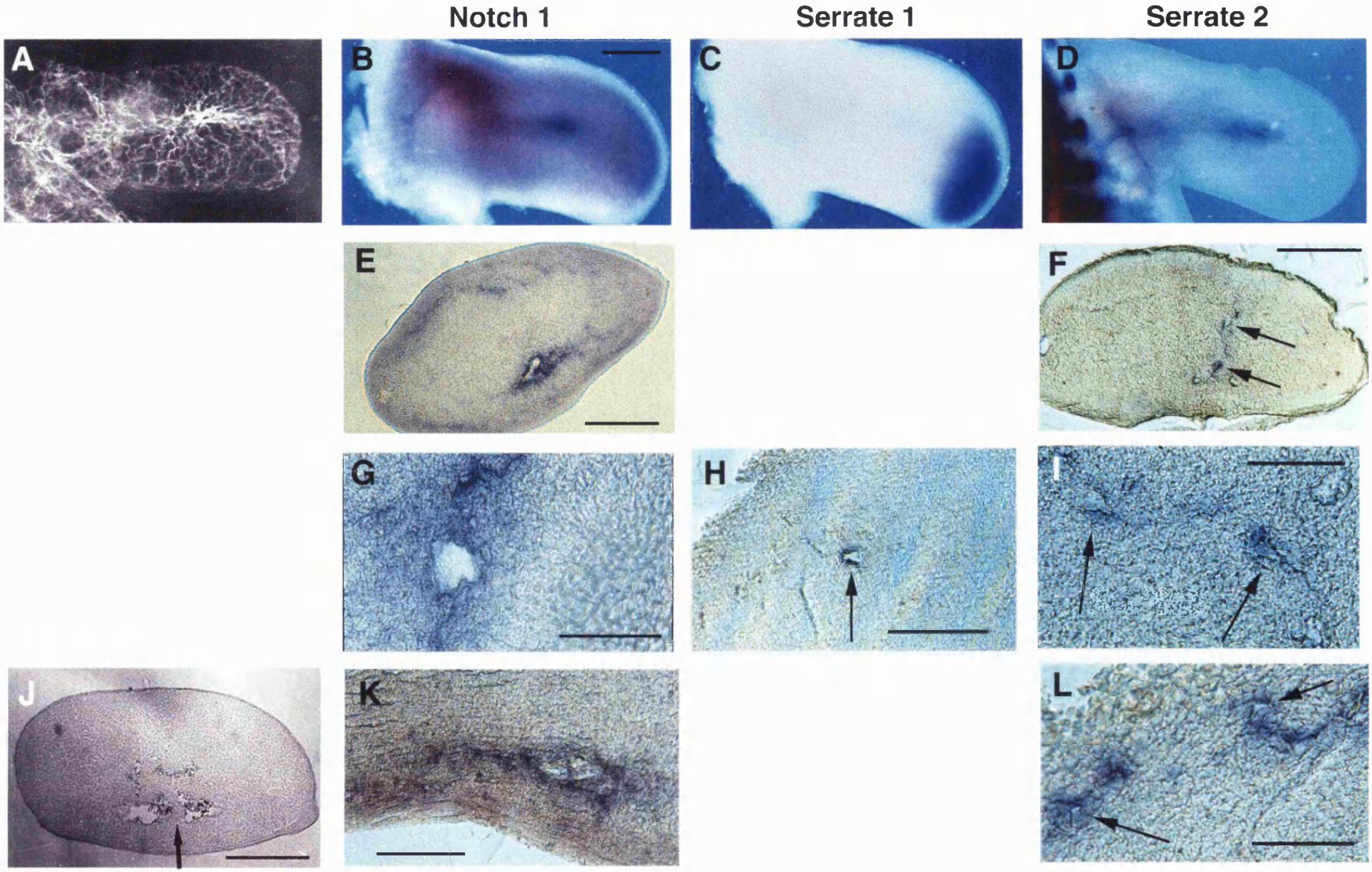
Notch 1
Serrate 1
Serrate 2
A
B
C
D
E
F
G
H
I
J
K
L

Figure 5.7

***Serrate 2* and *Delta 1* expression in muscle**

A-G ***Serrate 2*** **A)** Stage 25 whole mount limb showing expression in central proximal mesenchyme and also as indicated by arrowheads, two streams of faint expression between proximal limb regions and the central area of *Serrate 2* expression. Scale bar represents 250μm. **B)** Transverse central section of limb seen in A (Mag. X6; Scale bar represents 150μm in B, D). Note expression of *Serrate 2* in and around blood vessels, as indicated by the arrow, and expression also located beneath dorsal (up) and ventral ectoderm (bottom), as indicated by asterisks. **C)** Stage 30 limb showing discrete patches of *Serrate 2* expression (Scale bar represents 600μm in C, H). **D)** Is an example of a posterior longitudinal section of a stage 30 limb following whole mount in situ hybridisation *for Serrate 2* (Mag. X6). White box marks an area of muscle shown at a higher magnification (inset; Mag. X16). *Serrate 2* appears to be expressed in myotubes. **E)** Transverse section of the proximal radius/ulna region of a stage 30 limb, as shown in C (Mag. X6; Scale bar represents 200μm in E, G). Note the discrete patches of expression localised to muscles in both dorsal (top of image) and ventral (bottom of image) positions. Boxed area (inset) shown at a higher magnification in **F)** showing *Serrate 2* expression in and around a blood vessel (arrowed), within a ventral muscle mass (Mag. X16; scale bar 50μm). **G)** Transverse wrist section of a stage 31 limb (Mag. X6). Note the expression of *Serrate 2* in tendons beneath dorsal (top of image) and ventral (bottom of image) ectoderm, as indicated by the arrows. H-J ***Delta 1***. **H)** Stage 30 whole mount limb following in situ hybridisation for *Delta 1*. Note transcripts are only faintly observed above the metacarpals in the distal forearm and in between the radius and ulna. **I)** Transverse section of prospective forearm region of a stage 26 limb indicating two areas of expression one dorsally (nearer posterior margin; top of image) and one ventrally (midway between anterior and posterior margin; bottom of image; Mag. X6), which may be migrating myoblasts. Note also that that expression of *Delta 1* does not directly abut the ectoderm, which is also the case in earlier stages. Scale bar 150μm. **J)** Higher power view of the ventral *Delta 1* expression domain in **I** (Mag. X16. Scale bar 50μm).

For A, B, H Anterior is up, posterior down, distal to the left. Mag. X4.

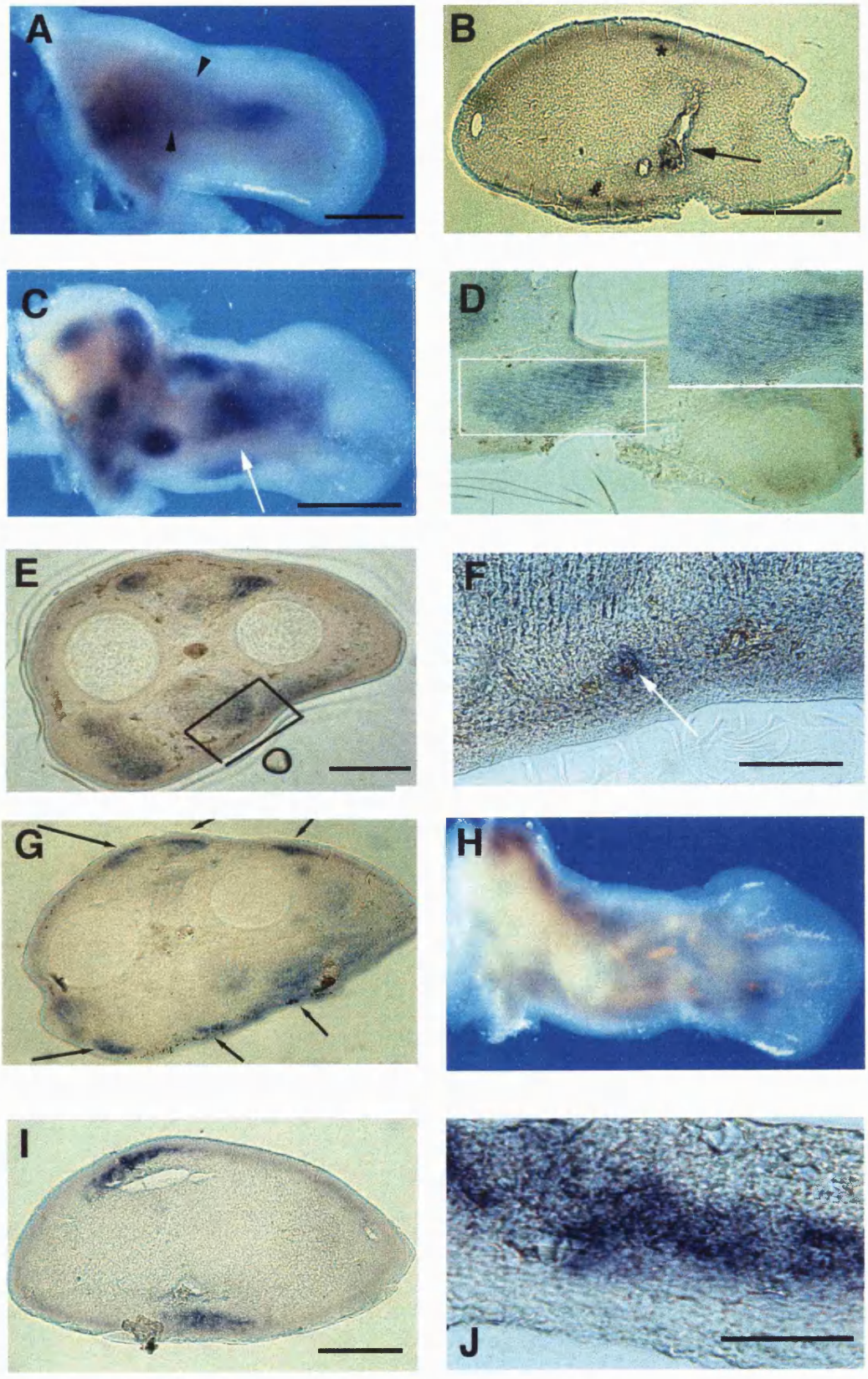
A
B
C
D
E
F
G
H
I
J

(Fig. 5.7C, D, E; Fig. 5.8F). By stage 31, sections show *Serrate 2* expression in tendons beneath the dorsal and ventral ectoderm (Fig. 5.7G, note arrows) at the distal part of the forearm.

Sections of stage 26 *Delta 1* limbs, indicate two separate populations of *Delta 1* expression, a stream dorsally in posterior mesenchyme and a stream ventrally in mid-limb mesenchyme (Fig. 5.7I). These streams are probably migrating myoblasts (Fig. 5.7J) which appear to express *Delta 1* transiently as by stage 30 the expression of *Delta 1* has practically gone and is only seen faintly at the base of the handplate and between the radius and ulna (Fig. 5.7H).

To establish more precisely the relationship of these patterns of gene expression to muscle development, gene expression patterns were compared to that of *MyoD*, a myogenic regulatory factor (Fig. 5.8). At stage 23/4, the central patch of *Delta 1* transcripts corresponds with the central patch of expression of *MyoD* whereas the transitory posterior distal patch of *Delta 1* expression does not (Fig. 5.8A). *Serrate 2* has a similar expression pattern to that of *MyoD* although *Serrate 2* expression appears slightly smaller than that of *MyoD* expression at stage 24 (compare Fig. 5.2J with Fig. 5.8A *MyoD* expression). Sections show that *Serrate 2* at this early stage appears to be expressed in and around blood vessels (Fig. 5.6F, I). By stage 26, the expression patterns of *Serrate 2* and *Delta 1* are strikingly similar to that of *MyoD* and all three genes express in two broad streams, one dorsally and one ventrally, running from proximal to central regions (Fig. 5.8B, D). Patterns of expression are still similar but not identical at stage 27/8. For example, *Serrate 2* and *Delta 1* has a large non-expressing central area within the broad dorsal domain of expression (compare arrows in Fig. 5.8C, E) whereas the *MyoD* domain has a small central domain not expressing *MyoD* (see arrow in Fig. 5.8C, E). Thus, *Serrate 2* and *Delta 1* seem to be expressed in regions of *MyoD* expression but not all cells expressing *MyoD*, express *Serrate 2* and *Delta 1*. *Serrate 2* is expressed in muscle up till at least stage 31 (Fig. 5.8F). Thus, *Serrate 2*, unlike *Delta 1* which is only expressed transiently in developing muscle, continues to be expressed in differentiating muscle tissue.

5.3 Discussion

I have described the expression patterns of *Notch 1, Serrate 1, Serrate 2,* and *Delta 1* in the chick wing bud. Interestingly each shows a distinct pattern in buds between stage 20 and stage 25. *Serrate 1* is expressed distally in mesenchyme; *Serrate 2* proximally. *Notch 1* is expressed distally and proximally in anterior

Figure 5.8

Relationship between *Serrate 2*, *Delta 1* and *MyoD* expression.

A-C shows examples of limbs after whole mount in situ hybridisation for *Delta 1* expression (left) and *MyoD* (right). **A**) stage 23/4 limbs. Note the central domains of dorsal expression are similar (scale bar represents 300μm); **B**) stage 26 limbs; the broad dorsal *Delta 1* expression domain is seen running from proximal regions into the central mesenchyme, which can be observed until stage 28. Note the central region of the *Delta 1* domain is faint, almost not expressing *Delta 1*. The edges of the *Delta 1* domain seems to be inside that of *MyoD*; **C**) stage 28 limbs. Note the similarity of the expression of the two genes (see arrow heads demarcating anterior boundary of dorsal domain of expression of each gene). Note the central dorsal region where *Delta 1* is not expressed (see asterisk). Compare the size of this region to the tiny region in the centre of the dorsal *MyoD* domain, indicated by an arrow. **D-F** show examples of limbs following whole mount in situ hybridisation for *MyoD* expression (left) as compared to *Serrate 2* (right). **D**) stage 26 limbs. The expression patterns correspond very closely, and like *Delta 1*, *Serrate 2* expression is seen in a broad dorsal stream running from proximal regions into the central mesenchyme; **E**) stage 28 limbs. The expression patterns of *Serrate 2* and *MyoD* are again similar and *Serrate 2* appears to be expressed around the border of *MyoD* expression. Arrows in the central region of the dorsal expression domains indicate the domains in which no transcripts are seen, compare *Serrate 2* with *MyoD* pattern. Scale bar represents 500μm in B, C, D, E; **F**) stage 31 limbs. Note the similarity between expression of the two genes and that *Serrate 2* appears to expressed in the majority of the limb muscles. Scale bar represents 1000μm.

In all limbs anterior is up; posterior is down. Left hand limbs - distal is to the left. Right hand limbs - distal is to the left.

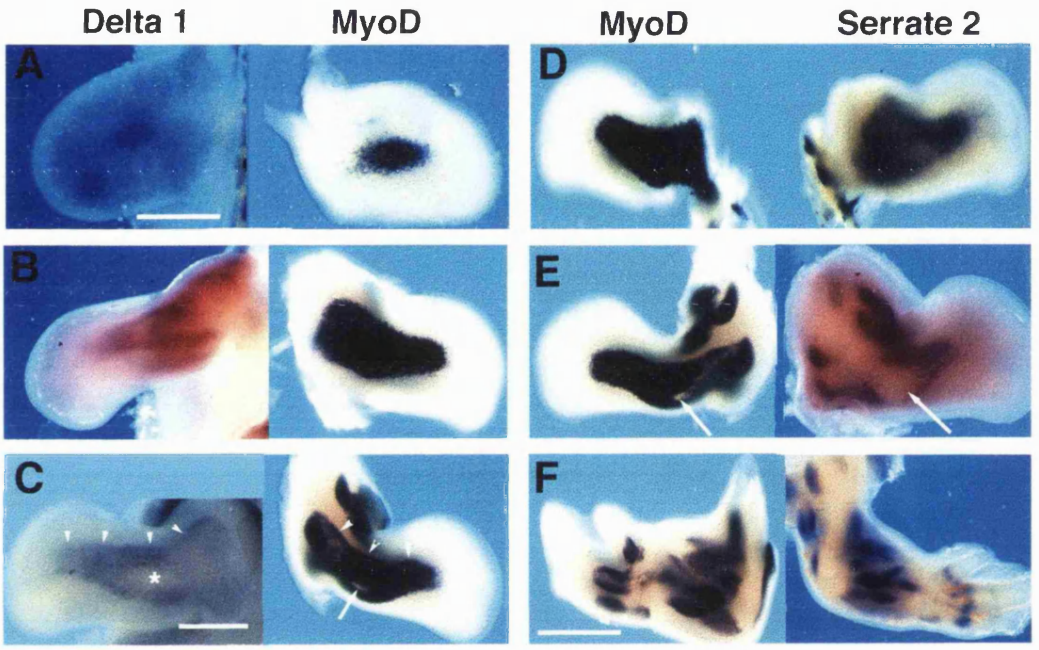
Delta 1
MyoD
MyoD
Serrate 2
A
B
C
D
E
F

mesenchyme and *Delta 1* is expressed in a transient distal domain and in a proximal domain. I have investigated the regulation and function of these genes. Mesenchymal expression of *Serrate 1* is apical ridge dependent and FGF-4 responsive and may have a role in limb outgrowth. Similarly, the distal domain of *Delta 1* expression is ridge dependent and can be maintained by FGF. In contrast, expression of *Serrate 2* and *Notch 1* appears to be independent of ridge signalling. In later limbs (stage 25 onwards), *Serrate 2* and *Notch 1* are expressed proximally in blood vessels and developing muscle. *Delta 1* is also expressed transiently in myoblasts, in proximal part of the limb. Thus, the *Notch* signalling pathway could be involved in establishing the musculature and vasculature of the limb. In the digital plate in limbs from stage 28, expression of *Serrate 1* and *Notch 1* appears to specify boundaries at digit/non-digit interfaces. This is more in line with the situation in *Drosophila* wing development where sharp borders between expression domains of *Notch* and *Serrate* and *Delta* are seen controlling cell fate.

5.3.1 Limb outgrowth

A possible role in limb bud outgrowth for *Notch 1* and *Serrate 1*, which are both expressed distally, could be a contribution to maintenance of the progress zone and in keeping undifferentiated cells in a proliferative state at the limb tip. These genes can not be the only progress zone maintenance factors as they are expressed after the progress zone is established. It is unclear at present whether all cells in the distal tip express both *Serrate 1* and *Notch 1* and mutual signalling maintains proliferation, such that when cells leave the distal tip and progress zone the loss of *Serrate 1* and *Notch 1* signalling allows the cells to differentiate. Alternatively *Serrate 1* and *Notch 1* expression may represent separate cell populations that signal to each other maintaining an undifferentiated state. Interestingly in the *Drosophila* wing, *Serrate* has been shown to be involved in proliferation of wing tissue (Speicher et al., 1994). The *Notch* pathway has also been shown to have an essential role in vertebrate neurogenesis (for review see Lewis 1996) where *Delta* expression in one cell, a prospective neuron, signals to neighbouring cells activating *Notch* which prevents these neighbouring cells from becoming neurons, maintaining the cells in an undifferentiated state. Unless *Serrate 1* is marking committed but undifferentiated cells in the distal chick limb and is signalling to neighbouring cells which express *Notch 1* to maintain an undifferentiated proliferating population, it is difficult to interpret *Notch* signalling at the tip of the limb in terms of a lateral inhibition model.

I have shown that expansion of *Serrate 1* expression is due to the incorporation of previously non-expressing anterior cells, which may involve some

proliferation. It is possible that a member of the FGF family may be responsible for inducing *Serrate 1* expression in anterior cells. *Serrate 1* expression is lost when the apical ridge is removed at stage 20 or stage 24, just when *Serrate 1* transcripts are first seen but expression of *Serrate 1* can be partially rescued by FGF-4 beads substituting for the ridge. In developing teeth in mouse embryos, *Serrate 1* expression is also enhanced by ectopic FGF-4 (Mitsiadis et al., 1997).

Interestingly, mesenchymal expression of both *Serrate 1* and *Notch 1* does not extend right up to the apical ridge. This pattern of expression has also been reported in mouse by Mitsiadis et al (1997) who suggested that this may be due to some negative regulation by a growth factor at a high concentration. It seems unlikely that this factor is FGF-4 because expression of *Notch 1* and *Serrate 1* is seen around and up to beads soaked in high concentrations of FGF-4. However it is not known how FGF-4 released from the ridge compares with concentration of FGF released from beads. Another ridge signal, such as BMPs, may inhibit expression of *Notch 1* and *Serrate 1* directly beneath the apical ridge.

The receptor *Notch 1* is expressed in the apical ridge from stage 20 to stage 24 and in the mesenchyme from stage 20 onwards. *Serrate 1* is not expressed in the apical ridge at all, suggesting that the ligand for *Notch 1* is not *Serrate 1* in the ridge. A ligand for *Notch 1* in the early chick limb may well be *Serrate 2* (Hayashi et al., 1996) which is expressed in the apical ridge initially. A relationship between *Notch 1* and *Serrate 2* has been suggested to play roles in several aspects of chick and rat development notably limb and brain development (Hayashi et al., 1996; Shawber et al., 1996). Recently Laufer et al. (1997) and Rodriguez-Esteban et al. (1997) suggested that *Notch 1* and *Serrate 2* which are both expressed in the early apical ridge may mediate the action of *Radical fringe*, which is involved in positioning and formation of the apical ridge, and, by analogy with *Drosophila,* perhaps be involved in maintenance of apical ridge signalling.

5.3.2 Digit spacing

Notch 1 and *Serrate 1* are both expressed interdigitally by stages 27/28. It therefore seems likely that these genes are involved in organising, fine tuning and/or modelling of digit condensations and spaces i.e. the distance between the condensations. *Serrate 1* and *Notch 1* expression at stage 28 appears complementary (Fig. 5.5C, F). *Notch 1* appears to be expressed at the edges of the digit condensations, whereas *Serrate 1* is expressed in the interdigital mesenchymal webs. Thus, it looks as though in late wing development the *Notch 1* and *Serrate 1* interface marks the edges of the digits and demarcates digit forming from non-digit forming

regions. This may prevent ectopic digit formation in the immediate vicinity. This could be directly tested by inhibiting or knocking out *Serrate 1* function but also by investigating *Notch 1* and *Serrate 1* expression in the chick mutant *talpid* which has multiple digit condensations. Are new *Notch 1* and *Serrate 1* interfaces present at the edges of each of the digits? Also of interest will be to see if *Notch 1* and *Serrate 1* expression is changed following the induction of duplicated digits via polarising region signal manipulations in normal limb buds.

There are some interesting parallels between *Notch* and *Serrate* expression in chick wing digit spacing and wing venation in *Drosophila*. In the *Drosophila* wing, *Notch* is involved in positioning the wing vein and extent of the wing vein competent tissue (Huppert et al., 1997; de Celis, 1997; see also de Celis and Garcia-Bellido, 1994). Thus, the boundary of *Notch* expression may specify position of either the wing vein in *Drosophila* or digit border in vertebrates. In the prospective wing vein, *Delta* is expressed which signals to *Notch* expressed in cells around the edge of the vein and via a lateral inhibition mechanism inhibits lateral intervein cells from adopting the vein fate until proper numbers of intervein cells are produced, controlling the position of the vein (Huppert et al., 1997; de Celis, 1997). Thus, in *Drosophila* and possibly the vertebrate wing, *Notch* may interact with a ligand at the sharp expression boundary, to determine position of the 'scaffolding' and to prevent overgrowth or ectopic structures forming.

5.3.3 Angiogenesis

Serrate 1, *Notch 1, Notch 3* and *Notch 4* have been shown to be expressed in the vascular system (Myat et al., 1996; Bettenhausen et al., 1995; Uyttendaele et al., 1996; Mitsiadis et al., 1997) and in the present study *Serrate 2* transcripts have also been shown to localise to blood vessels. The expression of *Serrate 1*, *Serrate 2* and *Notch 1* in the limb vasculature after limb initiation suggests these genes may be involved in angiogenesis, where new blood vessels sprout from existing vessels via the differentiation of endothelial cells, but are not involved in the initial vascularisation of the limb. The fact that several receptors and ligands are expressed in the developing vascular system suggests that angiogenesis, the endothelial cell population and the differentiation of cells in the vasculature could be controlled by various receptor-ligand combinations. Interestingly human *Jagged 1* (*Serrate 1*) expression in cultured endothelial cells on fibrin is upregulated in response to endothelial cell injury (Zimrin et al., 1996). Moreover when *Jagged 1*antisense oligonucleotides are introduced into this culture system this potentiates the rate of

angiogenesis, suggesting a role for *Jagged 1* in regulation and control of angiogenesis (Zimrin et al., 1996).

5.3.4 Muscle development

I have shown that *Serrate 2* and *Delta 1* transcripts are associated with development of differentiated muscle which expresses *MyoD* a bHLH transcription factor (Fig. 5.8). Expression of *Delta 1* is observed in streams of cells beneath the ectoderm, which co-localises with *MyoD* expression, and expression of *Delta 1* is almost gone by stage 30. This suggests that *Delta 1* may be marking migrating myoblasts. *Serrate 2* transcripts are also observed in streams of cells beneath the ectoderm at stage 26 and, in addition, are found within muscle condensations from stage 28 (Fig. 5.7) suggesting that *Serrate 2* may mark migrating undifferentiated myoblasts early in development but then mark differentiating muscle, including myotubes (Fig. 5.7). Thus, *Notch-Serrate-Delta* interaction may provide a regulatory mechanism controlling the production of muscle.

Notch 1 has been shown to inhibit the differentiation of muscle cell types (Lindsell et al., 1995). *Notch 1* expression overlaps with that of *Delta 1* and *Serrate 2* in central mesenchyme between stages 24 and 27. Thus, myoblasts expressing *Delta 1* (and *Serrate 2*) in central mesenchyme either also express *Notch 1* preventing muscle differentiation or signal to adjacent *Notch 1* expressing cells preventing muscle differentiation. In contrast, in proximal regions where *Notch 1* is not expressed, muscle differentiation can occur. Thus, like in neurogenesis, populations of potential myoblasts are inhibited from differentiating too early, thus patterning the musculature throughout the limb and allowing proximal muscle to form before distal muscle. Myogenesis provides another example of a specific interaction between *Notch 1* and *Serrate 2* which has already been suggested for apical ridge positioning (Laufer et al., 1997; Rodriguez-Esteban et al., 1997).

CHAPTER SIX

Conclusions

I have produced a detailed fate map for mesenchyme of the developing chick limb and, for the first time, for the apical ectodermal ridge. I have shown that there is an anterior shift of subapical mid-limb mesenchyme into the anterior tip of the limb but that posterior subapical mesenchyme populations do not shift anteriorly, but instead form wide streams of label along the posterior margin. Strikingly, an anterior shift of cell populations also occurs in the apical ridge. Apical ridge and mesenchyme do not remain in concert; the apical ridge expands more anteriorly than the mesenchyme. Moreover, cell populations in the anterior apical ridge at stage 20 'fall out' of the ridge and become incorporated into anterior non-ridge ectoderm, as development proceeds. Furthermore, these results do not appear consistent with theories of limb evolution (see Shubin and Alberch, 1986), which suggest that mesenchyme at the posterior margin should expand across the antero-posterior axis of the handplate and contribute to each of the digits and should therefore be linearly related.

I have used the fate maps to relate cell lineage and behaviour with patterns of gene expression. I looked at the distribution of a signalling molecule, FGF-4, in the apical ridge and have shown that the change in distribution of *Fgf-4* transcripts as development proceeds is due to the expansion of cell populations. The comparison of cell lineage with gene expression pattern could also be applied to other signalling regions in the limb bud, for example, the polarising region.

I have also looked at expression domains of two genes, *Hoxa-13* and *Hoxd-13,* implicated in hand plate formation. Limbs of mice mutant for both these genes have no hand plates. *Hoxa-13* and *Hoxd-13* expression is resticted to early postero-distal mesenchyme in early buds but later extends across the hand plate. I show that the change in expression pattern of *Hoxd-13* as development proceeds is related to cell lineage. In contrast the change in expression pattern of *Hoxa-13* involves the recruitment of previously non-expressing cells. This suggests that the dynamic expression patterns of *HoxD* and *HoxA* genes are elaborated by different mechanisms, and this may be important to maintain specific *Hox* codes in different regions of the limb bud.

It is important to understand how overlapping patterns of *HoxA* gene expression are established in order to gain insights into how *HoxA* genes may govern digit development. I have shown that *Hoxa-13* activation occurs 8-12 hours after that of *Hoxd-13*. Moreover *Hoxa-13* expression is apical ridge dependent. What causes the difference in timing of activation is not clear as *Hoxa-13* expression cannot be activated prematurely. Following activation of *Hoxd-13* and *Hoxa-13* the difference in elaboration of the expression domains could be due to different enhancers within the *Hox* complexes and/or different responses to combinations of mesenchymal and/or ridge signals.

I examined the cellular basis for pattern changes in manipulated limbs. I have investigated which cells have changed fate to compensate for loss of tissue and which cells were respecified by polarising region signals to form duplicated structures. In both cases, only cells in the progress zone can respond. The progress zone can be re-established in proximal cells. This can happen by amputation of the distal tip and the application of an FGF-4 bead and, also after large pieces of mesenchyme are removed, when the apical ridge contracts onto the proximal base of the bud. I have shown that proximal cells can give rise to distal structures. Moreover following application of polarising region signals, I showed that anterior subapical cell populations can give rise to posterior structures. Furthermore duplicated digits are initially specified as anterior but with prolonged exposure to the signal are respecified to a posterior fate. Duplicated digits which arise in response to polarising region signals, originate from a small area of subapical mesenchyme, as is the case in normal fate maps, suggesting signals controlling digital development act over a short distance.

Taken together these results highlight the general rules that proximal tissue can produce distal structures, but distal tissue can not produce proximal structures. Moreover anterior cell populations can produce posterior structures but not vice-versa. This could be connected with *Hox* gene functioning and activation. Thus, for example, a 5' (posterior) located gene is dominant over its 3' neighbour. Thus, proximal cells can produce distal structures by expressing the more 5' gene but distal structures, expressing a 5' *Hox* gene, cannot change to a proximal *Hox* code as *Hox* gene activation is irreversible. The developing limb may have this regulatory potential in order to monitor and control the correct growth of the limb, making up for a lack of cells in a region and/or may prevent misexpression or overexpression of a gene.

I investigated the patterns of expression of genes in the *Notch* signalling pathway. This pathway was first identified in *Drosophila* and shown to have an essential role in *Drosophila* wing development. I have shown that the *Notch* signalling

pathway may have several functions during vertebrate limb development. The pathway is implicated in limb outgrowth, vascularisation, muscle development and also in digit spacing. Interestingly, digit positioning seems to occur at boundaries of *Notch 1* and *Serrate 1* expression. This mechanism of signalling at boundaries of gene expression is used throughout *Drosophila* development. It remains to be seen if other vertebrate limb patterning events involving the *Notch* pathway, also utilise boundaries. It is unclear presently whether every cell in the overlapping expression domains of *Notch*, *Serrate* and *Delta* in developing vasculature and musculature are expressing all the genes. It is possible that single cells within these domains express individual genes and thus signal to adjacent cells controlling patterning and development.

Recent work has shown that understanding the regulation and function of the genes examined in this thesis, has clinical implications. For example, mutations in *Hoxd-13* and *Hoxa-13* are the basis of severe digit defects in mice and humans. Mutations in *Hoxd-13* cause synpolydactyly in mice and humans (Zakany and Duboule, 1996; Muragaki et al., 1996) and mutations in *Hoxa-13* cause hypodactyly in mice (Mortlock et al., 1996) and hand-foot-genital syndrome in humans (Mortlock and Innis, 1997). It has been recently suggested that *Serrate* may be implicated in Human Holt-Oram syndrome which causes defects in the heart and hand (Banfi et al., 1996). However *Tbx-5*, a member of the *Brachyury* family is also associated with the syndrome (Li et al.,1997; Basson et al., 1997). Patients with Holt-Oram syndrome can exhibit a wide range of defects from malformations of the carpal bones to phocomelia suggesting the possibility of a family of diseases caused by mutations in several signalling pathways. Furthermore as mutations in *Hox* genes and in the *Notch* pathway may both lead to digital defects this is suggestive of a potential link between *Notch* and the *Hox* genes.

Notch is also implicated in human mammary cancer (Uyttendaele et al., 1996), neoplastic lesions of the human cervix (Zagouras et al., 1995) as well as in dementia and stroke (Joutel et al., 1996) suggesting the *Notch* pathway appears to be involved in growth and differentiation control and also has extremely diverse functions throughout development and adult life. This further underlines the importance of using *Drosophila* to identify important vertebrate genes.

REFERENCES

Akasaka, T., Kanno, M., Balling, R., Mieza, M. A., Taniguchi, M. and Koseki, H. (1996). A role for *mel-18*, a Polycomb group-related vertebrate gene, during the antero-posterior specification of axial skeleton. *Development* **122**, 1513-1522.

Akita, K. (1996). The effect of the ectoderm on the dorsoventral pattern of epidermis, muscles and joints in the developing chick leg: a new model. *Anat. Embryol.* **193**, 377-386.

Altabef, M., Clarke, J. D. W. and Tickle, C. (1997). Dorso-ventral ectodermal compartments and origin of apical ectodermal ridge in developing chick limb.*Development* **124**, 4547-4556.

Anderson, R., Landry, M. and Muneoka, K. (1993). Maintenance of ZPA signalling in cultured mouse limb bud cells. *Development* **117**, 1421-1433.

Anderson, R., Landry, M., Reginelli, A., Taylor, G., Achkar, C., Gudas, L. and Muneoka, K. (1994). Conversion of anterior limb bud cells to ZPA signalling cells *in vitro* and *in vivo*. *Dev. Biol.* **164**, 241-257.

Artavanis-Tsakonas, S., Matsuno, K. and Fortini, M. E. (1995). Notch signalling. *Science* **268**, 225-232.

Banfi, S., Borsani, G., Rossi, E., Bernard, L., Guffanti, A., Rubboli, F., Marchitiello, A., Giglio, S., Coluccia, E., Zollo, M., Zuffardi, O. and Ballbio, A. (1996). Identification and mapping of human cDNAs homologous to *Drosophila* mutant genes through EST database searching. *Nature Genetics* **13**, 167-174.

Barasa, A. (1964). On the regulative capacity of the chick embryo limb bud. *Experentia* **20**, 444.

Basson, C., Bachinsky, D., Lin, R., Levi, T., Elkins, J., Soults, J., Grayzel, D., Kroumpouzou, E., Traill, T., Leblanc-Straceski, J., Renault, B., Kucherlapti, R., Seidman, J. and Seidman, C. (1997). Mutations in human TBX-5 cause limb and cardiac malformation in Holt-Oram syndrome. *Nature Genetics* **15**, 30-35.

Bettenhausen, B., Hrabe de Angelis, M., Simon, D., Guenet, J-L. and Gossler, A. (1995). Transient and restricted expression during mouse embryogenesis of *Dll1*, a murine gene closely related to *Drosophila Delta*. *Development* **121**, 2407-2418.

Bitgood, M. J. and McMahon, A. P. (1995). *Hedgehog* and *Bmp* genes are co-expressed at many diverse sites of cell-cell interaction in the mouse embryo. *Dev. Biol.* **172**, 126-138.

Blair, S. S. (1995). Compartments and appendage development in *Drosophila*. *BioEssays* **17**, 299-309.

Blair, S. S. (1997). Marginal fringe benefits. *Curr. Biol.* **7**, R686-R690.

Bowen, J., Hinchliffe, J. R., Horder, T. J. and Reeve, A. M. F. (1989). The fate map of the chick forelimb-bud and its bearing on hypothesised developmental control mechanisms. *Anat. Embryol.* **179**, 269-283.

Brockes J. P. (1997). Amphibian limb regeneration: rebuilding a complex structure.*Science* **276**, 81-87.

Brook, W. J., Diaz-Benjumea, F. J. and Cohen, S. M. (1996). Organizing spatial patterning limb development. *Annu. Rev. Cell Dev. Biol.* **12**, 161-180.

Bryant, S. V., French, V. and Bryant, P. J. (1981). Distal regeneration and symmetry. *Science* **212**, 993-1002.

Buxton, P. G., Kostakopoulou, K., Brickell, P., Thorogood, P. and Ferretti, P. (1997). Expression of the transcription factor *Slug* correlates with growth of limb bud and is regulated by FGF-4 and retinoic acid. *Int. J. Dev. Biol.* **41**, 559-568.

Carrington and Fallon, J. F. (1984). The stages of flank ectoderm capable of responding to ridge induction in the chick embryo. *J. Embryol. exp. Morph.* **84**, 19-34.

Chan, W. Y., Lee, K. K. H. and Tam, P. P. L. (1991). Regenerative capacity of forelimb buds after amputation in mouse embryos at the early organogenesis stage. *J. Exp. Zool.* **260**, 74-83.

Charite, J., de Graff, W., Shen, S. and Deschamps, J. (1994). Ectopic expression of *Hoxb-8* causes duplication of the ZPA in the forelimb and homeotic transformation of axial structures. *Cell* **78**, 589-601.

Chevallier, A., Kieny, M. and Mauger, A. (1977). Limb-somite relationship: origin of the limb musculature. *J. Embryol. exp. Morph.* **41**, 245-258.

Chevallier, A., Kieny, M. and Mauger, A. (1978). Limb somite relationship: effect of removal of somitic mesoderm on the wing musculature. *J. Embryol. exp. Morph.* **43**, 263-278.

Chiang, C., Litingtung, Y., Lee, E., Young, K. E., Cordoen, J. L., Westphal, H. and Beachy, P. A. (1996). Cyclopia and axial patterning defects in mice lacking Sonic hedgehog gene function. *Nature* **383**, 407-413.

Chitnis, A., Henrique, D., Lewis, J., Ish-Horowicz, D. and Kintner, C. (1995). Primary neurogenesis in Xenopus embryos regulated by a homologue of the *Drosophila* neurogenic gene *Delta*. *Nature* **375**, 761-766.

Christ, B., Jacob, H. J. and Jacob, M. (1977). Experimental analysis of the origin of the wing musculature in avian embryos. *Anat. Embryol.* **150**, 171-186.

Coates, M. I. (1991). New palaeontological contributions to limb ontogeny and phylogeny. In *Developmental Patterning of the Vertebrate Limb* (ed. J. R. Hinchliffe, J. M. Hurle and D. Summerbell), NATO ASI, Series A, **205**, 325-337. New York: Plenum.

Coates, M. I. (1995). Fish fins or tetrapod limbs - a simple twist of fate?. *Curr. Biol.* **5**, 844-848.

Cohn. M. J., Izpisua-Belmonte, J-C., Abud, H., Heath, J. K. and Tickle, C. (1995). Fibroblast growth factors induce additional limb development from the flank of chick embryos. *Cell* **80**, 739-746.

Conlon, R. A., Reaume, A. G. and Rossant, J. (1995). *Notch 1* is required for the coordinate segmentation of somites. *Development* **121**, 1533-1545.

Cooke, J. and Summerbell, D. (1980). Cell cycle and experimental pattern duplication in the chick wing during embryonic development. *Nature* **287**, 697-701.

Core, N., Bel, S., Gaunt, S. J., Lions-Aurrand, M., Pearce, J., Fisher, A. and Djabali, M. (1997). Altered cellular proliferation and mesoderm patterning in Polycomb-M33-deficient mice. *Development* **124**, 721-729.

Couso, J. P., Knust, E. and Martinez Arias, A. (1995). *Serrate* and *Wingless* cooperate to induce vestigial gene expression and wing formation in *Drosophila*. *Curr. Biol.* **5**, 1437-1448.

Crossley, P. H. and Martin, G. R. (1995). The mouse *Fgf-8* gene encodes a family of polypeptides and is expressed in regions that direct outgrowth and patterning in the developing embryo. *Development* **121**, 439-451.

Crossley, P. H., Minowada, G., MacArthur, C.A. and Martin, G. R. (1996). Roles for FGF-8 in the induction, initiation, and maintenance of chick limb development. *Cell* **84**, 127-136.

de Celis, J. F. and Garcia-Bellido, A. (1994). Roles of the *Notch* gene in Drosophila wing morphogenesis. *Mech. Dev.* **46**, 109-122.

de Celis, J. F., Garcia-Bellido, A. and Bray, S. (1996). Activation and function of *Notch* at the dorsal-ventral boundary of the wing imaginal disc. *Development* **122**, 359-369.

de Celis, J. F. (1997). Expression and function of *decapentaplegic* and *thick veins* during the differentiation of the veins in the *Drosophila* wing. *Development* **124**, 1007-1018.

de Celis, J. F. and Bray, S. (1997). Feedback mechanisms affecting *Notch* activation at the dorso-ventral boundary in *Drosophila* wing. *Development* **124**, 3241-3251.

de la Pompa, J. L., Wakeham, A., Correia, K. M., Samper, E., Brown, S., Aguilera, R. J., Nakano, T., Honjo, T., Mak, T. W., Rossant, J. and Conlon, R. A. (1997). Conservation of the *Notch* signalling pathway in mammalian neurogenesis. *Development* **124**, 1139-1148.

Davidson, D. (1995). The function and evolution of *Msx* genes: pointers and paradoxes. *Trends Genet.* **11**, 405-411.

Davidson, D. R., Crawley, A., Hill, R. E. and Tickle, C. (1991). Position dependent expression of two related homeobox genes in developing vertebrate limbs.*Nature* **352**, 429-431.

Davis, A. P. and Capecchi, M. (1994). Axial homeosis and appendicular skeleton defects in mice with a targeted disruption of *Hoxd-11. Development* **120**, 2187-2198.

Davis, A. P., Witte, D. P., Hsieh- Li, H. M., Potter, S. S. and Capecchi, M. R. (1995). Absence of radius and ulna in mice lacking *Hoxa-11* and *Hoxd-11. Nature* **375**, 791-795.

Dealy, C. N., Roth, A., Ferrari, D., Brown, A. M. and Kosher, R. A. (1993). *Wnt-5a* and *Wnt-7a* are expressed in the developing chick limb bud in a manner suggesting roles in pattern formation along the proximo-distal and dorso-ventral axes. *Mech. Dev.* **43**, 175-186.

Deng, C., Bedford, M., Li, C., Xu, X., Yang, X., Dunmore, J. and Leder, P. (1997). Fibroblast growth factor receptor-1 (FGFR-1) is essential for normal neural tube and limb development. *Dev. Biol.* **185**, 42-54.

Doherty, D., Feger, G., Younger-Shepard, S., Jan, L. Y. and Jan, Y. N. (1996). *Delta* is a ventral to dorsal signal complementary to *Serrate*, another *Notch* ligand, in *Drosophila* wing formation. *Genes Dev.* **10**, 421-434.

Dolle, P., Izpisua-Belmonte, J-C., Falkenstein, H., Renucci, A. and Duboule, D. (1989). Coordinate expression of the murine Hox-5 complex homoeobox containing genes during limb pattern formation. *Nature* **342**, 767-772.

Duboule, D. (1992). The vertebrate limb: A model system to study the *Hox*/HOM gene network during development and evolution. *BioEssays* **14**, 375-384.

Duboule, D. (1994). Temporal colinearity and the phylotypic progression: a basis for the stability of a vertebrate Bauplan and the evolution of morphologies through heterochrony. *Development* **Supplement**, 135-142.

Duboule, D. (1995). Vertebrate *Hox* genes and proliferation: an alternative pathway to homeosis?. *Curr. Op. Gen. & Dev.* **5**, 525-528.

Duboule, D. and Morata, G. (1994). Colinearity and functional hierarchy among genes of the homeotic complexes. *Trends Genet.* **10**, 358-364.

Dunwoodie, S. L., Henrique, D., Harrison, S. M. and Beddington, R. S. P. (1997). Mouse *Dll3*: a novel divergent *Delta* gene which may complement the function of other *Delta* homologues during early pattern formation in the mouse embryo. *Development* **124**, 3065-3074.

Duprez, D. M., de H. Bell, E. J., Richardson, M. K., Archer, C. W., Wolpert, L., Brickell, P. M. and Francis-West, P. H. (1996a). Overexpression of BMP-2 and BMP-4 alters the size and shape of developing skeletal elements in the chick limb. *Mech. Dev.* **57**, 145-157.

Duprez, D. M., Kostakopoulou, K., Francis-West, P. H., Tickle, C. and Brickell, P. (1996b). Activation of *Fgf-4* and *HoxD* gene expression by BMP-2 expressing cells in the developing chick limb. *Development* **122**, 1821-1828.

Echelard, Y., Epstein, D. J., St-Jacques, B., Shen, L., Mohler, J., McMahon, J. A. and McMahon, A. P. (1993). Sonic hedgehog, a member of a family of putative signaling molecules, is implicated in the regulation of CNS polarity. *Cell* **75**, 1417-1430.

Fallon, J. F., Lopez, A., Ros, M. A., Savage, M. P., Olwin, B. B. and Simandl, B. K. (1994). FGF-2: Apical ectodermal ridge growth signal for chick limb development. *Science* **264**, 104-107.

Feinberg, R. N. and Noden, D. M. (1991). Experimental analysis of blood vessel development in the avian wing bud. *Anat. Rec.* **231**, 136-144.

Feinberg, R. N. and Saunders, J. W. Jr. (1982). Effects of excising the apical ectodermal ridge on the development of the marginal vasculature of the wing bud in the chick embryo. *J. Exp. Zool.* **219**, 345-354.

Fleming, R. J., Gu, Y. and Hukriede, N. A. (1997). *Serrate* mediated activation of *Notch* is specifically blocked by the product of the gene *Fringe* in the dorsal compartment of *Drosophila* wing imaginal disc. *Development* **124**, 2973-2981.

Fleming, R. J., Scottgale, T. N., Diederich, R. J. and Artavanis-Tsakonas, S. (1990). The gene *Serrate* encodes a putative EGF-like transmembrane protein essential for proper ectodermal development in *Drosophila melanogaster.Genes Dev.* **4**, 2188-2201.

Francis, P. H., Richardson, M. K., Brickell, P. M. and Tickle, C. (1994). Bone morphogenetic proteins and a signalling pathway that controls patterning in the developing chick limb. *Development* **120**, 209-218.

French, V., Bryant, P. J. and Bryant, S. V. (1976). Pattern regulation in epimorphic fields. *Science* **193**, 969-81

Fromental-Ramain, C., Warot, X., Messadecq, N., LeMeur, M., Dolle, P. and Chambon, P. (1996). *Hoxa-13* and *Hoxd-13* play a crucial role in the patterning of the limb autopod. *Development* **122**, 2997-3011.

Gaunt, S. J. and Singh, P. B. (1990). Homeogene expression patterns and chromosonal imprinting. *Trends Genet.* **6**, 208-212.

Geduspan, J. S. and MacCabe, J. A. (1987). The ectodermal control of mesodermal patterns of differentiation in the developing chick wing. *Dev. Biol.* **124**, 398-408.

Geduspan, J. S. and MacCabe, J. A. (1989). Transfer of dorso-ventral information from mesoderm to ectoderm at onset of limb development. *Anat. Rec.* **224**, 79-87.

Gerard, M., Chen, J-Y., Gronemeyer, H., Chambon, P., Duboule, D. and Zakany, J. (1996). In vivo targeted mutagenesis of a regulatory element required for positioning the *Hoxd-11* and *Hoxd-10* expression boundary. *Genes Dev.* **10**, 2326-2334.

Grieshammer, U., Minowada, G., Pisenti, J. M., Abbott, U. K. and Martin, G. (1996). The chick *limbless* mutation causes abnormalities in limb bud dorsal-ventral patterning: implications for the mechanism of apical ridge formation. *Development* **122**, 3851-3861.

Goff, D. J. and Tabin, C. (1997). Analysis of *Hoxd-13* and *Hoxd-11* misexpression in chick limb buds reveals that *Hox* genes affect both bone condensation and growth. *Development* **124**, 627-636.

Gould, A. (1997). Functions of mammalian Polycomb and trithorax group relayted genes. *Curr. Opin. Gen. Dev.* **7**, 488-494.

Haack, H. and Gruss, P. (1993). Establishment of murine Hox-1 expression domains during patterning of the limb. *Dev. Biol.* **157**, 410-422.

Hamburger, V. and Hamilton, H. L. (1951). A series of normal stages in the development of the chick embryo. *J. Exp. Morphol.* **88**, 49-92.

Hammerschmidt, M., Brook, A. and McMahon, A. P. (1997). The world according to *hedgehog*. *Trends Genet.* **13**, 14-21.

Hayamizu, T., Wanek, N., Taylor, G., Trevino, C., Shi, C., Anderson, R., Gardiner, D. M., Muneoka, K. and Bryant, S. V. (1994). Regeneration of *HoxD* expression domains during pattern regulation in chick wing buds. *Dev. Biol.* **161**, 504-512.

Hayashi, H., Mochii, M., Kodama, R., Hamada, Y., Mizuno, N., Eguchi, G. and Tachi, C. (1996). Isolation of a novel chick homolog of *Serrate* and co-expression with *C-Notch* in chick development. *Int. J. Dev. Biol.* **40**, 1089-1096.

Heikinheimo, M., Lawshe, A., Shackleford, G. M., Wilson, D. B. and MacArthur, C. A. (1994). *Fgf-8* expression in the post-gastrulation mouse suggests roles in the development of the face, limbs and central nervous system. *Mech. Dev.* **48**, 129-138.

Henrique, D., Adam, J., Myat, A., Chitnis, A., Lewis, J. and Ish-Horowicz, D. (1995). Expression of a *Delta* homologue in prospective neurons in the chick. *Nature* **375**, 787-790.

Herault, Y., Fraudeau, N., Zakany, J. and Duboule, D. (1997). *Ulnaless* (*Ul*). A regulatory mutation inducing both loss-of-function and gain-of-function of posterior *Hoxd* genes. *Development* **124**, 3493-3500.

Helms, J. A., Kim, C. H., Eichele, G. and Thaller, C. (1996). Retinoic acid signalling is required during early chick limb development. *Development* **122**, 1385-1394.

Hogan, B. L. M. (1996). Bone morphogenetic proteins:multifunctional regulators of vertebrate development. *Genes Dev.* **10**, 1580-1594.

Honig, L. S. (1982). Effects of ultraviolet light on the activity of an avian limn positional signalling region. *J. Embryol. exp. Morph.* **71**, 223-232.

Honig, L. S. and Summerbell, D. (1985). Maps of strength of positional signalling activity in the developing chick wing. *J. Embryol. exp. Morph.* **87**, 163-174.

Honig, M. G. and Hume, R. I. (1986). Fluorescent carbocyanine dyes allow living neurons of identified origin to be studied in long-term cultures. *J. Cell Biol.* **103**, 171-187.

Honig, M. G. and Hume, R. I. (1989). DiI and DiO: versatile fluorescent dyes for neuronal labelling and pathway tracing. *Trends Neurosci.* **12** (9), 333-341.

Hornbruch, A. (1980). Abnormalities along the proximo-distal axis of the chick wing bud: The effect of surgical intervention. In *'Teratology of the limbs'* 191-197 (ed. H. J. Merker, H. Nou, D. Newbert) Walter de Gruyter and Co., Berlin.

Hornbruch, A. and Wolpert, L. (1970). Cell division in the early growth and morphogenesis of the chick limb bud. *Nature* **226**, 764-766.

Hornbruch, A. and Wolpert, L. (1986). Positional signalling by Hensons node, when grafted to the chick limb bud. *J. Embryol. exp. Morph.* **94**, 257-265.

Hornbruch, A. and Wolpert, L. (1991). The spatial and temporal distribution of polarizing activity in the flank of the pre-limb bud stages in the chick embryo. *Development* **111**, 725-731.

Hrabe de Angelis, M., McIntyre, J. and Gossler, A., (1997). Maintenance of somite borders in mice requires the *Delta* homologue *Dll1*. *Nature* **386**, 717-721.

Hui, C. C. and Joyner, A. L. (1993). A mouse model of greig cephalopolysyndactyly syndrome: the *extra toes* mutation contains an intragenic deletion of the *Gli-3* genes. *Nature Genet.* **3**, 241-246.

Huppert, S. S., Jacobsen, T. L. and Muskavitch, M. A. T. (1997). Feedback regulation is central to *Delta-Notch* signalling required for Drosophila wing vein morphogenesis. *Development* **124**, 3282-3291.

Irvine, K. D. and Vogt, T. F. (1997). Dorsal-ventral signalling in limb development. *Curr. Op. Cell Biol.* **9**, 867-876.

Irvine, K. D. and Wieschaus, E. (1994). *Fringe*, a boundary specific signalling molecule, mediates interactions between dorsal and ventral cells during *Drosophila* wing development. *Cell* **79**, 595-606.

Izpisua-Belmonte, J-C., Brown, J. M., Crawley, A., Duboule, D. and Tickle, C. (1992a). *Hox-4* gene expression in mouse/chicken heterospecific grafts of signalling regions to limb buds reveals similarities in patterning mechanisms. *Development* **115**, 553-560.

Izpisua-Belmonte, J-C., Brown, J. M., Duboule, D. and Tickle, C. (1992b). Expression of *Hox-4* genes in the chick wing links pattern formation to the epithelial-mesenchymal interactions that mediate growth. *EMBO J.* **11**, 1451-1457.

Izpisua-Belmonte, J-C., Tickle, C., Dolle, P., Wolpert, L. and Duboule, D. (1991). Expression of the homeobox *Hox-4* genes and the specification of position in chick wing development. *Nature* **350**, 585-589.

Jacob, M., Christ, B. and Jacob, H. J. (1978). On the migration of myogenic stem cells into the prospective wing region of chick embryos. *Anat. Embryol.* **153**, 179-193.

Janners, M. Y. and Searls, R. L. (1970). Changes in the rate of cellular proliferation during the differentiation of cartilage and muscle in the mesenchyme of the embryonic chick wing. *Dev. Biol.* **23**, 136-165.

Johnson, R. L. and Tabin, C. J. (1997). Molecular models for vertebrate limb development. *Cell* **90**, 979-990.

Joutel, A., Corpechot, C., Ducros, A., Vahedi, K., Chabriat, H., Mouton, P., Alamowitch, S., Domenga, V., Cecillion, M., Marechal, E., Maciazek, J., Vayssiere, C., Cruaud, C., Cabanis, E-A., Ruchoux, M., Weissenbach, J., Bach, J., Bousser, M. and Tournier-Lasserve, E. (1996). *Notch 3* mutations in CADASIL, a hereditary adult-onset condition causing stroke and dementia. *Nature* **383**, 707-710.

Kim, J., Irvine, K. D. and Carroll, S. B. (1995). Cell recognition, signal induction and symmetrical gene activation at the dorsal-ventral boundary of the developing *Drosophila* wing. *Cell* **82**, 795-802.

Kim, J., Sebring, A., Esch, J. J., Kraus, M. E., Vorwerk, K., Magee, J. and Carroll, S. (1996). Integration of positional signals and regulation of wing formation and identity by Drosophila *vestigial* gene. *Nature* **382**, 133-138.

Knezevic, V., De Santo, R., Schugart, K., Huffstadt, U., Chiang, C., Mahon, K. A. and Mackem, S. (1997). *Hoxd-12* differentially affects preaxial and postaxial chondrogenic branches in the limb and regulates *Sonic hedgehog* in a positive feedback loop. *Development* **124**, 4523-4536.

Kostakopoulou, K., Vogel, A., Brickell, P. and Tickle, C. (1996). 'Regeneration' of wing bud stumps of chick embryos and reactivation of *Msx-1* and *Shh* expression in response to FGF-4 and ridge signals. *Mech. Dev.* **55**, 119-131.

Kostakopoulou, K., Vargesson, N., Clarke, J. D. W., Brickell, P. M. and Tickle, C. (1997). Local origin of cells in FGF-4 induced outgrowth of amputated chick wing bud stumps. *Int. J. Dev. Biol.* **41**, 747-750.

Krumlauf, R. (1994). *Hox* genes in vertebrate development. *Cell* **78**, 191-201.

Laufer, E., Nelson, C. E., Johnson, R. L., Morgan, B. A. and Tabin, C. (1994). *Sonic hedgehog* and *Fgf-4* act through a signaling cascade and a feedback loop to integrate growth and patterning of the developing limb bud. *Cell* **79**, 993-1003.

Laufer, E., Dahn, R., Orozco, O. E., Yeo, C. Y., Pisenti, J., Henrique, D., Abbot, U. K., Fallon, J. F. and Tabin, C. (1997). Expression of *Radical fringe* in limb bud ectoderm regulates apical ectodermal ridge formation. *Nature* **386**, 366-373.

Lee, J. and Tickle, C. (1985). Retinoic acid and pattern formation in the developing chick wing: SEM and quantitative studies of early effects on the apical ectodermal ridge and bud outgrowth. *J. Embryol. exp. Morph.* **90**, 139-169.

Lewis, J. (1996). Neurogenic genes and vertebrate neurogenesis. *Curr. Opin. Neurobiol.* **6**, 3-10.

Lewis, J. H. (1975). Fatemaps and the pattern of cell division. *J. Embryol. exp. Morph.* **33**, 419-434.

Li, Q., Newbury-Ecob, R., Terrett, J., Wilson, D., Curtis, A., Yi, C., Gebuhr, T., Bullen, P., Robson, S., Strachan, T., Bonnet, D., Lyonnet, S., Young, I., Raeburn, J. A., Buckler, A., Law, D. and Brook, J. D. (1997). Holt-Oram syndrome is caused by mutations in TBX-5, a member of the *Brachyury* (T) gene family. *Nature Genetics* **15**, 21-29.

Li, S., Anderson, R., Reginelli, A. and Muneoka, K. (1996). FGF-2 influences cell movements and gene expression during limb development. *J. Exp. Zool.* **274**, 234-247.

Lindsell, C. E., Shawber, C. J., Boulter, J. and Weinmaster, G. (1995). Jagged: A mammalian ligand that activates Notch 1. *Cell* **80**, 909-917.

Logan, C. C., Hornbruch, A., Campbell, I. And Lumsden, A. (1997). The role of *Engrailed* in establishing the dorso-ventral axis in chick limb. *Development* **124**, 2317-2324.

Lohnes, D., Mark, M., Mendelsohn, C., Dolle, P., Dierich, A., Gorry, P., Gansmuller, A. and Chambon, P. (1994). Function of the retinoic acid receptors (RARs) during development. (I) Craniofacial and skeletal abnormalities in RAR double mutants. *Development* **120**, 2723-2748.

Loomis, C. A., Harris, E., Michaud, J., Wurst, W., Hanks, M. and Joyner, W. L. (1996). The mouse *Engrailed-1* gene and ventral limb patterning. *Nature* **382**, 360-363.

Lopez-Martinez, A., Chang, D. T., Chiang, C., Porter, J. A., Ros, M. A., Simandl, B. K., Beachy, P. A. and Fallon, J. F. (1995). Limb patterning activity and restricted posterior localization of the amino-terminal product of Sonic hedgehog cleavage. *Curr. Biol.* **5**, 791-796.

Lu, H-C., Revelli, J. P., Goering, L., Thaller, C. and Eichele, G. (1997). Retinoid signalling is required for the establishment of a ZPA and for expression of *Hoxb-8*, a mediator of ZPA formation. *Development* **124**, 1643-1651.

MacCabe, J. A. and Parker, B. W. (1975). The in vitro maintenance of the apical ectodermal ridge of the chick embryo wing bud: an assay for polarizing activity. *Dev. Biol.* **45**, 349-57

MacCabe, J. A., Errick, J. and Saunders, J. W. Jr. (1974). Ectodermal control of the dorsoventral axis in the leg bud of the chick embryo. *Dev. Biol.* **39**, 69-82.

Mahmood, R., Bresnick, J., Hornbruch, A., Mahony, C., Morton, N., Colquhoun, K., Martin, P., Lumsden, A., Dickson, C. and Mason, I. (1995). A role for FGF-8 in the initiation and maintenance of vertebrate limb bud outgrowth. *Curr. Biol.* **5**, 797-806.

Marigo, V., Johnson, R. L., Vortkamp, A. and Tabin, C. J. (1996). Sonic hedgehog differentially regulates expression of *GLI* and *GLI3* during limb development. *Dev. Biol.* **180**, 273-283.

Masuya, H., Sagai, T., Moriwaki, K. and Shiroishi, T. (1997). Multigenic control of the localization of the zone of polarising activity in limb morphogenesis in the mouse. *Dev. Biol.* **182**, 42-51.

Masuya, H., Sagai, T., Wakana, S., Moriwaki, H. and Shiroishi, T. (1995). A duplicated zone of polarising activity in polydactylous mouse mutants. *Genes Dev.* **9**, 1645-1653.

Mendelsohn, C., Ruberte, E. and Chambon, P. (1992). Retinoid receptors in vertebrate limb development. *Dev. Biol.* **152**, 50-61.

Meyer, A. (1998). *Hox* gene variation and evolution. *Nature* **391**, 225-228.

Micchelli, C. A., Rulifson, E. J. and Blair, S. S. (1997). The function and regulation of *Cut* expression on the wing margin of Drosophila: *Notch*, *Wingless* and a dominant negative role for *Delta* and *Serrate*. *Development* **124**, 1485-1495.

Michaud, W. L., Lapointe , F. and Le Douarin, N. M. (1997). The dorso-ventral polarity of the presumptive limb is determined by signals produced by the somites and by the lateral somatopleure. *Development* **124**, 1453-1463.

Mitsiadis , T. A., Henrique, D., Thesleff, I. And Lendahl, U. (1997). Mouse *Serrate-1* (*Jagged-1*): expression in the developing tooth is regulated by epithelial-mesenchymal interactions and Fibroblast growth factor-4. *Development* **124**, 1473-1483.

Morgan, B. A. and Tabin, C. (1994). *Hox* genes and growth: early and late roles in limb bud morphogenesis. *Development* **Suppl**, 181-186.

Mortlock, D. P. and Innis, J. W. (1997). Mutation of *HOXA13* in hand-foot-genital syndrome. *Nature Genetics* **15**, 179-180.

Mortlock, D. P., Post, L. C. and Innis, J. W. (1996). The molecular basis of hypodactyly (*Hd*): a deletion in *Hoxa13* leads to arrest of digital arch formation. *Nature Genetics* **13**, 284-289.

Muneoka, K. and Sassoon, D. (1992). Molecular aspects of regeneration in developing vertebrate limbs. *Dev. Biol.* **152**, 37-49.

Muneoka, K., Wanek, N. and Bryant, S. (1989). Mammalian limb bud development: In situ fate maps of early hindlimb buds. *J. Exp. Zool.* **249**, 50-54.

Muragaki, Y., Mundlos, S., Upton, J. Olsen, B. R. (1996). Altered growth and branching patterns in synpolydactyly caused by mutations in *HOXD13*. *Science* **272**, 548-551.

Muskavitch, M. A. T. (1994). Delta-Notch signalling and *Drosophila* cell fate choice. *Dev. Biol.* **166**, 415-430.

Myat, A., Henrique, D., Ish-Horowicz, D. and Lewis, J. (1996). A chick homologue of *Serrate* and its relationship with *Notch* and *Delta* homologues during central neurogenesis. *Dev. Biol.* **174**, 233-247.

Nelson, C. E., Morgan, B. A., Burke, A. C., Laufer, E., DiMambro, E., Murtaugh, L. C., Gonzales, E., Tessarollo, L., Parada, L. F. and Tabin, C. (1996). Analysis of *Hox* gene expression in the chick limb bud. *Development* **122**, 1449-1466.

Nieto, M. A., Patel, K. and Wilkinson, D. G. (1996). *In situ* hybridization analysis of chick embryos in whole mount and tissue sections in *Methods in Cell Biology*, **51**, 219-235. Academic Press.

Nikbakht, N. and McLachlan, J. C. (1997). A proximo-distal gradient of FGF like activity in the embryonic chick limb bud. *Cell. Mol. Life Sci.* **53**, 447-451.

Niswander, L. and Martin, G. R. (1992). *Fgf-4* expression during gastrulation, myogenesis, limb and tooth development in mouse. *Development* **114**, 755-768.

Niswander, L., Tickle, C., Vogel, A., Booth, I. and Martin, G. R. (1993). FGF-4 replaces the apical ectodermal ridge and directs outgrowth and patterning of the limb. *Cell* **75**, 579-587.

Niswander, L., Jeffrey, S., Martin, G. R. and Tickle, C. (1994). A positive feedback loop coordinates growth and patterning in the vertebrate limb.*Nature***371**, 609-612.

Nohno, T., Noji, S., Koyama, E., Ohyama, K., Myokai, F. et al. (1991). Involvement of the *Chox-4* chicken homeobox genes in determination of antero-posterior axial polarity during limb development. *Cell* **64**, 1197-1205.

Noji, S., Nohno, T., Koyama, E., Muto, K., Ohyana, K., Aoki, Y., Tamura, K., Ohsugi, K., Ide, H., Taniguchi, S. and Saito, T. (1991). Retinoic acid induces polarising activity but is unlikely to be a morphogen in the chick limb bud. *Nature* **350**, 83-86.

Noramly, S., Pisenti, J., Abbott, U. and Morgan, B. (1996). Gene expression in the limbless mutant: Polarized gene expression in the absence of *Shh* and an AER. *Dev. Biol. 179*, 339-346.

Nye, J. S. (1997). *Notch* signals *Kuz* it's cleaved. *Curr. Biol.* **7**, 716-720.

Ohuchi, H., Nakagawa, T., Yamamoto, A., Araga, A., Ohata, A., Ishimaru, Y., Yoshioka, H., Kuwama, T., Nohno, T., Yamasaki, M., Itoh, N. and Noji, S. (1997). The mesenchymal factor, FGF-10, initiates and maintains the outgrowth of the chick limb bud through interaction with FGF-8, an apical ectodermal factor. *Development* **124**, 2235-2244.

Pagan, S. M., Ros, M. A., Tabin, C. and Fallon, J. F. (1996). Surgical removal of limb bud *Sonic hedgehog* results in posterior skeletal defects. *Dev. Biol.* **180**, 35-40.

Panin, V. M., Papayannopoulos, V., Wilson, R. and Irvine, K. D. (1997). *Fringe* modulates Notch-ligand interactions. *Nature* **387**, 908-912.

Papageorgiou, S. and Almirantis, Y. (1996). Gradient model describes the spatial-temporal expression pattern of *HoxA* genes in the developing vertebrate limb. *Dev. Dynamics* **207**, 461-469.

Pardanaud, L., Yassine, F. and Dieterlen-Lievre, F. (1989). Relationship between vasculogenesis, angiogenesis and haemopoiesis during avian ontogeny. *Development* **105**, 473-485.

Paro, R. (1990). Imprinting a determined state into the chromatin of *Drosophila*. *Trends Genet.* **6**, 416-421.

Parr, B. A. and McMahon, A. P. (1995). Dorsalising signal *Wnt-7a* required for normal polarity of D-V and A-P axes of mouse limb. *Nature* **374**, 350-353.

Peichel, C. L., Prabhakaran, B. and Vogt, T. F. (1997). The mouse *Ulnaless* mutation deregulates posterior *HoxD* gene expression and alters appendicular patterning. *Development* **124**, 3481-3492.

Peters, K. G., Werner, S., Chen, G. and Williams, L. T. (1992). Two FGF receptor genes are differentially expressed in epithelial and mesenchymal tissues during limb formation and organogenesis in the mouse. *Development* **114**, 233-243.

Pirrotta, V. (1997). Chromatin-silencing mechanisms in *Drosophila* maintain patterns of gene expression. *Trends Genet.* **13**, 314-318.

Rebay, I., Fleming, R. J., Fehon, R. G., Cherbas, L., Cherbas, P. and Artavanis-Tsakonas, S. (1991). Specific EGF repeats of *Notch* mediate interactions with *Delta* and *Serrate*: Implications for *Notch* as a multifunctional receptor. *Cell* **67**, 687-699.

Reginelli, A. D., Wang, Y-Q., Sassoon, D. and Muneoka, K. (1995). Digit tip regeneration correlates with regions of *Msx-1* (*Hox-7*) expression in fetal and newborn mice. *Development* **121**, 1065-1076.

Riddle, R. D., Johnson, R. L., Laufer, E. and Tabin, C. (1993). *Sonic hedgehog* mediates the polarizing activity of the ZPA. *Cell* **75**, 1401-1416.

Riddle, R. D., Ensini, M., Nelson, C., Tsuchida, T., Jessell, T. M. and Tabin, C. (1995). Induction of the LIM homeobox gene *Lmx-1* by WNT7A establishes dorsoventral pattern in the vertebrate limb. *Cell* **83**, 631-640.

Risau, W. (1997). Mechanisms of angiogenesis. *Nature* **386**, 671-674.

Robert, B., Sassoon, D., Jacq, B., Gehring, W. and Buckingham, M. (1989). *Hox-7*, a mouse homeobox gene with a novel pattern of expression during mouse embryogenesis. *EMBO J.* **8**, 91-100.

Robey, E. (1997). Notch in vertebrates. *Curr. Biol.* **7**, 551-557.

Robson, L. G. and Hughes, S. M. (1996). The distal limb environment regulates MyoD accumulation and muscle differentiation in mouse-chick chimaeric limbs. *Development* **122**, 3899-3910.

Robson, L. G., Kara, T., Crawley, A. and Tickle, C. (1994). Tissue and cellular patterning of the musculature in chick wings. *Development* **120**, 1265-1276.

Rodriguez-Esteban , C., Schwabe, J. W., De La Pena, J., Foys, B., Eshelman, B. and Izpisua-Belmonte, J-C. (1997). Radical fringe positions the apical ectodermal ridge at the dorso-ventral boundary of the vertebrate limb. *Nature* **386**, 360-366.

Roelink, H. Porter, J., Chiang, C., Tanabe, Y., Chang, D. T., Beachy, P. A. and Jessell, T. M. (1995). Floor plate and motor neuron induction by different concnetrations of the amino-terminal cleavage product of Sonic hedgehog autoproteolysis. *Cell* **81**, 443-455.

Roelink, H., Tanabe, Y. and Jessell, T. M. (1996). Sonic hedgehog: a mediator of inductive signalling in the ventral neural tube. *Semin. Cell Dev. Biol.* **7**, 121-127.

Ros, M. A., Lopez-Martinez, A., Simandl, B. K., Rodriguez, C., Izpisua-Belmonte, J-C., Dahn, R. and Fallon, J. F. (1996). The limb field mesoderm determines initial limb bud anteroposterior asymmetry and budding independent of Sonic hedgehog or apical ectodermal gene expression. *Development* **122**, 2319-2330.

Ros, M. A., Sefton, M. and Nieto, M. A. (1997). *Slug*, a zinc finger gene previously implicated in the early patterning of the mesoderm and the neural crest, is also involved in chick limb development. *Development* **124**, 1821-1829.

Rowe, D. A. and Fallon, J. F. (1981). The effect of removing posterior apical ectodermal ridge of the chick wing and leg on pattern formation. *J. Embryol. exp. Morph.* **65** (supp), 309-325.

Rowe, D. A. and Fallon, J. F. (1982). The proximo-distal determination of skeletal parts in the developing chick leg. *J. Embryol. exp. Morph.* **68**, 1-7.

Ruddle, F. H., Bartels, J. L., Bentley, K. L., Kappen, C., Murtha, M. T. and Pendleton, J. W. (1994). Evolution of *Hox* genes. *Annu. Rev. Genet.* **28**, 423-442.

Ruji, F. M. and Chambon, P. (1997). Genetic interactions of *Hox* genes in limb development: learning from compound mutants. *Curr. Opin. Gen. Dev.* **7**, 481-487.

Saunders, J. W. Jr. (1948). The proximo-distal sequence of origin of the parts of the chick wing and the role of the ectoderm. *J. Exp. Zool.* **108**, 363-403.

Saunders, J. W. Jr. and Gasseling, M. T. (1963). Trans-filter propagation of apical ectoderm maintenance factor in the chick embryo wing. *Dev. Biol.* **7**, 64-78.

Saunders, J. W. Jr. and Gasseling, M. T. (1968). Ectodermal-mesenchymal interactions in the origin of limb symmetry. In *Epithelial-mesenchymal interactions* (ed. R. Fleischmaier and R. E. Billingham), 78-97. Williams and Wilkins, Baltimore.

Saunders, J. W. Jr., Gasseling, M. T. and Saunders, L. C. (1962). Cellular death in morphogenesis of the avian wing. *Dev. Biol.* **5**, 147-178

Saunders, J. W. Jr., Gasseling, M. T. and Errick, J. E. (1976). Inductive activity and enduring cellular constitution of a supernumerary apical ectodermal ridge grafted to the limb bud of the chick embryo. *Dev. Biol.* **50**, 16-25..

Saunders, J. W. Jr. and Reuss, C. R. (1974). Inductive and axial properties of prospective wing-bud mesoderm in the embryo. *Dev. Biol.* **38**, 41-50.

Savage, M. P., Hart, C. E., Riley, B. B., Sasse, J., Olwin, B. B. and Fallon, J. F. (1993). Distribution of FGF-2 suggests it has a role in chick limb bud growth. *Dev. Dynamics* **198**, 159-170.

Searls, R. L. and Janners, M. Y. (1971). The initiation of limb bud outgrowth in the embryonic chick. *Dev. Biol.* **24**, 198-213.

Shawber, C., Boulter, J., Lindsell, C. E. and Weinmaster, G. (1996). Jagged 2: a Serrate-like gene expressed during rat embryogenesis. *Dev. Biol.* **180**, 370-376.

Shellswell, G. B. and Wolpert, L. (1977). The pattern of muscle and tendon development in the chick wing. In: *Vertebrate limb and somite morphogenesis*. pp 71-86. (ed. D. A. Ede, J. R. Hinchliffe and M. Balls) Cambridge University Press.

Shubin, N. H. and Alberch, P. (1986). A morphogenetic approach to the origin and basic organisation of the tetrapod limb. *Evol. Biol.* **20**, 319-387.

Sidow, A., Bulotsky, M. S., kerrebrock, A. W., Bronson, R. T., Daly, M. J., Reeve, M. P., Hawkins, T. L., Bimen, B. W., Jaenisch, R. and Lander, E. S. (1997). *Serrate 2* is disrupted in the mouse limb development mutant syndactylism (sm). *Nature* **389**, 722-725.

Small, K. M. and Potter, S. S. (1993). Homeotic transformations and limb defects in *HoxA11* mutant mice. *Genes Dev.* **7**, 2318-2328.

Smith, J. C., Tickle, C. and Wolpert, L. (1978). Attenuation of positional signalling in the chick limb by high doses of radiation. *Nature* **272**, 612-613.

Song, K., Wang, Y. and Sassoon, D. (1992). Expression of *Hox-7.1* in myoblasts inhibits terminal differentiation and induces cell transformation. *Nature* **360**, 477-481.

Sordino, P., van der Hoeven, F. and Duboule, D. (1995). *Hox* gene expression in teleost fins and the origin of vertebrate digits. *Nature* **375**, 678-681.

Speicher, S. A., Thomas, U., Hinz, U. and Knust, E. (1994). The *Serrate* locus of *Drosophila* and its role in morphogenesis of the wing imaginal discs: control of cell proliferation. *Development* **120**, 535-544.

Stark, R. J. and Searls, R. L. (1973). A description of chick wing bud development and a model of limb morphogenesis. *Dev. Biol.* **33**, 138-153.

Stark, R. J. and Searls, R. L. (1974). The establishment of the cartilage pattern in the embryonic chick wing and evidence for a role of the dorsal and ventral ectoderm in normal wing development. *Dev. Biol.* **38**, 51-63.

Stratford, T., Horton, C. and Maden, M. (1996). Retinoic acid is required for the initiation of outgrowth in the chick limb bud. *Curr. Biol.* **6**, 1124-1133.

Stratford, T., Kostakopoulou, K. and Maden, M. (1997). *Hoxb-8* has a role in establishing early antero-posterior polarity in chick forelimb but not hindlimb. *Development* **124**, 4225-4234.

Summerbell, D. (1974). A quantitative analysis of the effect of excision of the AER from the chick limb bud. *J. Embryol. exp. Morph.* **32** (3), 651-660.

Summerbell, D. (1976). A descriptive study of the rate of elongation and differentiation of the skeleton and developing chick wing. *J. Embryol. exp. Morph.* **35**, 241-260.

Summerbell, D. (1977). Regulation of deficiencies along the proximal distal axis of the chick wing bud: a quantitative analysis. *J. Embryol. exp. Morph.* **41**, 137-159.

Summerbell, D. and Lewis, J (1975). Time, place and positional value in the chick limb-bud. *J. Embryol. Exp. Morphol.* **33**, 621-43.

Summerbell, D. and Wolpert, L. (1972). Cell density and cell division in the early morphogenesis of the chick wing. *Nature* **238**, 24-26.

Summerbell, D., Lewis, J. H. and Wolpert, L. (1973). Positional information in chick limb morphogenesis. *Nature* **244**, 492-496.

Swiatek, P. J., Lindsell, C. E., del Amo, F. F., Weinmaster, G. and Gridley, T. (1994). *Notch 1* is essential for post-implantation development in mice. *Genes Dev.* **8**, 707-719.

Tabin, C. J. (1991). Retinoids, homeoboxes, and growth factors: Toward molecular models for limb development. *Cell* **66**, 199-217.

Taylor, G. P., Anderson, R., Reginelli, A. D. and Muneoka, K. (1994). FGF-2 induces regeneration of the chick limb bud. *Dev. Biol.* **163**, 282-284.

Thaller, C. and Eichele, G. (1987). Identification and spatial distribution of retinoids in the developing chick limb bud. *Nature* **327**, 625-628.

Thomas, U., Speicher, S. A. and Knust, E. (1991). The *Drosophila* gene *Serrate* encodes an EGF-like transmembrane protein with a complex expression pattern in embryos and wing discs. *Development* **111**, 749-761.

Tickle, C. (1981). The number of polarizing region cells required to specify additional digits in the developing chick wing. *Nature* **289**, 295-298.

Tickle, C. (1995). Vertebrate limb development. *Curr. Op Genet. Dev.* **5**, 478-484.

Tickle, C. and Eichele, G. (1994). Vertebrate limb development. *Annu. Rev. Cell Biol.* **10**, 121-152.

Tickle, C., Alberts, B., Wolpert, L. and Lee, J. (1982). Local application of retinoic acid to the limb bud mimics the action of the polarizing region. *Nature* **296**, 564-566.

Tickle, C., Lee, J. and Eichele, G. (1985). A quantitative analysis of the effect of all-trans-retinoic acid on the pattern of chick wing development. *Dev. Biol.* **109**, 82-95.

Tickle, C., Shellswell, G., Crawley, A. and Wolpert, L. (1976). Positional signalling by mouse limb polarising region in the chick limb bud. *Nature* **259**, 396-397.

Tickle, C., Summerbell, D. and Wolpert, L., (1975). Positional signalling and specification of digits in chick limb morphogenesis. *Nature* **254**, 199-202.

Todt, W. L. and Fallon, J. F. (1984). Development of the apical ectodermal ridge in the chick limb bud. *J. Embryol. exp. Morph.* **80**, 21-41.

Uyttendaele, H., Marazzi, G., Wu, G., Yan, Q., Sassoon, D. and Kitajewski, J. (1996). *Notch4/int-3*, a mammary proto-oncogene, is an endothelial cell specific mammalian *Notch* gene. *Development* **122**, 2251-2259.

van der Hoeven, F., Zakany, J. and Duboule, D. (1996). Gene transpositions in the *HoxD* complex reveal a hierarchy of regulatory controls. *Cell* **85**, 1025-1035.

van der Lugt, N. M. T., Alkema, M., Berns, A. and Deschamps, J. (1996). The Polycomb-group homolog *Bmi-1* is a regulator of murine *Hox* gene expression. *Mech. Dev.* **58**, 153-164.

Vargesson, N., Clarke, J. D. W., Vincent, K., Coles, C., Wolpert, L. and Tickle, C. (1997). Cell fate in the chick limb bud and relationship to gene expression. *Development* **124**, 1909-1918.

Vassin, H., Bremer, K. A., Knust, E. and Campos-Ortega, J. A. (1987). The neurogenic gene *Delta* of *Drosophila melanogaster* is expressed in neurogenic territories and encodes a putative transmembrane protein with EGF-like repeats. *EMBO J.* **6**, 3431-3440.

Vogel, A. and Tickle, C. (1993). FGF-4 maintains polarizing activity of posterior limb bud cells in vivo and in vitro. *Development* **119**, 199-206.

Vogel, A., Roberts-Clarke, D. and Niswander, L. (1995a). Effect of FGF on gene expression in chick limb bud cells in vivo and in vitro. *Dev. Biol.* **171**, 507-520.

Vogel, A., Rodriguez, C., Warnken, W. and Izpisua-Belmonte, J-C. (1995b). Dorsal cell fate specified by chick *Lmx-1* during vertebrate limb development. *Nature* **378**, 716-720.

Vogel, A., Rodriguez, C. and Izpisua-Belmonte, J-C. (1996). Involvement of FGF-8 in initiation, outgrowth and patterning of the vertebrate limb. *Development* **122**, 1737-1750.

Wagner, M., Thaller, C., Jessell, T. and Eichele, G. (1990). Polarising activity and retinoid synthesis in the floor plate of the neural tube. *Nature* **345**, 819-822.

Wanek, N., Gardiner, D. M., Muneoka, K. and Bryant, S. V. (1991). Conversion by retinoic acid of anterior cells into ZPA cells in the chick wing bud. *Nature* **350**, 81-83.

Webster, M. K. and Donoghue, D. J. (1997). FGFR activation in skeletal disorders: too much of a good thing. *Trends Genet.* **13**, 178-182.

Wilkie, A. O. M., Morriss-Kay, G. M., Jones, E. Y. and Heath, J. K. (1995). Functions of fibroblast growth factors and their receptors. *Curr. Biol.* **5**, 500-507.

Wilson, D. (1983). The origin of the endothelium in the developing marginal vein of the chick wing bud. *Cell Differ.* **13**, 63-67.

Wolpert, L. (1969). Positional information and the spatial pattern of cellular differentiation. *J. Theoret. Biol.* **25**, 1-47.

Wolpert, L. and Hornbruch, A. (1981). Positional signalling along the antero-posterior axis of the chick wing: the effect of multiple polarizing region grafts. *J. Embryol. exp. Morphol.* **63**, 145-159.

Wolpert, L., Tickle, C. and Sampford, M. (1979). The effect of cell killing by X-irradiation on pattern formation in the chick limb. *J. Embryol. exp. Morph.* **50**, 175-198.

Wolpert, L., Beddington, R., Brockes, J., Jessell, T., Lawrence, P. and Meyerowitz. E. (1998). In *'Principles of DevelopmentÕ.* pp 63. Current Biology Ltd. Oxford University Press.

Xu, X., Weinstein, M., Li, C., Naski, M., Cohen, R. I., Ornitz, D. M., Leder, P. and Deng, C. (1998). Fibroblast growth factor receptor 2 (FGFR2)-mediated reciprocal regulation loop between FGF8 and FGF10 is essential for limb induction. *Development* **125**, 753-765.

Yallup, B. and Hinchliffe, J. R. (1983). Regulation along the antero-posterior axis of the chick wing bud. In *Limb development and regeneration* (ed. J. Fallon and A. Caplan), 131-140. A. R. Liss Inc.

Yamaguchi, T. P and Rossant, J. (1995). Fibroblast growth factors in mammalian development. *Curr. Op. Gen. Dev.* **5**, 485-491.

Yang, Y. and Niswander, L. (1995). Interaction between the signalling molecules WNT7A and SHH during vertebrate limb development: Dorsal signals regulate anteroposterior patterning. *Cell* **80**, 939-947.

Yang, Y. and Drossopoulou, G., Chuang, P-T., Duprez, D., Marti, E., Bumcrot, D., Vargesson, N., Clarke, J., Niswander, L., McMahon, A. and Tickle, C. (1997). Relationship between dose, distance and time in Sonic hedgehog-mediated regulation of anteroposterior polarity in the chick limb. *Development* **124**, 4393-4404.

Yokouchi, Y., Ohsugi, K., Sasaki, H. and Kuroiwa, A. (1991a). Chicken homeobox gene *Msx-1*: structure, expression in limb buds and effect of retinoic acid. *Development* **113**, 431-444.

Yokouchi, Y., Sasaki, H. and Kuroiwa, A. (1991b). Homeobox gene expression correlated with the bifurcation process of limb cartilage development. *Nature* **353**, 443-445.

Yokouchi, Y., Nakazato, S., Yamamoto, M., Goto, Y., Kameda, T., Iba, H. and Kuroiwa, A. (1995). Misexpression of *Hoxa-13* induces cartilage homeotic transformation and changes cell adhesiveness in chick limb buds.*Genes & Dev.* **9**, 2509-2522.

Yokouchi, Y., Sakiyama, J., Kameda, T., Iba, H., Suzuki, A., Ueno, N. and Kuroiwa, A. (1996). BMP-2/-4 mediate programmed cell death in chicken limb buds. *Development* **122**, 3725-3734.

Yuan, Y. P., Schultz, J., Mlodzik, M. and Bork, P. (1997). Secreted *Fringe*-like signalling molecules may be glycosyltransferases. *Cell* **88**, 9-11.

Zagouras, P., Stifani, S., Blaumueller, C. M., Carcangiu, M. L. and Artavanis-Tsakonas, S. (1995). Alterations in *Notch* signalling in neoplastic lesions of the human cervix. *Proc. Natl. Acad. Sci. U-S-A.* **92**, 6414-8.

Zakany, J. and Duboule, D. (1996). Synpolydactyly in mice with a targeted deficiency in the *HoxD* complex. *Nature* **384**, 69-71.

Zeller, R. and Duboule, D. (1997). Dorso-ventral polarity and origin of the ridge: on the fringe of independence?. *BioEssays* **19**, 541-546.

Zimrin, A. B., Pepper, M. S., McMahon, G. A., Nguyen, F., Montegano, R. and Maciag, T. (1996). An antisense oligonucleotide to the *Notch* ligand *Jagged* enhances FGF-induced angiogenesis in vitro. *J. Biol. Chem.* **271** (51), 32499-32502.

Zwilling, E. (1956). Interaction between limb bud ectoderm and mesoderm in the chick embryo: II Experimental limb duplication. *J. Exp. Zool.* **132**, 173-187.